DANIELA NOGUEIRA DA ROCHA MAR

PhD Thesis

Impact of Mechanotransduction in the Context of Central Nervous System Diseases

Dissertação submetida à Faculdade de Engenharia da Universidade do Porto
para obtenção do grau de Doutora em Engenharia Biomédica

Faculdade de Engenharia

Universidade do Porto

2015

This thesis was supervised by:

Doutora Ana Paula Gomes Moreira Pêgo (supervisor)

INEB – Instituto de Engenharia Biomédica

I3S – Instituto de Investigação e Inovação em Saúde

FEUP – Faculdade de Engenharia da Universidade do Porto

ICBAS – Instituto de Ciências Biomédicas Abel Salazar

Doutor João Bettencourt Relvas (co-supervisor)

IBMC – Instituto de Biologia Celular e Molecular

I3S – Instituto de Investigação e Inovação em Saúde

ICBAS – Instituto de Ciências Biomédicas Abel Salazar

The work was performed at:

INEB – Instituto de Engenharia Biomédica

IBMC – Instituto de Biologia Celular e Molecular, Divisão de Neurociências, Glial Cell Biology Laboratory

This work was financially supported by:

FCT through the PhD grant SFRH/BD/64079/ 2009.

European Commission FP6 NEST Program (Contract 028473)

FEDER funds through the Programa Operacional Factores de Competitividade – COMPETE

Portuguese funds through the Fundação para a Ciência e a Tecnologia (FCT) (PEst-C/SAU/LA0002/2011 and PEst-C/SAU/LA0002/2013-14)

PTDC/SAU-NMC/119937/2010 - FCT — R&D

Devagar se vai ao longe.

(Provérbio popular Português)

Agradecimentos

Aos meus orientadores Ana Paula e João que me apoiaram durante estes anos, e com quem aprendi muito.

Obrigada à Cristina Barrias pelo apoio, pela ajuda e input valioso no que toca à matrizes de alginato. Neste contexto, tenho ainda que agradecer à Keila Fonseca e à Raquel Maia pela ajuda preciosa nesta temática. Claro está que, no caso da Raquelita o meu muito obrigado vai bem para além do alginato. Obrigada pela amizade, que espero preservar por muitos e muitos anos. E claro não podia deixar de agradecer pela ajuda e companhia na hora de escolher o meu vestido de noiva.

Liliana Pires, obrigada pelas fibras de P(TMC-CL), pela camaradagem, pela amizade e pelas nossas longas conversas que ainda hoje temos, embora mais curtas e menos frequentes. Foi um prazer fazer ciência contigo!

À Isabel Carvalho com quem aprendi muito (senão quase tudo) do que sei de animais de laboratório, e experimentação animal. Apesar de já não estares no IBMC-ONEH há alguns anos, foste quem me introduziu neste mundo da experimentação animal e não poderia ter aprendido com melhor pessoa. Obrigada pela partilha de conhecimento.

Um obrigada muito especial também à Márcia Liz com quem tive o prazer de explorar o mundo dos western blots e da GSK3β. O P(TMC-CL) e os neurónios corticais deram-nos muitos desafios mas valeu a pena e, acima de tudo, foste uma excelente professora.

Obrigada Mónica pela disponibilade e ajuda na exploração da via da GSK3β.

Obrigada às minhas companheiras de viagem científica, amizades fabulosas que o INEB me deu: Nilza, Fabíola e Daniela muito obrigada pela vossa amizade! Foi bom partilhar este percurso convosco. Nilza e Fabíola obrigada ainda pela partilha e pelo convívio extra-INEB, pelos jantares, pelos lanches e pelas viagens à retrosaria do Sr. Simpático que fala pelos cotovelos. Pelas nossas conversas sobre trabalhos manuais e costuras, que espero que continuem a existir no futuro.

Ao GCB ou melhor, aos elmentos do GCB – Joana, Maria, Ana, Sofias e Nuno - que tão bem me receberam no seu laboratório, fazendo a integração super fácil. Gostei imenso de trabalhar convosco e de partilhar esta viagem científica. Obrigapa pela vossa paciência sempre que monopolizava o agitador orbital com as minhas mega membranas. Obrigada por me introduzirem ao maravilhoso mundo das culturas de OPCs e, Maria, obrigada por todas as vezes que nos últimos tempos me cedeste OPCs.

Obrigada Claúdia e Manuel pela ajuda com os meus géis grandes de western blot, e pelos conselhos tão úteis. Obrigada Prof. Jorge Azevedo por me deixar usar os seus sistemas para correr os meus géis.

Obrigada Maria Oliveira pelo input valioso no meu artigo de revisão, ficou seguramente mais valioso depois do teu contributo.

Obrigada Tiago pela ajuda preciosa no Huygens para a edição das imagens de confocal das fibras de P(TMC-CL), finalmente dá para ver que estão mielinizadas.

Tenho ainda que agradecer aos meu colegas de turma do MBA que foram a minha companhia neste último ano tão desafiante. Obrigada pela camaradagem, obrigada pelas amizades (seguramente para a vida), pelo apoio e carinho a esta Bioquímica/ *R&D investigator* que decidiu ir para o meio dos economistas e engenheiros.

Obrigada às minhas “pulguinhas” de quem gosto tanto e que me dão tantas alegrias de cada vez que vejo os seus sorrisos, que me pedem fatos de carnaval e halloween ou abracinhos apertadinhos.

Um obrigada gigante aos meus pais. Meus fãs, que me apoiam e apoiaram sempre, incondicionalmente. Obrigada por acreditarem em mim, por me desafiarem a ir sempre um bocadinho mais longe. O vosso apoio e carinho foi crucial neste processo.

A ti Fernando obrigada por tudo e mais alguma coisa. Obrigada pelo carinho, pela partilha, pela paciência e resiliência. Obrigada por acreditares em mim por me estimulares a ser sempre melhor. Obrigada por partilhares a vida comigo.

Table of Contents

Abbreviation List vii

Abstract xi

Resumo xiii

Chapter I – General Introduction and Motivations 1

Chapter II – Mechanotransduction: exploring new therapeutic avenues in CNS Pathology 21

Chapter III – Extracellular Environment Contribution to Astrogliosis – Lessons Learned from a Tissue Engineered 3D Model of the Glial Scar 61

Chapter IV – Poly (Trimethylene Carbonate-co-ε-Caprolactone) Pomotes Axonal Growth 93

Chapter V – Astrocytes Affect Oligodendrocyte Precursor Cell Differentiation 125

Chapter VI – Concluding Remarks 145

APPENDIX

Abbreviation list

AFM	Atomic force microscopy
Alg	Alginate
ATP	Adenosine 5´- triphosphate
BBB	Blood-brain-barrier
BIO	6-bromoindirubin-3'-acetoxime
BSA	Bovine serum albumin
CM	Conditioned medium
CNS	Central Nervous System
Col IV	Collagen IV
CRMP4	Collapsin response mediator protein 4
CSF	Cerebrospinal fluid
CSPG	Chondroitin sulphate proteoglycans
C4S	Chondroitin 4 sulphate
DMEM	Dulbecco's modified eagle medium
DMSO	Dimethyl sulfoxide
DNA	Deoxiribonucleic acid
DTT	DL-dithiothreitol
ECM	Extracellular matrix
EDTA	Ethylenediaminetretaacetic acid
EGTA	Ethylene glycol tretaacetic acid
FAK	Focal adhesion kinase
FBS	Fetal bovine serum
FITC	Fluorescein isothiocyanate
FRET	Foster Resonance Energy Transfer
G'	Elastic modulus

G’’	Viscous modulus
GAPDH	Glyceraldehyde-3-phosphate dehydrogenase
GBM	Glioblastoma multiforme
GFAP	Glial fibrillary protein
GPC	Gel permeation chromatography
GSK	Glycogen synthase kinase
GSK3β	Glycogen synthase kinase 3 beta
GTPases	Rho family guanosine-5-triphosphatases
HBSS	Hank’s balanced salt solution
HMW	High molecular weight
HPRT	Hypoxanthine guanine phosphoribosyl transferase
HRP	Horseradish peroxidase
IBU	Ibuprofen
iNPH	Idiopathic normal pressure hydrocephalus
IOP	Intraocular pressure
KD	Knockdown
LMW	Low molecular weight
LPA	Lysophosphatidic acid
MAIs	Myelin associated inhibitors
MAPK	Mitogen activated protein kinase
MBP	Myelin basic protein
MMPs	Matrix metalloproteinases
MMP-2	Matrix metalloproteinase 2
MMP-9	Matrix metalloproteinase 9
MOPS	3-(n-morpholino) propanesulfonic acid
MRE	Magnetic resonance elastography
MRI	Magnetic resonance imaging
MS	Multiple Sclerosis

NG2	Neural/glial antigen 2
NGS	Normal goat serum
NMR	Nuclear magnetic resonance
NSCs	Neural stem cells
OLs	Oligodendrocytes
OPCs	Oligodendrocyte precursor cells
PBS	Phosphate buffered saline
PKC	Protein kinase C
PLA_2	Phospholipase A2
PN	Perineuronal net
RMS	Root mean square
RPE	Retinal pigment epithelium
RT	Room temperature
RT-PCR	Real-time polymerase chain reaction
P(CL)	Poly(ε-caprolactone)
PLL	Poly(L-lysine)
PMSF	Phenyl-methanesulfonyl fluoride
PNS	Peripheral nervous system
P(TMC)	Poly(trimethylene carbonate)
P(TMC-CL)	Poly(trimethylene-carbonate-co-ε-caprolactone)
qPCR	Quantitative real- time polymerase chain reaction
RNA	Ribonucleic acid
ROCK	Rho-associated kinase
RPE	Retinal pigment epithelium
SCI	Spinal cord injury
Ser	Serine
shRNA	Small/Short hairpin ribonucleic acid
SRC	Proto-oncogene tyrosine-protein kinase SRC

TBS	Tris-buffered saline
Tyr	Tyrosine
VIM	Vimentin
VSVG	Vesicular Stomatitis Virus Glycoprotein
YAP	Yes-associated protein

Abstract

To understand the chain of alterations that occur in the aftermath of a central nervous system (CNS) lesion and how these condition the progress of the tissue response and ultimately of the disease, requires a systematic approach, as scar formation results from a plethora of events.

Cells within tissues are continuously exposed to physical forces and the CNS is no exception. Several CNS disorders have now been intimately correlated with mechanotransduction issues. As such, this thesis aimed at exploring the impact of mechanotransduction in the CNS, specifically in pathological conditions, envisaging its modulation towards the design of new complementary CNS regenerative therapies. In particular, the work here presented explores the impact of mechanotransduction on CNS key cellular players and subsequent signaling activation pathways.

Due to the lack of a screening platform, which could allow *in vitro* testing of mechanotransduction in CNS cells, up to now no comprehensive study has addressed and clarified this subject. Consequently, the first challenge was the development of a tissue-engineered platform, which lead to the establishment of an *in vitro* alginate-based three-dimensional (3D) glial scar model. Using this model we have further explored the implications of matrix mechanical properties in the process of astrocyte activation. Here mechanotransduction was found to play a pivotal role in modulating astrocyte phenotype and its subsequent extracellular matrix (ECM) production.

Afterwards, the reader is further challenged to look at the effect of substrate mechanical properties on neuronal regeneration capacity. The use of biomaterials to bridge CNS lesions and create an environment which favors axonal regeneration is currently under investigation by several authors but, mechanical properties have not been fully explored in this context. Here, mechanotransduction was found to play a pivotal role in axonal outgrowth as, poly(trimethylene-co-ε-caprolactone) (P(TMC-CL)) substrates with high caprolactone content promoted neuronal polarization and axonal elongation, prompting neurons into regeneration mode, even under inhibitory conditions such as in the presence of myelin debris.

One of the major mechanisms responsible for the loss of function observed in several neurological diseases is the loss of myelin sheet insulating the nerves - demyelination. In the adult CNS myelin loss can only be partially rescued by spontaneous remyelination of

spared axons, process essential to preserve axonal integrity and to ensure recovery of the lost physiological activity. Though the mechanisms responsible for chronic remyelination failure have not yet been identified, evidence of the presence of oligdendrocyte progenitor cells (OPCs) in chronic Multiple Sclerosis lesions suggests the existence of a critical regulatory mechanism inhibiting OPC differentiation.

Finally, the combination of the tissue engineered glial scar with an artificial axon system further revealed the inhibitory influence of reactive astrocytes on oligodendrocyte cell (OPC) differentiation. The use of an “artificial axon” enabled the uncoupling of neuron-oligodendrocyte cross-talk, showing that, contrarily to what many authors have suggested, neurons and their axons are not crucial for OPCs to differentiate and myelinate and that physical support can trigger these processes. Furthermore mechanotransduction was also revealed as a key player in OPCs differentiation and myelination processes via astrocytic activation.

A common signalling pathway has emerged in all these mechanotransduction scenarios – the Rho/ROCK signalling pathway – and, consequently, RhoA was explored as a mediator of the mechanoransduction processes. Its inhibition was reconnoitred as a potential therapeutic target.

Overall, besides developing two new *in vitro* culture systems which can be of added value in future neurodegenerative mechanism studies, as well as in drug screenings envisaging the development of new therapeutic approaches, we have established mechanotransduction as a key modulator of CNS cell behavior in pathological conditions.

Resumo

Para entender a cadeia de eventos que ocorrem na sequência de uma lesão no sistema nervoso central, e como condicionam o progresso da resposta tecidular e, finalmente, da doença, é necessária uma abordagem sistemática uma vez que a formação de uma cicatriz glial resulta de um vasto conjunto de eventos.

Nos tecidos as células estão constantemente expostas a forças físicas e, o sistema nervoso central não é excepção. Vários patologias do sistema nervoso central foram já intimamente correlacionadas com questões de mecanotransdução. Como tal, esta tese tem como objectivo explorar o impacto da mecanotransdução no sistema nervoso central, especificamente em condições patológicas, com vista à sua modulação para a concepção de novas terapias regenerativas complementares. Em particular, o trabalho aqui apresentado explora o impacto da mecanotransdução no sistema nervoso central nos principais agentes celulares e na subsequente activação das vias de sinalização.

Devido à falta de uma plataforma de triagem, que poderia permitir testes *in vitro* de mecanotransdução em células do sistema nervoso central, não há até ao momento nenhum estudo abrangente que tenha abordado e clarificado este assunto. Por conseguinte, o primeiro desafio foi o desenvolvimento de uma plataforma, o que conduziu ao estabelecimento de um modelo tridimensional (3D) *in vitro* da cicatriz glial com base em alginato. Usando este modelo exploramos as implicações das propriedades mecânicas da matriz no processo de activação de astrócitos. Deste modo, a mecanotransdução mostrou desempenhar um papel central na modulação do fenótipo dos astrócitos bem como na subsequente produção de matriz extracelular.

Em seguida, o leitor é ainda desafiado a olhar para o efeito das propriedades mecânicas do substrato na capacidade de regeneração neuronal. O uso de biomateriais para regenerar lesões do sistema nervoso central e criar um ambiente que favorece a regeneração axonal está atualmente a ser investigado por vários autores mas, as propriedades mecânicas não foram ainda devidamente exploradas neste contexto. Aqui, mostrou-se que a mecanotransdução desempenha um papel fundamental no crescimento axonal uma vez que, subatratos de poli (trimetileno - co - ε - caprolactona) (P(TMC - CL)) com elevado teor de caprolactona promoveram a polarização neuronal e a elongação axonal, promovendo um “modo de regeneração” nos neurónios, mesmo em condições inibitórias tais como a presença de restos de mielina.

Um dos principais mecanismos responsáveis pela perda de função observada em diversas doenças neurológicas, é a perda da folha de mielina que isola os nervos - desmielinização. No sistema nervoso central adulto a perda de mielina só pode ser parcialmente resgatada por remielinização espontânea de axónios que sobrevivem à lesão, processo essencial para preservar a integridade axonal e para assegurar a recuperação da atividade fisiológica perdida. Embora os mecanismos responsáveis pelo fracasso da remielinização crónica ainda não tenham sido identificados, a evidência da presença de células progenitoras de oligodendrócitos em lesões crónicas de esclerose múltipla sugere a existência de um mecanismo de regulação crítico que inibe a diferenciação destas células.

Finalmente, a combinação da cicatriz glial mimética com um sistema de axónios artificial revelou ainda a influência inibidora dos astrócitos reactivos na diferenciação de oligodendrócitos. O uso de "axónios artificiais" permitiu eliminar a comunicação neurónio - oligodendrócito, mostrando que, ao contrário do que muitos autores têm sugerido, os neurónios e os seus axónios não são cruciais para células progenitoras de oligodendrócitos se diferenciem em oligodendrócitos capazes de produzir mielina e que o suporte físico pode desencadear estes processos. Além disso, mosrou-se que a mecanotransdução desempenha um papel chave no processo de diferenciação das células progenitoras de oligodendrócitos em oligodendrócitos capazes de produzir mielina, através da ativação astrocitica.

Uma via de sinalização comum emergiu em todos esses cenários de mecanotransdução - a via de sinalização Rho / ROCK - e, consequentemente, o RhoA foi explorado como um mediador dos processos de mecanotransdução. A sua inibição foi reconhecida como um potencial alvo terapêutico.

No geral, para além de desenvolver dois novos modelos de cultura *in vitro* que podem ser de valor acrescentado em futuros estudos mecanisticos em neurodegeneração, bem como em screenings de fármacos com vista ao desenvolvimento de novas abordagens terapêuticas, identificamos a mecanotransdução como um modulador chave do comportamento das células do sistema nervoso central em condições de patologia.

“...ao contrário do que geralmente se crê, por muito que

se tente convencer-nos do contrário, as verdades únicas

não existem: as verdades são múltiplas,

só a mentira é global. “

(José Saramago)

CHAPTER I

General Introduction and Motivation

The Central Nervous System Milieu

The central nervous system (CNS) is composed by the brain, the spinal cord and the optic nerves. These are covered by three layers of connective tissue: the dura mater, the arachnoid mater and the pia mater, collectively referred to as the meninges. At the cellular level the main constituents of the CNS are the neurons, astrocytes, oligodendrocytes and microglia.

Neurons, the nerve impulse transmitting cells, are probably the most widely studied CNS cell type. For many years neurons were seen as the most important, if not the only important, cells of the CNS. Nowadays studies on the other CNS cells, like astrocytes and oligodendrocytes, have shown that these have equally important roles in CNS function and dynamics. Neurons have high levels of energy expenditure - it has been estimated that cortical neurons use about five billion ATP molecules per second [1]. They control their vast peripheral axonal and dendritic network through fast and slow axonal transport, which shuttles organelles and substrates between the soma and the synapses. The length and shape of the axons, as well as dendrites and synapses, are all important features of axonal function.

Astrocytes are the most abundant cells in the CNS. In the past their function has been mainly associated with pathological states, but currently their involvement in several homeostasis processes is being unraveled. They play an important role as support cells to neurons, as they maintain ion and pH homeostasis, store glycogen and clear neuronal wastes [2, 3]. Moreover, astrocytes are also crucial for the synaptic function [4, 5]. Additionally, they play a pivotal role in the function of the blood-brain-barrier (BBB) [6], as they surround CNS capillaries modulating the blood-brain-barrier (BBB) function and communication with neurons. Also in development, they are known to be instrumental in the process of neurite extension and path finding [7, 8].

Oligodendrocyte precursor cells (OPCs) are proliferative, migratory precursor cells [9]. Later, mature oligodendrocytes play a key role in the production of myelin and in wrapping axons. These insulating myelin sheaths, which isolating capacity is achieved by the high amount of lipids present in myelin, are crucial for the saltatory conduction along the axons. Oligodendrocytes are polarized cells as the plasma membrane of the myelin sheath is continuous with the plasma membrane of the cell body but their protein and lipid compositions are significantly different. They are able to form multiple processes and myelinate multiple axons.

Microglia constitutes the resident population of macrophages of the CNS and have an important function in immune surveillance and defense. These are the first to respond to harmful stimuli, aiming to preserve CNS health. Some authors have also correlated microglia with neuronal activity and synaptic plasticity as microglia's highly motile ramifications directly interact with neurons [10]. Microglia's response to adverse stimuli is characterized by profound morphological and secreted molecular profile alterations [11].

It is widely accepted that cells are influenced by the surrounding environment, which is composed of chemical, structural and physical cues. While the CNS is one of the most densely cellularized tissues of our body, the extracellular matrix (ECM), which occupies 20% of the CNS space [12], is an extremely important constituent. As it fills the space between cells, it establishes a complex scaffold comprised of secreted proteins and sugars, which play an important role in several processes such as cellular communication, stabilization of synapses, cell migration, maturation and differentiation, as well as cell survival. CNS ECM is rather unique in composition as it contains relatively small amounts of fibrous proteins. Its main constitutes include hyluronan and proteoglycans. Additionally, the native CNS ECM is extremely dynamic as it is constantly being remodeled by several proteases, including matrix metalloproteases (MMPs). In fact, MMPs have a great capacity to remodel CNS ECM as many members of this protein family have the ability to cleave laminin, chondroitin sulphate proteoglycans (CSPGs) and ECM receptors like integrins [13]. ECM components represent key components to which cell receptors are able to bind therefore regulating cell phenotype. It is known that tissue function relies on proper control of the biochemical and biophysical cues from the surrounding microenvironment. In fact, not only is the rigidity of the tissue determined by ECM's structure but also by its composition and as such, different local concentrations of the different components may result in differences in cell signaling and adhesion. Furthermore, ECM architecture provides physical cues to cells, either by the form of fiber diameter, crosslinking patterns or even through surface irregularities, the so-called surface nanomechanical properties.

In CNS disease scenarios, ECM composition and structure are frequently altered, disturbing cell-cell and cell-ECM interactions. It is known that astrocyte and microglia activation is an early event that occurs in response to insults to the CNS. It is also recognized that ECM molecules can affect for instance the phenotype and magnitude of the inflammatory response [14, 15]. Moreover the enzymes and inflammatory molecules excreted by immune cells will further alter ECM composition. In pathological conditions ECM is mostly recalled for its components which inhibit regeneration - increased levels of CSPGs [16], which are known to inhibit axonal regeneration; hyaluronan, known to bind to

CSPGs and further inhibit OPC maturation [17, 18]; tenascin, known to alter the adhesion properties of human monocytes, B cells and T cells [19]; myelin associated inhibitors and collagen IV, known to inhibit axonal outgrowth [20, 21], among others - but, it also has some protective features. Hyaluronan, one of the major components of CNS ECM, has anti-inflammatory properties. In fact, the inflammatory response has been the target of several studies in individuals with CNS disorders [22, 23]. ECM forms special stable structures around some subtype of neurons, called perineuronal net (PN) (Figure 1). In neurodegenerative diseases such as Alzheimer and Parkinson disease an inverse relationship between the abundance of PNs and the vulnerability of the neurons was found, suggesting a contribution of the matrix components of the PNs [24], indicating that CNS ECM also provides protective potential under conditions of CNS pathology. In multiple sclerosis (MS) lesions ECM also plays a dual role as on one hand the abnormal basement membrane, the membrane that lines the parenchymal side of the micro vessels, enables immune cell infiltration into the CNS; and on the other hand, collagen expression increases and the fibrils aggregate around blood vessels constituting a physical barrier for immune infiltration [25].

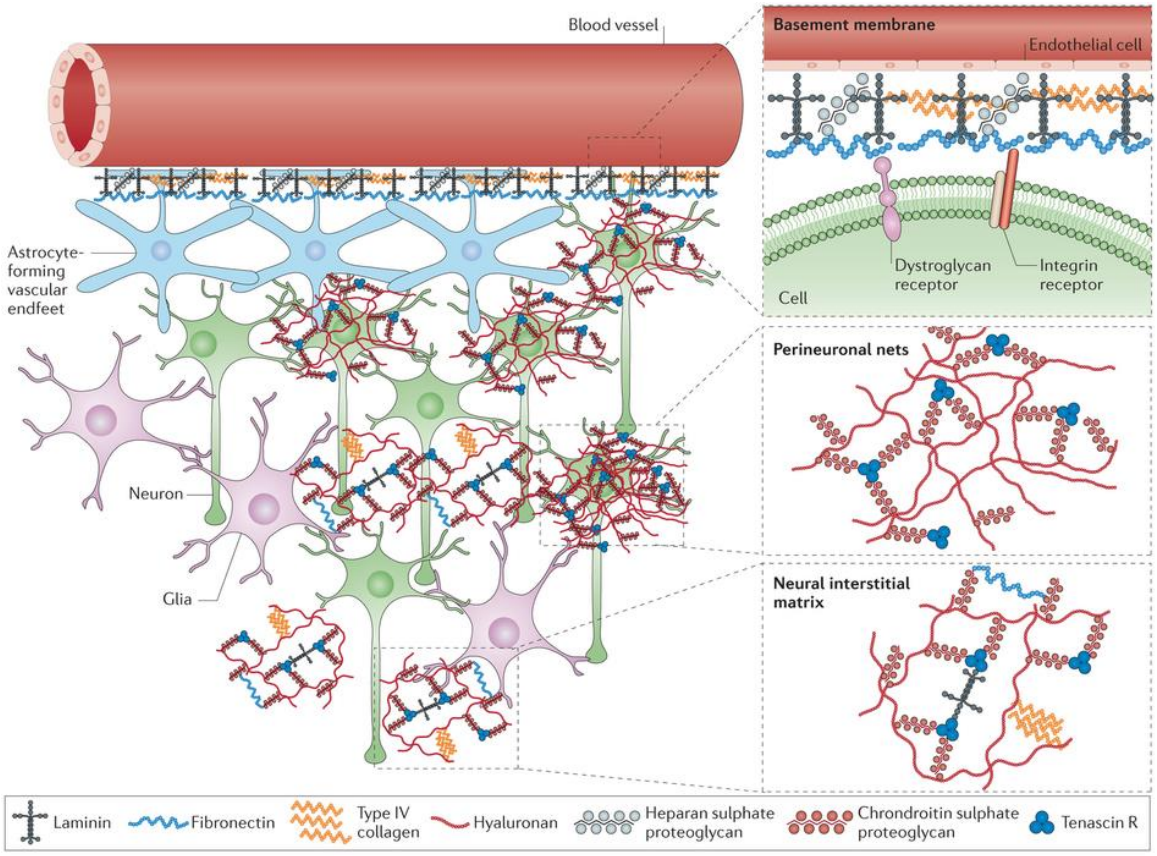

Figure 1 – The three major compartments of the extracellular matrix (ECM) in the CNS. ECM components arranged into basement membranes that lie outside cerebral vessels, condensed as perineuronal nets around

the cell bodies and dendrites of neurons or diffusely distributed as the neural interstitial matrix between cells of the CNS parenchyma. The pink glial cells depict astrocytes, oligodendrocytes or microglia. Reprinted by permission from Macmillan Publishers Ltd: Nature Reviews, Lau et al, copyright 2013.

So, upon injury, not only cellular content and morphology are affected but also the extracellular matrix environment is altered. Consequently, lesions to the CNS, either traumatic or as a result of a pathological condition such as tumors, Parkinson disease, Alzheimer's disease or Multiple Sclerosis (MS), result in several tissue architectural abnormalities and, as a consequence, culminate in functional deficits.

Ramon e Cajal have stated many decades ago that the CNS regenerative capacity is limited [26], today this statement is still true. This lack of regenerative capacity is mainly attributed to the inhibitory environment created at the lesion site as described above. Besides all the ECM alterations that occur there are also several cellular related events that contribute towards this inhibitory environment. Astrocytes react by initially building dense filamentous processes around the lesion, stromal cells migrate to the lesion core and produce several connective tissue elements, while OPCs proliferate within the lesion as an attempt to replace the dead oligodendrocytes.
Even though the glial scar may provide several beneficial functions such as the restoration of the BBB, prevention of a devastating inflammatory response and limit the action of cellular degeneration, it also contributes to the establishment of a physical and chemical barrier to axonal regeneration. Nevertheless, it is important to stress that although most CNS pathologies are known to result in a glial scar which have many common features, glial scars are not all exactly alike, probably due to the different lesion triggers (Figure 2). For instance, depending on the degree of deregulation of the BBB permeability the amount of infiltrated inflammatory cells, namely macrophages, may vary considerably (Figure 2).

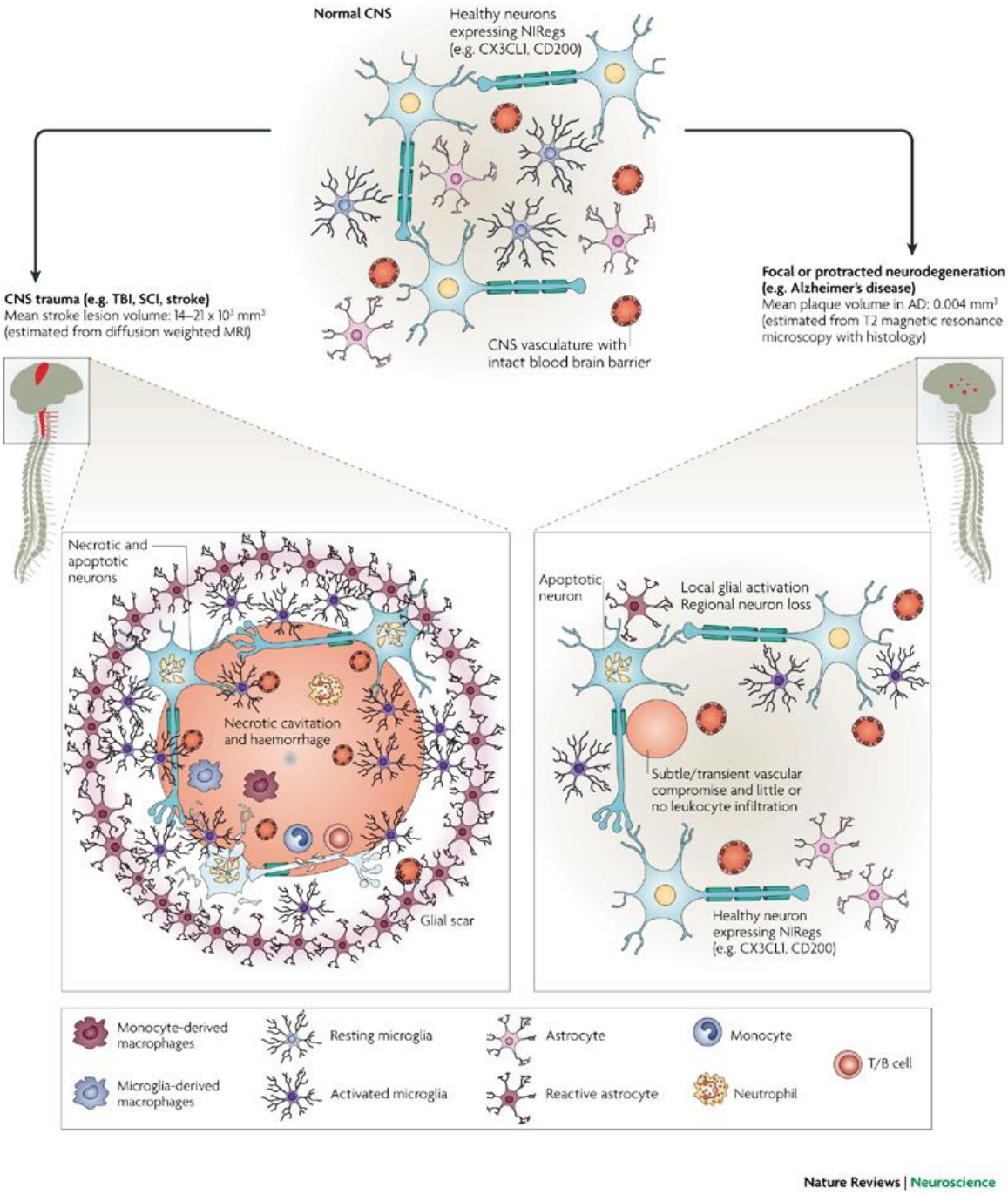

Figure 2 – The magnitude and rate of tissue pathology influences the nature of neuroimmune interactions. This figure illustrates differences in size and composition of lesions that form in response to trauma or neurodegenerative disease. In response to blunt CNS trauma or ischemia/reperfusion injury, in which there is extensive hemorrhage and leukocyte recruitment, a wound-healing response is elicited culminating in vascular repair, angiogenesis, gliosis and scarring. In contrast, slow and protracted neurodegeneration, in which vascular compromise is minimal, elicits glial activation and cytokine synthesis but not classical inflammation or wound healing. Reprinted by permission from Macmillan Publishers Ltd: Nature Reviews, Popovich et al [27], copyright 2008.

Several strategies aiming to increase the regenerative capacity of the CNS have already been proposed. Many authors have explored cell transplantation in order to improve neuroprotection and recovery. Transplanted cells include Schwan cells [28-32], bone marrow stromal cells [33], neural stem cells [34, 35], olfactory ensheathing cells [36, 37], activated macrophages [38, 39], mesenchymal stem cells derived from adipocyte tissues [40, 41], and more recently, induced pluripotent stem cells [42, 43]. Despite the obtained benefits, cells implanted as suspensions usually show poor cell survival, and when applicable limited differentiation along neuronal lineage, as a result of the inhibitory milieu of the injured tissue.

Given the extensive inflammation that occurs in most CNS lesions, administration of anti-inflammatory drugs has also been extensively studied [44-46]. Inhibition of macrophage migration has also been tested in order to reduce the inhibitory environment of the CNS [47]. In fact, oral administration of a DNA vaccine encoding full-length human myelin basic protein (MBP) was able to reduce inflammatory lesions in the brain of MS patients in a phase I/II clinical trial [48].

As stated above, many ECM components are known to somehow inhibit regeneration. As such, another classical target has been myelin. The presence of myelin debris at injury site has long been considered as one of the main contributors for the failure of regeneration in the CNS. Aiming to overcome the inhibitory environment of the glial scar many authors have studied the possibility of blocking myelin inhibition using antibodies [49-51]. Moreover, given the correlation of CSPGs with inhibition of axonal outgrowth and OPC maturation [52, 53], the use of chondroitinase ABC (chABC) in order to digest CSPGs produced in excess as a consequence of the injury, attempts to recover the initial ECM environment both chemically and mechanically have been explored. It has been established that treatment with chABC reduces inhibitory effects of CSPGs both in vitro [54] and in vivo [55, 56]. These results emphasize the importance of ECM structure and mechanical properties.

Moreover, exploration of signaling pathways involved in disease and health of the CNS has also lead to the establishment of promising therapeutic targets such as the Rho/ROCK signaling pathway [57-61], bone morphogenetic protein signaling [62], MAPK signaling [63], among others.

Given the complexity of a CNS lesion it is difficult to select one single strategy to approach this problem. It appears that the best way to reach effective neuroregeneration may rely in a multicomponent combinatorial approach. In fact, tissue engineering and regenerative medicine have a multidisciplinary approach to clinical problems by combining the principles of engineering, clinical medicine, biology and materials science, which may be

an important tool for CNS regeneration. A combination of strategies involving biomaterials, cells and/or bioactive molecules have been pursued over the past several years. Biomaterials can serve as delivery vehicles for several therapeutic molecules, such as proteins, drugs or growth factors and as cell delivery vehicles providing cellular support, which ensures their retention and may improve their survival. Delivery of bioactive molecules may target several components of the CNS regeneration problem. Depending on the delivered molecules it may promote neuroprotection and plasticity [64], modulate the inflammatory response [65, 66] or even stimulate endogenous stem cells to proliferate and differentiate [67-69]. Given the multifactorial nature of most CNS pathologies single drug development may be extremely hard to accomplish. Nevertheless it is important to stress the advantages of biomaterials as delivery systems as these can provide localized and sustained delivery while protecting the biomolecules from *in vivo* degradation. Additionally, considering the existent information regarding ECM's important role in CNS function it appears that a combination strategy that considers chemical, cellular and physical stimuli is an interesting approach to regenerate the CNS. Altering ECM's composition and on the regenerative milieu with the use of implanted scaffolds, can influence cellular signaling and consequently cellular response, as these stimuli can be seen as instructive cues towards mechanisms of CNS repair. Nevertheless, more knowledge on CNS mechanisms of repair and regeneration is still needed to accomplish these objectives. Our understanding of such matters could be enhanced with the use of 3D culture systems that enable the control of its mechanical, chemical and biological environment. The use of biomaterials for this purpose is also extremely appealing as these can serve as powerful artificial microenvironments enabling the detailed study of CNS cellular mechanisms.

Motivation

The work developed, which is presented in this thesis, aimed at exploring the impact of mechanotransduction in the CNS, particularly in pathological conditions, envisaging its modulation towards the design of novel regenerative therapies.

Specific objectives were:

- The development of a tunable alginate-based 3D in vitro platform to mimic CNS astrogliosis, as a tool to study cellular behavior and response to biochemical and physical properties.

- Assess the impact of substrate nanomechanical properties on cortical neuron's axonal outgrowth and their potential towards the achievement of overcoming myelin inhibition.

- Explore the substrate's influence on OPC differentiation ability. Dissection of the astrocyte - OPCs cross-talk, particularly the effect of astrocyte reactivity on OPC differentiation.

- Investigate common signaling mechanisms, which can be interesting future targets for the design of novel therapeutic strategies.

Thesis Outline

This thesis has been organized into six chapters and one appendix.

Chapter II provides the reader with a literature review, which specifically covers the role and influence of mechanical properties in the CNS. It discusses the work of several research groups in studying CNS mechanical properties in pathologic conditions. The possibility of modulating cellular behavior, and possible disease outcome, by tuning mechanical properties is also addressed in this chapter.

The subsequent chapters describe the developed experimental work:

Chapter III explores the use of 3D hydrogels as a bioengineered platform to mimic astrogliosis, serving as a powerful tool to study cellular behavior and response to biochemical and physical properties. Primary rat astrocytes were cultured within 3D alginate discs. Cellular activation was modulated by changing the hydrogel's mechanical properties, achieved by varying the alginate content, and by culturing these cells in the presence of meningeal fibroblasts conditioned medium (CM). Reactive astrocytes were found to inhibit axonal outgrowth and to produce higher levels of ECM components, such as CSPG and collagen. Furthermore, the Rho/ROCK signaling pathway was explored as a possible regulator of astrocyte activation.

Chapter IV describes the influence of substrate nanomechanical properties on cortical neurons' morphology and axonal outgrowth. With this work it was possible to establish what appears to be an optimum value of stiffness and hardness for cortical neuron's axonal elongation. This was found to be valid even when neurons were cultured under inhibitory conditions. These results have shown that a biomaterial can per se modulate cellular behavior and activate the GSK3β signaling pathway which was further found to impact the interaction of collapsin response mediator protein 4 (CRMP4) and RhoA through CRMP4 de-phosphorylation.

Chapter V dissects the cross-talk between activated astrocytes and OPCs, particularly the effect of astrocyte reactivity on OPC differentiation ability. For this, we have established an *in vitro* rapid myelinating system with electrospun polymeric fibers as artificial axons. The Rho/ROCK pathway was once more explored and RhoA was seen as a therapeutic target to promote OPC differentiation. Using this culture system we have further uncoupled

axonal signalling and OPC differentiation and myelination events, showing the important role of mechanotransduction in these complex cellular processes.

To finish, **Chapter VI** provides the concluding remarks, with an overall analysis of the preceding chapters, as well as future perspectives.

Appendix I constitutes the filed patent WO2014116132 A1, which resulted from the work presented in chapter IV.

REFERENCES

[1] Zhua XH, Qiaoa h, Dua F, Xionga Q, Liua X, Zhanga X, et al. Quantitative imaging of energy expenditure in human brain. NeuroImage. 2012;60:2107-17.
[2] Nair A, Frederick TJ, Miller SD. Astrocytes in multiple sclerosis: A product of their environment. Cell Mol Life Sci. 2008;65:2702-20.
[3] Nedergaard M, Ranson B, Goldman SA. New roles for astrocytes: redefining the functional architecture of the brain. Trends Neurosci. 2003;26:523-30.
[4] Perea G, Navarrete M, Araque A. Tripartite synapses: astrocytes process and control synaptic information. Trends Neurosci. 2009;32:421-31.
[5] Barker AJ, Ullian EM. Astrocytes and synaptic plasticity. The Neuroscientist : a review journal bringing neurobiology, neurology and psychiatry. 2010;16:40-50.
[6] Abbott NJ. Astrocyte-endothelial interactions and blood-brain barrier permeability. Journal of anatomy. 2002;200:629-38.
[7] Guizzetti M, Moore NH, Giordano G, Costa LG. Modulation of neuritogenesis by astrocyte muscarinic receptors. The Journal of biological chemistry. 2008;283:31884-97.
[8] Powell EM, Meiners S, DiProspero NA, Geller HM. Mechanisms of astrocyte-directed neurite guidance. Cell and tissue research. 1997;290:385-93.
[9] Kessaris N, Pringle N, Richardson WD. Specification of CNS glia from neural stem cells in the embryonic neuroepithelium. Philosophical transactions of the Royal Society of London Series B, Biological sciences. 2008;363:71-85.
[10] Tremblay ME, Lowery RL, Majewska AK. Microglial interactions with synapses are modulated by visual experience. PLos One. 2010;8.
[11] Delpech JC, Madore C, A. N, Joffre C, Wohleb E, S. L. Microglia in neuronal plasticity: Influence of stress. Neuropharmacology. 2015:1-10.
[12] Nicholson C, Sykova E. Extracellular space structure revealed by diffusion analysis. Trends Neurosci. 1998;21:207-15.
[13] Sternlicht MD, Werb Z. How matrix metalloproteinases regulate cell behavior. Annual review of cell and developmental biology. 2001;17:463-516.
[14] Arroyo AG, Iruela-Arispe ML. Extracellular matrix, inflammation, and the angiogenic response. Cardiovascular research. 2010;86:226-35.
[15] Sorokin L. The impact of the extracellular matrix on inflammation. Nature reviews Immunology. 2010;10:712-23.
[16] Busch SA, Silver J. The role of extracellular matrix in CNS regeneration. Current opinion in neurobiology. 2007;17:120-7.
[17] Back SA, Tuohy TM, Chen H. Hyaluronan accumulates in demyelinated lesions and inhibits oligodendrocyte progenitor maturation. Nat Med. 2005;11:966-72.
[18] Sloane JA, Batt C, Ma Y. Hyaluronan blocks oligodendrocyte progenitor maturation and remyelination through TLR2. Proc Natl Acad Sci. 2010;107:11555-60.
[19] Ruegg CR, Chiquet-Ehrismann R, Alkan SS. Tenascin, an extracellular matrix protein, exerts immunomodulatory activities. Proceedings of the National Academy of Sciences of the United States of America. 1989;86:7437-41.
[20] Liesi P, Kauppila T. Induction of Type IV collagen and other basement-membrane associated proteins after spinal cord injury and the adult rat may participate in formation of the glial scar. Exp Neurol. 2002;173:31-45.
[21] Stichel CC, Hermanns S, Luhmann HJ, Lausberg F, Niermann H, D'Urso D, et al. Inhibition of collagen IV deposition promotes regeneration of injured CNS axons. The European journal of neuroscience. 1999;11:632-46.
[22] Lucas SM, Rothwell NJ, Gibson RM. The role of inflammation in CNS injury and disease. British journal of pharmacology. 2006;147 Suppl 1:S232-40.
[23] Amor S, Peferoen LA, Vogel DY, Breur M, van der Valk P, Baker D, et al. Inflammation in neurodegenerative diseases--an update. Immunology. 2014;142:151-66.

[24] Wang D, Fawcett J. The perineuronal net and the control of CNS plasticity. Cell and tissue research. 2012;349:147-60.
[25] Mohan H, Krumbholz M, Sharma R, Eisele S, Junker A, Sixt M, et al. Extracellular matrix in multiple sclerosis lesions: Fibrillar collagens, biglycan and decorin are upregulated and associated with infiltrating immune cells. Brain pathology. 2010;20:966-75.
[26] S. RYC. Degeneration and regeneration of the nervous system: Oxford University Press; 1928.
[27] Popovich PG, Longbrake EE. Can the immune system be harnessed to repair the CNS? Nature. 2008;9.
[28] Deng LX, Walker C, Xu XM. Schwann cell transplantation and descending propriospinal regeneration after spinal cord injury. Brain research. 2014.
[29] Black JA, Waxman SG, Smith KJ. Remyelination of dorsal column axons by endogenous Schwann cells restores the normal pattern of Nav1.6 and Kv1.2 at nodes of Ranvier. Brain : a journal of neurology. 2006;129:1319-29.
[30] Honmou O, Felts PA, Waxman SG, Kocsis JD. Restoration of normal conduction properties in demyelinated spinal cord axons in the adult rat by transplantation of exogenous Schwann cells. The Journal of neuroscience : the official journal of the Society for Neuroscience. 1996;16:3199-208.
[31] Deng LX, Hu J, Liu N, Wang X, Smith GM, Wen X, et al. GDNF modifies reactive astrogliosis allowing robust axonal regeneration through Schwann cell-seeded guidance channels after spinal cord injury. Exp Neurol. 2011;229:238-50.
[32] Wiliams RR, Bunge MB. Schwann cell transplantation: a repair strategy for spinal cord injury? Progress in brain research. 2012;201:295-312.
[33] Mannoji C, Koda M, Kamiya K, Dezawa M, Hashimoto M, Furuya T, et al. Transplantation of human bone marrow stromal cell-derived neuroregenrative cells promotes functional recovery after spinal cord injury in mice. Acta neurobiologiae experimentalis. 2014;74:479-88.
[34] Bonner JF, Steward O. Repair of spinal cord injury with neuronal relays: From fetal grafts to neural stem cells. Brain research. 2015.
[35] Cusimano M, Biziato D, Brambilla E, Donega M, Alfaro-Cervello C, Snider S, et al. Transplanted neural stem/precursor cells instruct phagocytes and reduce secondary tissue damage in the injured spinal cord. Brain : a journal of neurology. 2012;135:447-60.
[36] Yui S, Fujita N, Chung CS, Morita M, Nishimura R. Olfactory ensheathing cells (OECs) degrade neurocan in injured spinal cord by secreting matrix metalloproteinase-2 in a rat contusion model. The Japanese journal of veterinary research. 2014;62:151-62.
[37] Liu J, Chen P, Wang Q, Chen Y, Yu H, Ma J, et al. Meta analysis of olfactory ensheathing cell transplantation promoting functional recovery of motor nerves in rats with complete spinal cord transection. Neural regeneration research. 2014;9:1850-8.
[38] Rapalino O, Lazarov-Spiegler O, Agranov E, Velan GJ, Yoles E, Fraidakis M, et al. Implantation of stimulated homologous macrophages results in partial recovery of paraplegic rats. Nat Med. 1998;4:814-21.
[39] Popovich PG, Guan Z, Wei P, Huitinga I, van Rooijen N, Stokes BT. Depletion of hematogenous macrophages promotes partial hindlimb recovery and neuroanatomical repair after experimental spinal cord injury. Exp Neurol. 1999;158:351-65.
[40] Yamada H, Ito D, Oki Y, Kitagawa M, Matsumoto T, Watari T, et al. Transplantation of mature adipocyte-derived dedifferentiated fat cells promotes locomotor functional recovery by remyelination and glial scar reduction after spinal cord injury in mice. Biochemical and biophysical research communications. 2014;454:341-6.
[41] Kim KS, Lee HJ, An J, Kim YB, Ra JC, Lim I, et al. Transplantation of Human Adipose Tissue-Derived Stem Cells Delays Clinical Onset and Prolongs Life Span in ALS Mouse Model. Cell transplantation. 2014;23:1585-97.
[42] Romanyuk N, Amemori T, Turnovcova K, Prochazka P, Onteniente B, Sykova E, et al. Beneficial effect of human induced pluripotent stem cell-derived neural precursors in spinal cord injury repair. Cell transplantation. 2014.

[43] Kondo T, Funayama M, Tsukita K, Hotta A, Yasuda A, Nori S, et al. Focal transplantation of human iPSC-derived glial-rich neural progenitors improves lifespan of ALS mice. Stem cell reports. 2014;3:242-9.
[44] Lee DH, Rotger C, Appeldoorn CC, Reijerkerk A, Gladdines W, Gaillard PJ, et al. Glutathione PEGylated liposomal methylprednisolone (2B3-201) attenuates CNS inflammation and degeneration in murine myelin oligodendrocyte glycoprotein induced experimental autoimmune encephalomyelitis. Journal of neuroimmunology. 2014;274:96-101.
[45] Alibai E, Zand F, Rahimi A, Rezaianzadeh A. Erythropoietin plus methylprednisolone or methylprednisolone in the treatment of acute spinal cord injury: a preliminary report. Acta medica Iranica. 2014;52:275-9.
[46] Streijger F, Lee JH, Duncan GJ, Ng MT, Assinck P, Bhatnagar T, et al. Combinatorial treatment of acute spinal cord injury with ghrelin, ibuprofen, C16, and ketogenic diet does not result in improved histologic or functional outcome. Journal of neuroscience research. 2014;92:870-83.
[47] Saxena T, Loomis KH, Pai BS, Karumbaiah L, Gaupp E, Patil K, et al. Nanocarrier Mediated Inhibition of Macrophage Migration Inhibitory Factor Attenuates Secondary Injury after Spinal Cord Injury. ACS nano. 2015.
[48] Bar-Or A, Vollmer T, Antel J, Arnold DL, Bodner CA, Campagnolo D, et al. Induction of antigen-specific tolerance in multiple sclerosis after immunization with DNA encoding myelin basic protein in a randomized, placebo-controlled phase 1/2 trial. Archives of neurology. 2007;64:1407-15.
[49] Bregman BS, Kunkel-Bagden E, Schnell L, Dai HN, Gao D, Schwab ME. Recovery from spinal cord injury mediated by antibodies to neurite growth inhibitors. Nature. 1995;378:498-501.
[50] Schnell L, Schwab ME. Axonal regeneration in the rat spinal cord produced by an antibody against myelin-associated neurite growth inhibitors. Nature. 1990;343:269-72.
[51] Wei YT, He Y, Xu CL, Wang Y, Liu BF, Wang XM, et al. Hyaluronic acid hydrogel modified with nogo-66 receptor antibody and poly-L-lysine to promote axon regrowth after spinal cord injury. Journal of biomedical materials research Part B, Applied biomaterials. 2010;95:110-7.
[52] Sloane JA, Batt C, Ma Y, Harris ZM, Trapp B, Vartanian T. Hyaluronan blocks oligodendrocyte progenitor maturation and remyelination through TLR2. Proceedings of the National Academy of Sciences of the United States of America. 2010;107:11555-60.
[53] Back SA, Tuohy TM, Chen H, Wallingford N, Craig A, Struve J, et al. Hyaluronan accumulates in demyelinated lesions and inhibits oligodendrocyte progenitor maturation. Nat Med. 2005;11:966-72.
[54] Steinmetz MP, Horn KP, Tom VJ, Miller JH, Busch SA, Nair D, et al. Chronic enhancement of the intrinsic growth capacity of sensory neurons combined with the degradation of inhibitory proteoglycans allows functional regeneration of sensory axons through the dorsal root entry zone in the mammalian spinal cord. The Journal of neuroscience : the official journal of the Society for Neuroscience. 2005;25:8066-76.
[55] Bradbury EJ, Moon LD, Popat RJ, King VR, Bennett GS, Patel PN, et al. Chondroitinase ABC promotes functional recovery after spinal cord injury. Nature. 2002;416:636-40.
[56] Caggiano AO, Zimber MP, Ganguly A, Blight AR, Gruskin EA. Chondroitinase ABCI improves locomotion and bladder function following contusion injury of the rat spinal cord. Journal of neurotrauma. 2005;22:226-39.
[57] Saal KA, Koch JC, Tatenhorst L, Szego EM, Ribas VT, Michel U, et al. AAV.shRNA-mediated downregulation of ROCK2 attenuates degeneration of dopaminergic neurons in toxin-induced models of Parkinson's disease in vitro and in vivo. Neurobiology of disease. 2015;73:150-62.
[58] Zhao YF, Zhang X, Ding ZB, Yang XW, Zhang H, Yu JZ, et al. The Therapeutic Potential of Rho Kinase Inhibitor Fasudil Derivative FaD-1 in Experimental Autoimmune Encephalomyelitis. Journal of molecular neuroscience : MN. 2014.

[59] Gu H, Yu SP, Gutekunst CA, Gross RE, Wei L. Inhibition of the Rho signaling pathway improves neurite outgrowth and neuronal differentiation of mouse neural stem cells. International journal of physiology, pathophysiology and pharmacology. 2013;5:11-20.
[60] Paintlia AS, Paintlia MK, Hollis BW, Singh AK, Singh I. Interference with RhoA-ROCK signaling mechanism in autoreactive CD4+ T cells enhances the bioavailability of 1,25-dihydroxyvitamin D3 in experimental autoimmune encephalomyelitis. The American journal of pathology. 2012;181:993-1006.
[61] Fujita Y, Yamashita T. Axon growth inhibition by RhoA/ROCK in the central nervous system. Frontiers in neuroscience. 2014;8:338.
[62] Zhong J, Zou H. BMP signaling in axon regeneration. Current opinion in neurobiology. 2014;27:127-34.
[63] Walker CL, Liu NK, Xu XM. PTEN/PI3K and MAPK signaling in protection and pathology following CNS injuries. Frontiers in biology. 2013;8.
[64] Jimenez Hamann MC, Tator CH, Shoichet MS. Injectable intrathecal delivery system for localized administration of EGF and FGF-2 to the injured rat spinal cord. Exp Neurol. 2005;194:106-19.
[65] Pires LR, Guarino V, Oliveira MJ, Ribeiro CC, Barbosa MA, Ambrosio L, et al. Ibuprofen-loaded poly(trimethylene carbonate-co-ε-caprolactone) electrospun fibres for nerve regeneration. J Tissues Eng Regen Med. 2013;16.
[66] Chan CC. Inflammation: beneficial or detrimental after spinal cord injury? Recent patents on CNS drug discovery. 2008;3:189-99.
[67] Erlandsson A, Lin CH, Yu F, Morshead CM. Immunosuppression promotes endogenous neural stem and progenitor cell migration and tissue regeneration after ischemic injury. Exp Neurol. 2011;230:48-57.
[68] Popa-Wagner A, Stocker K, Balseanu AT, Rogalewski A, Diederich K, Minnerup J, et al. Effects of granulocyte-colony stimulating factor after stroke in aged rats. Stroke; a journal of cerebral circulation. 2010;41:1027-31.
[69] Ohab JJ, Fleming S, Blesch A, Carmichael ST. A neurovascular niche for neurogenesis after stroke. The Journal of neuroscience : the official journal of the Society for Neuroscience. 2006;26:13007-16.

“As pessoas estão a desabituar-se de pensar;

e quando chegam a conclusões diferentes das

da maioria, acham que se enganaram.”

(José António Saraiva)

CHAPTER II

Mechanotransduction: exploring new therapeutic avenues in CNS pathology

D. N. Rocha[1,2,3], J. B. Relvas[2,4,5], MJ Oliveira[1,2] and A. P. Pêgo[1,2,3,5]

(1)INEB – Instituto de Engenharia Biomédica, Universidade do Porto, Porto, Portugal; (2) i3S – Instituto de Investigação e Inovação em Saúde, Universidade do Porto, Porto, Portugal; (3) FEUP – Faculdade de Engenharia da Universidade do Porto, Porto, Portugal; (4) IBMC – Instituto de Biologia Celular e Molecular da Universidade do Porto, Porto, Portugal; (5) ICBAS – Instituto de Ciências Biomédicas Abel Salazar, Universidade do Porto, Porto, Portugal

ABSTRACT

Cells within tissues are continuously exposed to physical forces and the central nervous system (CNS) is no exception. Cells dynamically adapt their behavior and remodel the surrounding environment in response to force. The importance of mechanotrasduction in the CNS is illustrated by exploring its role in CNS pathology development and progression. The cross-talk between the biochemical and biophysical components of the extracellular matrix are here explored, considering the recent explosion of literature demonstrating the powerful influence of biophysical stimuli like density, rigidity and geometry of the ECM on cell behavior. This review aims at integrating mechanical properties into our understanding of the molecular basis of CNS disease. Signaling pathways that mediate mechanotransduction events, like integrin and Rho/ROCK signaling pathways are reviewed. Analysis of CNS pathologies in this context has revealed that a wide range of neurological diseases share as hallmark alterations of the tissue mechanical properties. Therefore, it is our belief that the understanding of CNS mechanotransduction pathways may lead to development of improved medical devices and diagnostic methods as well as new therapeutic targets and strategies for CNS repair.

Contents

1. Introduction 26
2. Mechanotransduction in CNS pathology 27
2.1. Headache 28
2.2. Eye disorders 29
2.3. Neurodegenerative disorders 31
2.4. Traumatic CNS injury 34
2.5. Cancer 36
3. Mechanotransduction and CNS regeneration 39
4. The extracellular matrix role in the process of mechanotransduction 42
4.1. Integrins 43
4.2. Rho/ROCK Signaling pathway 45
4.3. Matrix metalloproteinases and ECM remodeling 47
5. Exploring mechanotransduction in the context of CNS diseases: current clinical strategies and future perspectives 48

1. Introduction

Mechanotransduction is the process by which a cell translates mechanical stimulus into biochemical signals. The transduced signals can vary in properties. Being electrical, as the ones involved in the depolarization of cellular membranes, chemical, as in producing a second messenger, or transcriptional, as in the activation of gene expression, among others. Mechanotransduction is ubiquitously present in several taxonomic domains such as *Eubacteria, Archaea* and *Eukarya* [1], suggesting an early evolutionary occurrence of mechanotransducers, which advocates the important role of mechanotransduction in living organisms.

The concept and the importance of mechanotransduction have been initially identified on cells that typically experience mechanical stimuli *in vivo*, like mesenchymal and epithelial cells, as well as on sensory cells, like the inner ear hair cells [2, 3]. Today it is known that mechanical forces influence the growth, shape and behavior of nearly every cell, tissue and organ of the human body. Cells can sense and respond to a wide range of external chemical and physical signals and, consequently, change its morphology, dynamics and

behavior. As such, mechanotransduction has become a topic of increasing awareness and consequently scientific interest in many fields of research. A vast body of research was mounted up to illustrate that forces are ubiquitous *in vivo* and that these can directly impact cell function.

Initial studies of mechanotransduction in the nervous system were performed with sensory cells – the somatosensory neurons. In mammals, detection of mechanical forces by the somatosensory system is performed by primary afferent neurons, which can detect a wide range of mechanical stimuli [1]. Psycho-physical techniques have established in 1882 that sensory spots, defined as regions of low threshold to a given kind of stimulus, existed in the human skin. Cutaneous somatosensory receptors detect a wide range of mechanical stimuli, including light brush of the skin, texture, vibration, touch and noxious pressure [4].

One of the main challenges in the study of sensory systems is to discover the basis of the transduction process. Rhodopsin, the light-transducing molecule, has been known for 130 years [5], olfactory receptors were discovered 20 years ago [6], but molecules that transduce physical forces as osmotic force, touch, vibration and texture, have been more difficult to identify. Corey and Hudspeth [7] have shown that neurosensory transduction is extremely rapid. Using hair cells they observed that the movement of a hair bundle produced an electrical response within 40 μs. Neurosensory mechanotransduction has been recently revised (see reference [4] for additional information) and will not be further explored.

This review will focus on the role of mechanical sensing in the central nervous system (CNS) in the context of disease, particularly highlighting the contribution of the mechanical properties of the extracellular matrix (ECM) to this process. Although there are some hints on how forces impact these regulatory functions, clarifying these mechanisms remains crucial for a better understanding of neuromechanics. This could thus lead to alternative prognostic and therapeutic options that can in the future improve tissue repair and regeneration.

2. Mechanotransduction in CNS pathology

Tissue architecture reflects a balance in which cells adapt their cytoskeletal tension to match the forces generated by neighboring cells and the surrounding ECM, and the disruption of this equilibrium can contribute to a variety of diseases [8]. Many times it is unclear whether mechanical changes at the tissue level are an early cause of the disease,

a mechanism of progression or a late symptom. One of the first diseases to be associated with biomechanics and mechanotransduction was atherosclerosis, for which it has been shown that low-oscillatory shear stress correlates with sites of atherosclerotic plaques [9, 10]. Since then many other diseases have been correlated with mechanotransduction alterations (Table 1).

CNS tissues are among the softest tissues in the body and due to their mechanical fragility, these are particularly susceptible to mechanical damage caused by trauma. As such, brain and spinal cord are protected by stronger structures such as the pia mater, the dura mater, the skull and vertebras. In some neurodegenerative diseases a change in stiffness of the affected tissues is partly accountable for the cell's physiological functions loss [11]. Recent studies on the mechanical properties of the glia have consistently demonstrated a decreased CNS stiffness tissue either as a result of CNS disorders [12-15] or of traumatic injuries [16]. Distinct CNS disorders described to be intimately related to alteration of mechanotransduction properties will be addressed in the following sections.

2.1. Headache

Pain can be evoked by mechanical stimuli and inflammatory conditions [17]. As such, increased mechanosensitivity has been considered to play a role in the pathophysiology of headache and of neuropathic pain [17, 18]. Migraine headaches, which are the most common type of primary headaches, are described as neurovascular disorders affecting up to 15-20% of the world population [19]. Migraine is characterized by attacks of moderate to severe headache that last from 4 to 72 hours, often unilateral, pulsating and associated with photophobia/phonophobia and/or nausea/vomiting [19], and one-third of the patients have associated symptoms of neurological aura [20].

Several studies have found elevated hypertension and dyslipidemia in migraineurs. [21-23]. Moreover, patients with sexual headache were found to show an abnormal increase of systemic blood pressure during exercise [24]. These studies suggest a role of vasodilation of cerebral and/or meningeal blood vessels on migraine, which is consistent with the role of mechanosensitivity. Calcitonin-related proteins, known to be coupled to protein kinase C (PKC) pathway, have been shown to play a role in this mechanical hypersensitivity in migraine [17, 18].

There has been an extensive debate on whether headaches have a vascular or neurogenic origin [25]. Nonetheless, headache is also a common symptom after lumbar

puncture, which has been associated with the intracranial hypotension due to cerebrospinal fluid (CSF) leakage [26]. Therefore, the genesis of this disorder is believed to be in the CNS and not a vascular cause, as vascular changes appear to be a consequence of the neural mechanisms at work, and not the initiator [27, 28]. In fact, a population of neurons suspected of transducing neuronal signals into vasomotor responses has been identified in the cerebral cortex [19]. These findings suggest that neurons send projections towards blood vessels in specific brain regions and that blood vessels have the ability to respond to changes in the level of neurotransmitters by modifying their diameters and consequently local blood flow.

These results hint a central role of the interaction between the CNS and the surrounding blood vessels, with mechanotransduction being a mechanism of disorder progression and, as such, a potential therapeutic target. The signaling pathways involved in this process are further explored in section 4 of this review.

2.2. Eye disorders

Changes in topography and/or stiffness of eye structures have also been correlated with pathologic conditions [29]. The optic nerve head constitutes an interesting biomechanical structure with a complex load-bearing tissue architecture, the *lamina cribrosa*, which is subjected to intraocular pressure stress [29, 30] (Figure 1). The biomechanical properties of the sclera are also extremely important as the sclera plays a pivotal role in controlling eye shape during events that promote eye deformation such as movement, accommodation and remodeling. In fact, the ECM and cellular constituents of the sclera contribute to the biomechanical environment that enables the sclera to accomplish these requirements.

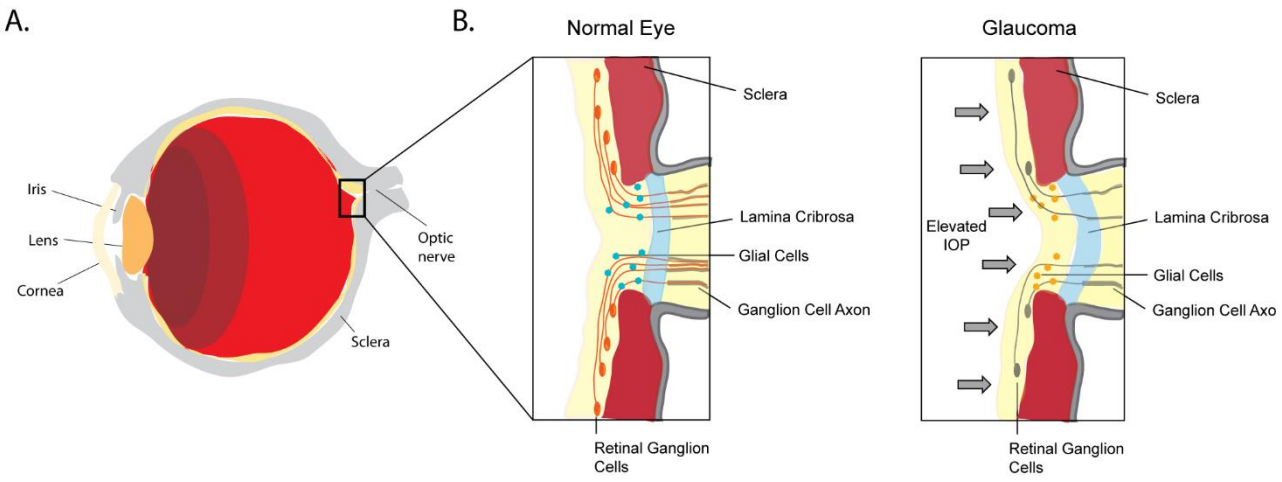

Figure 1 – Scheme of an eye **A.** Major anatomical structure and organization. **B.** Enlarged section of the lamina cribrosa and optic nerve representation of tissue deformation in response to increased intraocular pressure (IOP) representative of glaucomatous optic neuropathy.

Strouthidis et al [30] suggested that optic nerve biomechanics is the “link” by which intraocular pressure (IOP) can affect other factors such as ischemia, inflammation, autoimmunity and glial cell biology. This biomechanical theory may help to explain why some people are predisposed to develop glaucomatous optic neuropathy, independently of their IOP levels, while others are not. Moreover, the increasing predisposition related to ageing may also be explained by changes in biomechanical behavior through alterations of the connective tissue [30]. In glaucomatous optic neuropathy, one of the leading causes of blindness worldwide [31], IOP causes eye tissue stress, deformations and strain, leading eventually to damage and loss of retinal ganglion cell axons [32] (Figure 1). IOP reduction remains the only therapy used to preserve vision and retard glaucomatous progression [33, 34]. This suggests that the biomechanical effects of IOP to the tissues surrounding the optic nerve head are central to disease [35]. Therefore, the correct tuning of optic nerve head mechanics may constitute a potential therapeutic target in glaucomatous optic neuropathy.

Biomechanical properties may also affect ocular growth. Changes in sclera mechanical properties have been documented during development and pathological conditions as the cause of abnormal ocular growth such as myopia, where sclera becomes thinner, weaker and more extensible [36, 37]. Mechanical properties of eye structures have also been shown to play an important role on retinal detachment. Chou et al. [38] have developed a mathematical model to investigate the relationship between flows and pressures and

retinal detachment. This study has shown that the destabilization of retinal pigment epithelium (RPE) *per se* is not enough to induce large-scale delamination. Instead, spontaneous uniform tissue separation occurs when RPE pumps fail and the adhesion energy retina-RPE is globally reduced. Furthermore, it has also been suggested that retina elastic modulus is decreased in conditions such as retinal detachment [39]. Observation corroborated by thermodynamic calculations that have shown that supported membranes, like the normal retina, have greater stiffness values than unsupported membranes [40]. Another study from Davis and co-workers [39] has found a significant influence in gene regulation of Muller cells as a function of the stiffness of the substrate. This study emphasizes the role of YAP (Yes-associated protein) and TAZ (transcriptional coactivator with PDZ-binding motif) as important therapeutic targets for retina and optic nerve pathologies. These had previously been identified as nuclear relays of mechanical signals exerted by ECM rigidity and cell shape [41]. Overall, these studies suggest that eye mechanical properties, its mechanotransducers and mechanosensors, are key therapeutic targets in distinct eye pathologies. Nevertheless, although some clinical procedures already exploit mechanical forces like vitrectomies, laser photocoagulation or pneumatic retinopexy, deeper knowledge on the insights of mechanotransduction pathways is needed for further therapeutic developments.

2.3. Neurodegenerative disorders

The incidence of neurodegenerative disorders is increasing in the modern world, particularly within the aged population. So far, our understanding of the nature and origins of these disorders is still limited, as there exist a vast number of neurodegenerative disorders and they are, in general, heterogeneous in nature. Nevertheless, intense efforts are being performed to achieve a better understanding of these conditions.

The Alzheimer's disease is a chronic disorder characterized by cerebrovascular inflammation, accumulation of senile amyloid plaques in the brain and, ultimately, neuronal loss. Concerning mechanotransduction issues Alzheimer's is possibly the most studied neurodegenerative disease, due to its dependency on amyloid fibrils mechanical properties. In fact, the deposition of amyloid fibrils is associated with several other neurodegenerative diseases, as Parkinson disease and in neurodegenerative processes accompanying type-2 diabetes. Amyloid fibrils are highly ordered nanoscale assemblies of protein protofibrils composed predominantly of β-sheet structure. These have been found to alter cell membrane properties, such as fluidity, and molecular architecture,

leading to neurovascular dysfunction and chronic degeneration [42]. Interestingly, amyloid fibrils (Aβ fibers) deposits are correlated with the activation of phospholipase A2 (PLA_2) [43], which is known as a crucial modulator of membrane properties both in health and disease. In Alzheimer's diseased brains membrane reduced fluidity has been directly associated with decreased PLA_2 activity [44, 45]. Amyloid fibrils were shown to be stiffer than cytoskeleton components such as actin filaments, microtubules or intermediate filaments [46]. Recently several authors have been exploring amyloid fibrils mechanical properties, behavior and stability, as the understanding of these features may shed light on the fundamental mechanisms of formation and structure dynamics of these nanostructures. Depending on the peptide length of its monomers, Aβ fibers will present different rupture forces. In fact, Xu et al [47] have stated that longer amyloid fibrils are more stable, which is associated with their mechanical properties, mainly due to their close contact and denser structure, suggesting that size may imply pathological consequences the impact of the pathology can be correlated with the size of the fibrils. Additionally, Paparcone *et al*. [48] have shown that salt bridges contribute to stability, geometry and mechanical behavior of amyloid fibrils. Side chain interactions are described to influence the aggregation rate, as well as the chemistry and the mechanics of these fibrils.

Hattori and coworkers [49] have studied the diffusional properties of the corticospinal tract in patients with Alzheimer's disease, Parkinson disease and idiopathic normal pressure hydrocephalus (iNPH) by diffusion tensor imaging (DTI). DTI early became a popular Magnetic Resonance Imaging (MRI) technique to characterize microstructural changes in neuropathologies, as it enables the characterization of white matter fasciculi in three dimensions (3D). Many CNS pathologies influence tissue composition and architecture and the diffusion of water within these tissues is also altered [50]. iNPH is a rare case of a neurological disorder whose symptoms may be relieved by surgical intervention, which mainly consists on the implantation of a ventriculoperitoneal shunt in order to drain excess cerebrospinal fluid. The success of this interventions was related with mechanical re-ordering of the brain tissue [12] (Figure 2B and C). Patients with iNPH presented higher white matter damage such as myelin loss and ischemia [49]. Additionally, fractional anisotropy values and axial eigenvalues were significantly increased in these patients, suggesting alteration in the microstructure of the corticospinal tract, presumably consequence of the mechanical pressure resulting from ventricular enlargement [49]. This microstructural alterations have been further correlated with tissue's mechanical properties, using magnetic resonance elastography (MRE) [12]. MRE is a non-invasive [13] and reproducible [14] method that allows the evaluation of the mechanical properties of tissues and has recently been applied to assess biomechanical alterations of the living

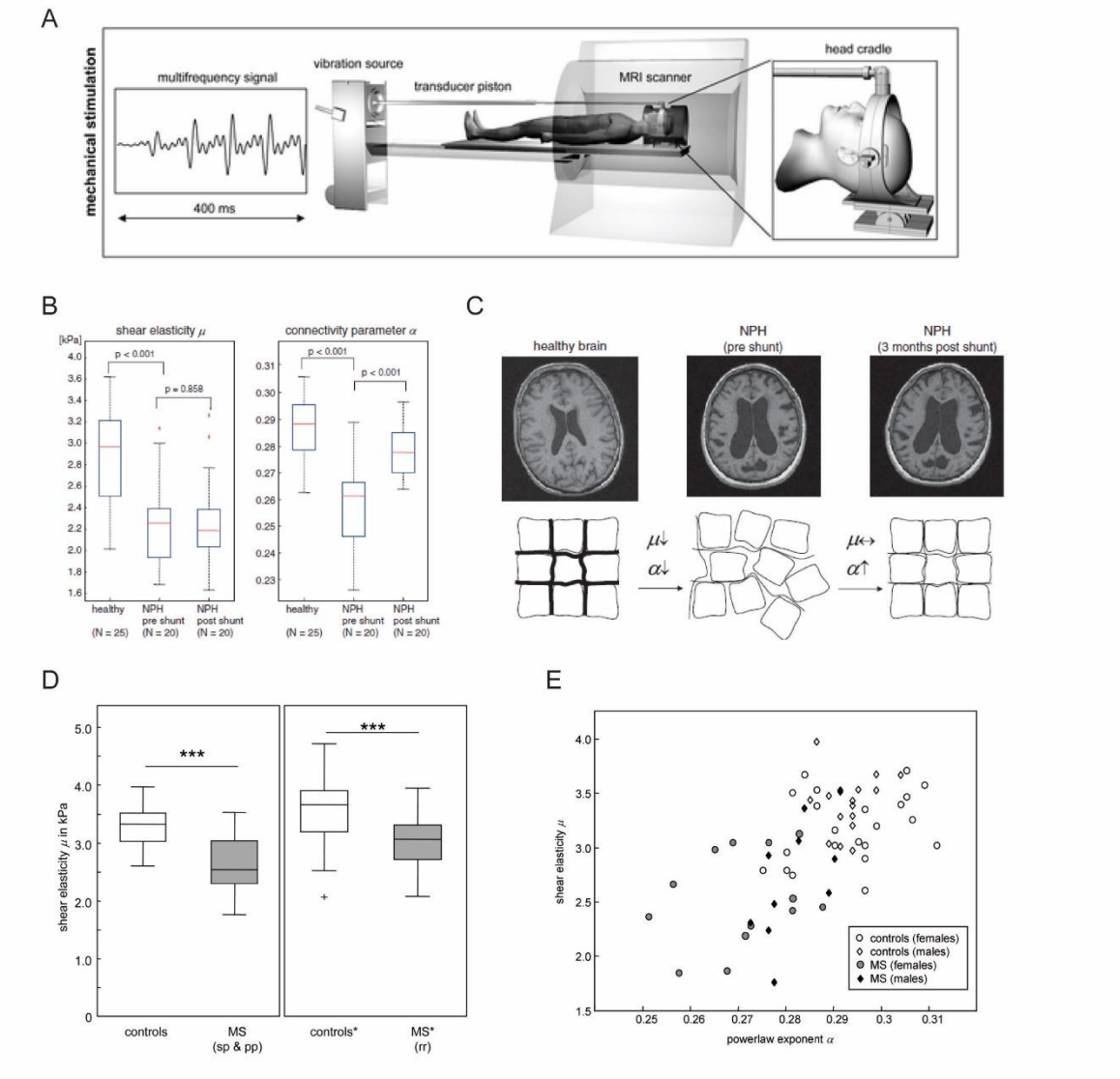

Figure 2 – Mechanical properties in neurodegeneration. **A.** Scheme of cereberal multifrequency MRE. The MRI scanner is combined with a device for acoustical head stimulations comprising a signal generator that produces a multifrequency signal composed from four harmonic frequencies of 25, 37.5, 50 and 62.5 Hz; a loudspeaker to generate acoustic vibrations; an extended piston that transfer the vibrations into the scanner and a head cradle to stimulate head vibrations mainly along the head-feet direction. Reprinted with kind permission from Springer Science and Business Media from Streitberger et al 2012 **B.** Brain viscoelastic properties in healthy volunteers and in NPH before and after surgical intervention. Reprinted with kind permission from Springer Science and Business Media from Freimann et al 2012 **C.** Cereberal MRE of NPH brains reveals a disease related decreased stiffness (μ), which is not recovered after surgical treatment. In contrast α increases after 3 months, to almost symptomatic values suggesting that the topology of the tissue's matrix is reorganized although its strength remains diminished. Reprinted with kind permission from Springer Science and Business Media from Freimann et al 2012 **D.** Reduction of brains elastic properties in healthy volunteers and MS patients. sp- secondary progressive, pp – primary progressive, rr – relapsing remitting. Reprinted with kind permission from Springer Science and Business Media from Streitberger et al 2012 **E.** Viscoleastic constants for prediction of brain pathology. Individual data of shear elasticity and power law exponent of brain of healthy volunteers and MS patients are represented. Reprinted with kind permission from Springer Science and Business Media from Streitberger et al 2012

brain (Fig. 2A). In general, patients with iNPH present lower tissue stiffness values when compared to healthy controls (Figure 2B). Patients with Alzheimer's disease also show significantly softer brain parenchyma than matched controls [14]. Several processes may impact tissue's mechanical properties in Alzheimer's disease but, the knowledge on amyloid fibrils being several orders of magnitude stiffer than neurons and glia [46-48] would, at a first glance, suggest increased stiffness of the patient's brain tissue. Indeed, the decreased tissue stiffness may be a consequence of microstructural events that have destroyed cytoarchitectural integrity such as degradation/alteration of the ECM. Moreover this loss of microstructural integrity, is in agreement with the findings, of diffusion anisotropy studies, of increased brain anisotropy in Alzheimer's patients [49]. Magnetic Ressonance Elastography (MRE) has also been used by several authors to study the biomechanical properties of multiple sclerosis patients' brains [15, 51]. The viscoelasticity and brain parenchymal volume of MS brains were shown to be reduced, both in human subjects and in animal models of MS [15, 51] in comparison with healthy controls (Fig. 2D). Once again, these differences are most certainly due to the loss of the brain's mechanical network geometry as a result of the characteristic MS associated neuroinflammation. Altogether, these data evidence that the above-mentioned pathologic conditions lead to significant changes of tissues' viscoelastic properties. Taking this in consideration, MRE presents great potential as an additional tool to improve diagnostic sensitivity as it provides a noninvasive, quantifiable "palpation" method of the brain (Figure 2E). Biomechanical properties of the brain parenchyma alone may not be enough but if correlated with other disease biomarkers and the clinical expression of the disease, can lead to a better diagnostic method. Nevertheless, the question remains on whether mechanical changes are an early cause of the disease, a mechanism of progression or a late symptom.

2.4. Traumatic CNS injury

Traumatic CNS injury results in disruption of the neural structures, local blood-brain barrier (BBB) disassemble and massive infiltration of immune cells. After the initial mechanical trauma (primary damage), cell damage is triggered and, within hours, the injury site and the surrounding hemorrhagic areas begin to undergo necrosis (secondary damage), recruiting more inflammatory cells and fibroblasts, which actively participate in ECM remodeling. In time a glial scar is formed, enriched in astrocytes, microglia and fibroblasts, as well as cell debris and *de novo* produced ECM deposits. Even though this glial scar

may provide several beneficial functions such as the restoration of the BBB, prevention of a devastating inflammatory response and delimiting cellular degeneration and death, it contributes to the establishment of a physical and chemical barrier to axonal regeneration [52].

Astrocytes, the most abundant cell type in the CNS [53], are the largest fraction of cells recruited to glial scars [11] and reactive astrogliosis one of its major hallmarks. Astrogliosis is commonly characterized by increased expression of glial fibrillary acidic protein (GFAP), hypertrophy, hyperplasia, and increased ECM component production/secretion by astrocytes (particularly chondroitin sulfate proteoglycans (CSPGs) and laminin) [54, 55]. The astrocyte response to CNS injury and disease has been the subject of several studies [54, 55]. Astrocytes naturally form a 3D meshwork/structure that extends throughout the brain which, as suggested by Masthewson and Berry in the 1980s [56], is the ideal morphology for sensing mechanical disturbances in the parenchyma. It is possible that the observed astrocytic accumulation in the scar is, at least in part, the result of their mechanosensitive response. Together with matrix degradation/remodelling and axonal disruption occurring after trauma, it is not surprising that tissue stiffness is altered, since nearly all brain pathologies result in some degree of deformation of the surrounding parenchyma. The ability of astrocytes to respond to mechanical stress could provide a general mechanism by which a variety of insults can be felt and managed in the CNS [57]. Understanding this structure and its mechanism of action could prove to be extremely important for future therapeutic strategies.

As previously mentioned, mechanotransduction events within the CNS have only been the subject of study more recently than in other tissues, probably because CNS tissues are not naturally subjected to intense mechanical stress as other structures in our body. Nevertheless, the spinal cord, like some cranial nerves, consistently experiences some physical stress during routine movements [58]. Schreiber et al have studied the role of glia in CNS tissue and concluded that despite of its individual stiffness, which is lower than neurons, glia significantly contributes to the tissue overall stiffness and strength, potentially by allowing many cells to act together and share the load [58], working somehow as a cellular cross-linkers. So the loss of this glial architecture/geometry may be one of the reasons why CNS stiffness is reduced in CNS injury scenarios. Other authors [53, 59, 60] have also attributed an important mechanical role to glia architecture suggesting that it plays a protective role against excessive tensile stress and strains, in order to limit injury. Intriguingly, *in vitro* data suggests an important role of substrate stiffness on astrocytic development and possibly on reactivity, with astrocytes becoming reactive in stiffer substrates [11, 60, 61]. This does not correlate with the *in vivo* data, where injured CNS

tissue shows decreased stiffness. Nevertheless, these studies were performed in flat substrates and, therefore, the important features of a 3D architecture are not represented. Moreover, after the correlation of CSPGs with inhibition of axonal outgrowth and oligodendrocyte precursor cell (OPC) maturation [62, 63], it has been already established that treatment with chondroitinase ABC (chABC) can tame/revert the inhibitory effects of CSPGs towards neural cells both *in vitro* [61, 64] and *in vivo* [65, 66]. This treatment, performed to digest CSPGs produced in response to injury, attempts to recover the initial ECM environment both chemically and mechanically. These results emphasize the importance of ECM structure and mechanical properties. Overall research has shown that glial cells play a pivotal role both in health and in disease, although initially these were only correlated with pathological states. Nevertheless, even in pathological scenarios these cells play a dual role, as the glial scar represents a physical barrier to regeneration but at the same time is crucial to protect the CNS from further damage when everything else fails. As such, it is important to further focus on glial cell health, as well as its response and behavior in CNS based investigations.

2.5. Cancer

Cancer is a disease characterized by the dysregulation of the cell cycle, particularly of the cell signaling pathways that control cell proliferation and apoptosis. CNS tumors are generally divided into several categories: astrocytomas, gliosarcomas and meningiomas. Gliosarcoma is a rare glioblastoma variant and there is still very little information on the disease. Consequently, it will not be focused here.

Meningiomas are the most common CNS tumors, constituting 25% of all primary intracranial cancers and being more frequent in middle-aged and elderly patients [67]. Most of the meningiomas are slow-growing tumors, which are well-encapsulated and tend to push the adjacent brain parenchyma, rather than infiltrate. During this process, tumor cells alter the surrounding ECM components, therefore, affecting tissue biomechanical properties [68].

Glioblastoma multiforme (GBM), a subtype of astrocytoma, is the most common and most aggressive brain tumor type. These tumors are extremely invasive due to their ability to remodel the surrounding ECM, through mechanisms that seem to involve integrin upregulation [69], MMP mediated proteolysis [70] and *de novo* secretion of ECM proteins by malignant cells [71]. Moreover, cultured GBM cellular activities, such as proliferation,

motility and mechanics were shown to be highly sensitive to changes in ECM stiffness [72, 73]. This knowledge indicates that alterations in tensional homeostasis may play a role in cancer progression. Indeed, mechanical properties of the cellular microenvironment of the brain were shown to fundamentally alter the migration of glioblastoma cells *in vitro* and *in vivo* [74, 75], and the expression of contractility-mediating signaling molecules, including RhoA and RhoB, are thought to correlate with tumor malignancy [76, 77]. Further discussion on the signaling pathways involved in this pathology will be addressed in section 4 of this review.

In all these CNS malignancies individual cells remodel and diffusely invade the surrounding ECM [69, 70], decreasing tissue stiffness [78]. In fact, tissue stiffness has been already exploited to detect cancer, using MRE and sono-elastography [79, 80]. In tumor tissues other than in the CNS, this decrease in stiffness has even been related with cellular malignancy and metastatic potential [81]. Qazi et al [82] have further suggested that the differential invasive potentials of tumors may be explained by mechanotransduction of flow forces, and that fluid shear stress may lower glioma cells motility through modulation of the activation of matrix metalloproteinases (MMPs). Nevertheless, MMP inhibitors have failed clinically in patients with several types of cancer, including glioblastoma [83, 84]. Moreover, there are some preclinical data suggesting that, in some instances, MMP inhibition stimulates disease progression [85]. Since focal adhesions are thought to play a central role in transducing mechanical signals between the cytoskeleton and the external ECM components, focal adhesion proteins have begun to emerge as targets of interest in GBM [8]. Taking this in consideration, Sen and coworkers showed that alpha-actinin isoforms participate in mechanomechanical feedback between glioma cells and the ECM [72]; later, talin-1 was identified as a focal adhesion protein crucial for regulation of glioma cell spreading, motility and adaptation to ECM stiffness [8]. These hypotheses need to be further validated in a 3D environment that presents a more complex combination of mechanical and topological cues.

As in other conditions it is still unknown if the alteration of ECM mechanical properties plays a key role in the establishment of brain tumors or if these can be correlated with tumor aggressiveness, but it is clear that it plays a vital role in tumor progression.

Table 1 – Analysis of several CNS pathologies and their impact in tissue structure.

Disorder	***Tissue Stiffness***	***ECM remodelling***	***Signalling Pathway Involved***	***Possible Therapeutic Target***	***Ref.***
Retinal Detachment	↓	Yes	Hippo pathway EGFR pathway Notch Pathway	RPE pumps	Morante et al Chou t al Dupont et al Sivak et al
Glaucoma		Yes	Hippo pathway	Optic nerve head mechanics	Dupont et al Heijl et al Kass et al Rosario Hernandez et al
Migraine	=	Yes (mild)	PKC pathway MMP activity	CNS-blood vessels crostalk	Goadsby et al Di Castro et al Nassini et al Lakhan et al Martins-Oliveira et al
CNS injury	↓	Yes	PKC pathway Rho/ROCK pathway MAP kinase pathway	BBB permeability	Krizbai et al
			EGFR pathway Rho/ROCK pathway	Glia architecture	Morante etal
			ERK pathway PKC pathway	MMP activity	Hsieh et al
Alzheimer's			Rho/ROCK pathway PKC pathway	CSPGs	Bush et al
		Yes	Rho/ROCK pathway PLA_2 pathway	Aβ fibrils	Moses et al
	↓		Rho-ROCK pathway	ROCK	Read et al Jagielska et al
			ERK pathway PKC pathway	MMP activity	Hsieh et al
Parkinson	↓	Yes	Rho/ROCK pathway	ROCK	Read et al Jagielska et al
			ERK pathway PKC pathway	MMP activity	Hsieh et al
Multiple Sclerosis	↓	Yes	Rho-ROCK pathway	ROCK	Read et al Jagielska et al
			ERK pathway PKC pathway	MMP activity	Hsieh et al
Cancer	↑	Yes	FAK signalling Rho/ROCK signaling	Talin-1 MMP activity	Sen et al Ulrich et al 2009

3. Mechanotransduction and CNS regeneration

Ramon e Cajal have stated that the CNS regenerative capacity is limited [86] and today, many decades later, this statement continues to be true. As previously discussed, alterations in the mechanical stimuli that the CNS cells are subjected to may be the trigger to pathological states or part of the response to an insult. But mechanotransduction can have a dual role in the process of CNS regeneration. If on the one hand CNS regeneration can be frustrated due to glial scar, to be successful it is believed that it will be dependent on physical cues.

Paul Weiss and co-workers [87] acquired early evidence that topographical features of the substrate might guide axons. More specifically, they noticed that the trajectory of axons aligned parallel to grooves generated by brushed clotting blood onto a glass coverslip. Recent studies have clarified the role of several physical parameters involved in the regenerative processes of CNS cells by carefully engineering substrates in which one is bale to vary rigidity and topography, while maintaining a constant chemical composition. Several authors have addressed the influence of mechanical properties on neural stem cell (NSC) differentiation, with potential impact both at the level of processes that can happen in the NSC niche or in the context of regenerative cell based therapies. These studies suggest a direct role of stiffness on the regulation of NSC lineage commitment [88, 89] as NSC can generate the three main cell types of the CNS (neurons, oligodendrocytes and astrocytes), or a role on differently favoring cell survival [89]. Regarding neuronal differentiation the majority of the studies had their focus on finding optimal neuronal differentiation stiffness conditions. The determined values were found to be within the elastic modulus of native brain tissue (E = 100 – 1000 Pa) [90], one of softest tissues in the body. A study with CNS cell lines using photocrosslinkable methacrylate-chitosan hydrogels with incorporated laminin showed different optimum stiffness values for neural proliferation (3.5 kPa) and neuronal differentiation (<1 kPa) [90]. Interestingly, oligodendrocyte and astrocyte differentiation ability were closely related to neural proliferation rates, as well as the presence of neurons. A myelinating population was found in all tested stiffness conditions. Concerning astrocytic differentiation contradictory results can be found in the literature. Jiang and co-workers [60] investigated cellular response to substrate compliance using polyacrylamide gels, suggesting an optimal range of stiffness values for immature astrocytes (vimentin but not GFAP expressing cells), and their proliferative or differentiating status. Authors state that astrocytes preferentially adhered to stiffer substrates (>300 Pa). On the other hand, the response of mature astrocytes (GFAP expressing cells) was different, with higher cell adhesion being observed on gels

of intermediate stiffness. Another study [11] has shown that mature astrocytes adhere to both soft (100 Pa) and stiff (10 kPa) polyacrylamide gels but with morphological differences, which is relevant in CNS disorder scenarios where tissue mechanical properties are altered. These studies report that astrocytes spread more and acquire more complex morphologies on stiff substrates, much like the morphology seen in tissue culture polystyrene and glass. Nevertheless, astrocytes cultured on soft substrates resembled the star-like shape of astrocytes *in vivo*. More recently, we have correlated substrate stiffness with astrocyte reactivity [61]. Astrocytes cultured within 3D alginate based hydrogels were shown to acquire a reactive phenotype when cultured within stiffer gels.

The relationship between astrocytes and neurons is known to be important *in vivo,* though for many years astrocyte's main function was believed to be serve simply as an inert support for neurons. Lu *et al* [53] have studied the viscoelastic properties of CNS individual glial cells and neurons. These have analyzed intact rodent and bovine hippocampal and retina tissue samples using a scanning force microscope and a rheometer. CNS tissues were found to display the rheological characteristics of elastic solids. Moreover, astrocytes were determined to be about twice as soft as neurons, suggesting that glial cells act as soft compliant substrates surrounding neurons, instead of a rigid scaffold, which mechanically supports them. This implies a glial cell role closer to the original idea of Rudolph Virchow, who considered it to act as "brain glue" [91]. Glial cells have further shown a viscoelastic behavior, much like shock absorbers, when subjected to deformation. Interestingly, this data is in line with reports showing that neuron outgrowth is favored by soft substrates [60, 92]. Also in agreement with these results, Georges *et al* [59] and Jiang *et al* [60] have demonstrated that while in the presence of astrocytes, neuron growth was independent of the substrate (polyacrylamide gel) stiffness. The same behavior was not seen when neurons were cultured alone, being able to extend neurites only on soft substrates. Therefore, a hard substrate may not constitute a problem for neuronal growth, as long as it is covered with a "cushioning" astrocytic layer. Here it is possible to conclude on the surface nanomechanical properties importance in relation to the bulk properties. Cells sense the microenvironment nanomechanical properties very closely and respond to them in a very effective way [92], as such neurons were able to sense the astrocytic layer overcoming the impact of the stiff substrate underneath.

During development, after neurons have reached their final destination and astrocytes have formed a 3D surrounding network, OPCs migrate and start to establish contact with axons. Myelination and its regenerative counterpart remyelination represent one of the most complex cell–cell interactions in the CNS [93]. Kippert *et al* [94] have shown that a particular balance of matrix rigidity and intracellular contractile forces, mediated by the

oligodendrocyte actomyosin cytoskeleton, is required for successful myelination and remyelination to occur. Moreover, Jagielska and co-workers [93] evidenced that OPCs can differentiate on a wide range of substrate stiffness (0,1 to 70 kPa), which includes the range of stiffness found in the human brain (0,1 – 1 kPa). Furthermore, Leipzig and Schoichet [90] have observed that maturation and myelination ability were higher at <1 kPa gels while OPC survival was found to be optimum between 0,7 – 1 kPa. This is consistent with the fact that in development OPCs need to migrate over a dense network of neurons and glia being subjected to a broad range of mechanical forces.

Altogether these studies suggest that as for other tissues, CNS cellular morphology is determined by a precisely regulated interplay of intracellular contractile forces and extracellular attachment. Neurons, which are generated first at the embryonic stage, prefer relatively soft surfaces for elaboration and branching of axons and dendrites. These softer substrates possibly correspond to the environmental conditions at the time of initial path-finding of neuronal processes [95]. Astrocytes grow on intermediate substrates while, myelin-forming oligodendrocytes that develop later, already at the newborn stage, myelinate best on more rigid surfaces. In figure 3 we present a schematic summary of the information here discussed, in terms of the characteristics of the tissue mechanical properties and its impact on cell behavior.

Microglial cells, key players in CNS immune response, were shown to be also influenced by substrate features. Bollmann et al have shown that although microglial cells preferentially migrate towards stiffer substrates, they have the ability to adapt their area, morphology and cytoskeleton according to the stiffness of the surrounding environment [96]. Additionally, we have shown that microglial cells presented a round shape when cultured on flat substrates, while cells cultured on fibrous substrates have shown elongated processes, responding with altered cytokine profile and myelin phagocytosis capacity to these physical cues [97].

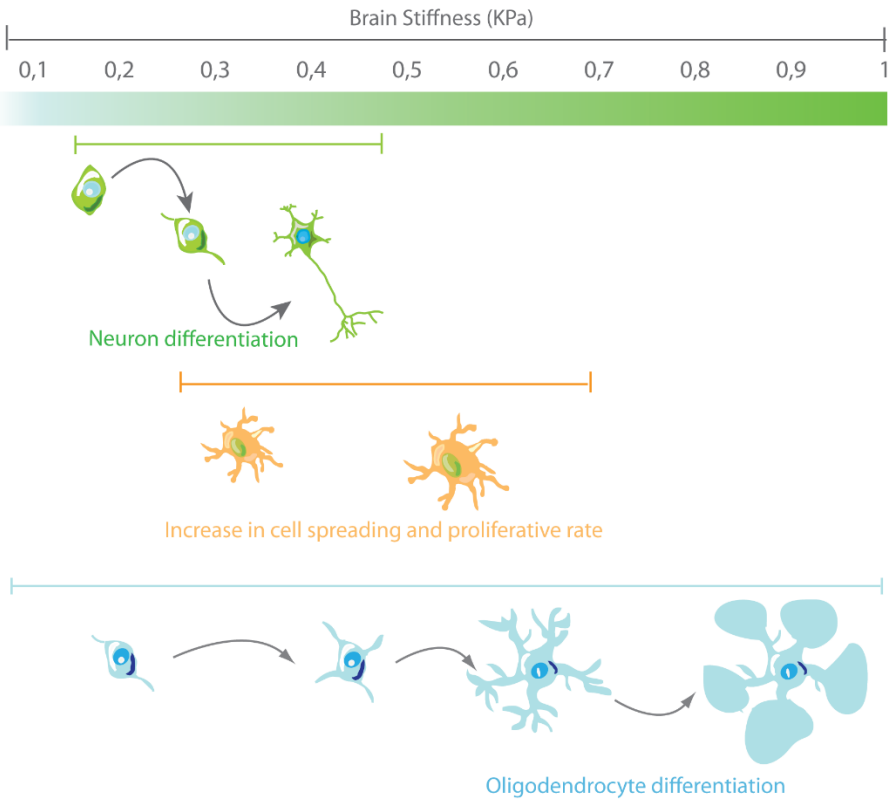

Figure 3 - CNS cell differentiation during development as a function of tissue stiffness.

4. The extracellular matrix role in the process of mechanotransduction

The ECM represents the secreted product of the CNS resident cells, serving a variety of cellular functions (survival, differentiation, proliferation, migration, proteolysis), regulating synaptic transmission and plasticity, and constituting a barrier against metastatic invasive cancer cells [98]. Initially considered as an inert meshwork providing just physical support to cells, it has now been demonstrated its role as an active cell signaling modulator, working as a reservoir of enzymes, growth factors and of immunomodulatory cytokines and chemokines. Moreover, the architecture of the ECM may direct cell fate by providing structural and mechanical cues, which can affect cell transcriptional events and associated cell phenotype and functions [99] . ECM is known to influence cell differentiation, proliferation, survival, migration and invasion by both biochemical interactions (directly through cell adhesion, indirectly through presentation of arrested signaling molecules) and mechanical cues (stiffness, deformability) [99-101]. It is thought to play a vital role in maintenance of the normal tissue microenvironment and its misregulation leads to

pathological conditions such as fibrosis, neuroinflammation, demyelination and cancer invasion [102-106]. With the exception of the meninges, vasculature and BBB, the ECM in the CNS has particular features as the proportion of fibrillar collagens and fibronectin is different than the one typically found in the ECM of other tissues. The CNS ECM is richer in adhesive glycoproteins and proteoglycans. Some matrix components such as fibronectin, collagen type IV, laminin and CSPGs are prominent and of known relevance to CNS plasticity and repair [107]. Nevertheless, the role of ECM components on mechanotransduction in this system is still poorly understood. Considering the large number of signaling receptors and mechanosensory motifs found in CNS cell surfaces, there are several potential pathways and engineering paradigms by which ECM mechanical signals could be transduced into biochemical signals [101, 108]. Among these, integrins have been considered as the most plausible candidates for mechanosensors since they physically connect the ECM and the cytoskeleton, while acting as a signal transducer across cell membranes [109].

4.1. Integrins

A growing body of evidence now suggests that the essential link between the mechanical properties of the extracellular environment and cellular decision-making are mechanotransductory processes at integrin-based cell-matrix contacts (Figure 4). Many of the generated forces concentrate at cell-ECM adhesion and at cell–cell adhesion sites. Consequently, mechanotransduction - transformation of physical stimuli into intracellular biochemical signaling - is thought to occur within the multi-protein complexes of these adhesion sites. Mammalian cells usually co-express several integrins, which recognize distinct ECM components by binding specific amino-acid residues, such as the Arg-Gly-Asp (RGD) motif present in fibronectin, laminin or vitronectin [110].

At the cell surface, integrins of focal adhesion complexes sense and respond to variations in force transmission in order to adapt cell-matrix adhesion to the ECM composition and properties [111]. The formation of integrins–ECM complexes promotes the integrin cytoplasmic domain to interact with the cytoskeleton and other focal adhesion proteins, such as paxillin, talin, vinculin, and F-actin, as well as the formation of stress fibers [112]. ECM components, which interact with transmembrane receptors of the integrin family, are known to trigger, upon mechanical stimuli, a number of intracellular signaling cascades initiated by the focal adhesion kinase (FAK) [111]. The intimate contact between proteins of these adhesive structures and the actin/tubulin network induces profound alterations at

the level of cell cytoskeleton organization, leading to pronounced cell morphology modifications. It has been observed that the application of force, using latex beads, on integrin-based contacts reinforced adhesive sites and mechanotransduction [113]. Later it has been shown that force exerted externally by a micropipette leads to growth of those focal adhesions which are tensed [114, 115]. There is some evidence that other adhesion structures, such as podosomes and fibrillar adhesions, which also connect ECM proteins to the actin cytoskeleton, can also participate in mechanotransduction [116], but these have not yet been thoroughly studied in the context of mechanotransduction.

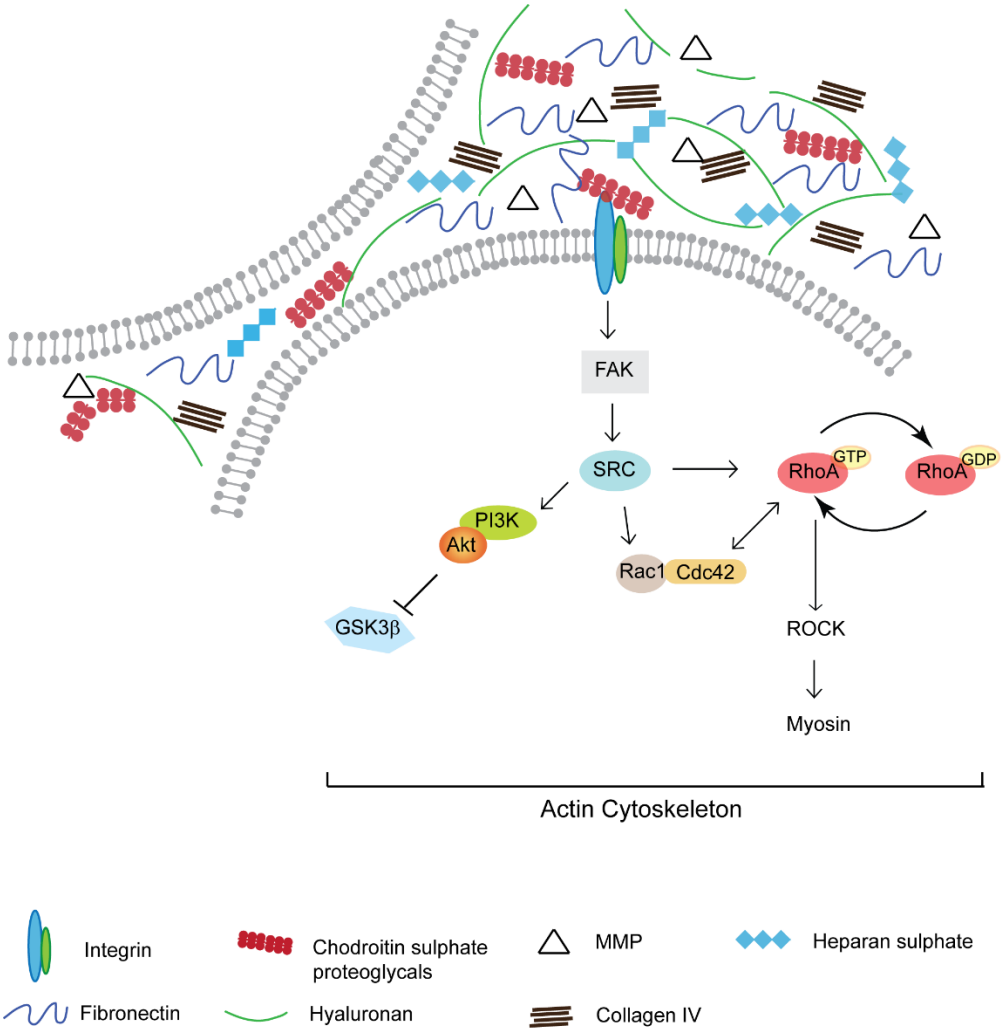

Figure 4 – Schematic representation of ECM biophysical dynamics via integrins.

FAK expression has been described in neurons [117-119] and in oligodendrocytes [120, 121]. FAK activity is known to be required for early events of cell adhesion in neuronal growth cones [122], which sense guidance cues and mechanically pull the axon forward.

During this process, novel adhesion complexes are established at the cell migratory front, while the cell cytoskeleton restructures leading to cell body contraction, old adhesion complexes are then lost and the cell moves forward, establishing novel ECM adhesion contacts at the rear [123]. Therefore, FAK is simultaneously implicated in both adhesion complexes assembly and disassembly. Similarly, the guidance of growth cones is a multistep process that involves adhesion, assembly and disassembly. Moore et al [124] have studied the physical interactions of growth cones with their guidance cues. The authors have demonstrated the need for mechanical forces during chemo-attraction to netrin-1 and for the regulation of FAK and Crk-associated substrate. In fact, in what concerns axon guidance, FAK has also been previously implicated in the guidance of axons to a growing number of other cues, including: ephrins, semaphorins, and brain-derived neurotrophic factor [125, 126]. As such, FAK may function as a mechanosensor in response to these guidance cues.

Oligodendrocytes are also cells that undergo important morphological changes through their maturation process. FAK as a key player in regulating cytoskeleton organization is also involved in the maturation and myelination process of oligodendrocytes. Indeed, Hoshimna et al [127] have that FAK mediates process outgrowth in an oligodendrocyte rat-derived cell line. Several other studies point to the idea that FAK is crucial for oligodendrocytes, particularly during the maturation process [128-131]. Moreover, Forrest and coworkers [132] have shown that FAK conditional knock-out mice have some inhibition or delay of normal myelination during development, reinforcing the idea of a pivotal role of FAK during oligodendrocyte maturation.

4.2. Rho/ROCK Signaling pathway

Lately it has become noticeable that there is cross-talk between integrins and GTPases, as a consequence of the adhesion signaling cascades triggered during integrin sensing of ECM mechanical properties. In fact, the activation of integrins by mechanical forces is thought to result in the recruitment of intracellular mediators that signal through the Rho/ Rho-associated coiled-coil-containing protein kinase (ROCK) signaling pathway to activate force-generating myosin II (Figure 4) [133]. As such, the Rho family guanosine-5-triphosphatases (GTPases) are also thought to be crucial in mechanosensing of matrix stiffness, cell morphological alterations, and cytoskeleton tension [134, 135]. Moreover, it has been proposed that these signaling molecules may work together as a complex network, depending on their subcellular location or the status of cells [136]. This complex

network could provide cell with the necessary structure and flexibility to tune cellular responses under various physiological conditions.

The small GTPases Ras superfamily comprises 20 members, which are widely expressed in mammals, including RhoA, Rac1, and Cdc42. RhoA, the best-characterized of the Ras proteins, acts as a molecular switch which cycles between an inactive GDP-bound and an active GTP-bound conformation. This molecule has been widely implicated in integrin-mediated signaling [137-139], regulation of the assembly and organization of the actin cytoskeleton network and the control of cell migration [140, 141]. RhoA plays a critical role in the assembly of actin stress fibers in response to various soluble stimuli, including serum, growth factors, and lysophosphatidic acid (LPA) [142-144], and to insoluble adhesion ligands such as fibronectin or other ECM components [137]. It is further known to play a critical role in the assembly of actin stress fibers in response to applied mechanical forces [145]. Moreover, it is a key regulator of intracellular contractility and, thus, allows cells to sense matrix stiffness and to respond to mechanical cues. This function is largely put forth through the RhoA major downstream effector, the serine/threonine Rho-associated protein kinase (ROCK). ROCK is involved in regulating neural cell migration, proliferation, survival, axon guidance, and regeneration [146]. Wozniak and coworkers[147] demonstrated that when ROCK or RhoA activity are altered, cells no longer respond effectively to mechanical forces induced by increased matrix stiffness. Some authors have suggested that stiff matrices, in general, lead to increased Rho activation [147, 148] whereas Rac1 activity remained unchanged, implicating that ECM stiffness preferentially activates specific Rho GTPases and consequently the formation of actin stress fibers [134].

Several studies have confirmed that Rho and their associated signaling molecules participate and actively mediate crucial neuron biological processes such as axon regeneration [149, 150], and have also been correlated with enhanced BBB permeability, which is targeted in distinct CNS disorders as are the formation of tumor metastases in the brain [151]. Interestingly, Rho has also been correlated with increased cell proliferation in many cancers [152-154]. ROCK, Rho A's main downstream effector, was found to be involved in focal adhesion formation by promoting myosin light chain (MLC) phosphorylation [155], as well as increasing cell contractility [143, 156], promoting cell migration, polarization and differentiation [147]. Moreover, RhoA was found to be closely related to the pathogenesis of several nervous system disorders [157], and involved in many aspects of neuronal functions including neurite outgrowth and retraction [158]. Recent studies provided additional evidences that ROCK inhibitors had potential therapeutic application for Alzheimer's disease [159, 160], Parkinson's disease [161],

epilepsy [162] and autoimmune neuritis [163]. Given the established role for RhoA-ROCK-mediated cytoskeletal tension, not only in cell migration but also cell proliferation, these pathways may play, therefore, an essential role in regulating both tissue homeostasis and malignant transformation.

4.3. Matrix metalloproteinases and ECM remodeling

The ECM has remodeling enzymes named matrix metalloproteinases (MMPs). MMPs are a large family of proteases involved in many cell-matrix and cell-cell signaling processes. Mammalian MMPs share a conserved domain structure that consists of a catalytic domain and of an autoinhibitory pro-domain [164]. Collectively they can cleave all protein components of the ECM, as well as other substrates including growth factors, cell adhesion molecules and receptors [165]. MMPs were initially thought to be enzymes that degrade structural components of the ECM. However, MMP proteolysis is now known to create space for cells to migrate, to produce specific substrate-cleavage fragments which are biologically active, to regulate tissue architecture and influence the activity of signaling molecules, both directly and indirectly [166].

Uncontrolled MMP activity underlies the pathophysiology of many disorders, such as cancer, asthma, rheumatoid arthritis and retinal detachment [167-169], and has also been associated with neurodegenerative diseases like glaucoma, migraine, Alzheimer's disease, Parkinson's disease, amyotrophic lateral sclerosis and multiple sclerosis [104-106, 170]. Although high levels of MMPs often correlated with poor prognosis in human patients [171], MMP up-regulation is believed to underlie reparative functions in the CNS at well-defined places and time points after an insult [105].

Given the presence of receptors, like integrins, for ECM components on cells, and the ability of MMPs to cleave virtually all ECM components, these enzymes may influence cellular function by regulating the ECM composition and concomitantly have a crucial role on ECM mechanical properties, playing a part in mechanotransduction events. Although this relationship has not been widely studied, particularly in the CNS, some authors have already found evidences of it in other systems. In the uterine cervix it has been shown that MMPs contribute to de-stiffening which precedes and facilitates the dilatation of the cervix during fetal delivery [172]. More recently MMPs were also shown to modulate the mechanical properties of the compass depressor ligaments of echinoderms [173]. Furthermore, MMPs have also been documented to be involved in osteocyte response to mechanical loading [174].

Moreover, it has been described that in injury scenarios MMP levels are increased [175-177]. This observation combined with the lower stiffness of the injured CNS tissue in relation to the healthy tissue suggest that increased MMP levels at the injury site lead to increased degradation/re-organization of the ECM, with a resulting alteration of the cell cytoskeleton network and mechanical properties.

5. Exploring mechanotransduction in the context of CNS diseases: current clinical strategies and future perspectives

Physical cues are important regulators of several biological functions during distinct momentums of cellular life. The disease contexts explored in this review demonstrate that the processes of mechanotransduction, are important contributors to the alteration of tissue function. But the interplay between mechanical induction of signaling pathways and disease is still a largely unexplored target for therapeutic intervention.

There are several reports relative to mechanosensing proteins, suggesting the existence of multiple mechanisms, though it is not known whether these are redundant or complementary mechanisms. The future work done in this field needs to better understand the molecular and biophysical basis of CNS mechanotransduction. This will require a multidisciplinary approach, with a combination of molecular biology and bioengineering techniques. For now, studies have been mainly focused on affecting one pathway, like knocking down or inhibiting one protein but most certainly, in the near future, there will be the need for high throughput systems which enable the simultaneous analysis of distinct and interrelated pathways and the evaluation of the effects of combinatorial drugs and treatments. Although efforts have been made at the molecular level we still need to increase our understanding of the dynamics of mechanotransduction in health and disease beyond the existent knowledge on focal adhesions and ion channels. Therefore, there is a growing effort to study such issues at the tissue and organ level, and recent imaging techniques such as the MRE will expectedly take us closer to future findings.

It must be highlighted that the interest on mechanotransduction issues in the context of CNS pathologies has already evolved from the bench to the bedside, as seen by the increasing number of studies with MRE neuroimaging techniques aiming at the correlation of brain mechanical properties with function, as well as the use of such techniques as a tool to aid disease diagnostic. In fact, MRE is currently under clinical trials to assess its

utility in the non-invasive diagnosis of normal pressure hydrocephalus (clinical trial # NCT02230124, in www.clinicaltrials.gov).

The enhancement of CNS regeneration by targeting ECM molecules known to inhibit regeneration has been also under evaluation. A few strategies have been tested such as the use of chABC, Nogo-A inhibitors and RhoA inhibitors. These will ultimately target mechanotransduction processes.

ChABC has been tested mainly in spinal cord injury scenarios, due to its ability to digest the scar tissue that prevents CNS regeneration after injury, with the final aim of enhancing plasticity and promoting effective rehabilitation. At the moment several veterinary clinical trials are running aiming to treat spinal cord injuries in dogs, namely at Iowa State University. In fact, this is one of the most commonly neurological pathologies in veterinary medicine due to the degeneration of intervertebral discs, which then rupture and cause injury to the spinal cord. Human clinical trials with chABC are now closer to becoming a reality as a modified enzyme is being investigated at the Cambridge Centre for Brain Repair towards the development of a human safe formulation.

Antibodies against Nogo-A is believed to work through inhibition of Nogo, a myelin associated neurite outgrowth inhibitorn. Nogo-A is known to activate the small GTPase RhoA which then binds to the Rho binding domain of the ROCK, activating this kinase.

Although Nogo has been widely correlated with axonal growth it may play important roles in other mechanisms and, anti-NogoA drugs were recently under phase I clinical trials in patients with Multiple Sclerosis (clinical trials # NCT01424423 and NCT01435993, in www.clinicaltrials.gov).

Regarding Rho inhibition two drugs have been currently under focus: ibuprofen and C3 transferase.

Ibuprofen has been on the market as an anti-inflammatory drug for a long time but new formulations and applications are currently under investigation. In fact, it is currently undergoing phase I clinical trials to treat acute traumatic spinal cord injury (clinical trial # NCT02096913, in www.clinicaltrial.gov) due to its ability to inhibit Rho and its putative neuroprotective effect, plasticity enhancement and consequent neurorestaurative potential. It is also under phase II clinical trials for the treatment of mild traumatic brain injuries (clinical trial # NCT02443142, in www.clinicaltrials.gov). Additionally, the interest in ibuprofen has been expanding to be used as a therapeutic agent in Alzheimer disease as it was found to reduce Aβ42 levels by modulating the activity of the γ-secretase enzyme

complex. However, it is important to mention that clinical trials in people with mild to moderate Alzheimer disease, which took place in 2003 and 2004, found no difference between the ibuprofen treated and placebo groups [178].

C3 transferase has entered clinical trials PhaseI/II under the name Cethrin® and results suggest an increase in neurological recovery after spinal cord injury. BioAxone BioSciences was planning a phase II/III trial for spinal cord injuries in USA and Canada (NCT02053883) in 2014. Meanwhile, cethrin® was also under pre-clinical trials during 2014 for optic nerve disorders applications and, if a positive outcome is reached, it may soon enter clinical trials.

While a large number of issues related to the process of mechanotransduction remain to be addressed, particularly in the context of CNS, basic and clinical research of the last decades led to increasing understanding of mechanostranduction events and put forward this process as a valuable diagnostic tool and therapeutic target. Undoubtedly an increasing number of therapies is currently seeking translation into human clinical trials. Nevertheless, one of the future challenges facing the biomedicine field will be the development of effective therapies based on the advances achieved on basic research.

REFRENCES

[1] Delmas P, Hao J, Rodat-Despoix L. Molecular mechanisms of mechanotransduction in mammalian sensory neurons. Nat Rev Neurosci. 2011;12:139-53.
[2] Davies PF, Barbee KA, Volin MV, Robotewskyj A, Chen J, Joseph L, et al. Spatial relationships in early signaling events of flow-mediated endothelial mechanotransduction. Annual Review of Physiology1997. p. 527-49.
[3] Davies PF, Robotewskyj A, Griem ML, Dull RO, Polacek DC. Hemodynamic forces and vascular cell communication in arteries. Archives of Pathology and Laboratory Medicine. 1992;116:1301-6.
[4] Delmas P, Hao J, Rodat-Despoix L. Molecular mechanisms of mechanotransduction in mammalian sensory neurons. Nature Reviews Neuroscience. 2011;12:139-53.
[5] Chalfie M. Neurosensory mechanotransduction. Nature Reviews Molecular Cell Biology. 2009;10:44-52.
[6] Buck L, Axel R. A novel multigene family may encode odorant receptors: A molecular basis for odor recognition. Cell. 1991;65:175-87.
[7] Corey DP, Hudspeth AJ. Response latency of vertebrate hair cells. Biophysical Journal. 1979;26:499-506.
[8] Sen S, Ng WP, Kumar S. Contributions of talin-1 to glioma cell-matrix tensional homeostasis. J R Soc Interface. 2012;9:1311-7.
[9] Hahn C, Schwartz MA. Mechanotransduction in vascular physiology and atherogenesis. Nature Reviews Molecular Cell Biology. 2009;10:53-62.
[10] Lehoux S, Tedgui A. Cellular mechanics and gene expression in blood vessels. Journal of Biomechanics. 2003;36:631-43.
[11] Moshayedi P, Da F Costa L, Christ A, Lacour SP, Fawcett J, Guck J, et al. Mechanosensitivity of astrocytes on optimized polyacrylamide gels analyzed by quantitative morphometry. Journal of Physics Condensed Matter. 2010;22.
[12] Freimann FB, Streitberger KJ, Klatt D, Lin K, McLaughlin J, Braun J, et al. Alteration of brain viscoelasticity after shunt treatment in normal pressure hydrocephalus. Neuroradiology. 2011;54:189-96.
[13] Murphy MC, Curran GL, Glaser KJ, Rossman PJ, Huston J, Poduslo JF, et al. Magnetic resonance elastography of the brain in a mouse model of Alzheimer's disease: Initial results. Magnetic Resonance Imaging. 2012;30:535-9.
[14] Murphy MC, Huston J, Jack CR, Glaser KJ, Manduca A, Felmlee JP, et al. Decreased brain stiffness in Alzheimer's disease determined by magnetic resonance elastography. Journal of Magnetic Resonance Imaging. 2011;34:494-8.
[15] Schregel K, Née Tysiak EW, Garteiser P, Gemeinhardt I, Prozorovski T, Aktas O, et al. Demyelination reduces brain parenchymal stiffness quantified in vivo by magnetic resonance elastography. Proceedings of the National Academy of Sciences of the United States of America. 2012;109:6650-5.
[16] Saxena T, Gilbert J, Stelzner D, Hasenwinkel J. Mechanical characterization of the injured spinal cord after lateral spinal hemisection injury in the rat. Journal of Neurotrauma. 2012;29:1747-57.
[17] Di Castro A, Drew LJ, Wood JN, Cesare P. Modulation of sensory neuron mechanotransduction by PKC- and nerve growth factor-dependent pathways. Proceedings of the National Academy of Sciences of the United States of America. 2006;103:4699-704.
[18] Nassini R, de Cesaris F, Pedretti P, Geppetti P. TRPS and migraine. Open Drug Discovery Journal. 2010;2:55-63.
[19] Edvinsson L, Uddman R. Neurobiology in primary headaches. Brain Research Reviews. 2005;48:438-56.
[20] Ferrari MD. Migraine. Lancet. 1998;351:1043-51.
[21] Kurth T, Schurks M, Logroscino G, Gaziano JM, Buring JE. Migraine, vascular risk, and cardiovascular events in women: prospective cohort study. BMJ (Clinical research ed). 2008;337.

[22] Scher AI, Terwindt GM, Picavet HSJ, Verschuren WMM, Ferrari MD, Launer LJ. Cardiovascular risk factors and migraine: The GEM population-based study. Neurology. 2005;64:614-20.
[23] Winsvold BS, Hagen K, Aamodt AH, Stovner LJ, Holmen J, Zwart JA. Headache, migraine and cardiovascular risk factors: The HUNT study. European Journal of Neurology. 2011;18:504-11.
[24] Evers S, Schmidt O, Frese A, Husstedt IW, Ringelstein EB. The cerebral hemodynamics of headache associated with sexual activity. Pain. 2003;102:73-8.
[25] Bahra A, Matharu MS, Buchel C, Frackowiak RS, Goadsby PJ. Brainstem activation specific to migraine headache. Lancet. 2001;357:1016-7.
[26] Lahoria R, Allport L, Glenn D, Masters L, Shnier R, Davies M, et al. Spontaneous low pressure headache - A review and illustrative patient. Journal of Clinical Neuroscience. 2012;19:1076-9.
[27] May A, Bahra A, Buchel C, Frackowiak RSJ, Goadsby PJ. PET and MRA findings in cluster headache and MRA in experimental pain. Neurology. 2000;55:1328-35.
[28] May A, Buchel C, Bahra A, Goadsby PJ, Frackowiak RSJ. Intracranial vessels in trigeminal transmitted pain: A PET study. NeuroImage. 1999;9:453-60.
[29] Morgan JT, Murphy CJ, Russell P. What do mechanotransduction, Hippo, Wnt, and TGFβ have in common? YAP and TAZ as key orchestrating molecules in ocular health and disease. Experimental Eye Research. 2013.
[30] Strouthidis NG, Girard MJA. Altering the way the optic nerve head responds to intraocular pressure - A potential approach to glaucoma therapy. Current Opinion in Pharmacology. 2013;13:83-9.
[31] Sigal IA, Grimm JL, Schuman JS, Kagemann L, Ishikawa H, Wollstein G. A method to estimate biomechanics and mechanical properties of optic nerve head tissues from parameters measurable using optical coherence tomography. IEEE Transactions on Medical Imaging. 2014;33:1381-9.
[32] Sigal IA, Ethier CR. Biomechanics of the optic nerve head. Experimental Eye Research. 2009;88:799-807.
[33] Heijl A, Leske MC, Bengtsson B, Hyman L, Hussein M. Reduction of intraocular pressure and glaucoma progression: Results from the Early Manifest Glaucoma Trial. Archives of Ophthalmology. 2002;120:1268-79.
[34] Kass MA, Heuer DK, Higginbotham EJ, Johnson CA, Keltner JL, Philip Miller J, et al. The Ocular Hypertension Treatment Study: A randomized trial determines that topical ocular hypotensive medication delays or prevents the onset of primary open-angle glaucoma. Archives of Ophthalmology. 2002;120:701-13.
[35] Sigal IA. Interactions between geometry and mechanical properties on the optic nerve head. Investigative Ophthalmology and Visual Science. 2009;50:2785-95.
[36] McBrien NA, Jobling AI, Gentle A. Biomechanics of the sclera in myopia: Extracellular and cellular factors. Optometry and Vision Science. 2009;86:E23-E30.
[37] Phillips JR, Khalaj M, McBrien NA. Induced myopia associated with increased scleral creep in chick and tree shrew eyes. Investigative Ophthalmology and Visual Science. 2000;41:2028-34.
[38] Chou T, Siegel M. A mechanical model of retinal detachment. Physical Biology. 2012;9.
[39] Davis JT, Wen Q, Janmey PA, Otteson DC, Foster WJ. Muller cell expression of genes implicated in proliferative vitreoretinopathy is influenced by substrate elastic modulus. Investigative ophthalmology & visual science. 2012;53:3014-9.
[40] Agrawal NJ, Radhakrishnan R. Calculation of free energies in fluid membranes subject to heterogeneous curvature fields. Physical Review E - Statistical, Nonlinear, and Soft Matter Physics. 2009;80.
[41] Dupont S, Morsut L, Aragona M, Enzo E, Giulitti S, Cordenonsi M, et al. Role of YAP/TAZ in mechanotransduction. Nature. 2011;474:179-84.
[42] Yang X, Askarova S, Lee JCM. Membrane biophysics and mechanics in alzheimer's disease. Molecular Neurobiology. 2010;41:138-48.

[43] Moses GSD, Jensen MD, Lue LF, Walker DG, Sun AY, Simonyi A, et al. Secretory PLA2-IIA: A new inflammatory factor for Alzheimer's disease. Journal of Neuroinflammation. 2006;3.
[44] Ross BM, Moszczynska A, Erlich J, Kish SJ. Phospholipid-metabolizing enzymes in Alzheimer's disease: Increased lysophospholipid acyltransferase activity and decreased phospholipase A2 activity. Journal of Neurochemistry. 1998;70:786-93.
[45] Eckert GP, Cairns NJ, Maras A, Gattaz WF, Muller WE. Cholesterol modulates the membrane-disordering effects of beta-amyloid peptides in the hippocampus: Specific changes in Alzheimer's disease. Dementia and Geriatric Cognitive Disorders. 2000;11:181-6.
[46] Sweers KKM, Bennink ML, Subramaniam V. Nanomechanical properties of single amyloid fibrils. Journal of Physics Condensed Matter. 2012;24.
[47] Zhiping Xu, Raffaella Paparcone, Buehler MJ. Alzheimer's Ab(1-40) Amyloid Fibrils Feature Size-Dependent Mechanical Properties. Biophysical Journal. 2010;98:2053–62.
[48] Raffaella Paparcone, Matthew A. Pires, Buehler MJ. Mutations Alter the Geometry and Mechanical Properties of Alzheimer's Aβ(1-40) Amyloid Fibrils. Biochemistry. 2010;49:8967–77.

[49] Hattori T, Yuasa T, Aoki S, Sato R, Sawaura H, Mori T, et al. Altered microstructure in corticospinal tract in idiopathic normal pressure hydrocephalus: Comparison with Alzheimer disease and Parkinson disease with dementia. American Journal of Neuroradiology. 2011;32:1681-7.

[50] Alexander AL, Lee JE, Field AS. Diffusion Tensor Imaging of the Brain. Neurotherapeutics. 2007;4:316-29.
[51] Streitberger KJ, Sack I, Krefting D, Pfuller C, Braun J, Paul F, et al. Brain viscoelasticity alteration in chronic-progressive multiple sclerosis. PLoS ONE. 2012;7.
[52] Liliana R Pires, Pêgo AP. Bridging the lesion--engineering a permissive substrate for nerve regeneration. Regenerative Biomaterials. 2015;2:203-14.
[53] Lu YB, Franze K, Seifert G, Steinhauser C, Kirchhoff F, Wolburg H, et al. Viscoelastic properties of individual glial cells and neurons in the CNS. Proceedings of the National Academy of Sciences of the United States of America. 2006;103:17759-64.
[54] Fawcett JW, Asher RA. The glial scar and central nervous system repair. Brain Research Bulletin. 1999;49:377-91.
[55] Morgenstern DA, Asher RA, Fawcett JW. Chondroitin sulphate proteoglycans in the CNS injury response. Progress in Brain Research2002. p. 313-32.
[56] Mathewson AJ, Berry M. Observations on the astrocyte response to a cerebral stab wound in adult rats. Brain Research. 1985;327:61-9.
[57] Ostrow LW, Sachs F. Mechanosensation and endothelin in astrocytes - Hypothetical roles in CNS pathophysiology. Brain Research Reviews. 2005;48:488-508.
[58] Shreiber DI, Hao H, Elias RA. Probing the influence of myelin and glia on the tensile properties of the spinal cord. Biomechanics and Modeling in Mechanobiology. 2009;8:311-21.
[59] Georges PC, Miller WJ, Meaney DF, Sawyer ES, Janmey PA. Matrices with compliance comparable to that of brain tissue select neuronal over glial growth in mixed cortical cultures. Biophysical Journal. 2006;90:3012-8.
[60] Jiang X, Georges PC, Li B, Du Y, Kutzing MK, Previtera ML, et al. Cell Growth in Response to Mechanical Stiffness is Affected by Neuron-Astroglia Interactions. The Open Neuroscience Journal. 2007;1:7-14.
[61] Rocha DN, Ferraz-Nogueira JP, Barrias CC, Relvas JB, AP P. Extracellular environment contribution to astrogliosis-lessons learned from a tissue engineered 3D model of the glial scar. Front Cell Neurosci. 2015;9.
[62] Back SA, Tuohy TM, Chen H, Wallingford N, Craig A, Struve J, et al. Hyaluronan accumulates in demyelinated lesions and inhibits oligodendrocyte progenitor maturation. Nat Med. 2005;11:966-72.

[63] Sloane JA, Batt C, Ma Y, Harris ZM, Trapp B, Vartanian T. Hyaluronan blocks oligodendrocyte progenitor maturation and remyelination through TLR2. Proc Natl Acad Sci U S A. 2010;107:11555-60.
[64] Steinmetz MP, Horn KP, Tom VJ, Miller JH, Busch SA, Nair D, et al. Chronic enhancement of the intrinsic growth capacity of sensory neurons combined with the degradation of inhibitory proteoglycans allows functional regeneration of sensory axons through the dorsal root entry zone in the mammalian spinal cord. J Neurosci. 2005;25:8066-76.
[65] Bradbury EJ, Moon LD, Popat RJ, King VR, Bennett GS, Patel PN, et al. Chondroitinase ABC promotes functional recovery after spinal cord injury. Nature. 2002;416:636-40.
[66] Caggiano AO, Zimber MP, Ganguly A, Blight AR, Gruskin EA. Chondroitinase ABCI improves locomotion and bladder function following contusion injury of the rat spinal cord. J Neurotrauma. 2005;22:226-39.
[67] Wilfred C Mezue, Samuel C Ohaegbulam, Chika C Ndubuisi, Mark C Chikani, Achebe DS. Intracranial meningiomas managed at Memfys hospital for neurosurgery in Enugu, Nigeria. J Neurosci Rural Pract. 2012;3:320-3.
[68] Martin Scholz, Volker Noack, Ioannis Pechlivanis, Martin Engelhardt, Britta Fricke, Ulf Linstedt, et al. Vibrography During Tumor Neurosurgery. J Ultrasound Med. 2005;24:985–92.
[69] Fukushima Y, Ohnishi T, Arita N, Hayakawa T, Sekiguchi K. Integrin alpha3beta1-mediated interaction with laminin-5 stimulates adhesion, migration and invasion of malignant glioma cells. Int J Cancer. 1998;76:63-72.
[70] Rao JS. Molecular mechanisms of glioma invasiveness: the role of proteases. Nat Rev Cancer. 2003;3:489-501.
[71] Demuth T, Berens ME. Molecular mechanisms of glioma cell migration and invasion. J Neurooncol. 2004;70:217-28.
[72] Sen S, Dong M, Kumar S. Isoform-specific contributions of alpha-actinin to glioma cell mechanobiology. PLoS One. 2009;4:e8427.
[73] Ulrich TA, de Juan Pardo EM, Kumar S. The mechanical rigidity of the extracellular matrix regulates the structure, motility, and proliferation of glioma cells. Cancer Res. 2009;69:4167-74.
[74] Hegedus B, Marga F, Jakab K, Sharpe-Timms KL, Forgacs G. The interplay of cell-cell and cell-matrix interactions in the invasive properties of brain tumors. Biophys J. 2006;91:2708-16.
[75] Thomas TW, DiMilla PA. Spreading and motility of human glioblastoma cells on sheets of silicone rubber depend on substratum compliance. Med Biol Eng Comput. 2000;38:360-70.
[76] Forget MA, Desrosiers RR, Del M, Moumdjian R, Shedid D, Berthelet F, et al. The expression of rho proteins decreases with human brain tumor progression: potential tumor markers. Clin Exp Metastasis. 2002;19:9-15.
[77] Yan B, Chour HH, Peh BK, Lim C, Salto-Tellez M. RhoA protein expression correlates positively with degree of malignancy in astrocytomas. Neurosci Lett. 2006;407:124-6.
[78] Selbekk T, Bang J, Unsgaard G. Strain processing of intraoperative ultrasound images of brain tumours: initial results. Ultrasound Med Biol. 2005;31:45-51.
[79] Butcher DT, Alliston T, Weaver VM. A tense situation: forcing tumour progression. Nat Rev Cancer. 2009;9:108-22.
[80] Sinkus R, Lorenzen J, Schrader D, Lorenzen M, Dargatz M, Holz D. High-resolution tensor MR elastography for breast tumour detection. Phys Med Biol. 2000;45:1649-64.
[81] Swaminathan V, Mythreye K, O'Brien ET, Berchuck A, Blobe GC, Superfine R. Mechanical stiffness grades metastatic potential in patient tumor cells and in cancer cell lines. Cancer Res. 2011;71:5075-80.
[82] Qazi H, Shi ZD, Tarbell JM. Fluid shear stress regulates the invasive potential of glioma cells via modulation of migratory activity and matrix metalloproteinase expression. PLoS One. 2011;6:e20348.

[83] Coussens LM, Fingleton B, Matrisian LM. Matrix metalloproteinase inhibitors and cancer: trials and tribulations. Science. 2002;295:2387-92.
[84] Brown PD. Ongoing trials with matrix metalloproteinase inhibitors. Expert Opin Investig Drugs. 2000;9:2167-77.
[85] Pozzi A, LeVine WF, Gardner HA. Low plasma levels of matrix metalloproteinase 9 permit increased tumor angiogenesis. Oncogene. 2002;21:272-81.
[86] S. RYC. Degeneration and regeneration of the nervous system: Oxford University Press; 1928.
[87] Weiss P. In vitro experiments on the factors determining the course of the outgrowing nerve fiber. Journal of Experimental Zoology. 1934;68:393-448.
[88] Banerjee A, Arha M, Choudhary S, Ashton RS, Bhatia SR, Schaffer DV, et al. The influence of hydrogel modulus on the proliferation and differentiation of encapsulated neural stem cells. Biomaterials. 2009;30:4695-9.
[89] Saha K, Keung AJ, Irwin EF, Li Y, Little L, Schaffer DV, et al. Substrate modulus directs neural stem cell behavior. Biophysical Journal. 2008;95:4426-38.
[90] Leipzig ND, Shoichet MS. The effect of substrate stiffness on adult neural stem cell behavior. Biomaterials. 2009;30:6867-78.
[91] R. V. Cellular pathology: as based upon physiological and pathological histology. In: Twenty lectures delivered in the pathological institute of Berlin during the months of February MaA, editor. First edition ed. Berlin: August Hirschwald1858.
[92] Rocha DN, Brites P, Fonseca C, Pego AP. Poly(trimethylene carbonate-co-epsilon-caprolactone) promotes axonal growth. PLoS One. 2014;9:e88593.
[93] Jagielska A, Norman AL, Whyte G, Vliet KJV, Guck J, Franklin RJM. Mechanical environment modulates biological properties of oligodendrocyte progenitor cells. Stem Cells and Development. 2012;21:2905-14.
[94] Kippert A, Fitzner D, Helenius J, Simons M. Actomyosin contractility controls cell surface area of oligodendrocytes. BMC Cell Biology. 2009;10:71.
[95] Bauer NG, Ffrench-Constant C. Physical forces in myelination and repair: a question of balance? Journal of Biology 2009. 2009;8.
[96] Bollmann L, Koser DE, Shahapure R, Gautier HO, Holzapfel GA, Scarcelli G, et al. Microglia mechanics: immune activation alters traction forces and durotaxis. Front Cell Neurosci 2015;9.
[97] Pires LR, Rocha DN, Ambrosio L, AP P. The role of the surface on microglia function: implications for central nervous system tissue engineering. J R Soc Interface. 2015;6.
[98] Crapo PM, Medberry CJ, Reing JE, Tottey S, van der Merwe Y, Jones KE, et al. Biologic scaffolds composed of central nervous system extracellular matrix. Biomaterials.33:3539-47.
[99] Eyckmans J, Boudou T, Yu X, Chen C. A Hitchhiker's Guide to Mechanobiology. Developmental Cell. 2011;21:35-47.
[100] Gieni RS, Hendzel MJ. Mechanotransduction From the ECM to the Genome: Are the Pieces now in Place? Journal of Cellular Biochemistry 2008;104:1964–87.
[101] Jansen KA, Donato DM, Balcioglu HE, Schmidt T, Danen EH, GH K. A guide to mechanobiology: Where biology and physics meet. Biochim Biophys Acta. 2015;15.
[102] Raghow R. The role of extracellular matrix in postinflammatory wound healing and fibrosis. FASEB Journal. 1994;8:823-31.
[103] Kim DH, Provenzano PP, Smith CL, Levchenko A. Matrix nanotopography as a regulator of cell function. Journal of Cell Biology. 2012;197:351-60.
[104] Klein T, Bischoff R. Physiology and pathophysiology of matrix metalloproteases. Amino Acids. 2011;41:271-90.
[105] Yong VW. Metalloproteinases: Mediators of pathology and regeneration in the CNS. Nature Reviews Neuroscience. 2005;6:931-44.
[106] Rosenberg GA. Matrix metalloproteinases and their multiple roles in neurodegenerative diseases. The Lancet Neurology. 2009;8:205-16.

[107] Burnside ER, Bradbury EJ. Review: Manipulating the extracellular matrix and its role in brain and spinal cord plasticity and repair. Neuropathology and Applied Neurobiology. 2014;40:26-59.
[108] Vogel V, Sheetz M. Local force and geometry sensing regulate cell functions. Nature Reviews Molecular Cell Biology. 2006;7:265-75.
[109] Martin KH, Slack JK, Boerner SA, Martin CC, Parsons JT. Integrin connections map: To infinity and beyond. Science. 2002;296:1652-3.
[110] Humphries JD, Byron A, Humphries MJ. Integrin ligands at a glance. Journal of Cell Science. 2006;119:3901-3.
[111] Geiger B, Spatz JP, Bershadsky AD. Environmental sensing through focal adhesions. Nature Reviews Molecular Cell Biology. 2009;10:21-33.
[112] Mitra SK, Hanson DA, Schlaepfer DD. Focal adhesion kinase: In command and control of cell motility. Nature Reviews Molecular Cell Biology. 2005;6:56-68.
[113] Choquet D, Felsenfeld DP, Sheetz MP. Extracellular matrix rigidity causes strengthening of integrin- cytoskeleton linkages. Cell. 1997;88:39-48.
[114] Riveline D, Zamir E, Balaban NQ, Schwarz US, Ishizaki T, Narumiya S, et al. Focal contacts as mechanosensors: Externally applied local mechanical force induces growth of focal contacts by an mDia1-dependent and ROCK-independent mechanism. Journal of Cell Biology. 2001;153:1175-85.
[115] Schiller HB, Hermann MR, Polleux J, Vignaud T, Zanivan S, Friedel CC, et al. B1- and v-class integrins cooperate to regulate myosin II during rigidity sensing of bronectin-based microenvironments. Nature Cell Biology. 2013;15:625-36.
[116] Collin O, Na S, Chowdhury F, Hong M, Shin ME, Wang F, et al. Self-organized podosomes are dynamic mechanosensors. Curr Biol. 2008;18:1288-94.
[117] Burgaya F, Toutant M, Studier JM, Costa A, Le Bert M, Gelman M, et al. Alternatively spliced focal adhesion kinase in rat brain with increased autophosphorylation activity. Journal of Biological Chemistry. 1997;272:28720-5.
[118] Contestabile A, Bonanomi D, Burgaya F, Girault JA, Valtorta F. Localization of focal adhesion kinase isoforms in cells of the central nervous system. International Journal of Developmental Neuroscience. 2003;21:83-93.
[119] Grant SGN, Karl KA, Kiebler MA, Kandel ER. Focal adhesion kinase in the brain: Novel subcellular localization and specific regulation by Fyn tyrosine kinase in mutant mice. Genes and Development. 1995;9:1909-21.
[120] Bacon C, Lakics V, Machesky L, Rumsby M. N-WASP regulates extension of filopodia and processes by oligodendrocyte progenitors, oligodendrocytes, and Schwann cells - Implications for axon ensheathment at myelination. GLIA. 2007;55:844-58.
[121] Kilpatrick TJ, Ortuno D, Bucci T, Lai C, Lemke G. Rat oligodendroglia express c-met and focal adhesion kinase, protein tyrosine kinases implicated in regulating epithelial cell motility. Neuroscience Letters. 2000;279:5-8.
[122] Robles E, Gomez TM. Focal adhesion kinase signaling at sites of integrin-mediated adhesion controls axon pathfinding. Nature Neuroscience. 2006;9:1274-83.
[123] Yamaguchi H, Wyckoff J, Condeelis J. Cell migration in tumors. Curr Opin Cell Biol. 2005;17:559-64.
[124] Moore SW, Zhang X, Lynch CD, Sheetz MP. Netrin-1 Attracts axons through FAK-dependent mechanotransduction. Journal of Neuroscience. 2012;32:11574-85.
[125] Falk J, Bechara A, Fiore R, Nawabi H, Zhou H, Hoyo-Becerra C, et al. Erratum: Dual functional activity of semaphorin 3B is required for positioning the anterior commissure (Neuron (October 6, 2005) 48 (63-75). Neuron. 2005;48:699.
[126] Woo S, Gomez TM. Rac1 and RhoA promote neurite outgrowth through formation and stabilization of growth cone point contacts. Journal of Neuroscience. 2006;26:1418-28.
[127] Hoshina N, Tezuka T, Yokoyama K, Kozuka-hata H, Oyama M, Yamamoto T. Focal adhesion kinase regulates laminin-induced oligodendroglial process outgrowth. Genes to Cells. 2007;12:1245-54.

[128] Miyamoto Y, Yamauchi J, Chan JR, Okada A, Tomooka Y, Hisanaga SI, et al. Cdk5 regulates differentiation of oligodendrocyte precursor cells through the direct phosphorylation of paxillin. Journal of Cell Science. 2007;120:4355-66.
[129] Rajasekharan S, Baker KA, Horn KE, Jarjour AA, Antel JP, Kennedy TE. Netrin 1 and Dcc regulate oligodendrocyte process branching and membrane extension via Fyn and RhoA. Development. 2009;136:415-26.
[130] Wang PS, Wang J, Xiao ZC, Pallen CJ. Protein-tyrosine phosphatase Î± acts as an upstream regulator of Fyn signaling to promote oligodendrocyte differentiation and myelination. Journal of Biological Chemistry. 2009;284:33692-702.
[131] Fox MA, Alexander JK, Afshari FS, Collelo RJ, Fuss B. Phosphodiesterase-I alpha/autotaxin controls cytoskeletal organization and FAK phosphorylation during myelination. Mol Cell Neurosci. 2004;27:140-50.
[132] Forrest AD, Beggs HE, Reichardt LF, Dupree JL, Colello RJ, Fuss B. Focal Adhesion Kinase (FAK): A regulator of CNS myelination. Journal of Neuroscience Research. 2009;87:3456-64.
[133] Bauer NG, Ffrench-Constant C. Physical forces in myelination and repair: A question of balance? Journal of Biology. 2009;8.
[134] Keung AJ, De Juan-Pardo EM, Schaffer DV, Kumar S. Rho GTPases mediate the mechanosensitive lineage commitment of neural stem cells. Stem Cells. 2011;29:1886-97.
[135] Holle AW, Engler AJ. More than a feeling: Discovering, understanding, and influencing mechanosensing pathways. Current Opinion in Biotechnology.22:648-54.
[136] Hoffman BD, Grashoff C, Schwartz MA. Dynamic molecular processes mediate cellular mechanotransduction. Nature. 2011;475:316-23.
[137] Ren XD, Kiosses WB, Schwartz MA. Regulation of the small GTP-binding protein Rho by cell adhesion and the cytoskeleton. EMBO Journal. 1999;18:578-85.
[138] Clark EA, King WG, Brugge JS, Symons M, Hynes RO. Integrin-mediated signals regulated by members of the rho family of gtpases. Journal of Cell Biology. 1998;142:573-86.
[139] Herzog D, Loetscher P, van Hengel J, Knüsel S, Brakebusch C, Taylor V, et al. The small GTPase RhoA is required to maintain spinal cord neuroepithelium organization and the neural stem cell pool. J Neuroscie. 2011;31.
[140] Etienne-Manneville S, Hall A. Rho GTPases in cell biology. Nature. 2002;420:629-35.
[141] Hall A. Rho GTpases and the actin cytoskeleton. Science. 1998;279:509-14.
[142] Chong LD, Traynor-Kaplan A, Bokoch GM, Schwartz MA. The small GTP-binding protein rho regulates a phosphatidylinositol 4-phosphate 5-kinase in mammalian cells. Cell. 1994;79:507-13.
[143] Chrzanowska-Wodnicka M, Burridge K. Rho-stimulated contractility drives the formation of stress fibers and focal adhesions. Journal of Cell Biology. 1996;133:1403-15.
[144] Ridley AJ, Hall A. The small GTP-binding protein rho regulates the assembly of focal adhesions and actin stress fibers in response to growth factors. Cell. 1992;70:389-99.
[145] Putnam AJ, Cunningham JJ, Pillemer BBL, Mooney DJ. External mechanical strain regulates membrane targeting of Rho GTPases by controlling microtubule assembly. American Journal of Physiology - Cell Physiology. 2003;284:C627-C39.
[146] González-Forero D, Montero F, Garcia-Morales V, Domínguez G, Gómez-Pérez L, García-Verdugo JM, et al. Endogenous rho-kinase signaling maintains synaptic strength by stabilizing the size of the readily releasable pool of synaptic vesicles. Journal of Neuroscience. 2012;32:68-84.
[147] Wozniak MA, Desai R, Solski PA, Der CJ, Keely PJ. ROCK-generated contractility regulates breast epithelial cell differentiation in response to the physical properties of a three-dimensional collagen matrix. Journal of Cell Biology. 2003;163:583-95.
[148] Provenzano PP, Inman DR, Eliceiri KW, Keely PJ. Matrix density-induced mechanoregulation of breast cell phenotype, signaling and gene expression through a FAK-ERK linkage. Oncogene. 2009;28:4326-43.

[149] Duffy P, Schmandke A, Sigworth J, Narumiya S, Cafferty WB, Strittmatter SM. Rho-associated kinase II (ROCKII) limits axonal growth after trauma within the adult mouse spinal cord. J Neurosci. 2009;29:15266-76.
[150] Sivasankaran R, Pei J, Wang KC, Zhang YP, Shields CB, Xu XM, et al. PKC mediates inhibitory effects of myelin and chondroitin sulfate proteoglycans on axonal regeneration. Nat Neurosci. 2004;7:261-8.
[151] Krizbai IA, Deli MA. Signalling pathways regulating the tight junction permeability in the blood-brain barrier. Cell Mol Biol (Noisy-le-grand). 2003;49:23-31.
[152] Faried A, Faried LS, Usman N, Kato H, Kuwano H. Clinical and prognostic significance of RhoA and RhoC gene expression in esophageal squamous cell carcinoma. Ann Surg Oncol. 2007;14:3593-601.
[153] Sterpetti P, Marucci L, Candelaresi C, Toksoz D, Alpini G, Ugili L, et al. Cell proliferation and drug resistance in hepatocellular carcinoma are modulated by Rho GTPase signals. Am J Physiol Gastrointest Liver Physiol. 2006;290:G624-32.
[154] Wang HB, Liu XP, Liang J, Yang K, Sui AH, Liu YJ. Expression of RhoA and RhoC in colorectal carcinoma and its relations with clinicopathological parameters. Clin Chem Lab Med. 2009;47:811-7.
[155] Kimura K, Ito M, Amano M, Chihara K, Fukata Y, Nakafuku M, et al. Regulation of myosin phosphatase by Rho and Rho-associated kinase (Rho-kinase). Science. 1996;273:245-8.
[156] Matthews BD, Overby DR, Mannix R, Ingber DE. Cellular adaptation to mechanical stress: role of integrins, Rho, cytoskeletal tension and mechanosensitive ion channels. J Cell Sci. 2006;119:508-18.
[157] Guan R, Xu X, Chen M, Hu H, Ge H, Wen S, et al. Advances in the studies of roles of Rho/Rho-kinase in diseases and the development of its inhibitors. European Journal of Medicinal Chemistry. 2013;70:613-22.
[158] Tan HB, Zhong YS, Cheng Y, Shen X. Rho/ROCK pathway and neural regeneration: A potential therapeutic target for central nervous system and optic nerve damage. International Journal of Ophthalmology. 2011;4:652-7.
[159] Hou Y, Zhou L, Yang QD, Du XP, Li M, Yuan M, et al. Changes in hippocampal synapses and learning-memory abilities in a streptozotocin-treated rat model and intervention by using fasudil hydrochloride. Neuroscience. 2012;200:120-9.
[160] Raad M, El Tal T, Gul R, Mondello S, Zhang Z, Boustany RM, et al. Neuroproteomics approach and neurosystems biology analysis: ROCK inhibitors as promising therapeutic targets in neurodegeneration and neurotrauma. Electrophoresis. 2012;33:3659-68.
[161] Tonges L, Frank T, Tatenhorst L, Saal KA, Koch JC, Szego EM, et al. Inhibition of rho kinase enhances survival of dopaminergic neurons and attenuates axonal loss in a mouse model of Parkinson's disease. Brain. 2012;135:3355-70.
[162] Inan SY, Buyukafsar K. Antiepileptic effects of two Rho-kinase inhibitors, Y-27632 and fasudil, in mice. British Journal of Pharmacology. 2008;155:44-51.
[163] Pineda AAM, Minohara M, Kawamura N, Matsushita T, Yamasaki R, Sun X, et al. Preventive and therapeutic effects of the selective Rho-kinase inhibitor fasudil on experimental autoimmune neuritis. Journal of the Neurological Sciences. 2011;306:115-20.
[164] Page-McCaw A, Ewald AJ, Werb Z. Matrix metalloproteinases and the regulation of tissue remodelling. Nat Rev Mol Cell Biol. 2007;8:221-33.
[165] McCawley LJ, Matrisian LM. Matrix metalloproteinases: They're not just for matrix anymore! Current Opinion in Cell Biology. 2001;13:534-40.
[166] Sternlicht MD, Werb Z. How matrix metalloproteinases regulate cell behavior. Annu Rev Cell Dev Biol. 2001;17:463-516.
[167] Imamura K, Takeshima T, Fusayasu E, Nakashima K. Increased plasma matrix metalloproteinase-9 levels in migraineurs. Headache. 2008;48:135-9.
[168] Martins-Oliveira A, Speciali JG, Dach F, Marcaccini AM, GonÃ§alves FM, Gerlach RF, et al. Different circulating metalloproteinases profiles in women with migraine with and without aura. Clinica Chimica Acta. 2009;408:60-4.

[169] Sivak JM, Fini ME. MMPs in the eye: Emerging roles for matrix metalloproteinases in ocular physiology. Progress in Retinal and Eye Research. 2002;21:1-14.
[170] Rosario Hernandez M, Pena JDO. The optic nerve head in glaucomatous optic neuropathy. Archives of Ophthalmology. 1997;115:389-95.
[171] Egeblad M, Werb Z. New functions for the matrix metalloproteinases in cancer progression. Nature Reviews Cancer. 2002;2:161-74.
[172] Rahkonen L, Rutanen EM, Unkila-Kallio L, Nuutila M, Nieminen P, Sorsa T, et al. Factors affecting matrix metalloproteinase-8 levels in the vaginal and cervical fluids in the first and second trimester of pregnancy. Hum Reprod. 2009;24:2693-702.
[173] Ribeiro AR, Barbaglio A, Oliveira MJ, Ribeiro CC, Wilkie IC, Candia Carnevali MD, et al. Matrix metalloproteinases in a sea urchin ligament with adaptable mechanical properties. PLoS One. 2012;7:e49016.
[174] Kulkarni RN, Bakker AD, Gruber EV, Chae TD, Veldkamp JB, Klein-Nulend J, et al. MT1-MMP modulates the mechanosensitivity of osteocytes. Biochem Biophys Res Commun. 2012;417:824-9.
[175] Szklarczyk A, Lapinska J, Rylski M, McKay RD, Kaczmarek L. Matrix metalloproteinase-9 undergoes expression and activation during dendritic remodeling in adult hippocampus. J Neurosci. 2002;22:920-30.
[176] Rosenberg GA, Cunningham LA, Wallace J, Alexander S, Estrada EY, Grossetete M, et al. Immunohistochemistry of matrix metalloproteinases in reperfusion injury to rat brain: activation of MMP-9 linked to stromelysin-1 and microglia in cell cultures. Brain Res. 2001;893:104-12.
[177] Rathke-Hartlieb S, Budde P, Ewert S, Schlomann U, Staege MS, Jockusch H, et al. Elevated expression of membrane type 1 metalloproteinase (MT1-MMP) in reactive astrocytes following neurodegeneration in mouse central nervous system. FEBS Lett. 2000;481:227-34.
[178] Pasqualetti P, Bonomini C, Dal Forno G, Paulon L, Sinforiani E, Marra C, et al. A randomized controlled study on effects of ibuprofen on cognitive progression of Alzheimer's disease. Aging Clin Exp Res. 2009;21:102-10.

“ Primeiro estranha-se, depois entranha-se.”

(Fernando Pessoa)

CHAPTER III

Extracellular Environment Contribution to Astrogliosis – Lessons Learned from a Tissue Engineered 3D Model of the Glial Scar *

D. N. Rocha [1,2,3], J. Ferraz-Nogueira [3,4], C.C. Barrias [1,3], J.B. Relvas [3,4], A.P. Pêgo [1,3,5]

[1] INEB – Instituto de Engenharia Biomédica, Porto, Portugal; [2] FEUP – Faculdade de Engenharia da Universidade do Porto, Porto, Portugal; [3] I3S – Instituto de Investigação e Inovação em Saúde, Universidade do Porto, Porto, Portugal; [4] IBMC – Instituto de Biologia Molecular e Celular, Porto, Portugal; [5] ICBAS - Ciências Biomédicas Abel Salazar, Universidade do Poro, Porto Portugal

* *Front Cell Neurosci. 2015 Sep 29;9:377. doi: 10.3389/fncel.2015.00377*

ABSTRACT

Glial scars are widely seen as a (bio)mechanical barrier to central nervous system regeneration. Due to the lack of a screening platform, which could allow in-vitro testing of several variables simultaneously, up to now no comprehensive study has addressed and clarified how different lesion microenvironment properties affect astrogliosis. Using astrocytes cultured in alginate gels and meningeal fibroblast conditioned medium, we have built a simple and reproducible 3D culture system of astrogliosis mimicking many features of the glial scar. Cells in this 3D culture model behave similarly to scar astrocytes, showing changes in gene expression (e.g. GFAP) and increased extra-cellular matrix production (chondroitin 4 sulphate and collagen), inhibiting neuronal outgrowth. This behavior being influenced by the hydrogel network properties.

Astrocytic reactivity was found to be dependent on RhoA activity, and targeting RhoA using shRNA-mediated lentivirus reduced astrocytic reactivity. Further, we have shown that chemical inhibition of RhoA with ibuprofen or indirectly targeting RhoA by the induction of extracellular matrix composition modification with chondroitinase ABC, can diminish astrogliosis.

Besides presenting the extracellular matrix as a key modulator of astrogliosis, this simple, controlled and reproducible 3D culture system constitutes a good scar-like system and offers great potential in future neurodegenerative mechanism studies, as well as in drug screenings envisaging the development of new therapeutic approaches to minimize the effects of the glial scar in the context of central nervous system disease.

INTRODUCTION

Astrocytes are the most abundant cells in the central nervous system (CNS) (Lu et al., 2006) and are known to play a pivotal role in glial scar formation. Reactive astrogliosis starts when a trigger-stimulus produced at the injury site drives astrocytes to leave their quiescent state and become activated. Reactive astrocytes are characterized by increased expression of intermediate filament proteins glial fibrillary acidic protein (GFAP) and vimentin (Holley et al., 2003, Robel et al., Wang et al., 2004), augmented production of extracellular matrix (ECM) constituents, such as collagen IV (Liesi and Kauppila, 2002) and chondroitin sulfate proteoglycans (CSPG) (Busch and Silver, 2007), and increase in the production of matrix metalloproteinases (MMPs) thought to be closely associated to ECM remodeling (Nair et al., 2008, Ogier et al., 2005, Ogier et al., 2006). The regeneration failure in the adult CNS is multi-factorial but the glial scar has been ascribed has a highly inhibitory environment. While it has been a widely explored therapeutic target (Jones et al., 2003, Koechling et al., 2011), very little is known about the causes and mechanisms underlying astrocyte activation.

Several animal models have been developed to study the processes of CNS degeneration and regeneration. Nevertheless, these are time consuming, costly, and raise technical and ethical issues when one intends to perform routine assays to elucidate molecular mechanisms or screening for potential therapeutics. These emphasize the need to develop simpler experimental systems. The existing 2D in vitro astrogliosis models have provided important insights (Kimura-Kuroda et al., Wanner et al., 2008, Koechling et al.) but they do not replicate key distinctive features of the ECM in a glial scar. As such, the development of a 3D model would be of added value, as this can better recapitulate several features of native cellular microenvironments, by incorporating both biochemical and mechanical components. The biggest challenge is to recreate simple, yet biologically meaningful matrices that support cells within the lesion environment, with a minimum number of model system variables. ECM-derived natural matrices such as Matrigel® or decellularized tissue provide factors that support cell function; however, the inherent complexity and variability of these scaffolds makes it difficult to isolate and dissect cell-signaling mechanisms (Owen and Shoichet, 2010). Here, a new in vitro alginate based 3D model of the glial scar is proposed to serve as a tool in the identification and modulation of molecular mechanisms underlying astrocyte activation. Mammalian cells do not interact with alginate, therefore it constitutes a relatively inert backbone structure (Lutolf and Blau, 2009, Rowley et al., 1999). Moreover, alginate based matrices are highly reproducible, a pivotal requirement for their application as 3D artificial ECM.

Cerebral astrocytes were cultured within 3D alginate discs with different alginate contents, and consequently different mechanical properties. These were further stimulated with conditioned medium from meningeal fibroblasts, in order to mimic the possible stimuli resultant from fibroblast infiltration occurring following CNS injury. Mechanical properties of CNS tissue are known to be altered when a glial scar is formed (Bonneh-Barkay and Wiley, 2009, Freimann et al., 2011, Murphy et al., 2012) and ECM components are thought to play a pivotal role on the mechanotransduction processes in healthy and diseased tissues. The correlation between astrocyte reactivity, ECM production and composition and the mechanical properties of the surrounding environment was explored. We show that the Rho-ROCK signaling pathway can regulate astrogliosis constituting a possible therapeutic target.

MATERIALS AND METHODS

Unless mentioned otherwise all reagents were supplied by GIBCO and were of cell culture grade.

Animals

Procedures involving animals and their care were conducted in compliance with institutional ethical guidelines (IBMC) and with the approval of Portuguese Veterinary Authorities. Animals had free access to food and water, being kept under a 12-h light/ 12-h dark cycle.

Cell isolation

Meningeal fibroblasts and cerebral astrocytes

Meningeal fibroblasts and astrocytes were obtained as previously described (Kimura-Kuroda et al., 2010). Briefly, meningeal fibroblasts were obtained from brain meninges of P2 Wistar Han rats. Upon isolation, meningeal tissue was digested in Hank's Balanced Salt Solution (HBSS) without calcium or magnesium, supplemented with papain (20 U/mL, Sigma-Aldrich), for 30 min. Dissociated meninges were plated in poly-L-lysine (Sigma-Aldrich) coated 75cm2 flasks (BioLite), and maintained in Dulbecco's Modified Eagle Medium (DMEM) supplemented with 10% (v/v) inactivated fetal bovine serum (FBS) and 1% (v/v) penicillin-streptomycin (PS).

Fibroblast conditioned medium (CM) was obtained by culturing 13.3 cells.cm^{-2} in DMEM supplemented with 10% FBS and 1% PS, for 72 hours. After collection, CM was centrifuged and stored at 4ºC until use.

Cerebral cortices were further dissected, after removal of the meninges. Isolated cortices were digested in HBSS without calcium or magnesium supplemented with papain (0.2 U/ml), for 30 minutes. Dissociated cortices were cultured in 75 cm2 flasks and maintained in DMEM supplemented with 10% (v/v) FBS and 1% (v/v) PS. When confluence was reached (~12 days) the flasks were shaken overnight on an orbital shaker (240 rpm) at 37ºC to remove loosely attached microglia, oligodendrocytes and neurons. The remaining cells, mainly astrocytes, adhered to the 75 cm2 flasks were then trypsinized and cultured in new flasks. Further tripsinizations were performed in order to increase culture purity.

Cortical neurons isolation and co-culture with astrocytes

To obtain cortical neurons, E18 Wistar Han rat embryos were recovered by cesarean section of pregnant rats. The isolated cortices were dissociated for 30 min at 37ºC in HBSS supplemented with 1 mM pyruvate, 2 mg.ml-1 albumin, and 10% (v/v) trypsin. Viable cells (trypan blue exclusion assay) were seeded at a density of 2.2×104 viable cells/cm2 in DMEM:Nutrient Mixture F-12 (3:1) supplemented with 10% (v/v) inactivated fetal calf serum. Two hours later, medium was changed to Neurobasal medium supplemented with 0.5 mM L-glutamine, 2% (v/v) B27 supplement, 1% (v/v) PS and 0.5% (v/v) Gentamicin. For the co-culture, astrocytes were cultured for 4 days, in DMEM supplemented with 10% FBS and 1% PS, prior to cortical neurons culture. At day 4 the DMEM culture medium was removed and cortical neurons were seeded on top of the adherent astrocytes. The co-culture were maintained for 4 additional days and then fixed with 4% paraformaldehyde in phosphate buffered saline (PBS).

Alginate discs preparation

In situ forming alginate hydrogel matrices were prepared as previously described (Maia et al., 2014). Briefly, PRONOVA ultrapure sodium alginates LVG and VLFG (hereafter designated as high and low molecular weight, HMW and LMW, respectively) with a high guluronic acid content (68%) were purchased from FMC Biopolymers. Hydrogel-precursor solutions with a bimodal molecular weight composition were prepared by combining HMW and LMW alginate at a 1:1 volume ratio and at different total polymer concentrations (0.5, 1 and of 2% w/v). Primary rat astrocytes were added to alginate solutions (4x106 cells.mL^{-1}) with $CaCO_3$ (Ca^{2+}/COO^- molar ratio = 0.288) and δ-gluconolactone (GDL, Ca^{2+}/GDL molar ratio= 0.125), and the mixture was pipetted (20 µL) onto the wells of pHEMA-treated culture plates. After crosslinking (1h, 37ºC), cell-laden 3D matrices were maintained in culture for 7 days, in DMEM or CM.

Ibuprofen (0.04 M) and chondroitinase ABC (chABC) (0.1 U.mL-1) were added to the 3D cultures at day 7 of culture, and were maintained for additional 48 hours.

ATP quantification

ATP quantification was performed using the CellTiter-Glo Luminescent Cell Viability Assay (Promega) according to the manufacturer's recommendations. Briefly, the CellTiter-Glo® Reagent was added directly to cells cultured in serum-supplemented medium. This resulted in cell lysis and generation of a luminescent signal proportional to the amount of ATP present, which was measured in a luminescent plate reader (SYNERGY MX, BioTek). An ATP standard curve was performed using ATP disodium salt hydrate (Sigma).

Cell viability

At culture days 1, 3 and 7 alginate discs were incubated with a solution of calcein-AM (Promega) for 20 minutes, followed by 5 minutes incubation with propidium iodide (Sigma). Discs were rinsed in culture medium twice to wash any excess of calcein-AM and propidium iodide and finally observed under the confocal microscope.

For flow cytometry analysis, cells were firstly incubated with a 6 µM solution of propidium iodide (PI, Sigma-Aldrich) for 10 min at 37ºC. Cells were further extracted from the alginate disks using trypsin-EDTA and transferred to 96-well round bottom plates and washed with 150 µL of FACS Buffer (2% FBS in PBS 1X) by centrifuging for 3 min, 244g at RT. For data acquisition, cells were suspended in 150 µL of FACS Buffer and analyzed on a BD FACS Canto II cytometer using 530/30 and 670/LP optical filters. The cell population of interest was gated according to forward (FSC), side scatter (SSC) and fluorescence parameters using untreated cells. Doublets were excluded with FSC-peak (height) versus FSC-integral (area) gating. A total of 20 000 events were acquired per sample. Data was analyzed using FlowJo software version vX.0.7.

Neurite outgrowth quantification and cell motility

For axonal outgrowth assessment the length of the longest neurite was determined using AxioVision image analysis software. Neuronal processes were manually traced and quantified on a total of 95 cells per condition from 3 different samples. Cell motility was assessed using ImageJ software with the MTrackJ pluggin. The motility profile was traced for 30 cells per condition from 3 different samples.

Astrocyte infection

HEK293T cells at 80% confluence were co-transfected with JetPrime (PolyPlus Transfection) according to the manufacturer's instructions. Transfection ratios were as

follows: 3 mg of shRNA plasmids to 4.2 mg of psPAX2 to 2.7 mg of Vesicular Stomatitis Virus Glycoprotein (VSVG). Medium was replaced 4h after transfection, and cells were cultured for additional 48h. Medium with viral particles was then collected and centrifuged. Finally, supernatants containing viral particles were collected.
Infection of primary astrocytes was performed at 80% confluence with viral supernatants overnight. Infection medium was then replaced by fresh medium with puromycin. Cells were kept in culture for 7 -12 days.

Gene expression analysis

Cell lysis and RNA purification were performed using Quick-RNA MiniPrep from Zymo Resarch, according to the manufacturer's instructions. Reverse transcription was done with SuperScript III (Invitrogen).

RT-PCR

Primer sequences used for RT-PCR were as follows:
Gfap sense 5'AGGCTGGAGGCGGAGAAC3';
Gfap anti-sense 5'GCTGTGAGGTCTGGCTTGG3';
Vimentin sense 5'CGTGATGTCCGCCAGCAGTATG3';
Vimentin anti-sense 5'GGCATCCACTTCGCAGGTGAG3';
Collagen IV sense 5'AAGGCGAGGAAGGCATCATG3';
Collagen IV anti-sense 5'GGGTGAGTAGGCTGGAGGTC3';
Hprt sense 5'ATGGACTGATTATGGACAGGACTG3';
Hprt anti-sense 5'GCAGGTCAGCAAAGAACTTATAGC3'.
PCR was performed using HotStarTaq DNA polymerase (Quiagen) for 34 cycles. Quantification of band intensity was done using ImageLab software.

Quantitative RT-PCR

Quantitative real-time PCR (qPCR) was performed using Hprt as endogenous control to normalize the expression levels of the genes of interest. Analyses were performed on iG5 (Bio-Rad) using SYBR Green (SYBR Green master mix, Applied Biosystems) according to the manufacturer’s recommendations. Reactions were carried out in triplicate (40 cycles). In order to verify the specificity of the amplification, a melt-curve analysis was performed immediately after the amplification protocol. Non-specific products of PCR were not found in any case. Primer sequences used for qRT-PCR were as follows:
Gfap sense 5’GCGGCTCTGAGAGAGATTCG3’;
Gfap anti-sense 5’TGCAAACTTGGACCGATACCA3’;
RhoA sense 5’TCAGCAAGGACCAGTTCCCAGAGG3’;

RhoA anti-sense 5'AGGCCGCAGGCGGTCATAATCTTC3';
RhoB sense 5' TTTGCTCTGCACAGAGAATG3';
RhoB anti-sense 5'TGGTAAAGGAAGGCAACACG3';
RhoC sense 5' TAGCCAAAGGCACTGATCCT3';
RhoC anti-sense 5'GCATACCAGGAGAGAGCTGG3';
ROCK1 sense 5'CGAGAGTGTGACTGGTGGTC3';
ROCK1 anti-sense 5'CTGGTGCTACAGTGTCTCGG3';
Src sense 5'GGACAGTGGCGGATTCTA3';
Src anti-sense 5'GGTAGTGAGACGGTGACA3';
Hprt sense 5'ATGGACTGATTATGGACAGGACTG3';
Hprt anti-sense 5'GCAGGTCAGCAAAGAACTTATAGC3'.

Rheological analysis

Rheological measurements were carried out using a Kinexus Pro rheometer from Malvern with parallel-plate geometry with sandblaster surfaces, at 37ºC and with 10% of compression. First, the linear viscoelastic region was analyzed for all the samples by performing a stress sweep at constant frequency of 0.1Hz. Frequency sweeps in the linear viscoelastic regimen were used to determine values of elastic (G') and viscous (G'') modulus. Samples were analyzed at day 1 and 7 of culture (n=3 for each).

Gelatin zymography

Cells were switched to serum-free conditions for 24 hours. After 24 hours, cell culture supernatants were collected and kept at -20ºC until use. MMP-2 activity was analyzed by gel zymography. Zymography was performed using a 10% SDS-Page separating gel with 0,1% gelatin (Sigma). After running, the gels were incubated in re-naturation buffer (2% triton X-100) for 30 minutes, with soft agitation. Then zymogram gels were changed to a development buffer (50mM Tris-HCL, 10mM $CaCl_2$) overnight at 37ºC. Afterwards gels were stained with Comassie Blue for 20 minutes and finally de-stained with water. Band intensity was quantified using a densitometer (Bio-Rad) and quantity one software.

Collagen quantification

Collagen quantification was performed with the Sircol Collagen Assay (Biocolor), according to the manufacturer's recommendations. Briefly, collagen from samples was precipitated with Sircol dye and further dissolved. Colorimetric alterations were measured at 555 nm and results were quantified using a standard curve for collagen.

Immunocytochemistry

2D cultured cells were fixed with 4% (v/v) paraformaldehyde. 3D cultured cells were fixed as in 2D, but $CaCl_2$ was added to the solution to keep hydrogel disc integrity. Cells were further permeabilized and blocked in phosphate buffered saline (PBS), or instead in tris buffered saline with calcium chloride (TBS-$CaCl_2$) for 3D discs, containing 5% (v/v). Normal Goat Serum (NGS) (Biosource) and 0.2 % (v/v) Triton X-100 (Sigma). Primary antibodies were diluted in PBS or TBS-$CaCl_2$ containing 1 % (v/v) NGS and 0.15 % (v/v) Triton X-100, and incubated overnight in a humid chamber at 4 ºC. The following primary antibodies were used: rabbit anti-GFAP (1:500, Dako), mouse anti-vimentin (1:100, ThermoScientific), mouse anti-NG2 (1:100, Abcam), rat anti-MBP (1:500, AbD Serotec) rabbit anti-TAU (1:100, Sigma), mouse anti-CSPG (1:200,Millipore). Secondary antibodies Alexa-Fluor 488, 568, 594 and 660 were applied for 1h at RT and subsequently treated for nuclear counterstaining at RT with Hoechst (Molecular Probes) at 2µl.ml^{-1}. 3D samples were then observed under confocal microscope.

Western blot

Cells were washed with PBS and lysed in lysis buffer (1 mM sodium orthovanadate, protease inhibitor cocktail (Amersham), 50mM TRIS, 1% (v/v) nonyl phenoxypolyethoxylethanol (v/v), 0.5% (wt/v) sodium deoxycholate, 0.1% (wt/v) sodium dodecyl sulphate. Protein lysates (30 µg/lane) were run on a 12% SDS-Page gel and then transferred to nitrocellulose membranes (Amersham). For Western blot analysis, membranes were blocked with blocking buffer (5% (w/v) non-fat dried milk in tris-buffered saline (TBS) plus 0.1% (v/v) Tween 20) and incubated overnight at 4°C in 5% (w/v) bovine serum albumin (BSA) in TBS plus 0.1% Tween 20 with primary antibodies. The following primary antibodies were used: mouse anti-GAPDH (1:10000, HyTest), rabbit anti-ROCK2 (1:10000, Abcam), rabbit anti-ROCK1 (1:3000, Abcam), rabbit anti-RhoA (1:1000, Cell Signalling), rabbit anti-RhoC (1:1000, Cell Signalling), rabbit anti-phospho-Src Tyr 409 (1:1000, Cell Signalling), rabbit anti-Src (1:1000, Cell Signalling), rabbit anti-CSK (1:1000, Cell Signalling), mouse anti-GFAP (1:500, BD Pharmingen), mouse anti-vimentin (1:500, Thermo Scientific), rabbit anti-profilin1 (1:3000, Abcam).

For chondroitin 4 sulphate quantification cell lysates were first treated with chondroitinase ABC 0.05 UN/ml for 2 hours at 37ºC, as previously described (Chan et al., 2007), and then loaded 12% SDS-Page gel and transferred to nitrocellulose membranes (Amersham). Mouse anti-C4S (1:1000, Millipore) primary antibody was used.

Band intensity was quantified using a densitometer (Bio-Rad) and quantity one software, for all membranes. For a semi-quantitative evaluation of the C4S expression all bands present in each lane were quantified.

Förster resonance energy transfer analysis

Astrocytes plated on glass-bottom culture dishes (µ-Dish 35 mm, iBidi) and transfected with the FRET probes for RhoA (Raichu-EV-RhoA, ref pmid 12860967) or Src (KRas-Src-YPet, ref pmid 18799748) were imaged in an inverted epifluorescence microscope (DMI6000B, Leica Microsystems). The donor fluorescent protein was excited with a mercury lamp coupled to a light attenuator (EL6000, Leica Microsystems), and the emission of both donor and acceptor fluorescent proteins was acquired with a digital CMOS camera (4x4 binning, ORCA-Flash4.0 V2, Hamamatsu Photonics). A 440-520 nm dichroic mirror (CG1, Leica Microsystems) was used together with appropriate emission and excitation filters mounted in external filter wheels (Fast Filter Wheels, Leica Microsystems). LAS AF software (Leica Microsystems) was used to control all modules. Raw images were background subtracted and time-lapse videos representing FRET ratio values (FRET/Donor or Donor/FRET) were generated. Regions of interest were drawn over cells and detailed analysis was performed to generate time-plots. Videos were converted to intensity modulated display mode using custom ImageJ macros and FRET channel as intensity modulator. Src kinase inhibitor (SKI-1) was added (200nM) as a chemical inhibitor of SRC.

Statistical analysis

Statistical analysis was performed using the Graphpad Prism program (version 5). Statistical differences between groups were determined based on one-way ANOVA tests followed by Tukey's post-hoc analysis (multiple comparisons) or t-student tests (2 group comparison). When Gaussian distribution was not confirmed (D'Agostino and Pearson omnibus normality analysis), non-parametric tests were applied. Man-Whitney test and Kruskal-Wallis test followed by the Dunn's multiple comparison test were used in the case of paired and multiple comparisons, respectively. Data are expressed as the mean ± standard deviation and p values <0.05 were considered significant.

RESULTS

Meningeal fibroblasts conditioned medium mimics fibroblast infiltration and activates astrocytes.

Astrocytes were cultured in the presence of meningeal fibroblasts conditioned medium (CM). The metabolic activity of astrocytes increased with culture time in both control and CM conditions (Figure 1A). Astrocytes cultured in the presence of CM showed increased

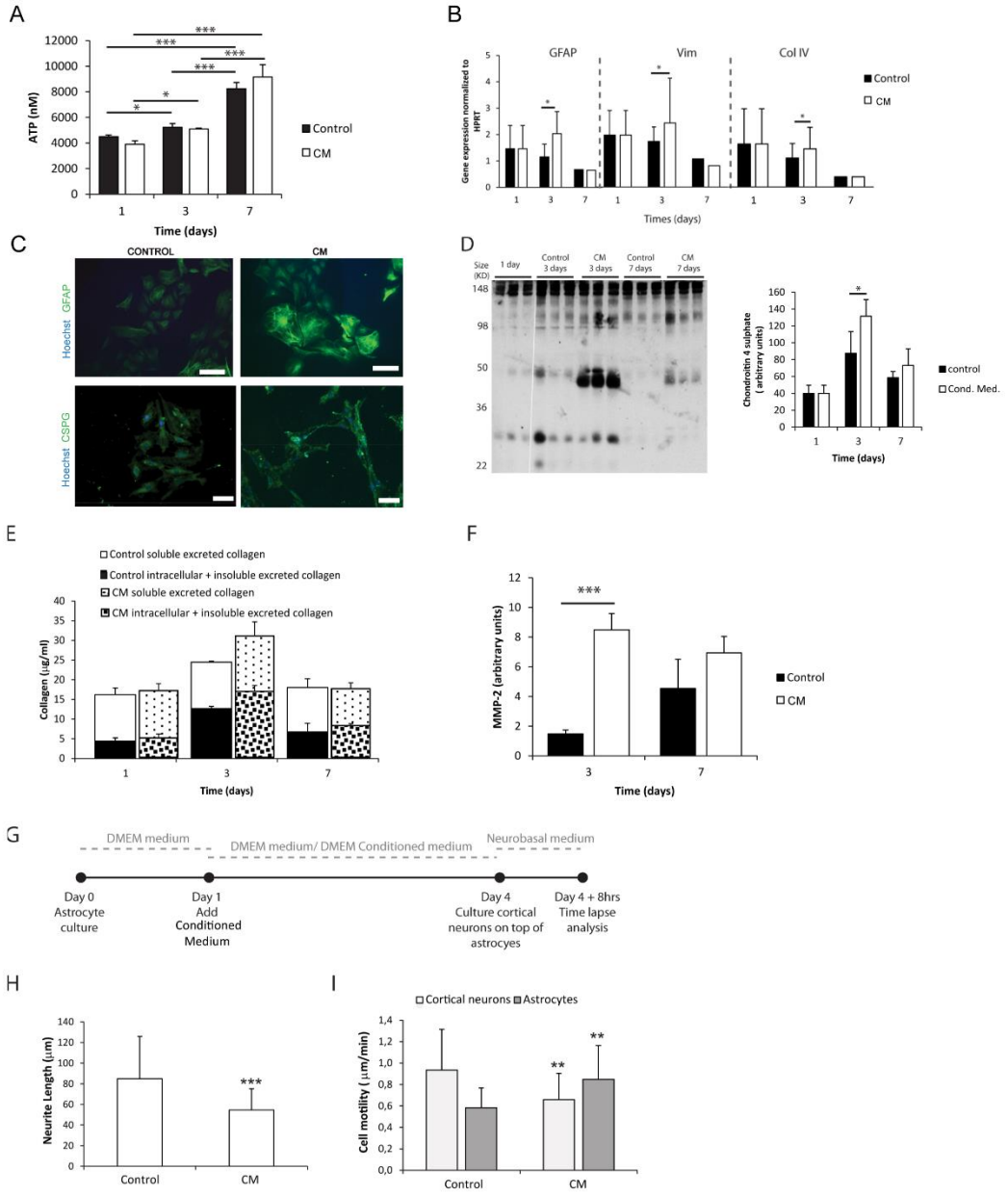

Figure 1 – Astrocyte 2D culture in the presence or absence of meningeal fibroblasts conditioned medium (CM). Results are shown as mean ± standard deviation; asterisks represent statistical differences, * $p < 0.05$, ** $p < 0.01$, ***$p < 0.001$ **A.** ATP levels at 1,3 and 7 days of culture (n=6, statistical analysis was performed

between all pairs of columns); **B.** mRNA levels of astrocytes at 1,3 and 7 days of culture (n=6, statistical analysis was performed between control and CM conditions at each time point); **C.** Immunocytochemistry of astrocytes cultured in the presence of CM and control conditions, scale bar 100 μm; **D.** Quantification of Chondroitin 4 sulphate (C4S) at 1, 3 and 7 days of culture. For each time point 3 samples from independent experiments were loaded in the gel. Quantification graph refers to whole lane (n=3, statistical analysis was performed between control and CM conditions at each time point); **E.** Collagen quantification during the cell culture time. Collagen was measured in the supernatant (collagen excreted to the culture medium) and in the culture well (Deposited and cytoplasmic collagen) (n=3; no statistical differences were found); **F.** MMP expression levels (n= 3, statistical analysis was performed between control and CM conditions at each time point).

Effect of control and CM treated astrocytes on cortical neurons; **G.** Experimental set-up. Astrocytes were cultured for 4 days with fresh medium or conditioned medium. At day 4 cortical neurons were cultured on top of the astrocytes for additional 4 days; **H.** Effect of astrocytes on axonal outgrowth (n = 95 cells); **I.** Cell migration velocity (n= 30 cells).

expression of astrogliosis hallmark genes as Gfap and Vimentin (Figure 1B) and proteins as GFAP and C4S at 3 days when compared to controls (Figure 1C and 1D). Although no statistical differences were found between control and CM, total collagen expression levels, both intracellular and deposited non-soluble collagen, also peaked upon 3 days of culture (Figure 1E). Additionally, astrocytes cultured with CM exhibited significantly increased levels of excreted active MMP-2 upon 3 days of culture compared with controls (Figure 1F). When neurons were co-cultured with astrocytes, which had been previously cultured in CM (Figure 1G), neurite length was significantly impaired (Figure 1H). Moreover, the motility of these neurons was diminished whereas astrocyte motility increased (Figure 1I).

Astrocytes can be successfully cultured within 3D alginate matrices.

Astrocytes were cultured within alginate hydrogel discs of different alginate content as illustrated in Figure 2A and Image 1, namely 2%, 1% and 0.5% alginate. Astrocytes remained viable throughout the 7-day culture period (Figure 2A-B). ATP consumption levels varied in time, deepening at the third day of culture to recover initial values at day 7 (Figure 2C). Such reduction in ATP levels was not the result of a decrease in cell viability, as flow cytometry analysis showed that independently of the culture time and tested conditions, 95% of cells were propidium iodide negative (Figure 2B).

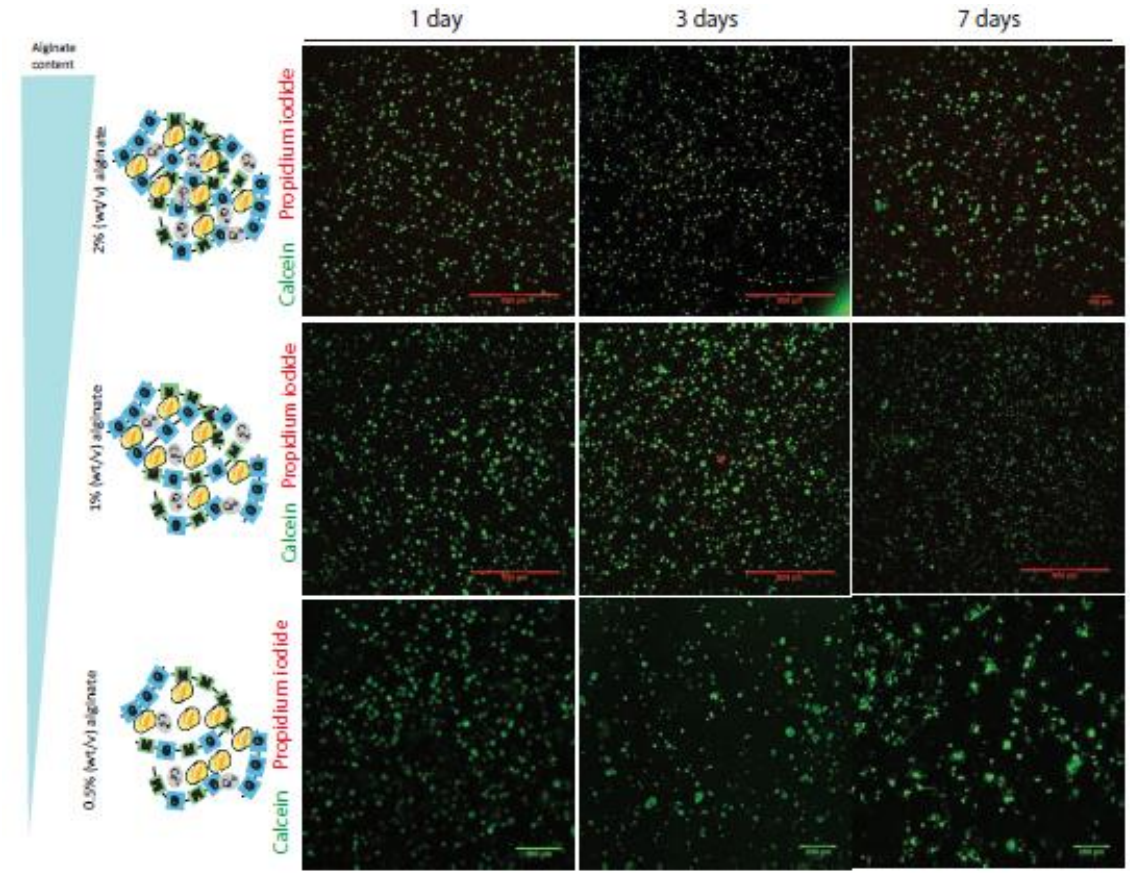

Image 1 – Evaluation of cell viability of 3D cultured control astrocytes. Representative photos of live-dead assay. Live cells are stained with Calcein-AM (green) and dead cells are stained with propidium iodide (red).

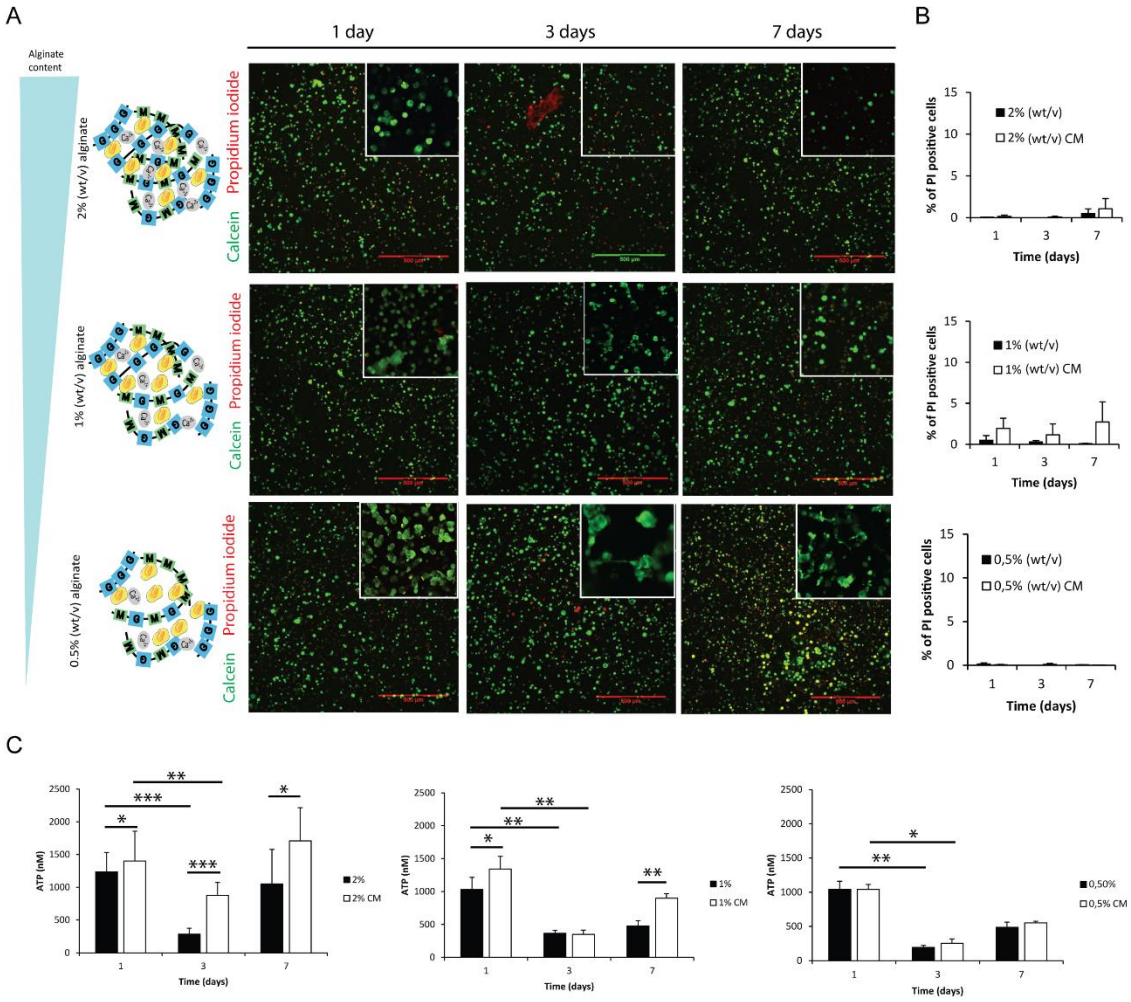

Figure 2 – Evaluation of cell viability and metabolic activity within 3D alginate discs. Results are shown as mean ± standard deviation; asterisks represent statistical differences * $p < 0.05$, ** $p < 0.01$, ***$p < 0.001$ **A.** Representative photos of live-dead assay for astrocytes cultured in the presence of fibroblast conditioned medium (CM). Live cells are stained with Calcein-AM (green) and dead cells are stained with propidium iodide (red); **B.** Quantification of dead cells (propidium iodide) by FACS analysis at 1,3 and 7 days of culture (n=3 pools of 10000 events); **C.** ATP levels of the 3D culture astrocytes at 1,3 and 7 days of culture (n=6).

3D cultured astrocytes acquire a reactive-like phenotype.

Astrocytes cultured within alginate matrices show different gene expression levels when cultured in the presence or absence of meningeal fibroblasts CM (Figure 3A). Particularly, Gfap and Vimentin levels are differently regulated after 7 days of culture. Only astrocytes cultured within 1% alginate discs showed increased expression of both Gfap and Vimentin when cultured in CM. Although Collagen IV mRNA expression levels were not significantly different between CM and control culture conditions (Figure 3A), the presence of CM induced astrocytes to increase collagen excretion levels at 1 and 3 days of culture (Figure 3B). At day 7, significant differences were only seen on astrocytes cultured in 1% alginate

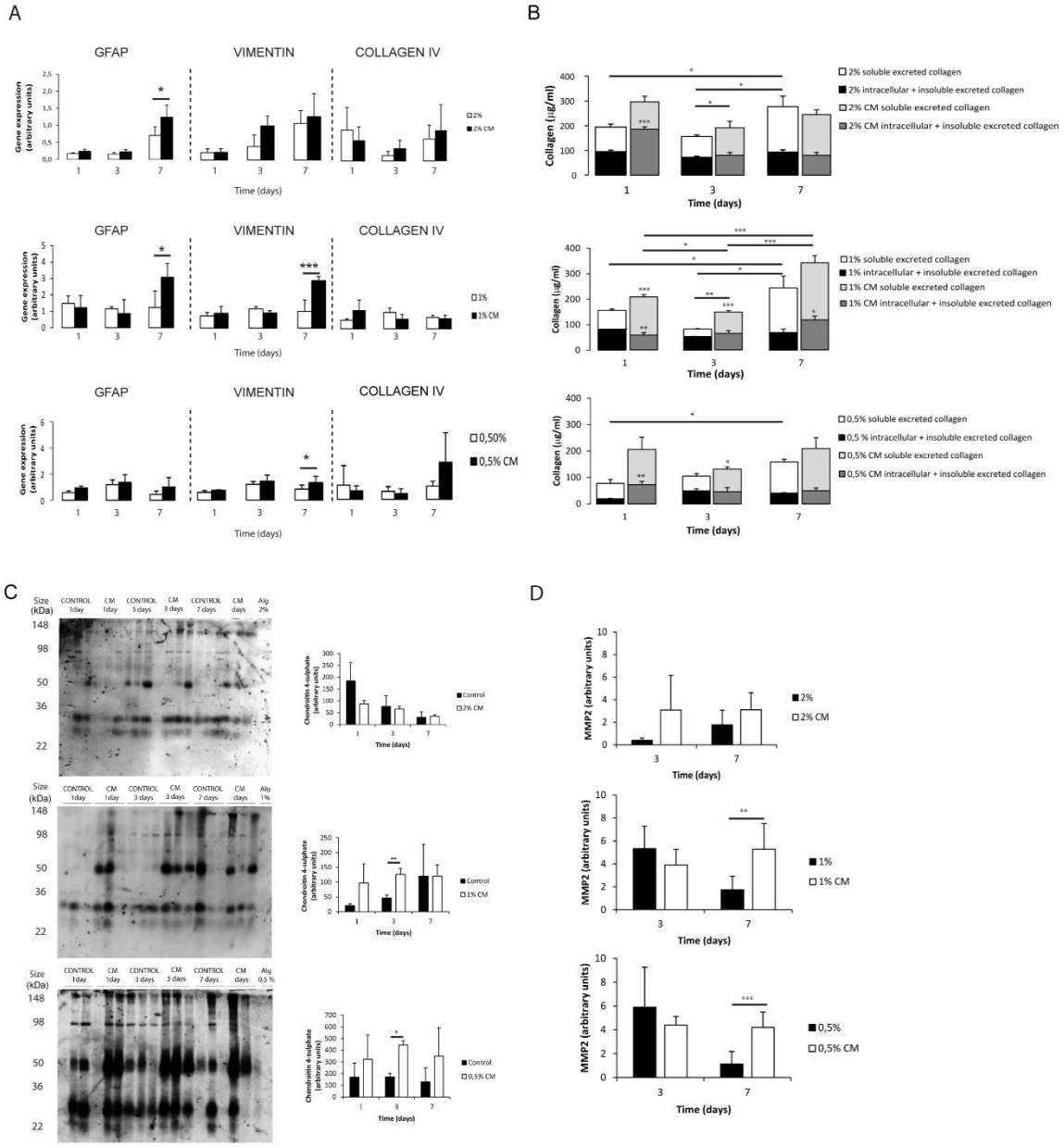

Figure 3 – Phenotype and matrix production of 3D seeded astrocytes. Results are shown as mean ± standard deviation; asterisks represent statistical differences, * $p < 0.05$, ** $p < 0.01$, ***$p < 0.001$ **A.** mRNA levels for Gfap, Vimentin and Collagen IV of astrocytes seeded within alginate discs; **B.** Collagen quantification at 1, 3 and 7 days of culture. Collagen was measured in the supernatant (collagen excreted to the culture medium) and in the alginate disc (Deposited and cytoplasmic collagen) (n= 3), regarding statistical analysis asterisks alone represent differences between of one component (excreted or intracellular collagen) and the control, asterisks above the bars with guidance line represent differences between total collagen levels; **C.** Quantification of chondroitin 4 sulphate (C4S) at 1, 3 and 7 days of culture. For each time point 3 samples from independent experiments were loaded in the gel. Quantification graphs refer to whole lane (n=3); **D.** MMP-2 activity at 3 and 7 days of culture (n= 4).

discs. Moreover, collagen levels were found to be 10 times higher in all alginate formulations than those found for 2D cultured astrocytes (Figure 1E, Figure 3B). Additionally, alginate content appears to affect collagen production levels, with cells cultured in gels with a higher alginate content producing, in general, more collagen than those seeded in gels with a lower alginate content. Nevertheless, it is important to say that this is not true for astrocytes seeded in 1% alginate discs in the presence of CM upon 7 days of culture, as these present higher levels of collagen production than the ones cultured in 2% alginate discs in the presence of CM. Furthermore, the presence of CM also induces 3D cultured astrocytes to produce higher levels of CSPG, with a significant increase of CSPG levels at day 3 of culture (Figure 3C). No significant differences were found between 2D and 3D conditions CSPG levels (Image 2). Upon 7 days of culture MMP-2 expression levels were also found to be upregulated in astrocyte cultures in 1% and 0.5% (Figure 3D).

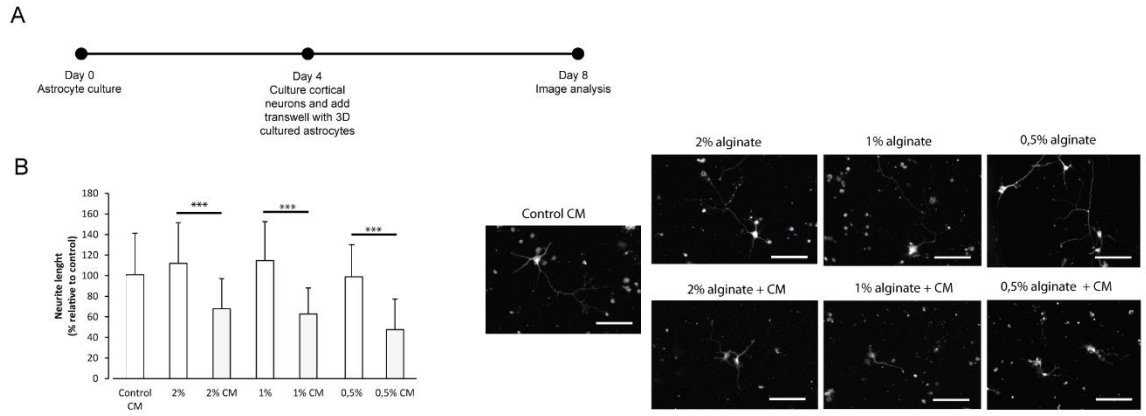

Figure 4 – Effect of control and CM treated astrocytes seeded in 3D alginate discs on cortical neurons. Results are shown as mean ± standard deviation; asterisks represent statistical differences ***p <0.001 **A.** Experimental set-up. Astrocytes were cultured for 4 days with fresh medium or conditioned medium. Neurons were cultured on glass cover-slips in 24 well-plates, alginate discs were placed on top of neurons using transwells; **B.** (Left) Effect of astrocytes on axonal outgrowth (n = 95 cells); (right) immunocytochemistry of cultured cortical neurons with anti-TAU, at the day of image analysis, scale bar 100 µm.

To further confirm the reactive phenotype of the 3D cultured astrocytes, cortical neurons were co-cultured with 3D astrocyte cultures. Neurite outgrowth was impaired when neurons were co-cultured with 3D astrocyte cultures treated with CM, for all alginate formulations (Figure 4).

3D seeded astrocytes influence hydrogels mechanical properties.

The calculated mesh size of the hydrogels was found to be dependent on alginate content. The 2% alginate discs showed a smaller mesh size than 1% alginate discs and 0.5% alginate discs presented the highest mesh size (Image 3).

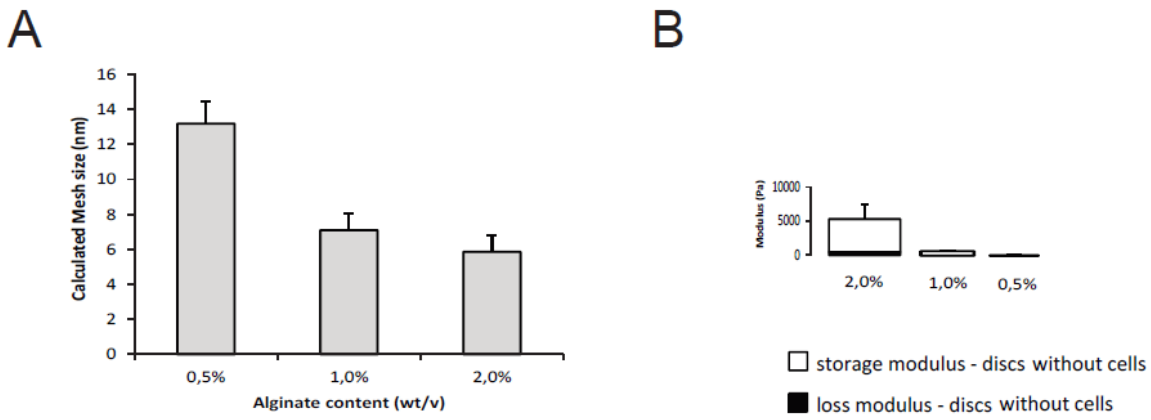

Image 3 – Physical properties of the alginate discs. A. Calculated mesh size of the tested alginate formulations; B. Rheological properties of alginate discs without astrocytes.

Mechanical properties of alginate discs with and without astrocytes were analyzed by rheometry. Alginate hydrogels presented typical mechanical spectra of gels with a solid-like character (G'-storage modulus) predominant over liquid-like viscous response (G''-loss modulus). Moreover, the mechanical properties of hydrogel discs varied in an alginate content dependent manner (Image 3). A 10-fold difference in stiffness was observed between consecutive alginate formulations (from 2% to 1%, and from the latter to 0.5%, Image 3 and Figure 5).

Astrocytes cultured in the presence of CM were able to dynamically alter their original mechanical environment and reinforce the overall disc mechanical properties. This stiffening of the storage modulus was particularly clear for astrocytes cultured with CM in 1% alginate discs at 24 hours (Figure 5), with statistically higher storage modulus values than those of discs with astrocytes and of discs without cells. In general, storage modulus values of discs with astrocytes, cultured with or without CM, decreased from day 1 to day 7.

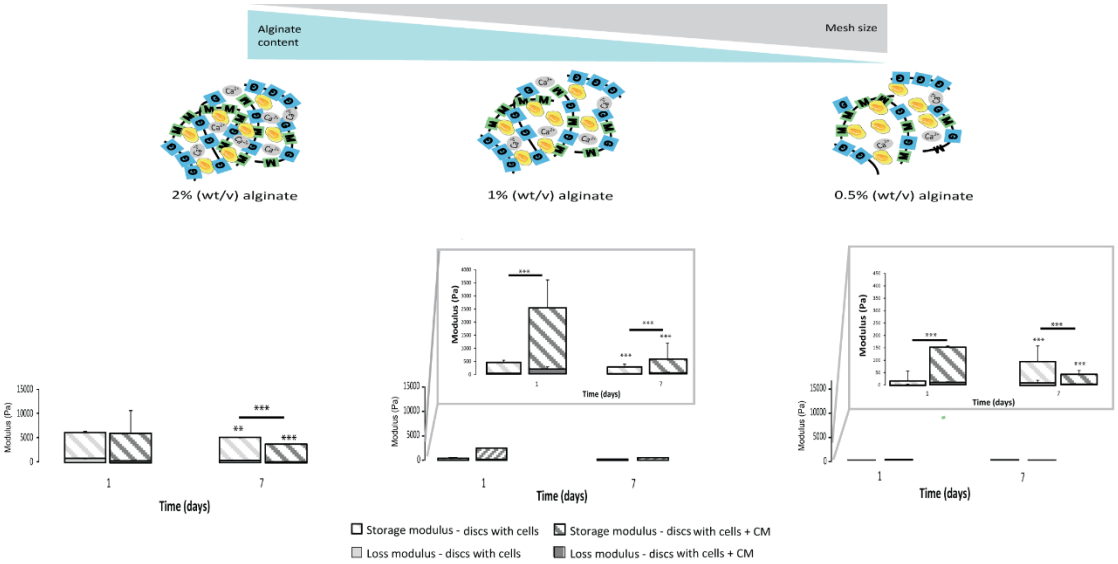

Figure 5 – Physical properties of the 3D alginate discs. Rheological properties of the 3D alginate discs incubated with culture medium or with astrocytes in the presence or absence of CM (n=3). Results are shown as mean ± standard deviation; asterisks represent statistical differences,), regarding statistical analysis asterisks alone represent differences between storage modulus, asterisks above the bars with guidance line represent differences between total levels, ** p < 0.01, ***p <0.001.

The Rho-ROCK signaling pathway regulates astrocyte reactivity

The Rho-ROCK signaling pathway was investigated as a possible mediator of astrocyte activation and consequent production of inhibitory molecules. Small hairpin RNAs were initially used to knockdown several members of the Rho family (RhoA, RhoB and RhoC).

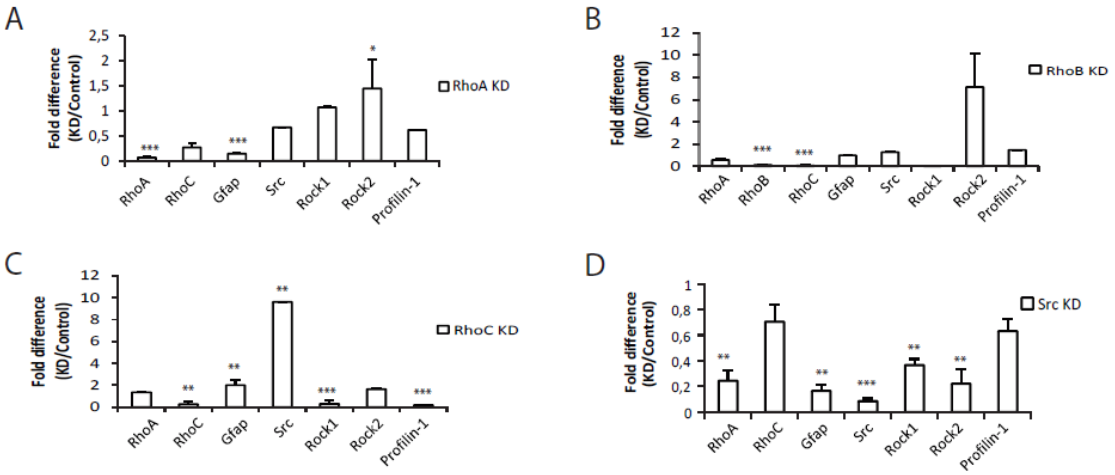

Image 4 – qPCR data for astrocyte knockdowns. Data is presented as mean ± standard deviation, statistical analysis was performed in relation to control samples, statistical comparisons were performed between conditions at each time point, * p < 0.05, ** p < 0.01, ***p <0.001 **A.** RhoA knockdown astrocytes; **B.** RhoB knockdown astrocytes; **C.** RhoC knockdown astrocytes; **D.** Src knockdown astrocytes.

Knockdowns were validated in astrocytes by qPCR, with consistent high gene-knockdown (superior to 70%) being achieved (Image 4).RhoA and RhoC knockdowns had a significant influence on Gfap expression in astrocytes, as RhoA knockdown resulted in decreased levels of Gfap, and RhoC knockdown in increased Gfap levels. Moreover, RhoA and RhoC knockdown also caused alteration in Src gene expression (Image 4).Knockdown influence on protein expression was determined by western blot (Figure 6A-B). All knockdowns resulted in significantly reduced levels of protein, with RHOA and RHOC protein levels decreased by 99%. Western blot analysis confirmed that RhoA and RhoC knockdown and respective proteins differently affect GFAP protein levels (Figure 6A-D), with RhoA knockdown resulting in down-regulation of GFAP protein levels and RhoC and RhoB knockdown in up-regulation of those levels. The effect of RhoA in GFAP levels was further confirmed following the ablation of RhoA in RhoAlox/lox astrocytes (Figure 6C-D).

c-src regulates rhoA activity

The src family has been shown to cross-talk with Rho during intracellular signaling, src kinase is further known to bind and phosphorylate RhoGDI both in vitro an in vivo at Tyr 156 (DerMardirossian et al., 2006, Belsches et al., 1997).

RhoA and RhoB knockdowns resulted in up-regulation of c-SRC while RhoC knockdown resulted in SRC down-regulation (Figure 6E-F). c-src knockdown not only resulted in c-SRC downregulation but also impacted the levels of total Src family tyrosine kinase (SFK) activity as demonstrated by the reduction in Tyrosine 416 phosphorylated SFK levels (Figure 6G-H).

Knocking down c-src also resulted in down-regulation of RHOA and RHOC protein levels. To investigate whether SRC regulates RHOA activation, we measured RHOA activity in astrocytes using a Förster Resonance Energy Transfer (FRET)-based sensor for RHOA with enhanced sensitivity, and show that inhibition of c-SRC by the SRC pharmacological inhibitor Ski-1 resulted in decreased RHOA activity (Figure 6I). In contrast, knocking down RhoA did not significantly influence c-SRC activity, as measured by a FRET-based sensor for c-SRC. Interestingly, c-SRC activity was significantly increased in RHOC knockdown astrocytes (Figure 6I).

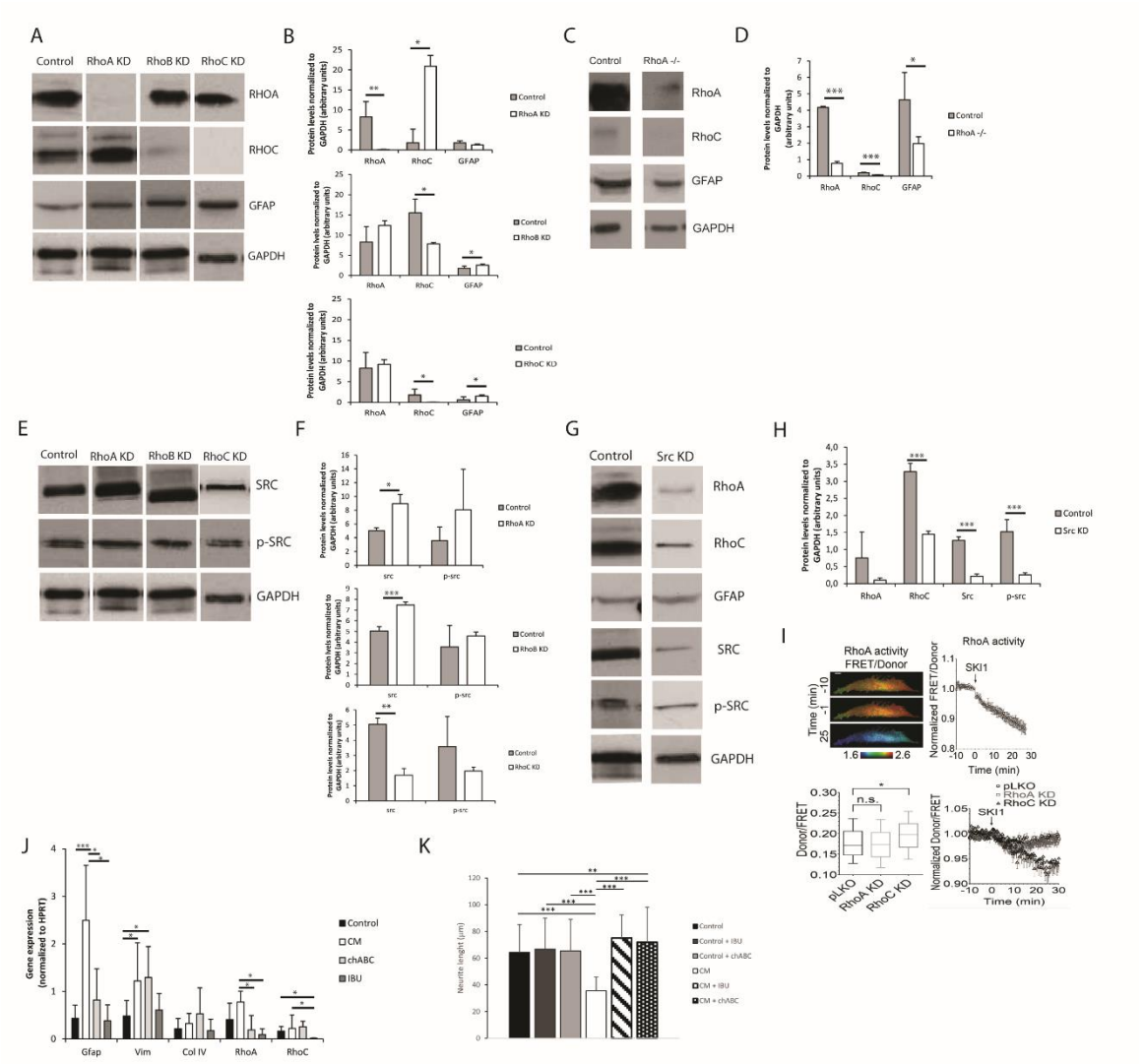

Figure 6 – The Rho-ROCK pathway influence on astrocyte reactivity. Results are shown as mean ± standard deviation; statistical analysis was performed between conditions at each time point, * $p < 0.05$, ** $p < 0.01$, ***$p < 0.001$ **A.** Representative images of western blots of RHOA, RHOC and GFAP levels on RhoA, RhoB and RhoC knockdown astrocytes; **B.** Western blot quantification (n=3); **C.** Representative images of western blot of lox/lox RhoA -/- ; **D.** Western blot quantification (n=3); **E.** Representative images of western blot of c-SRC levels on RhoA, RhoB and RhoC knockdown astrocytes; **F.** Western blot quantification (n=3); **G.** Representative images of western blot from Src Knockdown astrocytes; **H.** Western blot quantification (n=3); **I.** FRET analysis of RHOA and SRC activity in astrocytes. SKI-1 was used as a chemical inhibitor of SRC; **J.** Effect of the treatment of reactive astrocytes with 0.1 U/ml chABC and 0,04M ibuprofen. Astrocytes were cultured for 7 days in the presence of CM and then treated with chABC or Ibuprofen for 48 hours. (KD stands for knockdown); K. Effect of reactive astrocytes treated with chABC or ibuprofen (IBU) on cortical neurons. Neurons were cultured in glass coverslips and alginate discs with astrocytes were placed on top using transwells.

Astrocyte reactivity is reverted via RhoA inhibition.

Astrocytes were cultured within 1% alginate discs in the presence of CM, and after 7 days of culture chondroitinase ABC (chABC) or ibuprofen (IBU) were added to the culture medium. Activated astrocytes treated with chABC showed significantly lower RhoA levels than those untreated (CM-activated), and comparable to the control levels (Figure 6J). Gfap expression levels followed a similar trend. Nevertheless, Vimentin levels were not different from those of CM-treated astrocytes and were statistically higher than those of control cells. Regarding cells treated with ibuprofen, RhoA levels were also significantly reduced when compared to CM-treated astrocytes, to levels comparable to control cells. Gfap and Vimentin expression levels were also significantly reduced, when compared to CM-treated cells, and were at comparable levels of the control. RhoC levels were also significantly reduced in comparison to all tested conditions (Figure 6J).
In order to further confirm astrocyte phenotype recovery, astrocytes cultured within 1% alginate discs treated with chABC and IBU were co-cultured with cortical neurons (Figure 6K). Neurite outgrowth was not impaired when neurons were co-cultured with 3D cultured astrocytes treated with chABC or IBU (Figure 6K).

DISCUSSION

A tissue-engineered astrogliosis 3D-culture model is of added value. It is more physiologically relevant than the existing 2D models, as it can recapitulate better cellular interactions in vivo. This is particularly significant when considering astrocytes, which are known to form a 3D cellular network that extends throughout the brain (Mathewson and Berry, 1985). The role of this network is not well understood yet; however, it likely plays a pivotal role in astrocytic response to injury, since most brain pathologies result in some degree of deformation of this structure (Ostrow and Sachs, 2005). Alginate hydrogels are an attractive choice for such models for several reasons: firstly because of its mechanical properties, which are similar to the brain's mechanical properties (Banerjee et al., 2009); secondly, it works as an inert backbone structure that allows the control over system's complexity (Rowley et al., 1999, Lutolf and Blau, 2009); finally, an extremely relevant feature is that the cross-linking of these hydrogels can be reversed with the use of quelators (e.g. EDTA), enabling the recovery of the cultured cells for further biochemical and cellular assays. Here, the glial scar environment was closely recreated by stimulating astrocytes culture in alginate hydrogels with tuned mechanical properties with fibroblast CM.

Astrocyte activation with CM, and their consequent ability to inhibit axonal outgrowth, was validated in 2D astrocytic cultures (Figure 1). To the best of our knowledge meningeal fibroblast's CM has never been used to induce astrocyte reactivity. Some authors have previously explored co-cultures of cerebral astrocytes and meningeal fibroblasts (Kimura-Kuroda et al., Abnet et al., 1991, Struckhoff, 1995, Hirsch and Bahr, 1999, Wanner et al., 2008), nevertheless, the use of CM enables an increased control over the model system variables.

Given the mild gelation conditions, astrocytes remain viable when cultured within the tested alginate hydrogels (Figure 2A-B). The reduction of ATP levels at 3 days of culture may be explained by an initial adaptation phase of astrocytes to the new surrounding environment. Reactive astrocytes are known to have increased metabolic activity (Zamanian et al., 2012), and astrocytes cultured in the presence of CM showed increased activity in 2 and 1% alginate discs when compared to control (Figure 2C), which was not observed in 2D astrocytic cultures (Figure 1A). The presence of CM significantly induced an increase in expression levels of Gfap and Vimentin (Figure 1B, Figure 3A) in cultured astrocytes. Intermediate filaments augmentation is widely correlated with astrogliosis and glial scaring (Wanner et al., 2008, Kimura-Kuroda et al., 2010, Nair et al., 2008, Ogier et al., 2005, Wang et al., 2004, Middeldorp and Hol, 2011).

Increased deposition of ECM molecules and their interaction with local cells is considered an important factor in the non-permissive nature for CNS repair (Sobel and Mitchell, 1989, van Horssen et al., 2007). For this reason, ECM production was assessed. Increased CSPGs production is also a hallmark of astroglisosis and is known to play a pivotal role in neurite outgrowth inhibition (Jones et al., 2003, Galtrey and Fawcett, 2007). In fact, astrocytes seeded in the presence of CM have shown increased CSPGs production levels (Figure 1 C-D, Figure 3C) and were further shown to inhibit neuronal outgrowth (Figure 1H, Figure 4B). This is particularly relevant, as many authors have considered cultured astrocytes too immature to mimic reactive astrogliosis because they would promote rather than inhibit neurite outgrowth (Fallon, 1985, Smith et al., 1990). In addition to the CSPG analysis already mentioned, collagen levels were also assessed. Interestingly, collagen production was 10 times higher in 3D cultured astrocytes than in 2D (Figure 1E, Figure 3B). The increased collagen production in 3D astrocyte cultures in comparison to the 2D cultures, suggests an important role of the 3D structure in regulating ECM production. Within the 3D culture, collagen levels were significantly increased by the presence of CM in astrocytes cultured within 2 and 1% discs.

MMPs are known to be up-regulated in reactive astrocytes under pathological conditions (Rivera et al., 1997, Rathke-Hartlieb et al., 2000). In addition, MMP-2 (a type IV collagenase) was shown to be the most active enzyme in the degradation of myelin basic

protein (MBP) (Chandler et al., 1995). Increased MMP-2 activity was seen in 2D cultures at 3 days of culture (Figure 1F). In the established 3D systems, MMP-2 activity was found to be indirectly proportional to the alginate content (Figure 3D). Moreover, upon 7 days of culture, astrocytes cultured within 1 and 0.5% alginate in the presence of CM showed significantly increased MMP-2 activity.

Overall, astrocytes cultured in CM within 1% alginate discs resembled more closely scar astrocytes as these showed increased gene expression levels of Gfap and Vimentin (Figure 3A), as well as increased ECM production (Figure 3B-C). However, as the CM stimulus was present in all tested alginate formulations, astrocytes were probably capable of sensing and responding to the physical microenvironment they were in, as this was the only variable of the systems. Therefore, to further elucidate the differences in matrix stiffness of the different alginate formulations under study, rheological studies were performed and mesh size was estimated.

Calculated mesh size varied slightly, within the nanometer range, in the three tested alginate formulations with values below the cellular size (Image 3) so, it can be considered that it was possible to change the matrices mechanical properties independently of the mesh size. The prepared hydrogels showed a viscoelastic behavior, typically observed in ECM-derived hydrogels (Bott et al., 2010). As expected, the discs with higher alginate content showed higher stiffness values (Image 3). Furthermore, it was possible to observe that astrocytes in softer alginate matrices (1 and 0.5%) effectively stiffened the hydrogel after 24 hours of culture with CM (Figure 5). This effect was particularly evident for astrocytes cultured within 1% alginate matrices, which can be correlated with the increased production of collagen and/or CSPG (Figure 3B-C). As cellular behavior was significantly affected by the mechanical properties of the alginate 3D matrices, the only variable parameter, we hypothesized that astrocyte activation is mediated by a mechanosensing pathway.

The Rho/ROCK signaling pathway is known to play a critical role in the assembly of actin stress fibers in response to applied mechanical forces (Aikawa et al., 1999, Putnam et al., 2003). Moreover, the small GTPase Rho is a key regulator of intracellular contractility allowing cells to sense matrix stiffness and respond to mechanical cues (Wozniak et al., 2003). Taking this in consideration, the Rho/ROCK signaling pathway was explored as a possible mediator of astrocytic activation.

Data from qPCR and western blot have shown that RhoA and RhoC differently regulate Gfap expression, with RhoA knockdown decreasing Gfap expression while RhoC knockdown up-regulates it (Image 4, Figure 6). As such, RhoA is here promoting Gfap expression while RhoC is blocking it. Western blot data suggests that c-SRC regulation is closely correlated with RHOA (Figure 6). FRET analysis showed that c-SRC is positively

regulating RHOA activation levels, as chemical inhibition of SRC with SKI-1 in astrocytes induced a decrease in RHOA activity. Furthermore, these results show that in astrocytes c-SRC is responsible for part of the SFK activity.

RHOA has previously been shown to play a role in focal adhesion formation in astrocytes (Khatiwala et al., 2009, Matthews et al., 2006), and inhibition of the Rho/ROCK signaling pathway was shown to increase astrocyte reactivity (Chan et al., 2007, Lau et al., 2011); nonetheless, so far to the best of our knowledge no one has shown the individual influence of RHOA and RHOC on GFAP expression in astrocytes. This makes RHOA an interesting therapeutic target for astrogliosis treatment.

To further assess the role of Rho/ROCK signaling in the 3D culture model, astrocytes were cultured in the presence of two drugs known to affect RhoA: ibuprofen and chABC. Non-steroidal anti-inflammatory drug Ibuprofen was previously shown to effectively block RhoA (Wang et al., 2009, Dill et al., 2010), and the latter is known to mediate the inhibition of axonal regeneration by myelin and CSPGs (Walker et al., 2013, Yiu and He, 2006). Although RhoA has been mostly studied in neurons, our data suggests that it can be a pivotal modulator of astrocyte behavior. Astrocyte reactivity appeared to be achieved through increased RhoA levels and not RhoC's reduction. Moreover, analysis of gene expression levels revealed that treatment with Ibuprofen or chABC had an impact on RhoA levels as those of treated cells were significantly lower than those of reactive astrocytes. Moreover, Gfap levels were also significantly reduced to levels comparable to the control (Figure 6J). Although ibuprofen and chABC are known to target different molecules they both inhibited RhoA. Ibuprofen is known to directly inactivate RhoA while chABC is known to degrade the ECM. These results reinforce the idea that ECM remodeling is a cause of astrocyte reactivity and, as such, when ECM is degraded by chABC astrocyte phenotype is recovered. As such, RhoA inhibition on reactive astrocytes, either through chABC or ibuprofen treatment, generated an environment permissive to neurite outgrowth.

Overall, this work established the potential of a glial scar like hydrogel based 3D model. Cells in this culture model behaved similarly to scar astrocytes, showing changes in gene expression and increased ECM production leading to neuronal outgrowth inhibition. Moreover, exploring the mechanisms regulating astrogliosis showed a pivotal role of RhoA in astrocyte reactivity. As such, RhoA is here seen as a therapeutical target while Ibuprofen and chABC are explored as possible approaches to diminish astrogliosis.

This simple, controlled and reproducible 3D culture system constitutes a good scar-like system and offers great potential in future neurodegenerative mechanism studies, as well as in drug screenings envisaging the development of new therapeutic approaches.

ACKNOWLEDGEMENTS

The financial support of the FEDER funds through the Programa Operaional Factores de Competitividade – COMPETE and Portuguese funds through the Fundação para a Ciência e a Tecnologia (FCT) (PEstC/SAU/LA0002/2013) is gratefully acknowledged. DN Rocha acknowledges FCT for her PhD scholarship /SFRH/BD/64079/2009).
Authors thank Dr. Michiyuki Matsuda (Kyoto University, Japan) for the RhoA FRET probe with enhanced sensitivity and Dr. Yingxiao Wang (University of California, USA) for the Src FRET probe.

REFERENCES

ABNET, K., FAWCETT, J. W. & DUNNETT, S. B. 1991. Interactions between meningeal cells and astrocytes in vivo and in vitro. Brain Res Dev Brain Res, 59, 187-96.
AIKAWA, R., KOMURO, I., YAMAZAKI, T., ZOU, Y., KUDOH, S., ZHU, W., KADOWAKI, T. & YAZAKI, Y. 1999. Rho family small G proteins play critical roles in mechanical stress-induced hypertrophic responses in cardiac myocytes. Circ Res, 84, 458-66.
BANERJEE, A., ARHA, M., CHOUDHARY, S., ASHTON, R. S., BHATIA, S. R., SCHAFFER, D. V. & KANE, R. S. 2009. The influence of hydrogel modulus on the proliferation and differentiation of encapsulated neural stem cells. Biomaterials, 30, 4695-9.
BELSCHES, A. P., HASKELL, M. D. & PARSONS, S. J. 1997. Role of c-Src tyrosine kinase in EGF-induced mitogenesis. Front Biosci, 2, d501-18.
BONNEH-BARKAY, D. & WILEY, C. A. 2009. Brain extracellular matrix in neurodegeneration. Brain Pathology, 19, 573-585.
BOTT, K., UPTON, Z., SCHROBBACK, K., EHRBAR, M., HUBBELL, J. A., LUTOLF, M. P. & RIZZI, S. C. 2010. The effect of matrix characteristics on fibroblast proliferation in 3D gels. Biomaterials, 31, 8454-64.
BUSCH, S. A. & SILVER, J. 2007. The role of extracellular matrix in CNS regeneration. Current Opinion in Neurobiology, 17, 120-127.
CHAN, C. C., WONG, A. K., LIU, J., STEEVES, J. D. & TETZLAFF, W. 2007. ROCK inhibition with Y27632 activates astrocytes and increases their expression of neurite growth-inhibitory chondroitin sulfate proteoglycans. Glia, 55, 369-84.
CHANDLER, S., COATES, R., GEARING, A., LURY, J., WELLS, G. & BONE, E. 1995. Matrix metalloproteinases degrade myelin basic protein. Neurosci Lett, 201, 223-6.
DERMARDIROSSIAN, C., ROCKLIN, G., SEO, J. Y. & BOKOCH, G. M. 2006. Phosphorylation of RhoGDI by Src regulates Rho GTPase binding and cytosol-membrane cycling. Mol Biol Cell, 17, 4760-8.
DILL, J., PATEL, A. R., YANG, X. L., BACHOO, R., POWELL, C. M. & LI, S. 2010. A molecular mechanism for ibuprofen-mediated RhoA inhibition in neurons. J Neurosci, 30, 963-72.
FALLON, J. R. 1985. Preferential outgrowth of central nervous system neurites on astrocytes and Schwann cells as compared with nonglial cells in vitro. J Cell Biol, 100, 198-207.
FREIMANN, F. B., STREITBERGER, K. J., KLATT, D., LIN, K., MCLAUGHLIN, J., BRAUN, J., SPRUNG, C. & SACK, I. 2011. Alteration of brain viscoelasticity after shunt treatment in normal pressure hydrocephalus. Neuroradiology, 54, 189-196.
GALTREY, C. M. & FAWCETT, J. W. 2007. The role of chondroitin sulfate proteoglycans in regeneration and plasticity in the central nervous system. Brain Res Rev, 54, 1-18.

HIRSCH, S. & BAHR, M. 1999. Growth promoting and inhibitory effects of glial cells in the mammalian nervous system. Adv Exp Med Biol, 468, 199-205.
HOLLEY, J. E., GVERIC, D., NEWCOMBE, J., CUZNER, M. L. & GUTOWSKI, N. J. 2003. Astrocyte characterization in the multiple sclerosis glial scar. Neuropathology and Applied Neurobiology, 29, 434-444.
JONES, L. L., SAJED, D. & TUSZYNSKI, M. H. 2003. Axonal regeneration through regions of chondroitin sulfate proteoglycan deposition after spinal cord injury: a balance of permissiveness and inhibition. J Neurosci, 23, 9276-88.
KHATIWALA, C. B., KIM, P. D., PEYTON, S. R. & PUTNAM, A. J. 2009. ECM compliance regulates osteogenesis by influencing MAPK signaling downstream of RhoA and ROCK. J Bone Miner Res, 24, 886-98.
KIMURA-KURODA, J., TENG, X., KOMUTA, Y., YOSHIOKA, N., SANGO, K., KAWAMURA, K., RAISMAN, G. & KAWANO, H. 2010. An in vitro model of the inhibition of axon growth in the lesion scar formed after central nervous system injury. Molecular and Cellular Neuroscience, 43, 177-187.
KOECHLING, T., KHALIQUE, H., SUNDSTROM, E., ÁVILA, J. & LIM, F. 2011. A culture model for neurite regeneration of human spinal cord neurons. Journal of Neuroscience Methods, 201, 346-354.
LAU, C. L., O'SHEA, R. D., BROBERG, B. V., BISCHOF, L. & BEART, P. M. 2011. The Rho kinase inhibitor Fasudil up-regulates astrocytic glutamate transport subsequent to actin remodelling in murine cultured astrocytes. Br J Pharmacol, 163, 533-45.
LIESI, P. & KAUPPILA, T. 2002. Induction of type IV collagen and other basement-membrane-associated proteins after spinal cord injury of the adult rat may participate in formation of the glial scar. Experimental Neurology, 173, 31-45.
LU, Y. B., FRANZE, K., SEIFERT, G., STEINHAUSER, C., KIRCHHOFF, F., WOLBURG, H., GUCK, J., JANMEY, P., WEI, E. Q., KAS, J. & REICHENBACH, A. 2006. Viscoelastic properties of individual glial cells and neurons in the CNS. Proc Natl Acad Sci U S A, 103, 17759-64.
LUTOLF, M. P. & BLAU, H. M. 2009. Artificial stem cell niches. Advanced Materials, 21, 3255-3268.
MAIA, F. R., FONSECA, K. B., RODRIGUES, G., GRANJA, P. L. & BARRIAS, C. C. 2014. Matrix-driven formation of mesenchymal stem cell-extracellular matrix microtissues on soft alginate hydrogels. Acta Biomater, 10, 3197-208.
MATHEWSON, A. J. & BERRY, M. 1985. Observations on the astrocyte response to a cerebral stab wound in adult rats. Brain Res, 327, 61-9.
MATTHEWS, B. D., OVERBY, D. R., MANNIX, R. & INGBER, D. E. 2006. Cellular adaptation to mechanical stress: role of integrins, Rho, cytoskeletal tension and mechanosensitive ion channels. J Cell Sci, 119, 508-18.
MIDDELDORP, J. & HOL, E. M. 2011. GFAP in health and disease. Prog Neurobiol, 93, 421-43.
MURPHY, M. C., CURRAN, G. L., GLASER, K. J., ROSSMAN, P. J., HUSTON, J., PODUSLO, J. F., JACK, C. R., FELMLEE, J. P. & EHMAN, R. L. 2012. Magnetic resonance elastography of the brain in a mouse model of Alzheimer's disease: Initial results. Magnetic Resonance Imaging, 30, 535-539.
NAIR, A., FREDERICK, T. J. & MILLER, S. D. 2008. Astrocytes in multiple sclerosis: A product of their environment. Cellular and Molecular Life Sciences, 65, 2702-2720.
OGIER, C., BERNARD, A., CHOLLET, A. M., LE DIGUARDHER, T., HANESSIAN, S., CHARTON, G., KHRESTCHATISKY, M. & RIVERA, S. 2006. Matrix metalloproteinase-2 (MMP-2) regulates astrocyte motility in connection with the actin cytoskeleton and integrins. GLIA, 54, 272-284.
OGIER, C., CREIDY, R., BOUCRAUT, J., SOLOWAY, P. D., KHRESTCHATISKY, M. & RIVERA, S. 2005. Astrocyte reactivity to Fas activation is attenuated in TIMP-1 deficient mice. An in vitro study. BMC Neuroscience, 6.
OSTROW, L. W. & SACHS, F. 2005. Mechanosensation and endothelin in astrocytes--hypothetical roles in CNS pathophysiology. Brain Res Brain Res Rev, 48, 488-508.

OWEN, S. C. & SHOICHET, M. S. 2010. Design of three-dimensional biomimetic scaffolds. J Biomed Mater Res A, 94, 1321-31.
PUTNAM, A. J., CUNNINGHAM, J. J., PILLEMER, B. B. & MOONEY, D. J. 2003. External mechanical strain regulates membrane targeting of Rho GTPases by controlling microtubule assembly. Am J Physiol Cell Physiol, 284, C627-39.
RATHKE-HARTLIEB, S., BUDDE, P., EWERT, S., SCHLOMANN, U., STAEGE, M. S., JOCKUSCH, H., BARTSCH, J. W. & FREY, J. 2000. Elevated expression of membrane type 1 metalloproteinase (MT1-MMP) in reactive astrocytes following neurodegeneration in mouse central nervous system. FEBS Lett, 481, 227-34.
RIVERA, S., TREMBLAY, E., TIMSIT, S., CANALS, O., BEN-ARI, Y. & KHRESTCHATISKY, M. 1997. Tissue inhibitor of metalloproteinases-1 (TIMP-1) is differentially induced in neurons and astrocytes after seizures: evidence for developmental, immediate early gene, and lesion response. J Neurosci, 17, 4223-35.
ROBEL, S., BERNINGER, B. & GOTZ, M. 2011. The stem cell potential of glia: Lessons from reactive gliosis. Nature Reviews Neuroscience, 12, 88-104.
ROWLEY, J. A., MADLAMBAYAN, G. & MOONEY, D. J. 1999. Alginate hydrogels as synthetic extracellular matrix materials. Biomaterials, 20, 45-53.
SMITH, G. M., RUTISHAUSER, U., SILVER, J. & MILLER, R. H. 1990. Maturation of astrocytes in vitro alters the extent and molecular basis of neurite outgrowth. Dev Biol, 138, 377-90.
SOBEL, R. A. & MITCHELL, M. E. 1989. Fibronectin in multiple sclerosis lesions. Am J Pathol, 135, 161-8.
STRUCKHOFF, G. 1995. Cocultures of meningeal and astrocytic cells--a model for the formation of the glial-limiting membrane. Int J Dev Neurosci, 13, 595-606.
VAN HORSSEN, J., DIJKSTRA, C. D. & DE VRIES, H. E. 2007. The extracellular matrix in multiple sclerosis pathology. J Neurochem, 103, 1293-301.
WALKER, B. A., JI, S. J. & JAFFREY, S. R. 2013. Intra-axonal translation of RhoA promotes axon growth inhibition by CSPG. J Neurosci, 32, 14442-7.
WANG, K., BEKAR, L. K., FURBER, K. & WALZ, W. 2004. Vimentin-expressing proximal reactive astrocytes correlate with migration rather than proliferation following focal brain injury. Brain Research, 1024, 193-202.
WANG, X., BUDEL, S., BAUGHMAN, K., GOULD, G., SONG, K. H. & STRITTMATTER, S. M. 2009. Ibuprofen enhances recovery from spinal cord injury by limiting tissue loss and stimulating axonal growth. J Neurotrauma, 26, 81-95.
WANNER, I. B., DEIK, A., TORRES, M., ROSENDAHL, A., NEARY, J. T., LEMMON, V. P. & BIXBY, J. L. 2008. A new in vitro model of the glial scar inhibits axon growth. Glia, 56, 1691-709.
WOZNIAK, M. A., DESAI, R., SOLSKI, P. A., DER, C. J. & KEELY, P. J. 2003. ROCK-generated contractility regulates breast epithelial cell differentiation in response to the physical properties of a three-dimensional collagen matrix. J Cell Biol, 163, 583-95.
YIU, G. & HE, Z. 2006. Glial inhibition of CNS axon regeneration. Nat Rev Neurosci, 7, 617-27.
ZAMANIAN, J. L., XU, L., FOO, L. C., NOURI, N., ZHOU, L., GIFFARD, R. G. & BARRES, B. A. 2012. Genomic analysis of reactive astrogliosis. J Neurosci, 32, 6391-410.

“ Recomeça…

Se puderes,

Sem angústia e sem pressa,

E os passos que deres,

Nesse caminho duro

Do futuro,

Dá-os em liberdade,

Enquanto não alcances

Não descanses,

De nenhum fruto queiras só metade”

(Miguel Torga)

CHAPTER IV

Poly(Trimethylene Carbonate-co-ε-Caprolactone) Promotes Axonal Growth*

D. N. Rocha [1,2], P. Brites [3], C. Fonseca [1,2], A. P. Pêgo [1,2,4]

[1]INEB – Instituto de Engenharia Biomédica, Universidade do Porto, Porto, Portugal; [2] FEUP - Faculdade de Engenharia da Universidade do Porto, Porto, Portugal; (3) Nerve Regeneration Group, IBMC – Instituto de Biologia Molecular e Celular, Universidade do Porto, Porto, Portugal; (4) ICBAS – Instituto de Ciências Biomédicas Abel Salazar, Universidade do Porto, Porto, Portugal

PLOS ONE, 2014, 9 (2): e88593, doi:10.1371/journal.pone.0088593
This work originated a patent, please see Appendix I

ABSTRACT

Mammalian central nervous system (CNS) neurons do not regenerate after injury due to the inhibitory environment formed by the glial scar, largely constituted by myelin debris. The use of biomaterials to bridge the lesion area and the creation of an environment favoring axonal regeneration is an appealing approach, currently under investigation. This work aimed at assessing the suitability of three candidate polymers – poly(ε-caprolactone), poly(trimethylene carbonate-co-ε-caprolactone) (P(TMC-CL)) (11:89 mol%) and poly(trimethylene carbonate) - with the final goal of using these materials in the development of conduits to promote spinal cord regeneration. Poly(L-lysine) (PLL) coated polymeric films were tested for neuronal cell adhesion and neurite outgrowth. At similar PLL film area coverage conditions, neuronal polarization and axonal elongation was significantly higher on P(TMC-CL) films. Furthermore, cortical neurons cultured on P(TMC-CL) were able to extend neurites even when seeded onto myelin. This effect was found to be mediated by the glycogen synthase kinase 3β (GSK3β) signaling pathway with impact on the collapsin response mediator protein 4 (CRMP4), suggesting that besides surface topography, nanomechanical properties were implicated in this process. The obtained results indicate P(TMC-CL) as a promising material for CNS regenerative applications as it promotes axonal growth, overcoming myelin inhibition.

Keywords: degradable elastomers; nanomechanical properties; glycogen synthase kinase 3β; axonal outgrowth; atomic force microscopy; tissue engineering; central nervous system regeneration

INTRODUCTION

When an injury is inflicted to the spinal cord, the blood-brain barrier (BBB) breaks down locally and a massive infiltration of immune cells is observed. After the initial mechanical trauma (primary damage), cell damage is triggered such that within hours the injury site and the surrounding haemorrhagic areas begin to undergo necrosis (secondary damage), a progressive process that can last for several days. As the necrotic tissue is removed by macrophages, large fluid-filled cavities develop, which are bordered by areas of glial/connective tissue scarring. Even though this glial scar may provide several beneficial functions such as the restoration of the BBB, prevention of a devastating inflammatory response and limit the action of cellular degeneration [1, 2], it also contributes to the establishment of a physical and chemical barrier to axonal regeneration [1]. Strategies aimed at preventing primary and delaying secondary damage need to be administered within minutes to hours after injury making these unsuitable for the spinal cord injury (SCI) patients in a chronic stage [3]. Furthermore, none of the clinical approaches currently available to control or minimize the impact of a SCI lead to neuronal regeneration [4], nor there is an efficient regenerative therapeutic strategy for SCI treatment [4]. Although injured axons show the ability to regenerate when in a peripheral nervous system environment [5], the major factor contributing to the failure of the central nervous system (CNS) regeneration is the lack of capacity of injured axons to spontaneously regenerate in the glial scar microenvironment [6].

The use of biocompatible biomaterials to bypass the glial scar is one of the promising approaches being investigated to promote spinal cord regeneration [3, 7-13]. These tissue-engineering approaches are usually based on the use of either cell-free bridges or of cellularized biomaterial-based matrices. There are some advantages in the use of a cell-free bridging material, as on one hand cell purification and expansion methods are laborious, time consuming and expensive, and on the other hand when the transplantation of allogenic cells is required, the use of immunosuppressants cannot be circumvented [13]. Therefore, the idea of a cell-free bridging material that uses and controls endogenous cell population responses by having the ability to promote axon regeneration and control inflammatory and glial reactions is arguably appealing.

There are numerous polymeric materials under study for application in nerve repair strategies [3, 10, 14]. These can simultaneously provide a scaffold for tissue regeneration, serve as a cell-delivery vehicle and a reservoir for sustained drug delivery [15]. Within this class of materials, biodegradable polymers are particularly advantageous for the

preparation of these bridges, as polymer degradation can be tuned to match the neuronal cell growth. Besides the degradation rate, the mechanical properties of the selected material are also of extreme relevance and a property that can be fitted to one needs. While the implantable structures must be flexible but relatively strong, as well as easy to handle by surgeons, their mechanical properties have an influence on cell phenotype as well [16-19].

Poly(trimethylene carbonate-co-ε-caprolactone) (P(TMC–CL)) copolymers with high caprolactone (CL) content or the parental trimethylene carbonate (TMC) homopolymer are very flexible and tough materials that can be processed into highly porous three dimensional structures with degradation rates that can be modulated by adjusting the co-monomer content [20, 21]. As P(TMC-CL) has been shown to be processable in a variety of shapes and forms, including porous conduits [22] and electrospun fibers [23], it presents itself as a valuable tool in the design of new strategies for application in the treatment of spinal cord lesions. These materials have been shown to be biocompatible [21, 24] and have been previously explored for peripheral nerve regeneration conduits [20, 22, 24, 25]. Additionally, polymer degradation occurred with minimum swelling of the material [24], which is also an essential feature to prevent nerve compression that could compromise regeneration.

After the promising results obtained in the context of peripheral nerve regeneration, the suitability of P(TMC-CL) copolymers for application in the CNS and the possibility to modulate the biological response by tuning the surface properties at the nanoscale was explored, with the ultimate goal of contributing to the design of an artificial 3D scaffold able to promote spinal cord regeneration. Films based on a P(TMC-CL) copolymer with a high CL content and the respective homopolymers were prepared and cortical neuron cultures were conducted after the coating of all substrates with poly(L-lysine) (PLL). For each condition parameters like cell adhesion, neurite number and length of the longest neurite were determined, as these are key when assessing the potential of a substrate to promote axonal regeneration. It is hypothesized that the observed differential cell behaviour is related to the materials' nanomechanical properties that were characterized in this study. The involved cell signalling pathway was also investigated.

RESULTS

Cortical neurons adhere and extend neurites in a PLL dependent manner

As a first step in assessing P(CL), P(TMC-CL) and P(TMC) compatibility with the CNS and their potential application in devices for neuroregeneration, polymeric discs were tested as substrates for cortical neuron growth in vitro. Cortical neurons were seeded on PLL coated polymeric films and were found to adhere to the tested substrates in a PLL concentration dependent manner (Fig.1A). Cell number and neurite outgrowth on the coated polymeric films were evaluated using cover glasses coated with a PLL concentration of 24 µg.µl^{-1} for

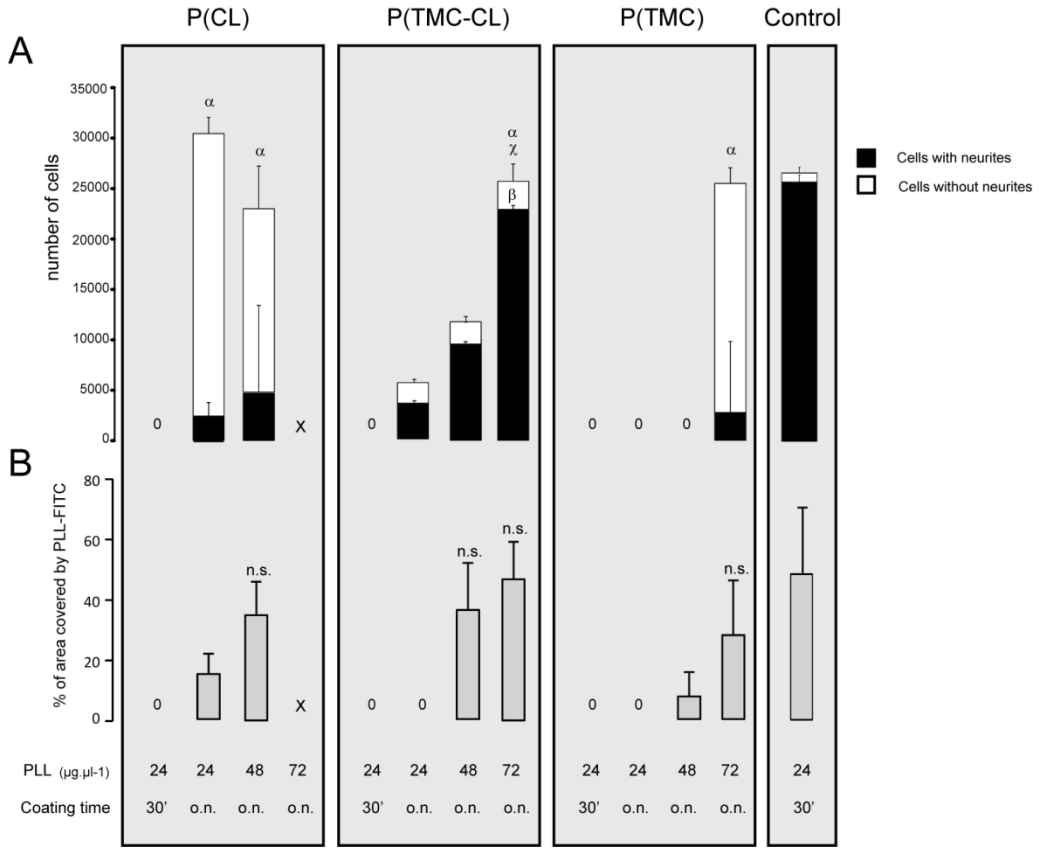

Figure 1. Cortical neuron culture on PLL coated films of P(TMC-CL) and respective homopolymers (2.7 x 10^4 viable cells were seeded per sample). **A.** Number of cortical neurons with and without neurite extensions on polymeric surfaces coated with aqueous solutions at different concentrations of PLL. Glass coated with 24 µg.µl^{-1} of PLL for 30 minutes was used as control. (n = 3 independent studies, mean ± SD, $p < 0.05$) **B.** Percentage of PLL covered surface area as a function of the coating conditions. (n= 3, mean ± SD, $p < 0.05$)

x = condition not tested, 0 = null value. n.s. = non-significantly different from the control, α = total number of cells not significantly different from the control, β = number of cells with neurite

extensions not significantly different from the control and χ = number of cells without extensions not significantly different from the control.

30 min as control. Cortical neurons adhered in comparable numbers to the control when the polymeric films were coated overnight with 24 $\mu g.\mu l^{-1}$ and 48 $\mu g.\mu l^{-1}$ of PLL in the case of P(CL) films, and 72 $\mu g.\mu l^{-1}$ of PLL in the case of TMC containing films (see Fig. 1A). However, only on P(TMC-CL) the majority of adhered cells was able to extend neurites as in the control.

To explain this PLL-dependent behaviour, the amount of PLL adsorbed to the polymeric films surface was evaluated by fluorescence quantification of PLL-FITC coated samples (see fig.1S for PLL-FITC coating fluorescence images).

As one can observe in Fig. 1B, the surface area covered by PLL (in %) was only comparable to the control conditions when the polymeric films were treated with a PLL solution of at least 48 $\mu g.\mu l^{-1}$ and 72 $\mu g.\mu l^{-1}$ in the case of the CL containing materials and P(TMC), respectively. Consequently, cell adhesion can be correlated with the PLL adsorption profile to the polymeric films.

Taking into consideration the obtained results, both in terms of cell adhesion and neurite extension, the coating conditions used in the subsequent studies were established to be polymer surface treatment overnight with 48 $\mu g.\mu l^{-1}$ for P(CL) and 72 $\mu g.\mu l^{-1}$ for P(TMC-CL) and P(TMC).

P(TMC-CL) stimulates axonal elongation

In order to evaluate neurite outgrowth on the different PLL-coated polymeric surfaces, the number of neurites per cell, as well as the neurite length were determined. As seen in Fig. 2A, neurons behave differently on each surface. More than 80% of the cells

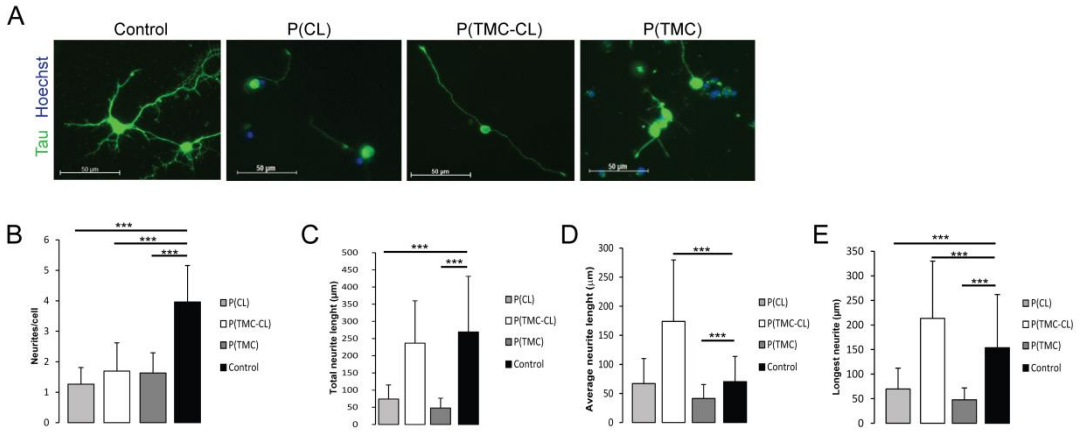

Figure 2. Effect of the PLL coated surfaces on neurite elongation and cellular polarization. **A**. Fluorescently labeled cortical neurons, immunostained for TAU (green); nuclei are counterstained with Hoechst (blue); **B.** Number of primary neurites per cell; **C.** Total neurite length; **D.** Average neurite length and **E.** Length of the longest neurite. (n= 130 cells, mean ± SD, *** for $p < 0.001$)

seeded on polymeric films show one or two neurites, while more than 80% of the cells seeded on glass (control) present between 3 to 5 neurites (Fig. 2B). Furthermore, as shown in Fig. 2A neurons seeded on the polymeric surfaces exhibit a lower degree of branching than those seeded on glass. However, on P(CL) and P(TMC) the adhered cells show smaller neurites than on P(TMC-CL) and the control (Fig. 2C-E). Despite the fact that for P(TMC-CL) the total neurite length was similar to the one observed on glass, given the lower number of neurites per cell in this condition, the average neurite length was higher (Fig. 2D). More remarkably, the length of the longest neurite was increased relatively to the control (Fig. 2E).

P(TMC-CL)'s nanomechanical properties

As shown in Fig. 3A, atomic force microscopy (AFM) analysis indicated that the RMS roughness was similar for P(CL) and P(TMC-CL), with mean values of 21.8 ± 11.5 nm and 24.4 ± 12.1 nm respectively, while significantly lower for P(TMC) with a mean value of 1.6 ± 1.0 nm.

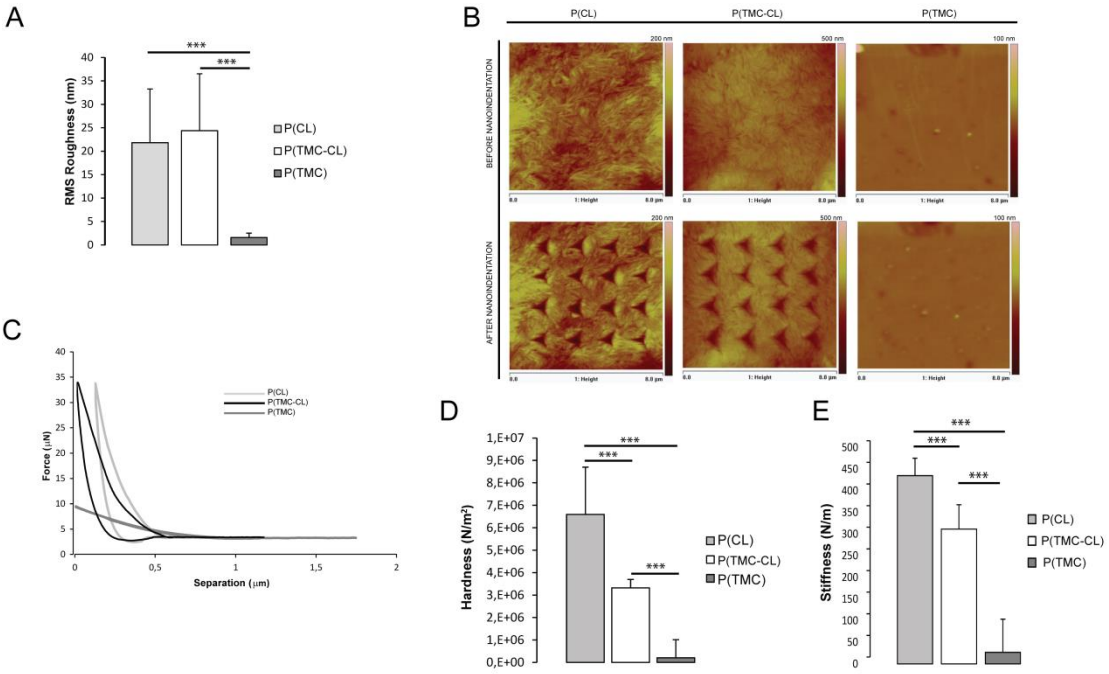

Figure 3. Morphology and mechanical properties of the tested polymeric surfaces. **A**. Root mean square (RMS) roughness of all polymeric surfaces; **B**. Representative photographs of the polymeric surfaces before and after nanoindentation; images are color coded, showing elevated areas in bright and lower areas in dark color. **C**. Representative nanoindentation force-displacement curves; D. Mean hardness values of all polymeric surfaces, calculated for the maximum load and E. Mean stiffness values for all polymeric surfaces. (n = 60 indentations, mean ± SD, *** for $p < 0.001$)

Nanoindentation is one of the most versatile techniques and particularly suited for the measurement of localized mechanical properties on the surface of materials [26]. Representative photos of the nanoindentations and force/displacement curves are represented in Fig. 3B and C, respectively. These show that P(CL) has a greater resistance to deformation in relation to the other two materials tested, as the force needed to achieve the same displacement is higher than for P(TMC-CL) or P(TMC). As shown in Fig. 3 D-E stiffness and hardness values are significantly different between the three different substrates. A stiffness value of 312 ± 56.4 $N.m^{-1}$ and a hardness of 3.32 $x10^6$ ± 0.373 x 10^6 $N.m^{-2}$ was found for P(TMC-CL), while P(CL) shows the highest values with a

stiffness of 435 ± 40.4 $N.m^{-1}$ and a hardness value of 6.60 x 10^6 ± 2.11 x 10^6 $N.m^{-2}$. As seen in the photos before and after nanoindentation, P(TMC) samples recover almost completely from the indentations and, consequently, show stiffness and hardness values close to zero.

P(TMC-CL) promotes restraining of myelin inhibition

Myelin-associated inhibitors (MAIs) are present at a spinal cord lesion site and are known to be among the major impediments of the spontaneous axonal regeneration after SCI. Cortical neurons were seeded on myelin coated surfaces with a reduction of adherent cells of 50 and 55% for P(TMC-CL) and glass, respectively.

P(TMC-CL) was chosen from the three tested surfaces as it showed the best results for neuronal adhesion and neurite extension, presenting a positive influence on axonal elongation. As seen in Fig. 4, when comparing surfaces coated and uncoated with myelin, the number of cells with neurites is smaller in the first case. Nevertheless, this decrease is not significant on P(TMC-CL) seeded neurons in contrast to the control where this reduction is statistically significant ($p < 0.01$).

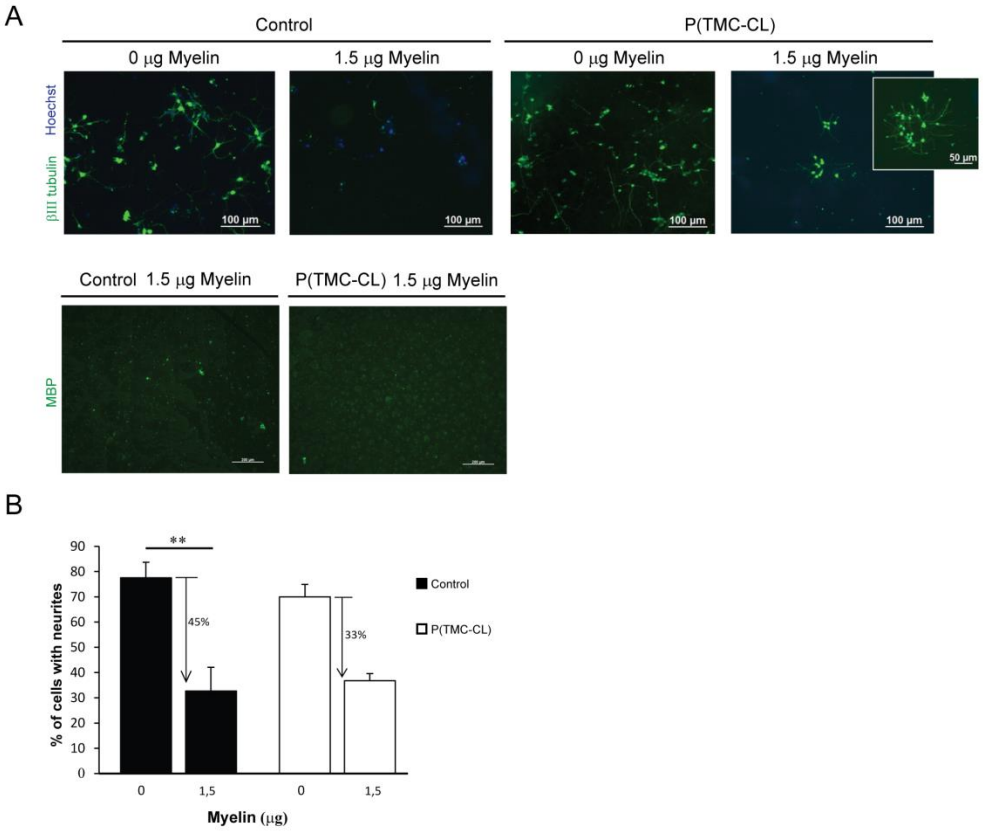

Figure 4. Effect of CNS myelin on neurite outgrowth of cortical neurons cultured for 4 days on PLL-P(TMC-CL) substrates coated with CNS myelin.. **A.** Cortical neurons are immunostained for β-III tubulin (green) and nuclei are counterstained with Hoechst (blue); myelin coating is immunostainned for MBP (green), surfaces were fully covered by myelin (see fig. 2S for myelin quantification) **B.** Effect of myelin on the ability of neurons to extend processes is presented as the % of cells with neurites in relation to the total number of cells. (n = 3 independent studies, mean ± SD; ** for $p < 0.01$).

GSK3β signalling pathway mediates neuronal behaviour on P(TMC-CL) substrates

Glycogen synthase kinase 3β (GSK3β) is implicated in many processes in the nervous system and is known to play a critical role in the regulation of neuron physiology. It is highly expressed in neurons and crucial for the establishment of neuronal polarity, as well as for the establishment of the branching-elongation equilibrium [27-29]. In view of this knowledge, the involvement of GSK3β as a mediator of P(TMC-CL) effect on neurite formation and axonal outgrowth was examined. GSK3β is regulated by phosphorylation and its activity can be reduced by phosphorylation at Ser-9. Contrarily, tyrosine phosphorylation at Tyr-216 increases the enzyme's activity (Fig. 5A) [30, 31]. As shown in Fig. 5B cortical neurons seeded on P(TMC-CL) present lower levels of GSK3β Ser-9

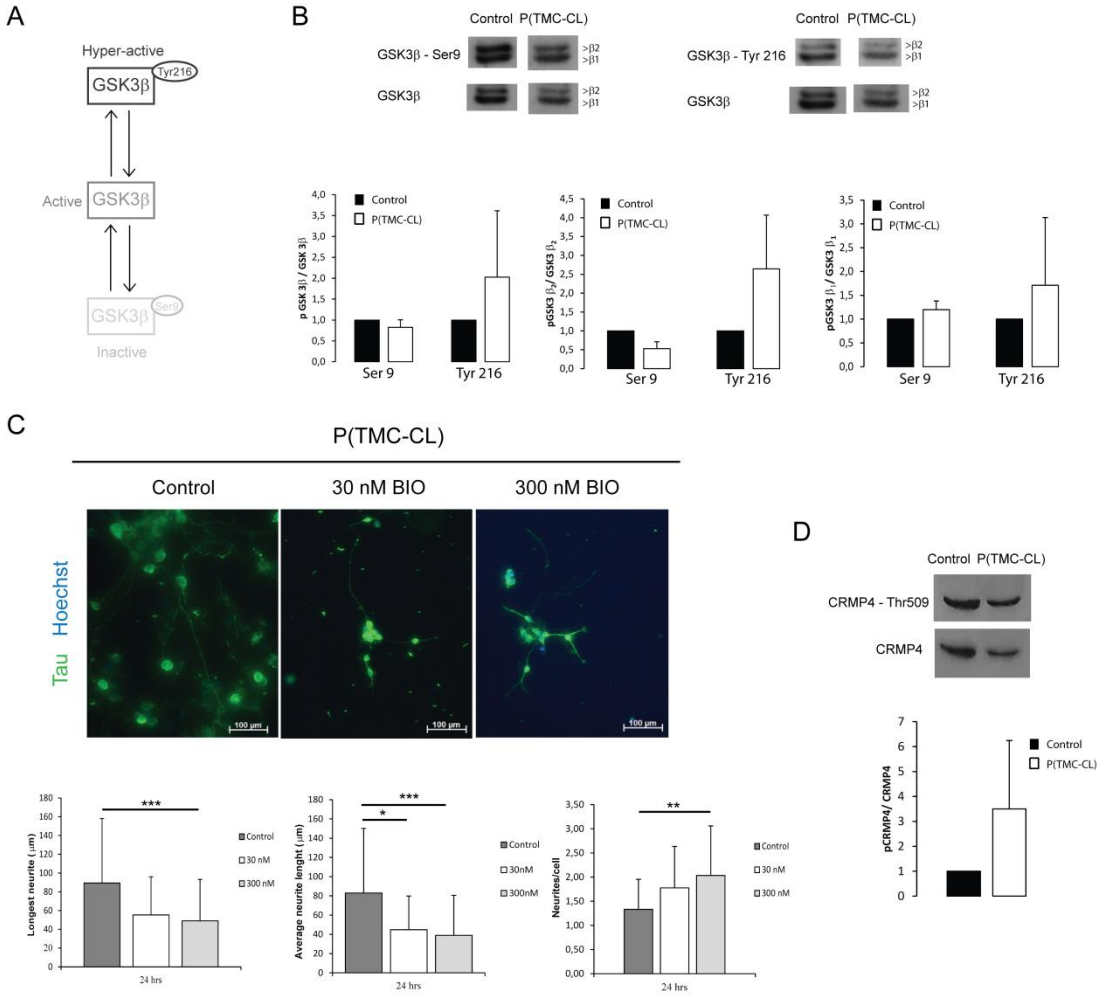

Figure 5. Analysis of GSK3β in cortical neurons plated on P(TMC-CL) and effects of GSK3β inhibition on neurite extension. **A.** Schematic representation of the different phosphorylation forms of GSK3β and their activity status; **B.** Analysis of the phosphorylated forms of GSK3β by western blot. Representative blots are shown. Expression levels of GSK3β isoforms, β1 and β2, are presented and quantified individually or together. (n = 3 independent studies, average ± SD); **C.** Morphology of neurons (immunostained for TAU in green and nuclei counterstained in blue) cultured for 24 hours in the presence of DMSO (control) or in the presence of 6-bromoindirubin-3'-acetoxime (BIO) at 30 and 300 nM. Quantifications of the longest neurite, average neurite length and the number of neurites per cell are shown (n = 130 cells, mean ± SD, * for $p < 0.05$, ** for $p < 0.01$ and *** for $p < 0.001$); **D.** Determination of CRMP4 phosphorylation levels in cortical neurons plated for 4 days on control or P(TMC-CL). Representative western blot is shown and below the quantification (n = 3 independent studies, average ± SD).

phosphorylation and higher level of Tyr-216 phosphorylation, in comparison to neurons cultured on glass. This indicates that neurons seeded on P(TMC-CL) display more kinase activity than hose on glass. It is also perceptible from Fig. 5B that the GSK3β isoform that

is differently expressed is GSK3β_2, which is known to be expressed exclusively in the nervous system [31, 32].

To further confirm the involvement of GSK3β as a mediator of the P(TMC-CL) effect on axonal outgrowth and number of neurites per cell, cortical neurons were cultured in the presence of a GSK3 pharmacologic inhibitor - 6-bromoindirubin-3'-acetoxime (BIO). It is expected that inhibiting GSK3 activity should inhibit the polymeric surface's effect on cortical neurons. In fact, as shown in Fig. 5C, when BIO is added to the culture medium one can observe a decrease in the length of the longest neurite and in the average neurite length, as well as an increase on the number of neurites per cell. These effects occur in a dose-dependent manner, with the highest concentration of BIO tested (300 nM) leading to statistically significant differences. Alabed et al. [33] have established that GSK3β phosphorylation and consequent inactivation, regulates the interaction of CRMP4 and RhoA through CRMP4 de-phosphorylation. If this mechanism is active in our setup, phospho-CRMP4 levels should be higher for neurons seeded on P(TMC-CL). To test this hypothesis, the levels of CRMP4 phosphorylation in cortical neurons seeded on P(TMC-CL) and glass surfaces were assessed. As expected, phospho-CRMP4 levels were increased for neurons cultured on P(TMC-CL) as shown in Fig. 5D.

DISCUSSION

In the aftermath of a SCI, a glial scar is formed. Despite its key role in constraining the damaging effects caused by the lesion, the glial scar also prevents axon regeneration. The astroglial scar not only contains secreted and transmembrane molecular inhibitors of axon growth but also constitutes an almost impenetrable physical barrier to regeneration [4]. Consequently, it was hypothesized that by creating a favourable environment at the lesion site, one will be able to enhance axonal regeneration and ultimately promote some gain of function. Therefore, the use of an implantable scaffold to bypass the glial scar area is one of the promising approaches being investigated to promote spinal cord regeneration. A prerequisite in the design of such biomaterial is its biocompatibility, which in this context means that it must support neuronal survival and axonal growth. The aim of this study was, therefore, to investigate the suitability of P(CL), P(TMC-CL) and P(TMC) as substrates for spinal cord regeneration purposes.

One of the most commonly used strategies to assess neuronal behaviour in vitro when testing biomaterials for nerve regeneration applications is to evaluate axonal growth [33-37]. In the present work rat cortical neurons were firstly seeded on the PLL-coated polymeric substrates to assess adhesion and neurite outgrowth ability. PLL is a synthetic

homo-poly (amino acid), characterized by an isopeptide bond between the ε-amino and the α-carboxyl groups of L-lysine, commonly used to coat cell culture substrates [38]. Initially, the polymer surface coating conditions were optimized - PLL concentration and time of contact - in order to achieve a comparable surface area covered by PLL and, consequently, similar cell adhesion in all tested surfaces. The observed PLL dependent behaviour can be explained by the different adsorption capacity of PLL on polymeric and glass surfaces. Differences that can be attributable to the surface properties of the tested materials, as these polymers present a more hydrophobic surface than glass [20]. Although after this process one could obtain comparable numbers of cortical neurons after 4 days of culture on the tested materials, significant morphological differences were found between neurons cultured on polymeric surfaces, particularly P(TMC-CL), and the control. Firstly, only on P(TMC-CL) the majority of neurons is able to extend neurites. Furthermore, our results show that among all the tested surfaces, including glass, seeding cortical neurons on P(TMC-CL) stimulates neuronal polarization and promotes axon elongation, as neurons on P(TMC-CL) show significantly enhanced neurite outgrowth and significantly lower numbers of neurites per cell. This switch to polarized and elongated morphology is noteworthy as successful regeneration requires that neurons survive and initiate rapid and directed neurite outgrowth [39-41]. A decreased number of neurites per cell were also found on P(CL) and P(TMC) but on these materials axonal outgrowth was significantly impaired. Moreover, while control neurons have, on average, twice the number of neurites of neurons seeded on P(TMC-CL), when one sums the length of all neurites of each cell (total neurite length) no significant differences are found. Altogether, cortical neurons seeded on P(TMC-CL) were found not only to be polarized but also to extend significantly longer neurites. To the best of our knowledge, no previous reports have shown this neuronal behaviour on any studied material.

The potential of materials to trigger specific cellular responses is getting to be a well-established phenomenon mediated by a number of factors that range from the properties of the surface that contacts with the cell, to the mechanical properties of the material [16, 17, 42-44]. We have previously characterized the family of these copolymers and when varying the monomer ratio mainly the thermal and, consequently, the mechanical properties of these materials are drastically affected [21]. P(TMC) and P(TMC-CL) copolymers with high CL content are flexible and though materials that range from amorphous to semi-crystaline elastomers when the CL content increases. Therefore, here we hypothesise that surface topography and the nanomechanical properties of the tested materials play a key role in influencing cell behaviour. The local characterization of roughness, hardness and elastic properties of a wide range of materials has been reported including for thin films and biomolecules [45-48] but so far the characterization of TMC-CL

copolymers has not been performed. The roughness of the three tested polymeric surfaces was first investigated. Values of 22 nm and 24 nm were found for P(CL) and P(TMC-CL) respectively, while for the P(TMC) the roughness values were found to be significantly lower. In 2002, Fan et al. [49, 50] showed that neuronal cells adherence and survival is optimum on surfaces with a RMS roughness ranging from 10 to 50 nm. Taking this data in consideration, both P(CL) and P(TMC-CL) show not only similar but also optimum roughness values for neural adhesion and survival, while P(TMC) is outside this optimum roughness range. Therefore, the different neuronal behaviour on these surfaces cannot be explained simply by topography. Aiming to measure localized mechanical properties on the surface of the polymeric films, nanoindentations were performed and force-displacement curves obtained for each indentation. Mean hardness and stiffness values were calculated and significant differences were found between all polymeric surfaces, with P(TMC-CL) being significantly less resistant to deformation than P(CL) and significantly more resistant to deformation than P(TMC). Although roughness values were similar between P(CL) and P(TMC-CL) and within the optimum range, P(CL) was two times harder than P(TMC-CL), which could explain the different cellular behaviour on these surfaces, indicating that changes in stiffness and hardness values may have caused changes in cell morphology, specifically in axonal elongation.

Having observed the ability of P(TMC-CL) surfaces in promoting neuronal polarization and axonal elongation under normal cell culture conditions, the capacity of P(TMC-CL) to positively affect cortical neurons in a typical CNS inhibitory environment was tested, envisaging its application in the design of an axonal regeneration promoting strategy. While axons in the context of a mature mammalian CNS do not regenerate if damaged, the immature mammalian CNS is able to regenerate after injury [51, 52]. Probably the most notable difference between the mature and the immature nervous system is the presence of myelin [34]. Indeed, the limited regenerative capacity of the mammalian CNS is known to be partially due to myelin inhibition. So far, no biomaterial has shown the ability to restrain myelin inhibition unless blockers of myelin protein receptors were used [53]. Recently, Mohammad and co-workers have shown that a nano-textured self-assembled aligned collagen hydrogel was able to promote directional neurite guidance and restrain inhibition by a recombinant myelin-associated glycoprotein of dorsal root ganglia cultures [54]. To assess P(TMC-CL)'s neuronal effect under adverse, and more biologically relevant conditions, cortical neurons were seeded on P(TMC-CL) films in the presence of myelin. As expected, in the glass control surface we observed a statistically significant reduction of the number of cells extending neurites when cultured in the presence of myelin. In contrast, when P(TMC-CL) was used as a substrate, this reduction was not statistically significant (Fig. 4 B), suggesting that P(TMC-CL) is, to some extent,

contributing to the promotion of the overcome of myelin inhibition. This is of extreme relevance as it has been already demonstrated that some degree of functional recovery can be obtained simply by counteracting the activity of myelin inhibition [55, 56]. The existence of a biomaterial that has the capacity to restrain this inhibition per se, without the need for the administration of antibodies or chemical inhibitors, can prove to be of great importance for therapeutic purposes.

The potential of materials to trigger specific cellular responses, such as interference and/or activation of defined pathways is extremely promising for tissue engineering. Stiffness and hardness sensing probably involves transduction into biological signals [15]. GSK3β is known to regulate axonal growth through the modification of the phosphorylation status of several microtubule-binding proteins and consequently the assembly of microtubules [31, 57]. Moreover, Alabed et al. [33] showed that the overexpression of active GSK3β attenuates MAI-dependent neurite outgrowth inhibition. For these reasons, GSK3 was studied as a possible mediator of P(TMC-CL)'s effect. Mammalian GSK3 is generated from two genes, GSK3α and GSK3β. GSK3 expression in neurons is further characterized by an alternative splicing of GSK3β originating two main variants: $GSK3\beta_1$ and $GSK3\beta_2$. $GSK3\beta_2$ is specifically expressed in the nervous system [31]. GSK3β is regulated by phosphorylation and its activity is dependent on the balance between tyrosine (Tyr-216) and serine (Ser-9) phosphorylation as shown in Fig. 5A, with a reduction of activity if phosphorylated at Ser-9, and its increase if phosphorylated at Tyr-216 [30, 31]. Our results show that GSK3β is differently regulated in neurons seeded on glass and P(TMC-CL), with the latter showing lower levels of Ser9 phosphorylation, a site of GSK3β inactivation, and higher levels of Tyr216 phosphorylation, which facilitates the activity of GSK3β by promoting substrate accessibility [31]. Neurite elongation and neuronal polarization on P(TMC-CL) may be promoted by an increase GSK3β activity in vitro. The relationship between axonal elongation and GSK3β activity was further confirmed through pharmacological inhibition of GSK3 in vitro. As expected, inhibition of GSK3β blocked P(TMC-CL) effect, as there was a decrease in neurite length and an increase on the numbers of neurites per cell. Cells seeded on P(TMC-CL) and treated with BIO acquired a morphology that resembles more closely the neurons seeded on glass Fig. 2A.

Activation of GSK3β activity occurs in cortical neurons when these are cultured on P(TMC-CL), resulting in an increase in neurite outgrowth and decrease on the number of neurites per cell. Increased axonal outgrowth in the presence of higher GSK3β activity has also been shown in prior reports, for cerebellar, dorsal root ganglia and hippocampal neurons [28, 33, 58].

The Rho signalling pathway is known to play an important role in neuronal growth regulation and it has been shown that inhibitors of RhoA, and/or its downstream effector

Rho kinase, facilitate growth on myelin substrates [59, 60]. Wozniak et al. [16] have studied the effects of stiffness on cell shape and shown that ROCK mediated contractility is essential for breast epithelial cells to sense the biophysical properties of the surrounding environment. Alabed et al. [61] have identified CRMP4 as a protein that functionally interacts with RhoA to mediate neurite outgrowth. Later on, this team has found that CRMP4-RhoA interaction is regulated by dephosphorylation of CRMP4 as a direct consequence of GSK3β inactivation by phosphorylation at Ser-9 [33]. This observation indicates that overexpression of GSK3β and consequent inhibition of CRMP4-RhoA complex formation may be protective in the context of myelin inhibition. Our findings are consistent with Alabed et al. [33] as for neurons seeded on P(TMC-CL), which show higher levels of GSK3β activity and longer neurites the levels of phospho-CRMP4 are higher than in glass seeded neurons. Overall these results suggest that the activation of GSK3β activity, and consequent neurite elongation, is mediated by the surface mechanical properties of P(TMC-CL).

CONCLUSION

This work shows that P(TMC-CL) with a high CL content can promote axonal regeneration, prompting neurons into a regeneration mode, even under inhibitory conditions. This effect is mediated by the GSK3β signalling pathway, which is triggered by P(TMC-CL)'s surface mechanical properties.

P(TMC-CL) being a material that can been processable in a variety of shapes and forms, including porous conduits and electrospun fibres, it presents itself as a valuable tool in the design of new strategies for application in the treatment of spinal cord lesions, while supporting axonal growth and taming myelin dependent neurite outgrowth inhibition without the need of the administration of any therapeutic drug.

MATERIALS AND METHODS

Polymeric film preparation

Poly(trimethylene carbonate) (P(TMC), poly(ε-caprolactone) (P(CL)) and poly(trimethylene carbonate-co-ε-caprolactone) (P(TMC-CL)) with 11 mol % of TMC were synthesized as previously described [20]. Briefly, prior to polymerization ε-caprolactone monomer (Fluka) was dried overnight over CaH_2 and distilled under reduced pressure. Trimethylene carbonate was obtained from Boehringer Ingelheim (Germany) and used as

received. Polymerizations were conducted by ring-opening polymerization in an argon atmosphere using stannous octoate as a catalyst. All polymerizations were carried out for a period of 3 days at 130°C ± 2°C. The obtained polymers were purified by dissolution in chloroform and subsequent precipitation into a ten-fold volume of ethanol. The precipitated polymers were recovered, washed with fresh ethanol and dried under reduced pressure at room temperature (RT) until constant weight. The prepared polymers were characterized with respect to chemical composition by nuclear magnetic resonance (NMR). Four hundred MHz ^{1}H-NMR (BRUKER AVANCE III 400) spectra were recorded using solutions of polymer in CDCl3 (Sigma). Number average and weight average molecular weights (Mn and Mw, respectively), polydispersity indexes (PDI) and intrinsic viscosities ([η]) of the (co)polymers were determined by gel permeation chromatography (GPC, GPCmax VE-2001, Viscotek, USA). The setup was equipped with ViscoGEL I-guard-0478, ViscoGEL I-MBHMW-3078, and ViscoGEL I-MBLMW-3078 columns placed in series and a TDA 302 Triple Detector Array with refractometer, viscometer, and light-scattering detectors, allowing the determination of absolute molecular weights. All measurements were performed at 30°C, using chloroform as the eluent at a flow rate of 1.0 ml.min^{-1}. The obtained results are compiled in Table 1.

Polymer films of 250 μm in thickness were prepared by casting the polymer solution in chloroform onto glass Petri dishes. After drying the films under reduced pressure at RT, disks with a diameter of 14 mm were punched out. Prior to cell culture, disks were sterilized by two incubation steps in a 70% (v/v) ethanol solution for 15 min, followed by two rinsing steps of 15 min in autoclaved MilliQ water (Millipore). After sterilization, polymer disks were placed in 24-well tissue polystyrene plates (BD Biosciences) and fixed with autoclaved silicon o-rings (EPIDOR, Barcelona).

Cortical neuron cell culture

Prior to cell seeding the air side surface of the polymeric disks was coated with 200 μl of a poly(L-lysine) (PLL, Sigma) solution in a concentration ranging from 24 to 73 μg.μl^{-1}, at 37ºC for 30 minutes or overnight and, subsequently, rinsed with autoclaved MilliQ water. Cover glass (Menzel) coated with 24 μg.μl^{-1}, at 37ºC for 30 minutes was used as control.

Procedures involving animals and their care were conducted in compliance with institutional ethical guidelines and with the approval of Portuguese Veterinary Authorities – Direcção Geral de Veterinária (DGV); approval reference 0420/000/000/2007. Female wistar rats were housed in pairs with free access to food and water, under a 12-h light/ 12-h dark cycle. E17 – E18 Wistar Han rat embryos were recovered by caesarean section of pregnant rats first anesthetized by intravenous injection of ketamine chlorohydrate

(IMALGENE® 1000, Merail) and medetomidine hydrochloride (DOMITOR®, Pfizer Animal Health) to confirm pregnancy by palpation, and then euthanized with sodium pentobarbital 20% (EUTASIL, CEVA Sante Animal) by intravenous injection. The isolated cortices were dissociated for 30 min at 37ºC in Hanks Balanced Salt Solution (HBSS) supplemented with 1.0 mM pyruvate, 2 $mg.ml^{-1}$ albumin, and 10% (v/v) trypsin (all from Gibco). Viable cells (trypan blue exclusion assay) were seeded at a density of 2.2×10^4 viable $cells.cm^{-2}$ onto PLL-coated polymeric discs or cover glasses in 24-well cell culture plates. Neural cells were seeded in 300 µl of Dubelcco's Modified Eagle Medium (DMEM) : Nutrient Mixture F-12 (F-12) (3:1) supplemented with 10% (v/v) inactivated fetal calf serum (FCS) (all from Gibco). Two hours later, medium and o-ring were removed and 1 ml of Neurobasal medium supplemented with 0.5 mM L-glutamine, 2% (v/v) B27 supplement, 1% (v/v) Penicillin-Streptomycin and 0.5% (v/v) Gentamicin (all from Gibco) was added and polymeric discs turned upside down. Cultures were maintained at 37ºC in a humidified atmosphere of 5% CO_2. Culture purity was determined by immunocytochemistry as described further down. Half of the cell culture medium was changed on the third day of culture. After 4 days in culture, samples were treated for immunocytochemistry.

Poly(L-lysine) adsorption quantification

Polymeric disks were coated with PLL-FITC (fluorescein isothiocyanate) (Sigma) as described in the previous section. Cover glass coated with 24 $µg.µl^{-1}$ of PLL, at 37ºC for 30 minutes, was used as control. Polymeric discs coated with PLL-FITC were further mounted on microscope slides using an aqueous mounting media (Sigma) and observed with an inverted fluorescence microscope (Axiovert 200M, Zeiss, Germany). Image analysis was performed with ImageJ 1.44 software.

Atomic force microscopy

Roughness analysis

The roughness of the polymer surfaces tested for cell culture was assessed by atomic force microscopy (AFM) using a PicoPlus scanning probe microscope interface with a PicoScan controller (Agilant Technologies, USA). A 10x10 $µm^2$ piezoscanner was used in tapping mode, with a scan speed of 1 $line.s^{-1}$. A bar shaped silicon cantilever (ACT probe, from AppNano), with a spring constant of 25-75 $N.m^{-1}$ was used and roughness analysis was performed from scanned areas of 7x7 $µm^2$ on five randomly chosen locations of each sample in air, at room temperature. The root-mean-square (RMS) roughness within the

sampling area was determined using the WSxM scanning probe microscope software, [62] according to

$$RMS = \sqrt{\frac{\sum_{i,j}(a_{i,j} - (a))^2}{N}} \qquad (1),$$

where **a** represents the image height and **N** the total number of points.

Nanoindentation

These measurements were performed at CEMUP (Centro de Materiais da Universidade do Porto), on a Veeco Metrology Multimode with Nanoscope IV controler (Veeco Instruments, Inc.) at RT conditions in Force-indent mode with a diamond tip, suitable for nanoindentation (DNISP Diamond-Tipped Probe from Veeco; spring constant 131 $N.m^{-1}$). Deflection sensitivity of the cantilever was calibrated by indenting a sapphire surface. Nanoindentations were made for 1 second and the peak load was confined up to 30 μN for P(TMC-CL) and P(CL) and 6.5 μN for P(TMC). Force-displacement curves were obtained during loading and unloading for each indentation, and further used to determine hardness and stiffness values according to the Oliver and Pharr method. [63] For each polymeric substrate type, 60 indents were done on the film side tested for cell culture, covering 3 randomly chosen regions of 4 different samples per material. In each region, a set of 16 indents were made at a distance of 2 μm of each other. Stiffness was calculated as the slope of the tangent line to the unloading curve at the maximum loading point and hardness values were calculated for the maximum load and taking into consideration the shape of the indenter probe.

Neurite outgrowth on myelin coated polymer films

Myelin isolation

Myelin was isolated from brains of C57BL/6 male mice, as previously described (for animal use ethics please see 5.2.). [64] Briefly, the isolated brains were homogenized in 0.32 M sucrose and after centrifugation at 900g, the post-nuclear supernatant was collected. The post-nuclear supernatant was carefully overlaid on an ultracentrifuge tube containing a 0.85 M sucrose solution on top of a 50% (w/v) sucrose cushion. After centrifugation for 1 hour at 37000 g at 4 ºC (Sorvall Pro80 centrifuge), the interphase between sucrose

solutions was transferred to a new ultracentrifuge tube. Two rounds of osmotic shocks were performed by adding ice-cold water and centrifugation at 20000 g. The final myelin pellet was stored at -80ºC until further use.

Myelin Coating

The polymeric disks and glass control were first coated overnight with PLL as described above and washed with 0.1M $NaHCO_3$. A myelin aqueous solution was subsequently dispensed onto the samples (total myelin protein 1.25 $\mu g.cm^{-2}$), left to dry overnight in the laminar flow hood as previously described by Cai et al. [28], and further used as substrates for cortical neuron culture. Myelin coating of control and polymer surfaces was quantified by fluorescence microscopy after immune labeling of myelin with anti-MBP SMI94 (1: 500, Abcam).

Pharmacologic inhibition of glycogen synthase kinase 3

For neuronal outgrowth assays in the presence of a pharmacologic inhibitor of glycogen synthase kinase 3 (GSK3), a 30 or 300 nM solution of 6-bromoindirubin-3'-acetoxime (BIO) in dimethyl sulfoxide (DMSO) was added to cortical neuron cultures (DMSO final concentration 0.05% (v/v)) at two different time points: at seeding (t = 0) being in contact with cells for 4 days, and at the third day of culture (t = 3) being in contact with cells for 24h. Neurons seeded on polymer discs in the presence of 0.05% (v/v) DMSO were used as controls. After 4 days in culture samples were treated for immunocytochemistry.

Immunocytochemistry

Cells were fixed for immunocytochemistry staining with 2% (v/v) paraformaldehyde at RT and further permeabilized and blocked in phosphate buffered saline (PBS) containing 5% (v/v) Normal Goat Serum (NGS) (Biosource) and 0.2% (v/v) Triton X-100 (Sigma). Primary antibodies were diluted in PBS containing 1% (v/v) NGS and 0.15% (v/v) Triton X-100, and incubated overnight in a humid chamber at 4ºC. Secondary antibodies were applied for 1h at RT and subsequently treated for nuclear counterstaining at RT with Hoechst (Molecular Probes) at 2 $\mu l.ml^{-1}$. Samples were mounted directly in aqueous mounting medium and observed with an inverted fluorescence microscope.

Culture purity was ≥99% in cortical neurons as determined by mouse anti-glial fibrillary acid protein (GFAP) (1:500, BD Biosciences)/ mouse anti-vimentin (1:100, Thermo Scientific)/ mouse anti-oligodendrocyte marker 4 (O4) (1:100, Chemicon)/ rabbit anti-Tau (TAU protein) (1:100, Sigma)/ 2 µg.ml-1 Hoechst fluorescent staining. Cells were counted from 18 radial fields and values were extrapolated to the total surface area of the sample (n=3). For axonal outgrowth assessment the length of the longest neurite and total primary neurite outgrowth per cell were determined using AxioVision image analysis software. Neuronal processes were manually traced and quantified on 130 cells per condition. Three independent experiments were performed.

For neuronal outgrowth analysis on myelin inhibition studies, neurons were stained with anti-βIII tubulin (1:500, Abcam) and myelin with anti-myelin basic protein (MBP) SMI-94 (1:500, Abcam). The secondary antibodies used were anti-rabbit Alexa 488 (1:500, Invitrogen), anti-mouse 594 (1:1000, Invitrogen).

Western Blot

Cortical neuron lysates were prepared by washing cells with PBS and further lysed in buffer containing 20 mM 3-(n-morpholino)propanesulfonic acid (MOPS), 2 mM ethylene glycol tetraacetic acid (EGTA), 5 mM ethylenediaminetetraacetic acid (EDTA), 30 mM NaF, 60 mM β-glycerophosphate, 20 mM sodium pyrophosphate, 1 mM sodium orthovanadate, 1% (v/v) Triton X-100, 1% (v/v) DL-dithiothreitol (DTT), 1 mM phenylmethanesulfonyl fluoride (PMSF) and protease inhibitor cocktail (Amersham). Protein lysates (25-100 µg/lane) were run on a 12% SDS-PAGE gel and then transferred to a nitrocellulose membrane (Amersham). For Western analysis, membranes were blocked with blocking buffer (5% (wt/v) non-fat dried milk in tris-buffered saline (TBS) 0.1% (v/v) Tween 20) and incubated overnight at 4°C in 5% (wt/v) bovine serum albumin (BSA) in TBS 0.1% Tween 20 with primary antibodies. The following primary antibodies were used: rabbit anti-phospho-GSK3β Ser9 (1:1000, Cell Signalling), rabbit anti-phospho-GSK3β Tyr216 (1:2000, Santa Cruz Biotechnology), mouse anti-GSK3α/β (1:2000, Santa Cruz Biotechnology), sheep anti-phospho- CRMP4 Thr 509 (1:1000, Kinasource) and mouse anti-total CRMP4 (1:500, Santa Cruz Biotechnology). After washing, membranes were incubated with secondary antibodies for 1h at RT. The secondary antibodies used were anti-rabbit HRP (1:10000, Jackson Immunoresearch), anti-mouse HRP (1:10000, Thermo Scientific) and anti-goat/sheep (1:10000, Binding Site). Proteins were detected using a chemiluminescent substrate Pierce ECL western blotting substrate (Thermo Scientific) according to the manufacturer's specifications. For each experiment

representative western blots are shown. Phospho-protein expression was quantified by densitometry with QuantityOne software (BioRad) and levels were normalized to the total level of the same protein.

Statistical analysis

For statistical analysis, one-way ANOVA followed by Tukey's post-hoc test were used. When Gaussian distribution was not confirmed non-parametric test Man-Whitney was applied, using the Graphpad Prism program. Data is expressed as the mean ± standard deviation (SD) and p values of < 0.05 were considered significant.

Acknowledgements

Authors acknowledge CEMUP (REEQ/1062/CTM/2005 from FCT), for the nanoindentation analysis. The authors would like to thank Manuela Brás (INEB) for help on the polymeric film rugosity determination by AFM and Dr. Mónica Sousa and Dr. Márcia Liz (IBMC) for their aid in the GSK3β role assessment as well as fruitful discussions of the obtained results.

Financial Disclosure

This work was done with the financial support of the FEDER funds through the Programa Operacional Factores de Competitividade – COMPETE and Portuguese funds through the Fundação para a Ciência e a Tecnologia (FCT) (contracts HMSPICT/0020/2010 and PEst-C/SAU/LA0002/2011), as well as of the European Commission FP6 NEST Program (Contract 028473); as well as Daniela N. Rocha PhD scholarship (SFRH/BD/64079/ 2009). The funders had no role in study design, data collection and analysis, decision to publish, or preparation of the manuscript.

References

[1] Silver J, Miller JH. Regeneration beyond the glial scar. Nature Reviews Neuroscience. 2004;5:146-56.
[2] Schwab JM, Brechtel K, Mueller CA, Failli V, Kaps HP, Tuli SK, et al. Experimental strategies to promote spinal cord regeneration - An integrative perspective. Progress in Neurobiology. 2006;78:91-116.
[3] Madigan NN, McMahon S, O'Brien T, Yaszemski MJ, Windebank AJ. Current tissue engineering and novel therapeutic approaches to axonal regeneration following spinal cord injury using polymer scaffolds. Respiratory Physiology and Neurobiology. 2009;169:183-99.
[4] Thuret S, Moon LDF, Gage FH. Therapeutic interventions after spinal cord injury. Nature Reviews Neuroscience. 2006;7:628-43.
[5] Richardson PM, McGuinness UM, Aguayo AJ. Axons from CNS neurones regenerate into PNS grafts. Nature. 1980;284:264-5.
[6] Prang P, Muller R, Eljaouhari A, Heckmann K, Kunz W, Weber T, et al. The promotion of oriented axonal regrowth in the injured spinal cord by alginate-based anisotropic capillary hydrogels. Biomaterials. 2006;27:3560-9.
[7] Willerth SM, Sakiyama-Elbert SE. Approaches to neural tissue engineering using scaffolds for drug delivery. Advanced Drug Delivery Reviews. 2007;59:325-38.
[8] Friedman JA, Windebank AJ, Moore MJ, Spinner RJ, Currier BL, Yaszemski MJ, et al. Biodegradable polymer grafts for surgical repair of the injured spinal cord. Neurosurgery. 2002;51:742-52.
[9] Straley KS, Foo CWP, Heilshorn SC. Biomaterial design strategies for the treatment of spinal cord injuries. Journal of Neurotrauma. 2010;27:1-19.
[10] Novikova LN, Novikov LN, Kellerth JO. Biopolymers and biodegradable smart implants for tissue regeneration after spinal cord injury. Current Opinion in Neurology. 2003;16:711-5.
[11] Wong DY, Leveque JC, Brumblay H, Krebsbach PH, Hollister SJ, LaMarca F. Macro-architectures in spinal cord scaffold implants influence regeneration. Journal of Neurotrauma. 2008;25:1027-37.
[12] Zhang N, Yan H, Wen X. Tissue-engineering approaches for axonal guidance. Brain Research Reviews. 2005;49:48-64.
[13] Geller HM, Fawcett JW. Building a bridge: Engineering spinal cord repair. Experimental Neurology. 2002;174:125-36.
[14] Pêgo AP, Kubinova S, Cizkiva D, Vanicky I, Mar FM, Sousa MM, et al. Regenerative Medicine for the Treatment of Spinal Cord Injury: More than Just Promises? Journal of Cellular and Molecular Medicine. 2012.
[15] Chen BK, Knight AM, De Ruiter GCW, Spinner RJ, Yaszemski MJ, Currier BL, et al. Axon regeneration through scaffold into distal spinal cord after transection. Journal of Neurotrauma. 2009;26:1759-71.
[16] Wozniak MA, Desai R, Solski PA, Der CJ, Keely PJ. ROCK-generated contractility regulates breast epithelial cell differentiation in response to the physical properties of a three-dimensional collagen matrix. Journal of Cell Biology. 2003;163:583-95.
[17] Chen CS. Mechanotransduction - a field pulling together? Journal of Cell Science. 2008;121:3285-92.
[18] Schuh E, Hofmann S, Stok KS, Notbohm H, Muller R, Rotter N. The influence of matrix elasticity on chondrocyte behavior in 3D. Journal of Tissue Engineering and Regenerative Medicine. 2011.
[19] Fioretta ES, Fledderus JO, Baaijens FPT, Bouten CVC. Influence of substrate stiffness on circulating progenitor cell fate. Journal of Biomechanics. 2012;45:736-44.
[20] Pêgo AP, Poot AA, Grijpma DW, Feijen J. Copolymers of trimethylene carbonate and epsilon-caprolactone for porous nerve guides: Synthesis and properties. Journal of Biomaterials Science, Polymer Edition. 2001;12:35-53.

[21] Pêgo AP, Poot AA, Grijpma DW, Feijen J. In vitro degradation of trimethylene carbonate based (Co)polymers. Macromolecular Bioscience. 2002;2:411-9.
[22] Vleggeert-Lankamp CLAM, Wolfs J, Pêgo AP, Van Den Berg R, Feirabend H, Lakke E. Effect of nerve graft porosity on the refractory period of regenerating nerve fibers: Laboratory investigation. Journal of Neurosurgery. 2008;109:294-305.
[23] LR Pires VG, MJ Oliveira, CC Ribeiro, MA Barbosa, et al. Ibuprofen-loaded poly(trimethylene carbonate–co–e-caprolactone) electrospun fibers for nerve regeneration. Journal of Tissue Engineering and Regenerative Medicine. 2013;(in press).
[24] Pêgo AP, Van Luyn MJA, Brouwer LA, Van Wachem PB, Poot AA, Grijpma DW, et al. In vivo behavior of poly(1,3-trimethylene carbonate) and copolymers of 1,3-trimethylene carbonate with D,L-lactide or Îμ-caprolactone: Degradation and tissue response. Journal of Biomedical Materials Research - Part A. 2003;67:1044-54.
[25] Vleggeert-Lankamp CLAM, De Ruiter GCW, Wolfs JFC, Pêgo AP, Feirabend HKP, Lakke EAJF, et al. Type grouping in skeletal muscles after experimental reinnervation: Another explanation. European Journal of Neuroscience. 2005;21:1249-56.
[26] Kurland NE, Drira Z, Yadavalli VK. Measurement of nanomechanical properties of biomolecules using atomic force microscopy. Micron. 2012;43:116-28.
[27] Peineau S. BC, Taghibiglou C., Doherty A., Bortolotto Z. A.,et al. The role of GSK-3 in synaptic plasticity. Br J Pharmacol. 2008;153:S428-S37.
[28] Juan José Garrido DS, Olga Varea, Francisco Wandosell. GSK3 alpha and GSK3 beta are necessary for axon formation. FEBS lett. 2007;581:1579-86.
[29] Li R. Neuronal polarity: Until GSK-3 do us part. Current Biology. 2005;15:R198-R200.
[30] Grimes CA, Jope RS. The multifaceted roles of glycogen synthase kinase 3b in cellular signaling. Progress in Neurobiology. 2001;65:391-426.
[31] Hur EM, Zhou FQ. GSK3 signalling in neural development. Nature Reviews Neuroscience. 2010;11:539-51.
[32] Castaño Z, Gordon-Weeks PR, Kypta RM. The neuron-specific isoform of glycogen synthase kinase-3b is required for axon growth. Journal of Neurochemistry. 2010;113:117-30.
[33] Alabed YZ, Pool M, Tone SO, Sutherland C, Fournier AE. GSK3b regulates myelin-dependent axon outgrowth inhibition through CRMP4. Journal of Neuroscience. 2010;30:5635-43.
[34] Cai D, Yingjing S, De Bellard ME, Tang S, Filbin MT. Prior exposure to neurotrophins blocks inhibition of axonal regeneration by MAG and myelin via a cAMP-dependent mechanism. Neuron. 1999;22:89-101.
[35] Fournier AE, GrandPre T, Strittmatter SM. Identification of a receptor mediating Nogo-66 inhibition of axonal regeneration. Nature. 2001;409:341-6.
[36] Fu Q, Hue J, Li S. Nonsteroidal anti-inflammatory drugs promote axon regeneration via RhoA inhibition. Journal of Neuroscience. 2007;27:4154-64.
[37] Oscar Siera RG, Vanessa Gil, Franc Llorens, Alejandra Rangel, et al. Neurites regowth of cortical neurons by GSK3b inhibition independently of Nogo receptor 1. Journal of Neurochemistry. 2010;113:1644-58.
[38] Muller H-J, Roder T. Microarrays: Elsevier Academic Press; 2006.
[39] Cafferty WBJ, Gardiner NJ, Gavazzi I, Powell J, McMahon SB, Heath JK, et al. Leukemia inhibitory factor determines the growth status of injured adult sensory neurons. Journal of Neuroscience. 2001;21:7161-70.
[40] Kerschensteiner M, Schwab ME, Lichtman JW, Misgeld T. In vivo imaging of axonal degeneration and regeneration in the injured spinal cord. Nature Medicine. 2005;11:572-7.
[41] Bareyre FM, Kerschensteiner M, Raineteau O, Mettenleiter TC, Weinmann O, Schwab ME. The injured spinal cord spontaneously forms a new intraspinal circuit in adult rats. Nature Neuroscience. 2004;7:269-77.
[42] Leach JB, Brown XQ, Jacot JG, Dimilla PA, Wong JY. Neurite outgrowth and branching of PC12 cells on very soft substrates sharply decreases below a threshold of substrate rigidity. Journal of Neural Engineering. 2007;4:26-34.

[43] Pelham Jr RJ, Wang YL. Cell locomotion and focal adhesions are regulated by substrate flexibility. Proceedings of the National Academy of Sciences of the United States of America. 1997;94:13661-5.
[44] Brunetti V, Maiorano G, Rizzello L, Sorce B, Sabella S, Cingolani R, et al. Neurons sense nanoscale roughness with nanometer sensitivity. Proceedings of the National Academy of Sciences of the United States of America. 2010;107:6264-9.
[45] Radmacher JDaM. Measuring the Elastic Properties of Thin Polymer Films with the Atomic Force Microscope. Langmuir. 1998;14:3320-5.
[46] J.H. Kinney MB, G. M. Marshall, S.J. Marshall, . A micromechanics model of the elastic properties of human dentine. Archives of oral Biology. 1999;44:813-22.
[47] Kol N, Shi Y, Tsvitov M, Barlam D, Shneck RZ, Kay MS, et al. A stiffness switch in human immunodeficiency virus. Biophysical Journal. 2007;92:1777-83.
[48] G. W. Marshall MB, R. R. Gallagher, S. A. Gansky, S. J. Marshall. Mechanical properties of the dentinoenamel junction: AFM studies of nanohardness, elastic modulus, and fracture. J Biomed Mat Res. 2001;54:87-95.
[49] Fan YW, Cui FZ, Chen LN, Zhai Y, Xu QY, Lee IS. Adhesion of neural cells on silicon wafer with nano-topographic surface. Applied Surface Science. 2002;187:313-8.
[50] Fan YW, Cui FZ, Hou SP, Xu QY, Chen LN, Lee IS. Culture of neural cells on silicon wafers with nano-scale surface topograph. Journal of Neuroscience Methods. 2002;120:17-23.
[51] Bates CA, Stelzner DJ. Extension and regeneration of corticospinal axons after early spinal injury and the maintenance of corticospinal topography. Experimental Neurology. 1993;123:106-17.
[52] Hasan SJ, Keirstead HS, Muir GD, Steeves JD. Axonal regeneration contributes to repair of injured brainstem-spinal neurons in embryonic chick. Journal of Neuroscience. 1993;13:492-507.
[53] Yue-Teng Wei YH, Chand-Lei Xu, Ying Wang, Bing-Fang Liu, et al. Hyaluronic acid hydrogel modified with nogo-66 receptor antibody and poly-L-lysine to promote axon regrowth after spinal cord injury. Journal of Biomedical Materials Research. 2010;95B:110-7.
[54] Abu-Rub MT, Billiar KL, Van Es MH, Knight A, Rodriguez BJ, Zeugolis DI, et al. Nano-textured self-assembled aligned collagen hydrogels promote directional neurite guidance and overcome inhibition by myelin associated glycoprotein. Soft Matter. 2011;7:2770-81.
[55] Bregman BS, Kunkel-Bagden E, Schnell L, Dai HN, Gao D, Schwab ME. Recovery from spinal cord injury mediated by antibodies to neurite growth inhibitors. Nature. 1995;378:498-501.
[56] Schnell L, Schwab ME. Axonal regeneration in the rat spinal cord produced by an antibody against myelin-associated neurite growth inhibitors. Nature. 1990;343:269-72.
[57] Dill J, Wang H, Zhou F, Li S. Inactivation of glycogen synthase kinase 3 promotes axonal growth and recovery in the CNS. Journal of Neuroscience. 2008;28:8914-28.
[58] Kim WY, Zhou FQ, Zhou J, Yokota Y, Wang YM, Yoshimura T, et al. Essential Roles for GSK-3s and GSK-3-Primed Substrates in Neurotrophin-Induced and Hippocampal Axon Growth. Neuron. 2006;52:981-96.
[59] Dergham P, Ellezam B, Essagian C, Avedissian H, Lubell WD, McKerracher L. Rho signaling pathway targeted to promote spinal cord repair. Journal of Neuroscience. 2002;22:6570-7.
[60] Maxine Lehmann AF, Immaculada Selles-Navarro, Pauline Dergham, Agnes Sebok, et al. Inactivation of Rho Signaling Pathway Promotes CNS Axon Regeneration. The Journal of Neuroscience. 1999;19:7537-47.
[61] Alabed YZ, Pool M, Tone SO, Fournier AE. Identification of CRMP4 as a convergent regulator of axon outgrowth inhibition. Journal of Neuroscience. 2007;27:1702-11.
[62] Horcas I, Fernandez R, Gomez-Rodriguez JM, Colchero J, Gomez-Herrero J, Baro AM. WSXM: A software for scanning probe microscopy and a tool for nanotechnology. Review of Scientific Instruments. 2007;78.

[63] Hobbs JK, Winkel AK, McMaster TJ, Humphris ADL, Baker AA, Blakely S, et al. Nanoindentation of polymers: An overview. Macromolecular Symposia. 2001;167:15-43.
[64] Norton WT PS. Myelination in rat brain: method of myelin isolation. J Neurochem. 1973;21:749-57.

SUPPLEMENTARY DATA

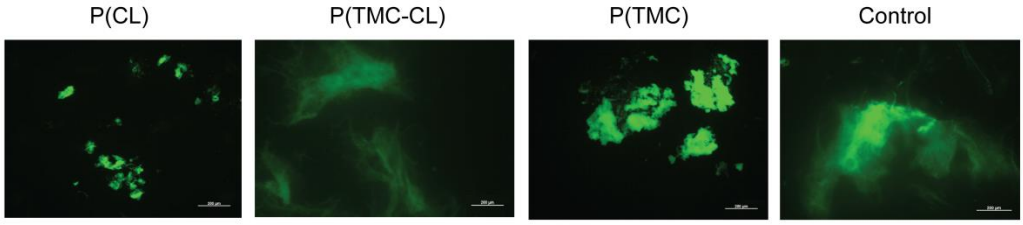

Figure 1S. Representative images of the PLL-FITC coating on the studied surfaces.

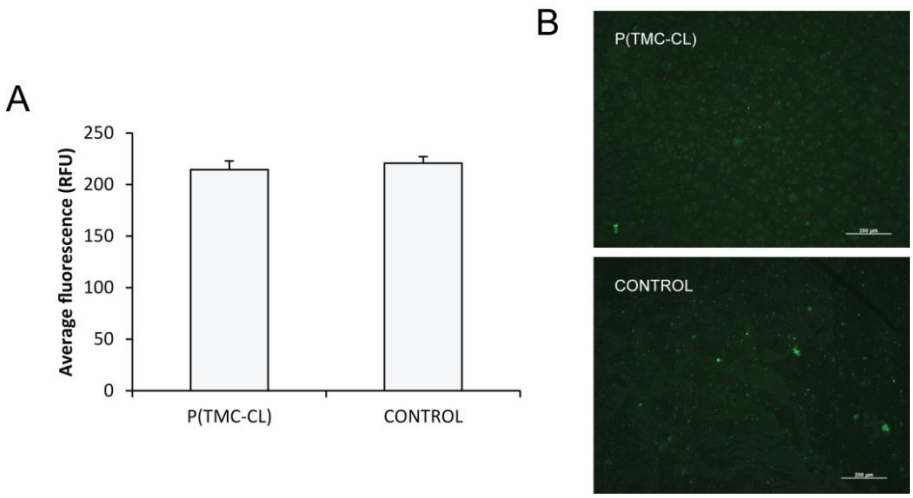

Figure 2S. Distribution of the myelin coating. **A)** Fluorescent quantification of the adsorbed myelin on P(TMC-CL) and glass surfaces.

“ Procurar o sonho é procurar a verdade.”

(Fernando Pessoa)

CHAPTER V

Astrocyte Activation Affects Oligodendrocyte Precursor Cell Differentiation

D. N. Rocha [1,2,3], L. R. Pires [1,2], João B. Relvas [3,4,5], Ana Paula Pêgo [1,3,5]

(1) INEB – Instituto de Engenharia Biomédica, Universidade do Porto, Porto, Portugal; (2) FEUP - Faculdade de Engenharia da Universidade do Porto, Porto, Portugal; (3) I3S – Instituto de Investigação e Inovação em Saúde (4) IBMC – Instituto de Biologia Molecular e Celular, Universidade do Porto, Porto, Portugal; (5) ICBAS – Instituto de Ciências Biomédicas Abel Salazar, Universidade do Porto, Porto, Portugal

ABSTRACT

The loss of the myelin sheath insulating axons is the hallmark of demyelinating diseases. These pathologies often lead to irreversible neurological impairment and patient disability and no effective therapies are currently available to promote remyelination.

Several elements contribute to the inadequacy of remyelination in diseases such as multiple sclerosis, and understanding the intricacies of the cellular and signaling microenvironment of the remyelination niche might help us to devise better strategies to enhance remyelination.

Here using a new *in vitro* rapid myelinating artificial axon system based on engineered microfibers, we investigated how reactive astrocytes influence oligodendrocyte precursor cell differentiation and myelination ability. This artificial axon culture system enables the effective uncoupling of molecular cues from the biophysical properties of the axons allowing the detailed study of the astrocyte-oligodendrocyte cross-talk. Oligodendrocyte progenitor cells were shown to adhere to uncoated engineered microfibers and differentiate into myelinating oligodendrocytes. Reactive astrocytes were found to significantly impair oligodendrocyte precursor cell differentiation ability. This inhibition could be reverted by rescuing the reactive astrocytic phenotype with ibuprofen, a chemical inhibitor of the small rhoGTPase RhoA.

Overall these findings show that modulating astrocytic function might be an interesting therapeutic option for demyelinating diseases. The use of these engineered microfibers as an artificial axon culture system will enable the screening for potential therapeutic agents that promote oligodendrocyte differentiation and myelination while providing valuable insight on the myelination/remyelination processes.

INTRODUCTION

The loss or destruction of the myelin sheet - a dielectric material produced by oligodendrocytes in the CNS that insulates axons is characteristic of numerous pathologies such as contusion-type spinal injury and stroke. In the adult central nervous system (CNS) myelin loss can only be partially rescued by remyelination of spared axons [1]. The newly formed myelin is not made by oligodendrocytes surviving an episode of demyelination, but from oligodendrocyte progenitor cells (OPCs), which become activated, proliferate and give rise to remyelinating oligodendrocytes [2]. Promoting myelin repair is potentially a highly effective means of long-term axon protection, and is a target for the treatment of demyelinating diseases [2-4].

CNS myelination is a complex process and though the mechanisms responsible for chronic remyelination failure have not yet been identified, evidence of the presence of OPCs in chronic multiple sclerosis (MS) lesions [5] suggests the existence of a regulatory mechanism inhibiting OPC differentiation under certain pathological conditions. Namely, it has been proposed that modulation of signalling-pathways like the Rho/ROCK signalling-pathway can rescue OPC differentiation phenotype s [6, 7]. Astrocytes have also been recognized to contribute to CNS myelination [8-10]. During development astrocytes and oligodendrocytes are known to communicate so that myelination can occur in an accurate and timely manner. However, under pathological conditions, such as in the context of demyelinating diseases, astrocytes are also severely affected, playing a pivotal role in the modulation of the CNS extracellular environment. In pathologic scenarios astrocytes become activated expressing increased levels of glial fibrillary acidic protein (GFAP) and also excreting high amounts of extracellular matrix (ECM) components such as chondroitin sulphate proteoglycans (CSPG) and collagen IV [11-13]. The cytokine profile expression of astrocytes is also altered affecting OPC differentiation and myelination capacity [15, 16]. All these components are known to contribute to the formation of the glial scar, which constitutes a barrier for cellular regeneration and myelination, preventing functional recovery [14]. Here, we hypothesize that astrocyte reactivity may play a critical role in the course of OPC differentiation into mature oligodendrocytes and that the reversion of the astrocyte phenotype to a non-activated status can lead to the recovery of OPC differentiation capacity.

We have previously reported an alginate-based 3D model of astrogliosis [13] where astrocytes behave similarly to glial scar astrocytes, showing changes in gene expression

(e.g. GFAP) and increased ECM production (chondroitin 4-sulphate and collagen), inhibiting neuronal outgrowth. Astrocyte activation is thought to be mediated via RhoA and its pharmacological inhibition rescued the astrocyte phenotype. In order to test our hypothesis an *in vitro* rapid myelinating artificial axon system combined with our tissue engineered glial scar was used as a tool to dissect the crosstalk between reactive astrocytes and OPCs. The use of engineered polymeric microfibers mimicking axons enabled the study of the astrocyte-OPC crosstalk and its influence on OPC differentiation ability. This approach allowed us to eliminate axon-OPC cross-talk, as well as achieve myelination in a significantly shorter period of time. Such an approach has been previously explored with success by Howe and his co-workers to study the myelination process [17]. Here, OPCs were cultured on electrospun poly(trimethylene-co-ε-caprolactone) (P(TMC-CL)) fibres in the presence of 3D cultured reactive astrocytes.

MATERIALS AND METHODS

Poly (trimethylene carbonate-co-ε-caprolactone) (P(TMC-CL)) fibre preparation and characterization

P(TMC-CL) was prepared as previously described [18]. Briefly, prior to polymerization ε-caprolactone monomer (Fluka) was dried overnight over CaH_2 and distilled under reduced pressure. Trimethylene carbonate was obtained from Boehringer Ingelheim (Germany) and used as received. Polymerizations were conducted by ring-opening polymerization in an argon atmosphere using stannous octoate as a catalyst. All polymerizations were carried out for a period of 3 days at 130°C±2°C. The obtained polymers were purified by dissolution in chloroform and subsequent precipitation into a ten-fold volume of ethanol. The precipitated polymers were recovered, washed with fresh ethanol and dried under reduced pressure at room temperature (RT) until constant weight. The prepared polymers were characterized with respect to chemical composition by nuclear magnetic resonance (NMR) and found to contain 11% mol of TMC, which was in accordance with the monomer ratio charged (10% mol TMC). The average number molecular weight and polydispersity index of the purified polymer were determined by size exclusion chromatography and were found to be 8.2×10^4 and 1.61, respectively.

P(TMC-CL) fibres were obtained by electrospinning using a polymer solution (10% w/v) in a dichloromethane:dimethylformamide 3:1 mixture (DCM:DMF; Merck, Germany) as

reported elsewhere [18]. The polymer solution was dispensed at a controlled flow rate of 1 $ml.h^{-1}$ using a syringe pump (Ugo Basile, Italy). An electric field of 1 $kV\ cm^{-1}$ was applied (Gamma High Voltage Research, Inc., FL, USA) between the spinneret (inner diameter 0.8 mm) and the flat collector (15 × 15 cm). Fibres were collected during 1–1.5 h onto 13 mm glass coverslips (Menzel-Glaser, Germany) distributed on top of aluminium foil.

Fibre morphology was analysed by scanning electron microscopy (SEM). A JEOL JSM 6301F/ Oxford INCA Energy 350/ Gatan Alto 2500 was used. Fibre diameter was quantified from SEM micrographs using image analysis software Image J (version 1.39; NIH, Bethesda, MD, USA). Fibre-mean diameter and fibre distribution were calculated from at least 100 measurements from three independent samples.

Cell culture

Procedures involving animals and their care were conducted in compliance with institutional ethical guidelines (IBMC) and with the approval of Portuguese Veterinary Authorities. Animals had free access to food and water, being kept under a 12-h light/ 12-h dark cycle.

Cells were obtained from the brains of P2 Wistar Han rats. Isolated cortices were digested in Hank's Balanced Salt Solution (HBSS) without calcium or magnesium supplemented with papain (0.2 $U.ml^{-1}$), for 30 minutes. Dissociated cortices were cultured in 75 cm^2 flasks and maintained in Dulbecco's Modified Eagle Medium (DMEM) supplemented with 10% (v/v) fetal bovine serum (FBS) and 1% (v/v) penicillin-streptomycin (PS). When confluence was reached (~12 days) the flasks were shaken overnight on an orbital shaker (240 rpm) at 37ºC to remove loosely attached microglia and oligodendrocytes. The cells in suspension were then seeded into non-tissue culture treated petri dishes for 2 hrs to remove microglial cells. Oligodendrocyte cells were then seeded on top of polymeric fibres and maintained for 24 hrs in DMEM medium supplemented with transferrin (0,01 mg/ml), bovine serum albumin (BSA) (0.01 $\mu g.ml^{-1}$), putrescin (0.0016 mg/ml), progesterone (0.0060 $\mu g.ml^{-1}$), thyroxine (0.0040 $\mu g.ml^{-1}$), sodium selenite (0.0040 $\mu g.ml^{-1}$), triiodo-l-thyroxine (0.0030 $\mu g.ml^{-1}$), insulin (0.025 µg/ml), platelet derived growth factor (PDGF) (0.01 $\mu g.ml^{-1}$) and fibroblast growth factor (FGF) (0.01 $\mu g.ml^{-1}$). Afterwards cells were cultured without FGF and FBS (0.5%) was added. The remaining cells adhered to the 75 cm^2 flasks were mainly astrocytes, which were trypsinized and re-cultured in new flasks. Further tripsinizations were performed in order to increase culture purity, final astrocyte culture purity was >98%.

Meningeal fibroblasts were obtained from brain meninges of P2 Wistar Han rats. Upon isolation, meningeal tissue was digested in HBSS without calcium or magnesium

supplemented with papain (20 $U.ml^{-1}$, Sigma-Aldrich), for 30 min. Dissociated meninges were plated in poly(L-lysine) (Sigma-Aldrich) coated 75 cm^2 flasks (BioLite), and maintained in DMEM supplemented with 10% (v/v) FBS and 1% (v/v) PS. Fibroblast conditioned medium (CM) was obtained by culturing 13.3 $cells.cm^{-2}$ in DMEM supplemented with 10% FBS and 1% PS, for 72 hours. After collection, CM was centrifuged and stored at 4ºC until use.

Tissue engineered glial scar

In situ forming alginate hydrogel matrices were prepared as previously described [13, 19]. Briefly, PRONOVA ultrapure sodium alginates LVG and VLVG (hereafter designated as high and low molecular weight, HMW and LMW, respectively) with a high guluronic acid content (68%) were purchased from FMC Biopolymers. Hydrogel-precursor solutions with a bimodal molecular weight composition were prepared by combining 1% (wt/v) HMW and LMW alginate solution in 0,9% NaCl, at a 1:1 volume ratio. Primary rat astrocytes were added to alginate solutions ($4x10^6$ $cells.ml^{-1}$) with $CaCO_3$ (Ca^{2+}/COO^- molar ratio = 0.288) and δ-gluconolactone (GDL, Ca^{2+}/GDL molar ratio= 0.125), and the mixture was pipetted (20 µL) onto the wells. After crosslinking (1h, 37ºC), cell-laden 3D matrices were maintained in culture for 4 days, in DMEM or meningeal fibroblast conditioned medium (CM). After these 4 days alginate discs were added to OPC cultures using a transwell, and co-cultures were maintained for additional 5 days.

For the experiments with the pharmacological inhibition of RhoA, ibuprofen (0.04 M) was added to the 3D cultured reactive astrocytes, after the 4 days activation period, for 48 hours.

Imunocytochemistry

Cells were fixed with 4 % (v/v) paraformaldehyde and further permeabilized and blocked in phosphate buffered saline (PBS) containing 5 % (v/v). Normal goat serum (NGS) (Biosource) and 0.2 % (v/v) Triton X-100 (Sigma). Primary antibodies were diluted in PBS containing 1 % (v/v) NGS and 0.15 % (v/v) Triton X-100, and incubated overnight in a humid chamber at 4 ºC. The following primary antibodies were used: mouse anti-NG2 (1:100, Abcam) and rat anti-MBP (1:500, AbD Serotec). Secondary antibodies Alexa-Fluor 488 and 568 were applied for 1h at RT and subsequently treated for nuclear counterstaining at RT with Hoechst (Molecular Probes) at $2µl.ml^{-1}$. Samples were then

observed under a confocal microscope. Cells positive for NG2 and MBP were counted from 10 radial fields.

Myelin geomorphological analysis was carried out in z-stacks taken with a 500µm z-stack step from OPCs cultured on P(TMC-CL) fibres. Images were achieved with the object analyzer tool for 3D microscopy images from Huygens Pro software (SVI) using a seed parameter of 0% and a threshold parameter of 13%.

Environmental Scanning Electron Microscopy

After treatment with 4 % (v/v) paraformaldehyde solution, OPCs cultured on P(TMC-CL) fibres were extensively rinsed with water. Samples were then imaged on a FEI Quanta 400FEG ESEM / EDAX Genesis X4M.

Statistical Analysis

Statistical analysis was performed using the Graphpad Prism program (version 5). Statistical differences between groups were determined based on t-student tests (2 group comparison) or one-way ANOVA tests followed by Tukey's post-hoc analysis (multiple comparisons). When Gaussian distribution was not confirmed (D'Agostino and Pearson omnibus normality analysis) non-parametric tests were applied. Man-Whitney test and Kruskal-Wallis test followed by the Dunn's multiple comparison test were used in the case of paired and multiple comparisons, respectively. Data are expressed as the mean ± standard deviation (SD) and p values <0.05 were considered significant.

RESULTS

P(TMC-CL) fibres promote OPC differentiation into MBP positive oligodendrocytes.

The prepared electrospun P(TMC-CL) fibres were found to have an average diameter of 0,67 ± 0,12 µm (Figure 1A) and the fibre mats depicted a random orientation (Figure 1B). Fibre diameter distribution values ranged from 0,2 µm to 3 µm, with only a very small percentage of the fibres having a diameter larger than 1,5 µm (Figure 1A).

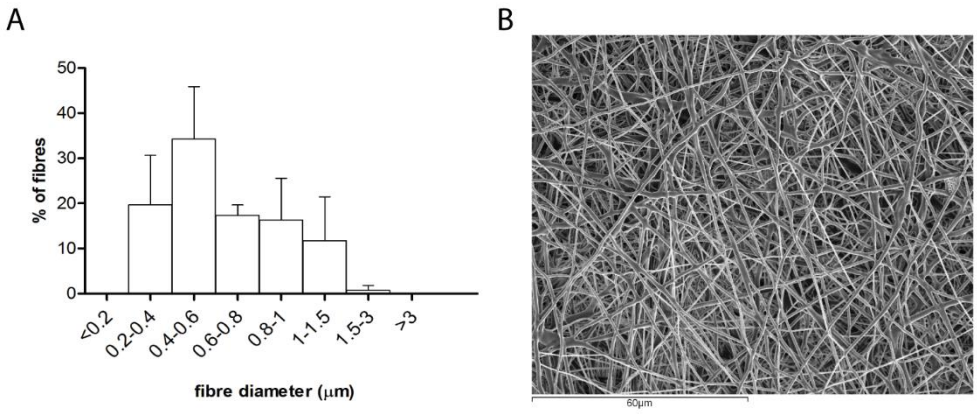

Figure 1 - P(TMC-CL) fibre characterization. **A.** P(TMC-CL) fibre diameter distribution (n = 3 ± SD, standard deviation represents variability between different samples) **B.** Scanning electron microscope image from the P(TMC-CL) fibres.

OPCs were able to adhere, survive and differentiate into MBP positive oligodendrocytes when cultured on the electrospun P(TMC-CL) fibres. After 4 days in culture they produced large membrane extensions, which in some cases contacted with multiple fibres, (Figure 2). Differentiated oligodendrocytes were not only found to extend their processes along nanofibers but also ensheathed them as shown in Figure 2B and in more detail in Figure 1S (supplementary information). It must be highlighted that this was observed without the need to coat the polymeric fibres with any adhesive molecule.

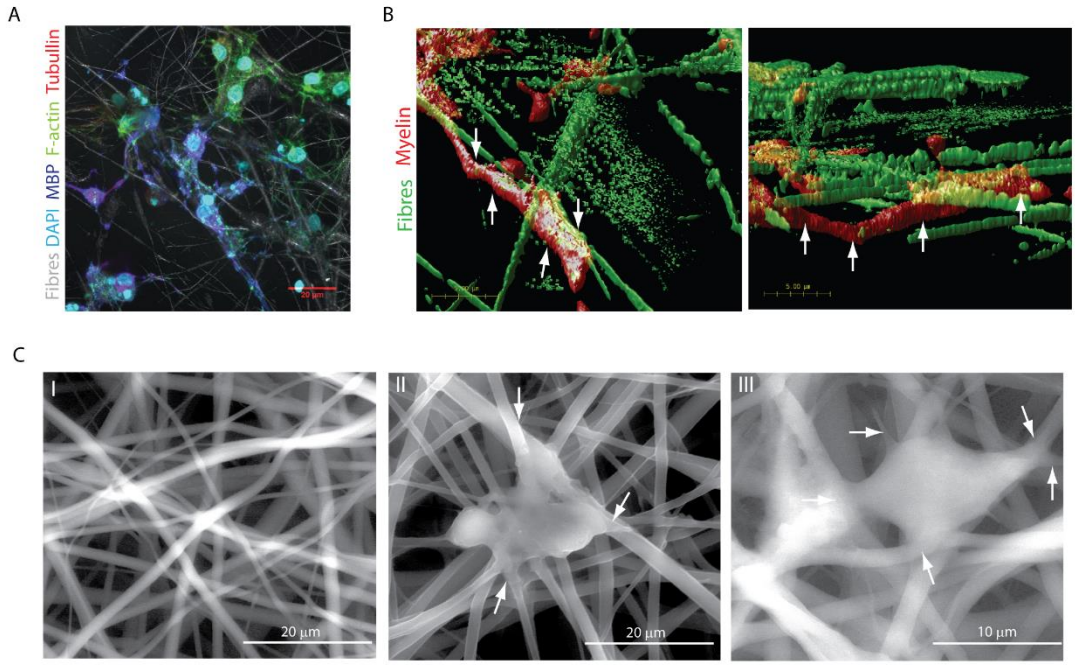

Figure 2 – Oligodendrocyte precursor cells cultured on P(TMC-CL) fibres. **A.** Confocal microscopy image from OPCs cultured on P(TMC-CL) fibres. Fibres can be seen in grey, nuclei are seen in light blue, MBP can be seen in blue, F-actin can be seen in green and tubulin in red. **B.** 3D image of myelinated P(TMC-CL) fibres. Arrows point to an ensheathead fibre segment **C.** Environmental Scanning Electron Microscopy (ESEM) images of OPCs cultured on P(TMC-CL) fibres. I. P(TMC-CL) fibre without cells. II. P(TMC-CL) fibres with oligodendrocytes. III. Detail of oligodendrocyte cell extending processes to several P(TMC-CL). Arrows point out cellular projections of the myelin membrane

Moreover, a significantly higher number of MBP positive oligodendrocytes were found on the P(TMC-CL) fibres than on PDL coated glass control surfaces (Figure 3C).

Reactive astrocytes inhibit OPC differentiation

Monocultures of astrocytes within alginate hydrogels and OPCs on P(TMC-CL) fibres were initially performed in the presence of meningeal fibroblast conditioned medium (CM) (Figure 3A). As previously observed [13], astrocytes were activated by the presence of CM (data not shown). However, no significant alteration in the percentage of MBP positive cells was observed in OPCs cultured on P(TMC-CL) fibres in the presence of meningeal fibroblast CM (Figure 2C and 2D). Conversely, OPC differentiation ability was inhibited in the presence of 3D cultured reactive astrocytes (Figure 3E), with a significant reduction of

the percentage of MBP positive cells (Figure 3E). The percentage of NG2 positive cells was not affected (Figure 3F).

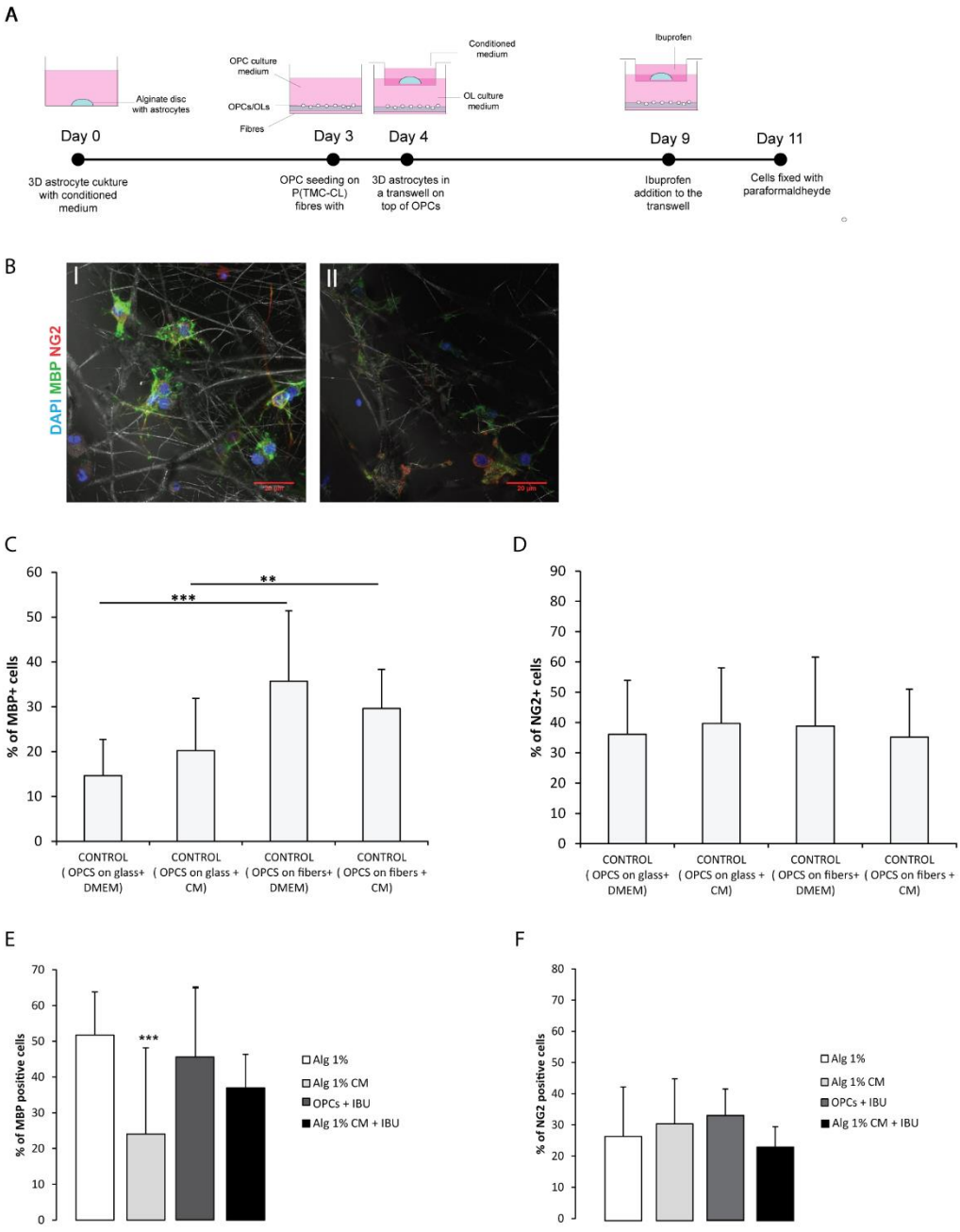

Figure 3 – Differentiation ability of oligodendrocyte precursor cells differentiation cultured on P(TMC-CL) fibres. **A.** Schematic representation of the experiment. Oligodendrocyte precursor cells were cultured on top of P(TMC-CL) fibres and 3D cultured astrocytes (within alginate discs) were cultured on top, in a cell culture insert. 3D cultured astrocytes had been previously activated for 4 days, with meningeal fibroblasts conditioned medium. OPC medium is DMEM medium supplemented with transferrin, bovine serum albumin, putrescin, progesterone, thyroxine, sodium selenite, triiodo-l-thyroxine, insulin, PDGF and FGF; and OL medium is DMEM medium supplemented with transferrin, bovine serum albumin, putrescin, progesterone, thyroxine, sodium selenite, triiodo-l-thyroxine, insulin, PDGF and FBS. **B.** Representative images of OPCs co-cultured

with astrocytes. **I.** OPCs cultured on P(TMC-CL) fibres with control astrocytes. **II.** OPCs cultured on P(TMC-CL) fibres with reactive astrocytes. **C.** Quantification of MBP positive oligodendrocytes in controls. **D.** Quantification of NG2 positive oligodendrocytes in controls. **E.** Quantification of MBP positive cells when OPCs were co-cultures with oligodendrocytes. F. Quantification of NG2 positive cells when OPCs were co-cultured with oligodendrocytes (n= 10 radial fields; average ± SD)

OPCs recover their differentiation ability after astrocyte phenotype rescue

When the 3D cultured reactive astrocytes, co-cultured with OPCs, were treated for 48 hrs with ibuprofen (Figure 3A), a pharmacological inhibitor of RhoA, the number of MBP positive cells on the surface of the polymeric fibres increased significantly, to levels comparable to those from OPCs cultured with non-reactive astrocytes (Figure 3E). Additionally, when ibuprofen was added for 48 hrs to OPC monocultures there was no effect on OPC differentiation ability, as the percentages of MBP and NG2 positive cells remained unchanged (Figure 3E and 3F).

DISCUSSION

Existing models to study oligodendrocyte myelination processes with primary neuron cultures have three major limitations: time, cost and reproducibility. With electrospinning techniques, fibres can be rapidly produced in a standardized way with a range of physical properties depending on the polymer used. Furthermore, these can be configured into various diameters, orientations and even densities. The simplicity of this artificial axon system enables the monitoring of oligodendrocyte behaviour, namely differentiation capacity and membrane wrapping, in the absence of neuronal signals. This model further allows the study of oligodendrocyte interactions with CNS cells in the absence of neurons. Here we explore this artificial axon system to investigate if reactive astrocytes directly affect OPC differentiation ability and, consequently if astrocytes may constitute an interesting therapeutic target for remyelination.

Myelinated axons of the CNS are known to have between 0.3 and 2 µm of diameter with an average diameter of 1 µm [20, 21]. As such, the selected P(TMC-CL) electrospun fibres, with a range of diameters between 0,4 µm and 3 µm, mimic a physiologically relevant mix of a CNS axon population. Remarkably, primary OPCs were able to adhere directly to bare polymeric fibres (Figure 2). To the best of our knowledge, this is the first report of the establishment of an artificial axon system without the need of an adhesive coating. Noteworthy, some authors have even considered that the use of a coating was essential

to promote myelin production in this model system [22]. The fact that these fibres do not need to be coated to support OPC adhesion and differentiation is of added value as several authors have already shown that many of the common coating molecules (e.g. laminin, fibronectin, etc) may affect several signalling transduction pathways [23, 24] in addition to those controlling cell adhesion. In fact, even poly(lysine), which has been for long used to promote non-specific cell adhesion, can activate the phosphatidylinositol 3-kinase (PI3K) signalling pathway [25], which is known to be involved in oligodendrocyte differentiation and CNS myelination [26-28]. Here, the number of cells differentiating into MBP expressing oligodendrocytes was significantly higher in the presence of P(TMC-CL) fibres than on glass control surfaces (Figure 3C). This suggests an important role of the physical 3D cues in the framework of the processes of OPC differentiation and myelin production. These results further demonstrate that although neurons undoubtedly play an important role in the myelination process, they are not crucial for OPC differentiation and myelin expression. Additionally, in an *in vitro* context, the presence of an adhesive substrate is also not essential for myelination to occur.

To test the hypothesis that astrocyte phenotype plays a direct role in OPC differentiation, OPCs were cultured in the presence of a tissue engineered glial scar, in which astrocytes are in a reactive state (Figure 3A). Astrocyte reactivity was achieved as we have previously described [13], by culturing astrocytes within an 1% (w/v) alginate-based hydrogels in the presence of meningeal fibroblast conditioning medium. In these settings astrocytes increased gene expression of astrogliosis hallmark genes including *Gfap* and *Vimentin*, and increased production and excretion of ECM molecules such as CSPG and collagen. Here OPCs were cultured on P(TMC-CL) fibres while in the presence of astrocytes cultures within 3D hydrogels maintained in the top compartment of a transwell system. Our data indicates that reactive astrocytes significantly impair OPC differentiation ability when compared to control astrocytes (Figure 3). These results contradict what was suggested by Nash and co-workers [29] who stated that quiescent astrocytes inhibit myelination. Nevertheless, one must highlight that only a limited verification of the quiescent state was performed in that study.

We have previously shown that RhoA is a pivotal modulator of astrocyte behaviour, with astrocyte reactivity being closely related to RhoA levels [13]. Chemical inhibition of RhoA with ibuprofen, a non-steroidal anti-inflammatory drug previously shown to block RhoA [30, 31], was shown to reduce astrogliosis by recovering normal astrocyte phenotype [13]. Although ibuprofen did not affect OPCs differentiation ability directly (Figure 3E-F), treatment of reactive astrocytes with ibuprofen for 48 hours reverted its inhibitory effect on OPC differentiation, with the percentage of MBP positive cells increasing to values

comparable to the control (Figure 3E). These results reinforce astrocytes' role in CNS myelination processes and highlight astrocytes' potential as a therapeutic target in demyelinating diseases.

CONCLUSIONS

This work shows that reactive astrocytes significantly inhibit OPC differentiation, and that pharmacological inhibition of astrogliosis, enables recovery of OPC differentiation ability. This knowledge is relevant in the context of demyelinating neurodegenerative diseases, such as multiple sclerosis, where astrogliosis is known to occur together with myelination failure. We have further been able to uncouple axonal signalling from OPC differentiation and myelination events, further reinforcing the importance of physical cues for the myelination process. Finally, the proposed *in vitro* artificial axon system may be of added value for further studies aiming to dissect the molecular mechanisms of myelination, as by removing the neuronal cell contribution to the process it allows a more controlled manipulation of defined variables of the culture system, constituting a complementary approach to currently available neuron-glia cell culture methodologies.

SUPPLEMENTARY DATA

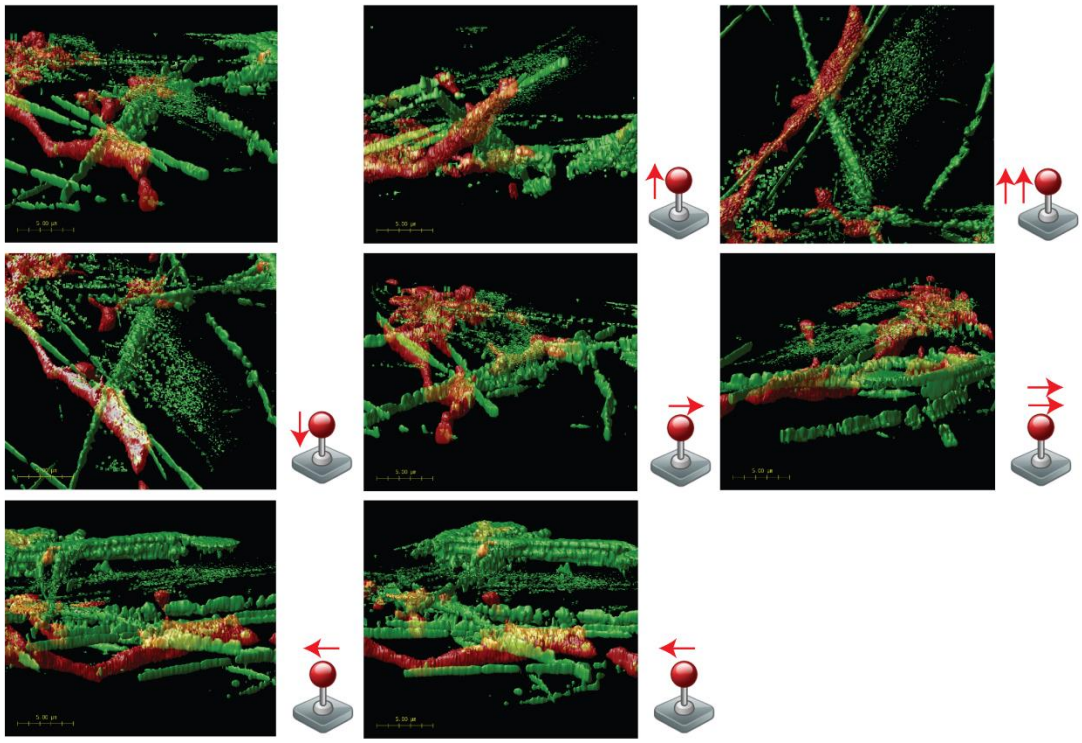

Supplementary Figure 1 – Sequence of 3D images of myelinated P(TMC-CL) fibres. Fibres are shown in green and myelin is shown in red. A joystick image is on the right side of each image, showing the rotation's direction of that image in relation to the first image.

REFERENCES

[1] Bruce CC FR, Relvas JB Remyelination of the central nervous system. In: Interaction Between Neurons and Glia in Aging and Disease Spinger ed. 2007.
[2] Veronique E. Mirona, Tanja Kuhlmannb, Antel JP. Cells of the oligodendroglial lineage, myelination, and remyelination. Molecular Basis of Multiple Sclerosis. 2011;1812:184–93.
[3] Labombarda F, González SL, Lima A, Roig P, Guennoun R, Schumacher M, et al. Effects of progesterone on oligodendrocyte progenitors, oligodendrocyte transcription factors, and myelin proteins following spinal cord injury. Glia. 2009;57.
[4] Zhang J, Zhang ZG, Li Y, Ding X, Shang X, Lu M, et al. Fingolimod treatment promotes proliferation and differentiation of oligodendrocyte progenitor cells in mice with experimental autoimmune encephalomyelitis. Neurobiol Dis. 2015;76:57-66.
[5] RJ F. Why does remyelination fail in multiple sclerosis? . Nat Rev Neurosci. 2002;3:705-14.
[6] Baer SB SY, Kang SU, Mitteregger D, Vig R, Ffrench-Constant C, Franklin RJM, Altmann F, Lubec G, Kotter MR Myelin-mediated inhibition of oligodendrocyte precursor differentiation can be overcome by pharmacological modulation of Fyn-RhoA and protein kinase C signalling. Brain. 2009;132:465-81.
[7] Chang A TW, Rudick R, Trapp BD Premyelinating oligodendrocytes in chronic lesions of multiple sclerosis. N Engl J Med 2002;346:165-73.
[8] Trent A. Watkins BE, Sara Mulinyawe, and Ben A. Barres. Distinct Stages of Myelination Regulated by g-Secretase and Astrocytes in a Rapidly Myelinating CNS Coculture System. Neuron. 2008;60:555-69.
[9] Sorensen A, Moffat K, Thomson C, Barnett SC. Astrocytes, but not olfactory ensheathing cells or Schwann cells, promote myelination of CNS axons in vitro. Glia. 2008;56:750-63.
[10] Ishibashi T, Dakin KA, Stevens B, Lee PR, Kozlov SV, Stewart CL, et al. Astrocytes promote myelination in response to electrical impulses. Neuron. 2006;49:823-32.
[11] Hering TM, Beller JA, Calulot CM, Centers A, Snow DM. Proteoglycans of reactive rat cortical astrocyte cultures: Abundance of N-unsubstituted glucosamine-enriched heparan sulfate. Matrix biology : journal of the International Society for Matrix Biology. 2015;41:8-18.
[12] Liesi P, Kauppila T. Induction of Type IV collagen and other basement-membrane associated proteins after spinal cord injury and the adult rat may participate in formation of the glial scar. Exp Neurol. 2002;173:31-45.
[13] Rocha DN, Ferraz-Nogueira J, Barrias CC, Relvas JB, Pêgo AP. Extracellular Environment Contribution to Astrogliosis – Lessons learned from a Tissue Engineered 3D Model of the Glial Scar. Front Cell Neurosci. 2015;9:377.
[14] García-Álvarez I, Fernández-Mayoralas A, Moreno-Lillo S, Sánchez-Sierra M, Nieto-Sampedro M, E D-P. Inhibition of glial proliferation, promotion of axonal growth and myelin production by synthetic glycolipid: A new approach for spinal cord injury treatment. Restor Neurol Neurosci. 2015.
[15] Wang Y, Cheng X, He Q, Zheng Y, Kim DH, Whittemore SR, et al. Astrocytes from the contused spinal cord inhibit oligodendrocyte differentiation of adult oligodendrocyte precursor cells by increasing the expression of bone morphogenetic proteins. J Neurosci 2011;31:6053-8.
[16] Su Z, Yuan Y, Chen J, Zhu Y, Qiu Y, Zhu F, et al. Reactive astrocytes inhibit the survival and differentiation of oligodendrocyte precursor cells by secreted TNF-α. J Neurotrauma. 2011;28:1089-100.
[17] Howe CL. Coated Glass and Vycril Microfibers as Artificial Neurons. Cells Tissues Organs. 2006;183:180-94.

[18] Pires LR, Guarino V, Oliveira MJ, Ribeiro CC, Barbosa MA, Ambrosio L, et al. Ibuprofen-loaded poly(trimethylene carbonate-co-epsilon-caprolactone) electrospun fibres for nerve regeneration. Journal of tissue engineering and regenerative medicine. 2013.
[19] Maia FR, Barbosa M, Gomes DB, Vale N, Gomes P, Granja PL, et al. Hydrogel depots for local co-delivery of osteoinductive peptides and mesenchymal stem cells. J Control Release. 2014;189:158-68.
[20] Berthold CH, Nilsson I, Rydmark M. Axon diameter and myelin sheath thickness in nerve fibres of the ventral spinal root of the seventh lumbar nerve of the adult and developing cat. Journal of anatomy. 1983;136:483-508.
[21] Ruit KG, Elliott JL, Osborne PA, Yan Q, Snider WD. Selective dependence of mammalian dorsal root ganglion neurons on nerve growth factor during embryonic development. Neuron. 1992;8:573-87.
[22] Howe CL. Coated glass and vicryl microfibers as artificial axons. Cells, tissues, organs. 2006;183:180-94.
[23] Liberio MS, Sadowski MC, Soekmadji C, Davis RA, Nelson CC. Differential effects of tissue culture coating substrates on prostate cancer cell adherence, morphology and behavior. PloS one. 2014;9:e112122.
[24] L'Hote C G, Thomas PH, Ganesan TS. Functional analysis of discoidin domain receptor 1: effect of adhesion on DDR1 phosphorylation. FASEB journal : official publication of the Federation of American Societies for Experimental Biology. 2002;16:234-6.
[25] Weiger MC, Wang CC, Krajcovic M, Melvin AT, Rhoden JJ, Haugh JM. Spontaneous phosphoinositide 3-kinase signaling dynamics drive spreading and random migration of fibroblasts. Journal of cell science. 2009;122:313-23.
[26] Kumar S, Patel R, Moore S, Crawford DK, Suwanna N, Mangiardi M, et al. Estrogen receptor beta ligand therapy activates PI3K/Akt/mTOR signaling in oligodendrocytes and promotes remyelination in a mouse model of multiple sclerosis. Neurobiol Dis. 2013;56:131-44.
[27] Flores AI, Narayanan SP, Morse EN, Shick HE, Yin X, Kidd G, et al. Constitutively active Akt induces enhanced myelination in the CNS. J Neurosci. 2008;28:7174-83.
[28] Narayanan SP, Flores AI, Wang F, Macklin WB. Akt signals through the mammalian target of rapamycin pathway to regulate CNS myelination. J Neurosci. 2009;29:6860-70.
[29] Nash B, Thomson CE, Linington C, Arthur AT, McClure JD, McBride MW, et al. Functional duality of astrocytes in myelination. The Journal of neuroscience : the official journal of the Society for Neuroscience. 2011;31:13028-38.
[30] Wang X, Budel S, Baughman K, Gould G, Song KH, Strittmatter SM. Ibuprofen enhances recovery from spinal cord injury by limiting tissue loss and stimulating axonal growth. J Neurotrauma. 2009;26:81-95.
[31] Dill J, Patel AR, Yang XL, Bachoo R, Powell CM, Li S. A molecular mechanism for ibuprofen-mediated RhoA inhibition in neurons. J Neurosci. 2010;30:963-72.

CHAPTER VI

Concluding Remarks

The Central Nervous System (CNS) is complex and all its constituents - neurons, astrocytes, oligodendrocytes, microglia and extracellular matrix (ECM) - play important roles in the homeostasis of this system.

An insult to the CNS usually results in astrogliosis and the formation of a glial scar. The glial scar is characterized by having a high number of reactive astrocytes and altered ECM composition, constituting a barrier to regeneration [1]. Although astrocytes have long been considered as central players in the glial scar formation, the dynamics of such process has not been uncovered yet. Furthermore, the perceived role of astrocytes has changed and evolved. Initially they were seen as only providing support to neurons and astrocytes. Now they are known to be complex, highly differentiated cells that make numerous essential contributions to normal function in the healthy CNS, like regulation of blood-flow, provision of energy metabolites to neurons, participation in synaptic function and plasticity, and maintenance of the extracellular balance of ions [2, 3]. To understand how the changes in a CNS lesion environment occur and how these condition the progress of the tissue response and ultimately of disease, requires a systematic approach, as scar formation results from a plethora of events.

Given this, the work here presented first introduces a tissue engineered 3D glial scar. An alginate-based 3D culture model has been designed with mechanical properties similar to those of CNS tissue [4] and to further work as an inert backbone structure [5] allowing the control over system's complexity, from which it is possible to recover the cultured cells for further biochemical and cellular assays. The glial scar environment was recreated by stimulating astrocytes with meningeal fibroblasts conditioned medium. The resulting tissue engineered glial scar presented numerous features of the glial scars as cells present the phenotype of scar astrocytes in terms of gene expression, increased ECM production and inhibition of axonal outgrowth. Overall this behavior was found to be influenced by alginate network mechanical properties.

Envisaging the use of biomaterials as bridges to support axonal regeneration in spinal cord injuries, a poly(trymethylene-carbonate-co-ε-caprolactone) (P(TMC-CL)) based culture system with high caprolactone content was used to study mechanotransduction's relevance and impact on axonal outgrowth and polarization. In the follow up of a spinal cord injury, axonal outgrowth inhibition has been mainly attributed to myelin debris that remains in the lesion area [6, 7]. In the described experimental setup, surface nanomechanical properties were also explored and found to modulate neuronal ability to extend axons, even under inhibitory conditions such as the presence of myelin debris.

These results further reinforce the idea that mechanical properties play a pivotal role in CNS lesion environments, and may be an important therapeutic target showing the importance of tuning the implantable material's mechanical properties.

At this stage, we hypothesized that if mechanotransduction affects important CNS events such as astrogliosis and axonal outgrowth, there are probably other complex events, which can be at least partially modulated via mechanotransduction. In fact, the combination of the developed tissue engineered 3D glial scar with a P(TMC-CL) based artificial axon culture system, has shown that mechanical stimuli can also affect OPC differentiation and myelination processes, addressing the cross-talk between astrocytes and OPCs. Reactive astrocytes were shown to negatively affect OPC differentiation and myelination processes. Nevertheless, when astrocyte phenotype was modulated to a non-activated state, OPC differentiation ability was recovered. Additionally, our data indicates that contrarily to what many authors have suggested [8] neurons and their axons are not crucial for OPCs to differentiate and myelinate.

In all these studies, which specifically explored the role of mechanotransduction in astrocyte activation, in axonal outgrowth and in OPC differentiation and myelination capacity, the molecular mechanisms underlying these events were explored. RhoA was found to play a pivotal role in the mechanotransduction events, and its inhibition, either pharmacologically, with ibuprofen or chondroitinase ABC (chABC), or via substrate mechanical properties, significantly enhanced regenerative features.

- Treatment with ibuprofen or chABC, drugs known to inhibit RhoA signaling [9, 10], reduced astrocyte reactivity.
- P(TMC-CL) promoted axonal elongation via GSK3β signaling pathway. GSK3β phosphorylation and consequent inactivation, was found to regulate the interaction of CRMP4 and RhoA through CRMP4 de-phosphorylation.
- Recovery of astrocyte phenotype with ibuprofen, in OPCs-reactive astrocytes co-cultures, enabled the recovery of OPCs differentiation ability.

Overall we have developed an *in vitro* 3D tissue engineered glial scar and an artificial axon culture system, which can be of added value in future neurodegenerative mechanism studies, as well as in drug screenings envisaging the development of new therapeutic approaches. Most importantly, we were able to show the importance of mechanotransduction in the CNS, particularly in neurons, astrocytes and OPCs. As such, mechanotransduction is here established as an interesting target for the development of new therapeutical combinatorial approaches to treat neurodegenerative diseases.

REFERENCES

[1] Wanner IB, Deik A, Torres M, Rosendahl A, Neary JT, Lemmon VP, et al. A new in vitro model of the glial scar inhibits axon growth. Glia. 2008;56:1691-709.
[2] Seifert G, Schilling K, Steinhauser C. Astrocyte dysfunction in neurological disorders: a molecular perspective. Nature reviews Neuroscience. 2006;7:194-206.
[3] Sofroniew MV. Molecular dissection of reactive astrogliosis and glial scar formation. Trends in neurosciences. 2009;32:638-47.
[4] Banerjee A, Arha M, Choudhary S, Ashton RS, Bhatia SR, Schaffer DV, et al. The influence of hydrogel modulus on the proliferation and differentiation of encapsulated neural stem cells. Biomaterials. 2009;30:4695-9.
[5] Lutolf MP, Blau HM. Artificial stem cell niches. Advanced Materials. 2009;21:3255-68.
[6] Mar FM, da Silva TF, Morgado MM, Rodrigues LG, Rodrigues D, Pereira MI, et al. Myelin Lipids Inhibit Axon Regeneration Following Spinal Cord Injury: a Novel Perspective for Therapy. Molecular neurobiology. 2015.
[7] Xu CJ, Wang JL, Jin WL. The Neural Stem Cell Microenvironment: Focusing on Axon Guidance Molecules and Myelin-Associated Factors. Journal of molecular neuroscience : MN. 2015.
[8] Nash B, Thomson CE, Linington C, Arthur AT, McClure JD, McBride MW, et al. Functional duality of astrocytes in myelination. J Neurosci. 2011;31:13028-38.
[9] Dill J, Patel AR, Yang XL, Bachoo R, Powell CM, Li S. A molecular mechanism for ibuprofen-mediated RhoA inhibition in neurons. J Neurosci. 2010;30:963-72.
[10] Wang X, Budel S, Baughman K, Gould G, Song KH, Strittmatter SM. Ibuprofen enhances recovery from spinal cord injury by limiting tissue loss and stimulating axonal growth. J Neurotrauma. 2009;26:81-95.

Appendix

(12) INTERNATIONAL APPLICATION PUBLISHED UNDER THE PATENT COOPERATION TREATY (PCT)

(19) World Intellectual Property Organization
International Bureau

(43) International Publication Date
31 July 2014 (31.07.2014)

WIPO | PCT

(10) International Publication Number
WO 2014/116132 A1

(51) International Patent Classification:
A61K 31/765 (2006.01) *A61P 25/00* (2006.01)
A61L 27/58 (2006.01) *A61K 31/198* (2006.01)

(21) International Application Number:
PCT/PT2014/000006

(22) International Filing Date:
28 January 2014 (28.01.2014)

(25) Filing Language: English

(26) Publication Language: English

(30) Priority Data:
1301461.8 28 January 2013 (28.01.2013) GB

(71) Applicant: **INEB - INSTITUTO NACIONAL DE ENGENHARIA BIOMÉDICA** [PT/PT]; Rrua do Campo Alegre, 823, P-4150-180 Porto (PT).

(72) Inventors: **PÊGO, Ana Paula**; Rua do Rosário 236, P-4050-522 Porto (PT). **ROCHA, Daniela**; Rua das Violetas, nº34 2º tras, P-4480-775 Vila do Conde (PT).

(74) Agent: **VIEIRA PEREIRA FERREIRA, Maria Silvina**; Clarke, Modet & Co., Rua Castilho, 50-9º, P-1269-163 Lisboa (PT).

(81) Designated States *(unless otherwise indicated, for every kind of national protection available)*: AE, AG, AL, AM, AO, AT, AU, AZ, BA, BB, BG, BH, BN, BR, BW, BY, BZ, CA, CH, CL, CN, CO, CR, CU, CZ, DE, DK, DM, DO, DZ, EC, EE, EG, ES, FI, GB, GD, GE, GH, GM, GT, HN, HR, HU, ID, IL, IN, IR, IS, JP, KE, KG, KN, KP, KR, KZ, LA, LC, LK, LR, LS, LT, LU, LY, MA, MD, ME, MG, MK, MN, MW, MX, MY, MZ, NA, NG, NI, NO, NZ, OM, PA, PE, PG, PH, PL, PT, QA, RO, RS, RU, RW, SA, SC, SD, SE, SG, SK, SL, SM, ST, SV, SY, TH, TJ, TM, TN, TR, TT, TZ, UA, UG, US, UZ, VC, VN, ZA, ZM, ZW.

(84) Designated States *(unless otherwise indicated, for every kind of regional protection available)*: ARIPO (BW, GH, GM, KE, LR, LS, MW, MZ, NA, RW, SD, SL, SZ, TZ, UG, ZM, ZW), Eurasian (AM, AZ, BY, KG, KZ, RU, TJ, TM), European (AL, AT, BE, BG, CH, CY, CZ, DE, DK, EE, ES, FI, FR, GB, GR, HR, HU, IE, IS, IT, LT, LU, LV, MC, MK, MT, NL, NO, PL, PT, RO, RS, SE, SI, SK, SM, TR), OAPI (BF, BJ, CF, CG, CI, CM, GA, GN, GQ, GW, KM, ML, MR, NE, SN, TD, TG).

Published:

— *with international search report (Art. 21(3))*

WO 2014/116132 A1

(54) Title: BIOMATERIAL COMPRISING POLY(TRIMETHYLENE CARBONATE-CO-E-CAPROLACTONE) FOR PROMOTING AXONALL GROWTH AND NEURONAL REGENERATION

(57) Abstract: Mammalian central nervous system (CNS) neurons do not regenerate after injury due to the inhibitory environment formed by the glial scar, largely constituted by myelin debris. The use of biomaterials to bridge the lesion area and the creation of an environment favoring axonal regeneration is an appealing approach, currently under investigation. This work aimed at assessing the suitability of three candidate polymers - poly(?-caprolactone), poly(trimethylene carbonate-co- ?-caprolactone) (P(TMC-CL)) (11:89 mol%) and poly(trimethylene carbonate) - with the final goal of using these materials in medicine, namely in the development of conduits to promote spinal cord regeneration. Cortical neurons cultured on P(TMC-CL) in the presence of myelin were able to tame myelin inhibition in comparison with the control condition (glass substrate). This effect was found to be mediated by the glycogen synthase kinase 3p (GSK3p) signaling pathway with impact on the collapsin response mediator protein 4 (CRMP4), suggesting that nanomechanical properties were implicated in this process. The obtained results indicate P(TMC-CL) as a promising material for CNS regenerative applications as it promotes axonal growth, taming myelin inhibition.

BIOMATERIAL COMPRISING POLY(TRIMETHYLENE CARBONATE-CO-E-CAPROLACTONE) FOR PROMOTING AXONAL GROWTH AND NEURONAL REGENERATION

Field of the Invention

The present invention relates to a biomaterial for use in medicine, in particular for promoting neuronal growth in the central nervous system, wherein the biomaterial comprises poly(trimethylene carbonate-co-ε-caprolactone) (P(TMC-CL)). This biomaterial can be used in the regeneration of neurons in the central nervous system (CNS), such as the spinal cord.

Background to the Invention

When an injury is inflicted to the spinal cord, the blood-brain barrier (BBB) breaks down locally and a massive infiltration of immune cells is observed. After the initial mechanical trauma (primary damage), cell damage is triggered such that within hours the injury site and the surrounding haemorrhagic areas begin to undergo necrosis (secondary damage), a progressive process that can last for several days. Tissue necrosis is thought to result from a combination of processes, including free-radical induced injury, excitotoxic amino acids and the release of toxic cytokines by inflammatory cells. As the necrotic tissue is removed by macrophages, large fluid-filled cavities develop, which are bordered by areas of glial/connective tissue scarring. Even though this glial scar may provide several beneficial functions such as the restoration of the BBB, prevention of a devastating inflammatory response and limit action of cellular degeneration [1, 2], it also contributes to the establishment of a physical and chemical barrier to axonal regeneration [1]. Strategies aimed at preventing primary and delaying secondary damage need to be administered within minutes to hours after injury [3]. Furthermore, none of the clinical approaches currently available to control or minimize the impact of a SCI lead to neuronal regeneration [4], nor is there an efficient regenerative therapeutic strategy for SCI treatment [4]. Although injured axons show the ability to regenerate when in a peripheral nervous system environment [5], the major factor contributing to the failure of the central nervous system (CNS) regeneration is the lack of capacity of injured axons to spontaneously regenerate in the glial scar microenvironment [6].

The use of biocompatible biomaterials to bypass the glial scar is one of the promising approaches being investigated to promote spinal cord regeneration [3, 7-13]. These tissue-engineering

approaches are usually based on the use of either cell-free bridges or of cellularized biomaterial-based matrices. There are some advantages in the use of a cell-free bridging material, as on one hand cell purification and expansion methods are laborious, time consuming and expensive, and on the other hand when the transplantation of allogenic cells is required, the use of immunosuppressants cannot be circumvented [13]. Therefore the idea of a cell-free bridging material that uses and controls endogenous cell population responses, by having the ability to promote axon regeneration and control inflammatory and glial reactions is appealing.

There are numerous polymeric materials under study for application in nerve repair strategies [3, 10, 14]. These can simultaneously provide a scaffold for tissue regeneration, as well as serve as a cell-delivery vehicle and a reservoir for sustained drug delivery [15]. Within this class of materials, biodegradable polymers are particularly advantageous for the preparation of these bridges, as polymer degradation can be tuned to match the neuronal cell growth. Besides the degradation rate, the mechanical properties of the selected material are also of extreme relevance, as they must be fitted to one's needs. While the implantable structures must be flexible but relatively strong, as well as easy to handle by surgeons, their mechanical properties have an influence on cell phenotype as well [16-19].

Poly(trimethylene carbonate-co-ε-caprolactone) (P(TMC–CL)) copolymers or the parental trimethylene carbonate (TMC) homopolymer are very flexible and tough materials that can be processed into highly porous three dimensional structures with degradation rates that can be modulated by adjusting the co-monomer content [20, 21]. These materials have been shown to be biocompatible [21-23] and have been previously explored for peripheral nerve regeneration conduits [20, 23-26]. Additionally, polymer degradation occurred with minimum swelling of the material [23], which is also an essential feature to prevent nerve compression that could compromise regeneration.

Although P(TMC–CL) copolymers have been previously explored for peripheral nerve regeneration, regeneration of nerves in the CNS is hampered by the inhibitory environment formed by the glial scar, largely constituted by myelin debris. For example, it has been shown that many materials, which have shown an effect in the periphery, do not promote nerve regeneration in the CNS. Furthermore, there is no material that has been found to be able to promote axonal elongation and neuronal polarization, even in the absence of myelin (an

inhibitory substrate). Therefore, there would be no expectation that P(TMC–CL) copolymers would be able promote neuronal growth in the CNS, in particular, axonal elongation and neuronal polarization.

Summary of the Invention

In a first aspect, the present invention provides a biomaterial for use in medicine, namely for promoting neuronal regeneration in the CNS, wherein the biomaterial comprises poly(trimethylene carbonate-co-ε-caprolactone) (P(TMC-CL)).

It has been surprisingly found that the copolymer poly(trimethylene carbonate-co-ε-caprolactone) is able to promote neuronal regeneration, in particular, neuronal polarization and axonal elongation, in the CNS, even under inhibitory conditions. This is especially surprising as polymers of the two constituents, i.e. poly(trimethylene carbonate) and poly(ε-caprolactone) do not promote this effect on their own.

The biomaterial can be used to treat conditions in which neuronal regeneration of the CNS is required. The CNS is defined as the brain and the spinal cord of a subject. The CNS does not include the sciatic nerves.

The biomaterial can be used to treat damage to the CNS. In this regard, the invention provides a biomaterial for use in treating damage to the CNS, wherein the biomaterial comprises poly(trimethylene carbonate-co-ε-caprolactone) (P(TMC-CL)). This damage may occur as a result of a number of different causes. The damage may occur due to a disease, which causes damage to the CNS, or injury. For example, damage to the CNS may occur as a result of: trauma, e.g. a spinal cord injury (SCI); an infection such as poliomyelitis; neurodegeneration such as amyotrophic lateral sclerosis; a tumour; an autoimmune and/or inflammatory disease such as multiple sclerosis; or spinal stroke. Where the damage to the CNS is caused by disease, the biomaterial causes regeneration of nerves in the CNS rather than treating the underlying cause of the damage.

The biomaterial can be used to treat injury or trauma to the CNS. In particular, the biomaterial can be used to treat spinal cord injury. This typically happens as a result of damage to the spinal cord of a subject.

Poly(trimethylene carbonate-co-ε-caprolactone) is a copolymer formed from the monomers trimethylene carbonate and ε-caprolactone. This copolymer can be formed in any suitable way. For example, polymerisation may be carried out using ring-opening polymerization. This may be done in an inert atmosphere such as an argon atmosphere or in solution. In some embodiments, the polymerization reaction is carried out in an inert atmosphere. A catalyst may be used such as stannous octoate or yttrium isopropoxide. In some embodiments, stannous octoate is used as a catalyst. The polymerization reaction may be carried out for a period of between 1 and 40 days depending on the temperature of polymerisation and the size of polymer required. The polymerization reaction may be carried out for a period of between 1 and 5 days. In some embodiments, the polymerization reaction is carried out for between 2 and 4 days. In particular embodiments, the polymerization reaction is carried out for 3 days. The polymerization reaction may be carried out at between about 60°C and about 200°C or between about 100°C and about 160°C. In some embodiments, the polymerisation reaction is carried out at between about 110°C and about 150°C. In further embodiments, the polymerisation reaction may be carried out at between about 120°C and about 140°C. The polymerisation reaction may be carried out at about 130°C, e.g. 130°C ± 2°C.

In certain embodiments, the polymerization reaction is carried out for between 2 and 4 days at between about 100°C and about 160°C. In some embodiments, the polymerization reaction is carried out for 3 days at between about 120°C and about 140°C such as about 130°C, e.g. 130°C ± 2°C.

The poly(trimethylene carbonate-co-ε-caprolactone) contains trimethylene carbonate and ε-caprolactone as monomers. The ratio of these monomers should be such that the polymer has the required physical properties to cause neuronal regeneration in the CNS. In some embodiments, the molar ratio of trimethylene carbonate to ε-caprolactone may be between about 1:20 and about 1:3, respectively. In other embodiments, the molar ratio of trimethylene carbonate to ε-caprolactone may be between about 1:19 and about 1:3. In further embodiments, the molar ratio of trimethylene carbonate to ε-caprolactone may be between about 1:17 and about 1:3. The molar ratio of trimethylene carbonate to ε-caprolactone may be between about 1:15 and about 1:3. In particular embodiments, the molar ratio of trimethylene carbonate to ε-caprolactone may be between about 1:20 and about 1:4. In certain embodiments, the molar ratio of trimethylene carbonate to ε-caprolactone may be between about 1:15 and about 1:5. The molar ratio of trimethylene carbonate to ε-caprolactone may be between about 1:10 and about 1:6. Further, the

molar ratio of trimethylene carbonate to ε-caprolactone may be between about 1:9 and about 1:7. The molar ratio of trimethylene carbonate to ε-caprolactone may be about 1:8.

Alternatively, in some embodiments, the molar ratio of trimethylene carbonate to ε-caprolactone may be between about 5:95 and about 25:75, respectively. In other embodiments, the molar ratio of trimethylene carbonate to ε-caprolactone may be between about 5:95 and about 23:77. In further embodiments, the molar ratio of trimethylene carbonate to ε-caprolactone may be between about 5:95 and about 21:79. In particular embodiments, the molar ratio of trimethylene carbonate to ε-caprolactone may be between about 5:95 and about 19:81. In certain embodiments, the molar ratio of trimethylene carbonate to ε-caprolactone may be between about 5:95 and about 17:83. The molar ratio of trimethylene carbonate to ε-caprolactone may be between about 7:93 and about 15:85. Further, the molar ratio of trimethylene carbonate to ε-caprolactone may be between about 9:91 and about 13:87. Furthermore, the molar ratio of trimethylene carbonate to ε-caprolactone may be between about 10:90 and about 12:88. The molar ratio of trimethylene carbonate to ε-caprolactone may be about 11:89.

The trimethylene carbonate and the ε-caprolactone should be polymerised to an appropriate degree to give a polymer with the required characteristics. The degree of polymerisation can be measured using the number average molecular weight (Mn).
The copolymer may have a number average molecular weight of at least about 0.2×10^5. The copolymer may have a number average molecular weight of less than about 2×10^5. In some embodiments, the copolymer has a number average molecular weight of less than about 1.5×10^5. The copolymer may have a number average molecular weight of less than about 1×10^5. In further embodiments, the copolymer may have a number average molecular weight of less than about 0.75×10^5. In other embodiments, the copolymer may have a number average molecular weight of less than about 0.5×10^5. In particular, embodiments, the copolymer has a number average molecular weight of at least about 0.2×10^5 and less than about 1×10^5. The copolymer may have a number average molecular weight of about 0.37×10^5.

The copolymer may have a stiffness of between about 200 N/m and about 400 N/m. The copolymer may have a stiffness of about 312 N/m.

The copolymer may have a hardness of between about 1 x 10^6 N/m^2 and about 6 x 10^6 N/m^2. In some embodiments, the copolymer has a hardness of between about 2 x 10^6 N/m^2 and about 5 x 10^6 N/m^2. In other embodiments, the copolymer has a hardness of between about 3 x 10^6 N/m^2 and about 4 x 10^6 N/m^2. The copolymer may have a hardness of about 3.32 x 10^6 N/m^2.
The copolymer may have a roughness of between about 10 nm and about 50 nm. The copolymer may have a roughness of about 24 nm.

The poly(trimethylene carbonate-co-ε-caprolactone) may be coated with a molecule that promotes cell adhesion to the polymer. This molecule may be any suitable molecule such as fibronectin, laminins (e.g. laminin-111), collagen (e.g. collagen type I), poly(ethylene imine) or synthetic oligopeptides or polypeptides (e.g. poly(L-lysine) (PLL)). In some embodiments the poly(trimethylene carbonate-co-ε-caprolactone) is coated with laminin-111 or PLL. In some embodiments, the poly(trimethylene carbonate-co-ε-caprolactone) is coated with PLL.

The term "about" as used herein is defined as meaning that the values referred to can vary by plus or minus 5% (i.e. ±5%).

The biomaterial and/or the P(TMC-CL) may be in any suitable form for use in promoting neuronal regeneration. For example, the biomaterial and/or the P(TMC-CL) may be in the form of a scaffold, e.g. a three dimensional scaffold. The scaffold may be porous. The biomaterial may be in the form of a nerve guide, e.g. with a hollow tubular shape (cylindrical). Such a nerve guide will serve as a conduit for axonal growth. The conduit may be constituted by an assembly of smaller diameter nerve guides. The biomaterial can also be in the form of fibres, for example, prepared from extrusion, electrospinning or spun from solution. These fibres can be aligned in the longitudinal orientation of the nerve fibres. The nerve guides can also be filled with the fibres. The biomaterial may be in the form of films, beads or microspheres. The biomaterial may be in the form of a patch. These can be implanted into the brain or spinal cord for promoting neuronal regeneration. The films can have topographical features, like aligned channels or poles that can be obtained by microfabrication techniques. The biomaterial and/or the P(TMC-CL) may be plasma treated to alter surface morphology and/or chemistry. The biomaterial and/or the P(TMC-CL) may comprise one or more active pharmaceutical ingredients. The pharmaceutical ingredient may be an active agent such as ibuprofen, rolipram or diclofenac.

A skilled person will appreciate that the various features described above can be combined together to form a biomaterial with certain characteristics. All the features can and are intended to be combined in any combination even if such combinations are not explicitly identified.
The present invention also provides the use of a biomaterial in the preparation of a composition for promoting neuronal regeneration in the CNS, wherein the biomaterial comprises poly(trimethylene carbonate-co-ε-caprolactone) (P(TMC-CL)).

Further, the invention provides the use of a biomaterial in the preparation of a composition for treating damage to the CNS, wherein the biomaterial comprises poly(trimethylene carbonate-co-ε-caprolactone) (P(TMC-CL)).

In a further aspect, the present invention provides a method of promoting neuronal regeneration in the CNS of a subject, the method comprising administering a biomaterial comprising poly(trimethylene carbonate-co-ε-caprolactone) to a site of damage in the CNS of the subject.

The characteristics and features of the biomaterial are as described above.

The biomaterial may be administered in any suitable way. It may be implanted or injected. Generally, the biomaterial will be implanted by surgery.

The subject may be any suitable subject in which neuronal regeneration of the CNS is required. The subject may be any suitable subject with a CNS, which may require neuronal regeneration such as a mammal, for example, a cat, a dog, a horse or a human. Preferably, the subject is a human.

When the biomaterial is implanted at the site of damage in the CNS, it will promote neuronal regeneration to at least partially repair the damage. Over time, the P(TMC-CL) will be degraded and will be at least partially replaced by neural tissue.

Detailed Description of the Invention

The invention will now be described in detail, by way of example only, with reference to the following figures:

Figure 1 – Cortical neuron culture on PLL coated films of P(TMC-CL) and respective homopolymers. A. Number of cortical neurons with and without neurite extensions on polymeric surfaces coated with aqueous solutions at different concentrations of PLL. Glass coated with 24 $\mu g.\mu l^{-1}$ of PLL for 30 minutes was used as control. (n = 3 independent studies, mean ± SD, $p < 0.05$) B. Percentage of PLL covered surface area as a function of the coating conditions. (n= 3, mean ± SD, $p < 0.05$) x = not tested condition. n.s. = non-significantly different from the control, α = total number of cells not significantly different from the control, β = number of cells with neurite extensions not significantly different from the control and χ = number of cells without extensions not significantly different from the control.

Figure 2 – Effect of the surface on neurite elongation and cellular polarization. A. Fluorescently labeled cortical neurons, immunostained for TAU (green); nuclei are counterstainned with Hoechst (blue); B. Number of neurites per cell; C. Total neurite length; D. Average neurite length and E. Length of the longest neurite. (n= 130 cells, mean ± SD, *** for $p < 0.001$)

Figure 3 – Morphology and mechanical properties of the tested polymeric surfaces. A. Root mean square (RMS) roughness of all polymeric surfaces; B. Representative photographs of the polymeric surfaces before and after nanoindentation; C. Representative nanoindentation force-displacement curves; D. Mean hardness values of all polymeric surfaces, calculated for the maximum load and E. Mean stiffness values for all polymeric surfaces. (n = 60 indentations, mean ± SD, *** for $p < 0.001$)

Figure 4 – Effect of CNS myelin on neurite outgrowth of cortical neurons cultured for 4 days on PLL-P(TMC-CL) substrates coated with CNS myelin. A. Cortical neurons are immunostained for β-III tubulin (green), myelin immunostained for MBP (red) and nuclei are counterstainned with Hoechst (blue); B. Effect of myelin on the ability of neurons to extend processes is presented as the % of cells with neurites in relation to the total number of cells. (n = 3 independent studies, mean ± SD; ** for $p < 0.01$)

Figure 5 – Analysis of GSK3β in cortical neurons plated on P(TMC-CL) and effects of GSK3β inhibition on neurite extension. A. Schematic representation of the different phosphorylation forms of GSK3β and their activity status; B. Analysis of the phosphorylated forms of GSK3β by western blot. Representative blots are shown. Expression levels of GSK3β isoforms, β1 and β2, are presented and quantified individually or together. (n = 3 independent studies, average ± SD); C. Morphology of neurons (immunostained for Tau in green and nuclei counterstained in blue) cultured for 24 hours in the presence of DMSO (Control) or in the presence of 6-bromoindirubin-3'-acetoxime (BIO) at 30 and 300 nM. Quantifications of the longest neurite, average neurite length and the number of neurites per cell are shown (n = 130 cells, mean ± SD, * for $p < 0.05$, ** for $p < 0.01$ and *** for $p < 0.001$); D. Determination of CRMP4 phosphorylation levels in cortical neurons plated for 4 days on control or P(TMC-CL). Representative western blot is shown and below the quantification (n = 3 independent studies, average ± SD).

1. SUMMARY

Mammalian central nervous system (CNS) neurons do not regenerate after injury due to the inhibitory environment formed by the glial scar, largely constituted by myelin debris. The use of biomaterials to bridge the lesion area and the creation of an environment favouring axonal regeneration is an appealing approach, currently under investigation. This work aims to assess the suitability of three candidate polymers – poly(ε-caprolactone), poly(trimethylene carbonate-co-ε-caprolactone) (P(TMC-CL)) (11:89 mol%) and poly(trimethylene carbonate) - with the final goal of using these materials in the development of conduits to promote spinal cord regeneration. Poly(L-lysine) coated polymeric films were tested for neuronal cell adhesion and neurite outgrowth, with P(TMC-CL) stimulating neuronal polarization and promoting axon elongation. Furthermore, cortical neurons cultured on P(TMC-CL) in the presence of myelin were able to overcome myelin inhibition in comparison with the control condition (glass substrate). This effect was found to be mediated by the glycogen synthase kinase 3β (GSK3β) signalling pathway with impact on the collapsin response mediator protein 4 (CRMP4), suggesting that besides surface topography, mechanical properties were implicated in this process. The obtained results indicate P(TMC-CL) as a promising material for CNS regenerative applications as it promotes axonal growth, overcoming myelin inhibition.

2. MATERIALS AND METHODS

2.1. Polymeric film preparation

Poly(trimethylene carbonate) (P(TMC), poly(ε-caprolactone) (P(CL)) and poly(trimethylene carbonate-co-ε-caprolactone) (P(TMC-CL)) with 11 mol % of TMC were synthesized as previously described [20]. Briefly, prior to polymerization ε-caprolactone monomer (Fluka) was dried overnight over CaH_2 and distilled under reduced pressure. Trimethylene carbonate was obtained from Boehringer Ingelheim (Germany) and used as received. Polymerizations were conducted by ring-opening polymerization in an argon atmosphere using stannous octoate as a catalyst. All polymerizations were carried out for a period of 3 days at 130°C ± 2°C. The obtained polymers were purified by dissolution in chloroform and subsequent precipitation into a ten-fold volume of ethanol. The precipitated polymers were recovered, washed with fresh ethanol and dried under reduced pressure at room temperature (RT) until constant weight. The prepared polymers were characterized with respect to chemical composition by nuclear magnetic resonance (NMR). Four hundred MHz ^{1}H-NMR (BRUKER AVANCE III 400) spectra were recorded using solutions of polymer in $CDCl_3$ (Sigma). Number average and weight average molecular weights (Mn and Mw, respectively), polydispersity indices (PDI) and intrinsic viscosities ([η]) of the (co)polymers were determined by gel permeation chromatography (GPC, GPCmax VE-2001, Viscotek, USA). The setup was equipped with ViscoGEL I-guard-0478, ViscoGEL I-MBHMW-3078, and ViscoGEL I-MBLMW-3078 columns placed in series and a TDA 302 Triple Detector Array with refractometer, viscometer, and light-scattering detectors, allowing the determination of absolute molecular weights. All measurements were performed at 30°C, using chloroform as the eluent at a flow rate of 1.0 ml.min^{-1}. The obtained results are compiled in Table 1.

Polymer films of 250 μm in thickness were prepared by casting the polymer solution in chloroform onto glass Petri dishes. After drying the films under reduced pressure at RT, disks with a diameter of 14 mm were punched out. Prior to cell culture, disks were sterilized by two incubation steps in a 70% (v/v) ethanol solution for 15 min, followed by two rinsing steps of 15 min in autoclaved MilliQ water. After sterilization, polymer disks were placed in 24-well tissue polystyrene plates (BD Biosciences) and fixed with autoclaved silicon o-rings (EPIDOR).

2.2. Cortical neuron cell culture

Prior to cell seeding the air side surface of the polymeric disks was coated with 200 μl of a poly(L-lysine) (PLL, Sigma) solution in a concentration ranging from 24 to 73 μg.μl^{-1}, at 37°C for 30 min or overnight and, subsequently, rinsed with autoclaved MilliQ water. Coverglass (Menzel) coated with 24 μg.μl^{-1}, at 37°C for 30 min was used as control.

Wistar Han rat embryos (embryonic day 17-18) were removed by caesarean section of the euthanized pregnant rats. The isolated cortices were dissociated for 30 min at 37°C in Hanks Balanced Salt Solution (HBSS) supplemented with 1.0 mM pyruvate, 2 $mg.ml^{-1}$ albumin, and 10% (v/v) trypsin (all from Gibco). Viable cells (trypan blue exclusion assay) were seeded at a density of 2.2×10^4 viable $cells.cm^{-2}$ onto PLL-coated polymeric discs or coverglasses in 24-well cell culture plates. Neural cells were seeded in 300 µl of Dubelcco's Modified Eagle Medium (DMEM) : Nutrient Mixture F-12 (F-12) (3:1) supplemented with 10% (v/v) inactivated fetal calf serum (FCS) (all from Gibco). Two hours later, medium and o-ring were removed and 1 ml of Neurobasal medium supplemented with 0.5 mM L-glutamine, 2% (v/v) B27 supplement, 1% (v/v) Penicillin-Streptomycin and 0.5% (v/v) Gentamicin (all from Gibco) was added and polymeric discs turned upside down. Cultures were maintained at 37 °C in a humidified atmosphere of 5 % CO_2. Culture purity was determined by immunocytochemistry as described further down. Half of the cell culture medium was changed on the third day of culture. After 4 days in culture, samples were treated for immunocytochemistry.

2.3. Poly(L-lysine) adsorption quantification

Polymeric disks were coated with PLL-FITC (fluorescein isothiocyanate) (Sigma) as described in the previous section. Coverglass coated with 24 $\mu g.\mu l^{-1}$ of PLL, at 37°C for 30 min, was used as control. Polymeric discs coated with PLL-FITC were further mounted on microscope slides using an aqueous mounting media (Sigma) and observed with an inverted fluorescence microscope (Axiovert 200M, Zeiss). Image analysis was performed with ImageJ 1.44 software.

2.4. Atomic force microscopy

2.4.1. Roughness analysis

The roughness of the polymer surfaces tested for cell culture was assessed by atomic force microscopy (AFM) using a PicoPlus scanning probe microscope interface with a PicoScan controller (Agilant Technologies, USA). A 10x10 μm^2 piezoscanner was used in tapping mode, with a scan speed of 1 $line.s^{-1}$. A bar shaped silicon cantilever (ACT probe, from AppNano), with a spring constant of 25-75 $N.m^{-1}$ was used and roughness analysis was performed from scanned areas of 7x7 μm^2 on five randomly chosen locations of each sample in air, at room temperature. The root-mean-square (RMS) roughness within the sampling area was determined using the WSxM scanning probe microscope software [25], according to

$$RMS = \sqrt{\frac{\sum i,j\ (a_{i,j} - \langle a \rangle)^2}{N}} \qquad (1),$$

where a represents the image height and N the total number of points.

2.4.2. Nanoindentation

These measurements were performed at CEMUP (*Centro de Materiais da Universidade do Porto*), on a Veeco Metrology Multimode with Nanoscope IV controler (Veeco Instruments, Inc.) at RT conditions in Force-indent mode with a diamond tip, suitable for nanoindentation (DNISP Diamond-Tipped Probe from Veeco; spring constant 131 $N.m^{-1}$). Deflection sensitivity of the cantilever was calibrated by indenting a sapphire surface. Nanoindentations were made for 1 second and the peak load was confined up to 30 μN for P(TMC-CL) and P(CL) and 6.5 μN for P(TMC). Force-displacement curves were obtained during loading and unloading for each indentation, and further used to determine hardness and stiffness values according to the Oliver and Pharr method [26]. For each polymeric substrate type, 60 indents were done on the film side tested for cell culture, covering 3 randomly chosen regions of 4 different samples per material. In each region, a set of 16 indents was made at a distance of 2 μm of each other. Stiffness was calculated as the slope of the tangent line to the unloading curve at the maximum loading point and hardness values were calculated for the maximum load and taking into consideration the shape of the indenter probe.

2.5. Neurite outgrowth on myelin coated polymer films

2.5.1. Myelin isolation

Myelin was isolated from brains of C57BL/6 male mice, as previously described [27]. Briefly, the isolated brains were homogenized in 0.32 M sucrose and after centrifugation at 900g, the post-nuclear supernatant was collected. The post-nuclear supernatant was carefully overlaid on an ultracentrifuge tube containing a 0.85 M sucrose solution on top of a 50% (w/v) sucrose cushion. After centrifugation for 1 hour at 37000 g at 4 °C (Sorvall Pro80 centrifuge), the interphase between sucrose solutions was transferred to a new ultracentrifuge tube. Two rounds of osmotic shocks were performed by adding ice-cold water and centrifugation at 20000 g. The final myelin pellet was stored at -80°C until further use.

2.5.2. Myelin coating

The polymeric disks and glass control were first coated overnight with PLL as described above and washed with 0.1M $NaHCO_3$. Myelin 1.25 μg myelin.cm^{-2} aqueous solution was dried overnight onto the PLL coated disks as described by Cai *et al.* [28], and further used as substrates for cortical neuron culture.

2.6. Pharmacologic inhibition of glycogen synthase kinase 3

For neuronal outgrowth assays in the presence of a pharmacologic inhibitor of glycogen synthase kinase 3 (GSK3), a 30 or 300 nM solution of 6-bromoindirubin-3'-acetoxime (BIO) in dimethyl sulfoxide (DMSO) was added to cortical neuron cultures (DMSO final concentration 0.05% (v/v)) at two different time points: at seeding (t = 0) being in contact with cells for 4 days, and at the third day of culture (t = 3) being in contact with cells for 24h. Neurons seeded on polymer discs in the presence of 0.05% (v/v) DMSO were used as controls. After 4 days in culture samples were treated for immunocytochemistry.

2.7. Immunocytochemistry

Cells were fixed for immunocytochemistry staining with 2% (v/v) paraformaldehyde at RT and further permeabilized and blocked in phosphate buffered saline (PBS) containing 5% (v/v) Normal Goat Serum (NGS) (Biosource) and 0.2% (v/v) Triton X-100 (Sigma). Primary antibodies were diluted in PBS containing 1% (v/v) NGS and 0.15% (v/v) Triton X-100, and incubated overnight in a humid chamber at 4°C. Secondary antibodies were applied for 1h at RT and subsequently treated for nuclear counterstaining at RT with Hoechst (Molecular Probes) at 2 μl.ml^{-1}. Samples were mounted directly in aqueous mounting medium and observed with an inverted fluorescence microscope.

Culture purity was ≥99% in cortical neurons as determined by mouse anti-glial fibrillary acid protein (GFAP) (1:500, BD Biosciences)/ mouse anti-vimentin (1:100, Thermo Scientific)/ mouse anti-oligodendrocyte marker 4 (O4) (1:100, Chemicon)/ rabbit anti-Tau (TAU protein) (1:100, Sigma)/ 2 μg.ml^{-1} Hoechst fluorescent staining. Cells were counted from 18 radial fields and values were extrapolated to the total surface area of the sample (n=3). For axonal outgrowth assessment the length of the longest neurite and total neurite outgrowth per cell were determined using AxioVision image analysis software. Neuronal processes were manually traced and quantified on 130 cells per condition. Three independent experiments were performed.

For neuronal outgrowth analysis on myelin inhibition studies, neurons were stained with anti-βIII tubulin (1:500, Abcam) and myelin with anti-myelin basic protein (MBP) SMI-94 (1:500, Abcam). The secondary antibodies used were anti-rabbit Alexa 488 (1:500, Invitrogen), anti-mouse 594 (1:1000, Invitrogen).

2.8. Western Blot

Cortical neuron lysates were prepared by washing cells with PBS and further lysed in buffer containing 20 mM 3-(n-morpholino)propanesulfonic acid (MOPS), 2 mM ethylene glycol tetraacetic acid (EGTA), 5 mM ethylenediaminetetraacetic acid (EDTA), 30 mM NaF, 60 mM β-glycerophosphate, 20 mM sodium pyrophosphate, 1 mM sodium orthovanadate, 1% (v/v) Triton X-100, 1% (v/v) DL-dithiothreitol (DTT), 1 mM phenylmethanesulfonyl fluoride (PMSF) and protease inhibitor cocktail (Amersham). Protein lysates (25-100 μg/lane) were run on a 12% SDS-PAGE gel and then transferred to a nitrocellulose membrane (Amersham). For Western analysis, membranes were blocked with blocking buffer (5% (wt/v) non-fat dried milk in tris-buffered saline (TBS) 0.1% (v/v) Tween 20) and incubated overnight at 4°C in 5% (wt/v) bovine serum albumin (BSA) in TBS 0.1% Tween 20 with primary antibodies. The following primary antibodies were used: rabbit anti-phospho-glycogen synthase kinase 3 beta (GSK3β) Ser9 (1:1000, Cell Signaling), rabbit anti-phospho-GSK3β Tyr216 (1:2000, Santa Cruz Biotechnology), mouse anti-GSK3α/β (1:2000, Santa Cruz Biotech.), sheep anti-phospho-collapsin response mediator protein 4 (CRMP4) Thr 509 (1:1000, Kinasource) and mouse anti-total CRMP4 (1:500, Santa Cruz Biotech.). After washing, membranes were incubated with secondary antibodies for 1h at RT. The secondary antibodies used were anti-rabbit HRP (1:10000, Jackson Immunoresearch), anti-mouse HRP (1:10000, Thermo Scientific) and anti-goat/sheep (1:10000, Binding Site). Proteins were detected using a chemiluminescent substrate Pierce ECL western blotting substrate (Thermo Scientific) according to the manufacturer's specifications. For each experiment representative western blots are shown. Phospho-protein expression was quantified by densitometry with QuantityOne software (BioRad) and levels were normalized to the total level of the same protein.

2.9. Statistical Analysis

For statistical analysis, one-way ANOVA followed by Tukey's post-hoc test were used. When Gaussian distribution was not confirmed non-parametric test Man-Whitney was applied, using

the Graphpad Prism program. Data is expressed as the mean ± standard deviation (SD) and p values of < 0.05 were considered significant.

3. RESULTS

3.1. Cortical neurons adhere and extend neurites in a PLL dependent manner

As a first step in assessing P(CL), P(TMC-CL) and P(TMC) compatibility with the CNS and their potential application in devices for neuroregeneration, polymeric discs were tested as substrates for cortical neuron growth *in vitro*. Cortical neurons were seeded on PLL coated polymeric films and were found to adhere to the tested substrates in a PLL concentration dependent manner (Fig. 1A). Cell number and neurite outgrowth on the coated polymeric films were evaluated using coverglasses coated with a PLL concentration of 24 $\mu g.\mu l^{-1}$ for 30 min as control. Cortical neurons adhered in comparable numbers to the control when these were coated overnight with 24 $\mu g.\mu l^{-1}$ and 48 $\mu g.\mu l^{-1}$ of PLL in the case of P(CL) films, and 72 $\mu g.\mu l^{-1}$ of PLL in the case of TMC containing films (see Fig. 1A). However, only on P(TMC-CL) the majority of adhered cells was able to extend neurites as in the control.

To explain this PLL-dependent behaviour, the amount of PLL adsorbed to the polymeric films surface was evaluated by fluorescence quantification of PLL-FITC coated samples. As one can observe in Fig. 1B, the surface area covered by PLL (in %) was only comparable to the control conditions when the polymeric films were treated with a PLL solution of at least 48 $\mu g.\mu l^{-1}$ and 72 $\mu g.\mu l^{-1}$ in the case of the CL containing materials and P(TMC), respectively. Consequently, cell adhesion can be directly correlated with the PLL adsorption profile to the polymeric films.

Taking into consideration the obtained results, both in terms of cell adhesion and neurite extension, the coating conditions used in the subsequent studies were established to be polymer surface treatment overnight with 48 $\mu g.\mu l^{-1}$ for P(CL) and 72 $\mu g.\mu l^{-1}$ for P(TMC-CL) and P(TMC).

3.2. P(TMC-CL) stimulates axonal elongation

In order to evaluate neurite outgrowth on the different PLL-coated polymeric surfaces, the number of neurites per cell, as well as the neurite length were determined. As seen in Fig. 2A, neurons behave differently on each surface. More than 80% of the cells seeded on polymeric films show one or two neurites, while more than 80% of the cells seeded on glass (control) present between 3 to 5 neurites (Fig. 2B). Furthermore, as shown in Fig. 2A neurons seeded on the polymeric surfaces exhibit a lower degree of branching than those seeded on glass. However,

on P(CL) and P(TMC) the adhered cells show smaller neurites than on P(TMC-CL) and the control (Fig. 2C-E). Despite the fact that for P(TMC-CL) the total neurite length was similar to the one observed on glass, given the lower number of neurites per cell in this condition, the average neurite length was higher (Fig. 2D). More remarkably, the length of the longest neurite was increased relatively to the control (Fig. 2E).

3.3. P(TMC-CL)'s mechanical properties stimulate axonal outgrowth

As shown in Fig. 3A, AFM analysis indicated that the RMS roughness was similar for P(CL) and P(TMC-CL), with mean values of 21.8 ± 11.5 nm and 24.4 ± 12.1 nm respectively, while significantly lower for P(TMC) with a mean value of 1.6 nm ± 1.0.

Nanoindentation is one of the most versatile techniques and particularly suited for the measurement of localized mechanical properties on the surface of materials [29]. Representative photos of the nanoindentations and force/displacement curves are represented in Fig. 3B and C, respectively. These show that P(CL) poses a greater resistance to deformation in relation to the other two materials tested, as the force needed to achieve the same displacement is higher than for P(TMC-CL) or P(TMC). As shown in Fig. 3 D-E stiffness and hardness values are significantly different between the three different substrates. A stiffness value of 312 ± 56.4 $N.m^{-1}$ and a hardness of 3.32 $x10^6$ ± 0.373 x 10^6 $N.m^{-2}$ was found for P(TMC-CL), while P(CL) shows the highest values with a stiffness of 435 ± 40.4 $N.m^{-1}$ and a hardness value of 6.60 $x10^6$ ± 2.11 x 10^6 $N.m^{-2}$. As seen in the photos before and after nanoindentation, P(TMC) samples recover almost completely from the indentations and, consequently, show stiffness and hardness values close to zero.

3.4. P(TMC-CL) promotes overcome of myelin inhibition

Myelin-associated inhibitors (MAIs) are present at a spinal cord lesion site and are known to be among the major impediments of the spontaneous axonal regeneration after SCI. Cortical neurons were seeded on myelin coated surfaces. P(TMC-CL) was chosen from the three surfaces tested as it showed the best results for neuronal adhesion and neurite extension, presenting a positive influence on axonal elongation. As seen in Fig. 4, when comparing surfaces coated and uncoated with myelin, the number of cells with neurites is smaller in the first case. Nevertheless, this decrease is not significant on P(TMC-CL) seeded neurons in contrast to the control where this reduction is statistically significant ($p < 0.01$).

3.5. GSK3β signalling pathway mediates neuronal sensing of P(TMC-CL) surface nanomechanical properties

GSK3β is implicated in many processes in the nervous system and is known to play a critical role in the regulation of neuron physiology. It is highly expressed in neurons and crucial for the establishment of neuronal polarity, as well as for the establishment of the branching-elongation equilibrium [30-32]. In view of this knowledge, the involvement of GSK3β as a mediator of P(TMC-CL) effect on neurite formation and axonal outgrowth was examined. GSK3β is regulated by phosphorylation and its activity can be reduced by phosphorylation at Ser-9. Contrarily, tyrosine phosphorylation at Tyr-216 increases the enzyme's activity (Fig. 5A) [33, 34]. As shown in Fig. 5B cortical neurons seeded on P(TMC-CL) present lower levels of $GSK3\beta_2$ Ser-9 phosphorylation and higher level of Tyr-216 phosphorylation, in comparison to neurons cultured on glass. This indicates that neurons seeded on P(TMC-CL) display more kinase activity than those on glass. It is also perceptible from Fig. 5B that the GSK3β isoform that is differently expressed is GSK3β2, which is known to be expressed exclusively in the nervous system [35]. To further confirm the involvement of GSK3β as a mediator of the P(TMC-CL) effect on axonal outgrowth and number of neurites per cell, cortical neurons were cultured in the presence of a GSK3 pharmacologic inhibitor - BIO. It is expected that inhibiting GSK3 activity should inhibit the polymeric surface's effect on cortical neurons. In fact, as shown in Fig. 5C, when BIO is added to the culture medium one can observe a decrease in the length of the longest neurite and in the average neurite length, as well as an increase on the number of neurites per cell. These effects occur in a dose-dependent manner, with the highest concentration of BIO tested (300 nM) leading to statistically significant differences. Alabed *et al.* [36] have established that GSK3β phosphorylation and consequent inactivation, regulates the interaction of CRMP4 and RhoA through CRMP4 de-phosphorylation. If this mechanism is active in our setup, phospho-CRMP4 levels should be higher for neurons seeded on P(TMC-CL). To test this hypothesis, the levels of CRMP4 phosphorylation in cortical neurons seeded on P(TMC-CL) and glass surfaces were assessed. As expected, phospho-CRMP4 levels were increased for neurons cultured on P(TMC-CL) as shown in Fig. 5D.

4. DISCUSSION

In the aftermath of a SCI, a glial scar is formed. Despite its key role in constraining the damaging effects caused by the lesion, the glial scar also prevents axon regeneration. The

astroglial scar not only contains secreted and transmembrane molecular inhibitors of axon growth but also constitutes an almost impenetrable physical barrier to regeneration [4]. Consequently, it was hypothethized that by creating a favourable environment at the lesion site, one will be able to enhance axonal regeneration and ultimately promote some gain of function. Therefore, the use of an implantable scaffold to bypass the glial scar area is one of the promising approaches being investigated to promote spinal cord regeneration. A prerequisite in the design of such biomaterial is its biocompatibility, which in this context means that it must support neuronal survival and axonal growth. The aim of this study was, therefore, to investigate the suitability of P(CL), P(TMC-CL) and P(TMC) as substrates for spinal cord regeneration purposes.

One of the most commonly used strategies to assess neuronal behaviour in vitro when testing biomaterials for nerve regeneration applications is to evaluate axonal growth [28, 36-39]. In the present work rat cortical neurons were firstly seeded on the PLL-coated polymeric substrates to assess adhesion and neurite outgrowth ability. PLL is a synthetic homo-poly-(amino acid), characterized by an isopeptide bond between the ε-amino and the α-carboxyl groups of L-lysine, commonly used to coat cell culture substrates [40]. Initially, the polymer surface coating conditions were optimized - PLL concentration and time of contact - in order to achieve a comparable surface area covered by PLL and, consequently, similar cell adhesion in all tested surfaces. The observed PLL dependent behaviour can be explained by the different adsorption capacity of PLL on polymeric and glass surfaces. Differences that can be attributable to the surface properties of the tested materials, as these polymers present a more hydrophobic surface than glass [20], although after this process one could obtain comparable numbers of cortical neurons after 4 days of culture on the tested materials, significant morphological differences were found between neurons cultured on polymeric surfaces, particularly P(TMC-CL), and the control. Firstly, only on P(TMC-CL) the majority of neurons is able to extend neurites. Furthermore, our results show that among all the tested surfaces, including glass, seeding cortical neurons on P(TMC-CL) stimulates neuronal polarization and promotes axon elongation, as neurons on P(TMC-CL) show significantly enhanced neurite outgrowth and significantly lower numbers of neurites per cell. This switch to polarized and elongated morphology is noteworthy as successful regeneration requires that neurons survive and initiate rapid and directed neurite outgrowth [41]. A decreased number of neurites per cell were also found on P(CL) and P(TMC) but on these materials axonal outgrowth was significantly impaired. Moreover, while control

neurons have, on average, twice the number of neurites of neurons seeded on P(TMC-CL), when one sums the length of all neurites of each cell (total neurite length) no significant differences are found. Altogether, cortical neurons seeded on P(TMC-CL) were found not only to be polarized but also to extend significantly longer neurites. To the best of our knowledge, no previous reports have shown this neuronal behaviour on any studied material.

The potential of materials to trigger specific cellular responses is getting to be a well established phenomenon mediated by a number of factors that range from the properties of the surface that contacts with the cell, to the mechanical properties of the material [16, 17, 42-44]. We have previously characterized the family of these copolymers and when varying the monomer ratio mainly the thermal and, consequently, the mechanical properties of these materials are drastically affected [21]. P(TMC) and P(TMC-CL) copolymers with high CL content are flexible and though materials that range from amorphous to semi-crystaline elastomers when the CL content increases. Therefore, we hypothesise that surface topography and the nanomechanical properties of the tested materials play a key role in influencing cell behaviour. The local characterization of roughness, hardness and elastic properties of a wide range of materials has been reported including for thin films and biomolecules [45-48] but so far the characterization of TMC-CL copolymers has not been performed. The roughness of the three tested polymeric surfaces was first investigated. Values of 22 nm and 24 nm were found for P(CL) and P(TMC-CL) respectively, while for the P(TMC) the roughness values were found to be significantly lower. In 2002, *Fan et al.* [49, 50] showed that neuronal cells adherence and survival is optimum on surfaces with a RMS roughness ranging from 10 to 50 nm. Taking this data in consideration, both P(CL) and P(TMC-CL) show not only similar but also optimum roughness values for neural adhesion and survival, while P(TMC) is outside this optimum roughness range. Therefore, the different neuronal behaviour on these surfaces cannot be explained simply by topography. Aiming to measure localized mechanical properties on the surface of the polymeric films, nanoindentations were performed and force-displacement curves obtained for each indentation. Mean hardness and stiffness values were calculated and significant differences were found between all polymeric surfaces, with P(TMC-CL) being significantly less resistant to deformation than P(CL) and significantly more resistant to deformation than P(TMC). Although roughness values were similar between P(CL) and P(TMC-CL) and within the optimum range, P(CL) was two times harder than P(TMC-CL), which could explain the different cellular

behaviour on these surfaces, indicating that changes in stiffness and hardness values may have caused changes in cell morphology, specifically in axonal elongation.

Having observed the ability of P(TMC-CL) surfaces in promoting neuronal polarization and axonal elongation under normal cell culture conditions, the capacity of P(TMC-CL) to positively affect cortical neurons in a typical CNS inhibitory environment was tested, envisaging its application in the design of an axonal regeneration promoting strategy. While axons in the context of a mature mammalian CNS do not regenerate if damaged, the immature mammalian CNS is able to regenerate after injury [51, 52]. Probably the most notable difference between the mature and the immature nervous system is the presence of myelin [28]. Indeed, the limited regenerative capacity of the mammalian CNS is known to be partially due to myelin inhibition. So far, no biomaterial has shown the ability to overcome myelin inhibition unless blockers of myelin protein receptors were used [53]. Recently, Mohammad and co-workers have shown that a nano-textured self-assembled aligned collagen hydrogel was able to promote directional neurite guidance and overcome inhibition by a recombinant myelin-associated glycoprotein of dorsal root ganglia cultures [54]. To assess P(TMC-CL)'s neuronal effect under adverse, and more biologically relevant conditions, cortical neurons were seeded on P(TMC-CL) films in the presence of myelin. As expected, in the glass control surface we observed a statistically significant reduction of the number of cells extending neurites when cultured in the presence of myelin. In contrast, when P(TMC-CL) was used as a substrate, this reduction was not statistically significant (Fig. 4 B), suggesting that P(TMC-CL) is, to some extent, contributing to the promotion of the overcome of myelin inhibition. This is of extreme relevance as it has been already demonstrated that some degree of functional recovery can be obtained simply by counteracting the activity of myelin inhibition [55, 56]. The existence of a biomaterial that has the capacity to overcome this inhibition *per se,* without the need for the administration of antibodies or chemical inhibitors, can prove to be of great importance for therapeutic purposes.

The potential of materials to trigger specific cellular responses, such as interference and/or activation of defined pathways is extremely promising for tissue engineering. Stiffness and hardness sensing probably involves transduction into biological signals [17]. GSK3β is known to regulate axonal growth through the modification of the phosphorylation status of several microtubule-binding proteins and consequently the assembly of microtubules [34, 57]. Moreover, Alabed *et al.* [36] showed that the overexpression of active GSK3β attenuates MAI-

dependent neurite outgrowth inhibition. For these reasons, GSK3 was studied as a possible mediator of P(TMC-CL)'s effect. Mammalian GSK3 is generated from two genes, GSK3α and GSK3β. GSK3 expression in neurons is further characterized by an alternative splicing of GSK3β originating two main variants: GSK3β1 and GSK3β2. GSK3β2 is specifically expressed in the nervous system [34]. GSK3β is regulated by phosphorylation and its activity is dependent on the balance between tyrosine (Tyr-216) and serine (Ser-9) phosphorylation as shown in Fig. 5A, with a reduction of activity if phosphorylated at Ser-9, and its increase if phosphorylated at Tyr-216 [33, 34]. Our results show that GSK3β is differently regulated in neurons seeded on glass and P(TMC-CL), with the later showing lower levels of Ser9 phosphorylation, a site of GSK3β inactivation, and higher levels of Tyr216 phosphorylation, which facilitates the activity of GSK3β by promoting substrate accessibility [34]. Neurite elongation and neuronal polarization on P(TMC-CL) may be promoted by an increase GSK3β activity *in vitro*. The relationship between axonal elongation and GSK3β activity was further confirmed through pharmacological inhibition of GSK3 *in vitro*. As expected, inhibition of GSK3β blocked P(TMC-CL) effect, as there was a decrease in neurite length and an increase on the numbers of neurites per cell. Cells seeded on P(TMC-CL) and treated with BIO acquired a morphology that resembles more closely the neurons seeded on glass Fig. 2A.

Activation of GSK3β activity occurs in cortical neurons when these are cultured on P(TMC-CL), resulting in an increase in neurite outgrowth and decrease on the number of neurites per cell. Increased axonal outgrowth in the presence of higher GSK3β activity has also been shown in prior reports, for cerebellar, dorsal root ganglia and hippocampal neurons [31, 36, 58].

The Rho signalling pathway is known to play an important role in neuronal growth regulation and it has been shown that inhibitors of RhoA, and/or its downstream effector Rho kinase, facilitate growth on myelin substrates [59, 60]. *Wozniak et al.* [16] have studied the effects of stiffness on cell shape and shown that ROCK mediated contractility is essential for breast epithelial cells to sense the biophysical properties of the surrounding environment. Alabed *et al.* [61] have identified CRMP4 as a protein that functionally interacts with RhoA to mediate neurite outgrowth. Later on, this team has found that CRMP4-RhoA interaction is regulated by dephosphorylation of CRMP4 as a direct consequence of GSK3β inactivation by phosphorylation at Ser-9 [36]. This observation indicates that overexpression of GSK3β and consequent inhibition of CRMP4-RhoA complex formation may be protective in the context of

myelin inhibition. Our findings are consistent with Alabed *et al.* [36] as for neurons seeded on P(TMC-CL), which show higher levels of GSK3β activity and longer neurites the levels of phospho-CRMP4 are higher than in glass seeded neurons. Overall these results suggest that the activation of GSK3β activity, and consequent neurite elongation, is mediated by the surface mechanical properties of P(TMC-CL).

5. CONCLUSIONS

This work shows that P(TMC-CL) with a high CL content can promote axonal regeneration, prompting neurons into a regeneration mode, even under inhibitory conditions. This effect is mediated by the GSK3β signalling pathway, which is triggered by P(TMC-CL)'s surface mechanical properties.

These findings establish P(TMC-CL) as a promising material in the design of devices to promote neural regeneration, serving as a protective barrier for *de novo* scar tissue formation while supporting axonal growth and rendering neurons insensitive to myelin dependent neurite outgrowth inhibition without the administration of any therapeutic drug.

REFERENCES

1. Silver J, Miller JH. Nature Reviews Neuroscience 2004;5(2):146-156.
2. Schwab JM, Brechtel K, Mueller CA, Failli V, Kaps HP, Tuli SK, et al. Progress in Neurobiology 2006;78(2):91-116.
3. Madigan NN, McMahon S, O'Brien T, Yaszemski MJ, Windebank AJ. Respiratory Physiology and Neurobiology 2009;169(2):183-199.
4. Thuret S, Moon LDF, Gage FH. Nature Reviews Neuroscience 2006;7(8):628-643.
5. Richardson PM, McGuinness UM, Aguayo AJ. Nature 1980;284(5753):264-265.
6. Prang P, Muller R, Eljaouhari A, Heckmann K, Kunz W, Weber T, et al. Biomaterials 2006;27(19):3560-3569.
7. Willerth S, Sakiyama-Elbert S. Advanced Drug Delivery Reviews 2007;59(4-5):325-338.
8. Friedman JA, Windebank AJ, Moore MJ, Spinner RJ, Currier BL, Yaszemski MJ, et al. Neurosurgery 2002;51(3):742-752.
9. Straley KS, Foo CWP, Heilshorn SC. Journal of Neurotrauma 2010;27(1):1-19.
10. Novikova L, Novikov L, Kellerth J. Current Opinion in Neurology 2003;16(6):711-715.
11. Wong DY, Leveque JC, Brumblay H, Krebsbach PH, Hollister SJ, LaMarca F. Journal of Neurotrauma 2008;25(8):1027-1037.
12. Zhang N, Yan H, Wen X. Brain Research Reviews 2005;49(1):48-64.
13. Geller HM, Fawcett JW. Experimental Neurology 2002;174(2):125-136.
14. Pêgo AP, Kubinova S, Cizkiva D, Vanicky I, Mar FM, Sousa MM, et al. Journal of Cellular and Molecular Medicine 2012.
15. Chen BK, Knight AM, De Ruiter GCW, Spinner RJ, Yaszemski MJ, Currier BL, et al. Journal of Neurotrauma 2009;26(10):1759-1771.

16. Wozniak MA, Desai R, Solski PA, Der CJ, Keely PJ. Journal of Cell Biology 2003;163(3):583-595.
17. Chen CS. Journal of Cell Science 2008;121(20):3285-3292.
18. Schuh E, Hofmann S, Stok KS, Notbohm H, Muller R, Rotter N. Journal of Tissue Engineering and Regenerative Medicine 2011.
19. Fioretta ES, Fledderus JO, Baaijens FPT, Bouten CVC. Journal of Biomechanics 2012;45(5):736-744.
20. Pêgo AP, Poot AA, Grijpma DW, Feijen J. Journal of Biomaterials Science, Polymer Edition 2001;12(1):35-53.
21. Pêgo AP, Poot A, Grijpma D, Feijen J. Macromolecular Bioscience 2002;2(9):411-419.
22. Pêgo AP, Van Luyn MJA, Brouwer LA, Van Wachem PB, Poot AA, Grijpma DW, et al. Journal of Biomedical Materials Research - Part A 2003;67(3):1044-1054.
23. Vleggeert-Lankamp CLAM, De Ruiter GCW, Wolfs JFC, Pêgo AP, Feirabend HKP, Lakke EAJF, et al. European Journal of Neuroscience 2005;21(5):1249-1256.
24. Vleggeert-Lankamp CLAM, Wolfs J, Pêgo AP, Van Den Berg R, Feirabend H, Lakke E. Journal of Neurosurgery 2008;109(2):294-305.
25. Horcas I, Fernandez R, Gomez-Rodriguez JM, Colchero J, Gomez-Herrero J, Baro AM. Review of Scientific Instruments 2007;78(1).
26. Hobbs JK, Winkel AK, McMaster TJ, Humphris ADL, Baker AA, Blakely S, et al. Macromolecular Symposia 2001;167:15-43.
27. Norton WT PS. J Neurochem 1973;21(4):749-757.
28. Cai D, Yingjing S, De Bellard ME, Tang S, Filbin MT. Neuron 1999;22(1):89-101.
29. Kurland NE, Drira Z, Yadavalli VK. Micron 2012;43(2-3):116-128.
30. Peineau S. BC, Taghibiglou C., Doherty A., Bortolotto Z. A., Wang Y. T. and Collingridge G.L. Br J Pharmacol 2008;153(Suppl. 1):S428-S437.
31. Juan José Garrido DS, Varea O, Wandosell F. FEBS lett 2007;581:1579-1586.
32. Li R. Current Biology 2005;15(6):R198-R200.
33. Grimes CA, Jope RS. Progress in Neurobiology 2001;65(4):391-426.
34. Hur EM, Zhou FQ. Nature Reviews Neuroscience 2010;11(8):539-551.
35. Castaño Z, Gordon-Weeks P, Kypta R. Journal Neurochemistry 2010;113(1):117-130.
36. Alabed YZ, Pool M, Tone SO, Sutherland C, Fournier AE. Journal of Neuroscience 2010;30(16):5635-5643.
37. Fournier AE, GrandPre T, Strittmatter SM. Nature 2001;409(6818):341-346.
38. Fu Q, Hue J, Li S. Journal of Neuroscience 2007;27(15):4154-4164.
39. Oscar Siera RG, Vanessa Gil, Franc Llorens, Alejandra Rangel, Eduardo Soriano, and José Antonio del Rio. Journal of Neurochemistry 2010;113:1644-1658.
40. Muller H-J, Roder T. Microarrays: Elsevier Academic Press, 2006.
41. Cafferty WBJ, Gardiner NJ, Gavazzi I, Powell J, McMahon SB, Heath JK, et al. Journal of Neuroscience 2001;21(18):7161-7170.
42. Leach JB, Brown XQ, Jacot JG, Dimilla PA, Wong JY. Journal of Neural Engineering 2007;4(2):26-34.
43. Pelham Jr RJ, Wang YL. Proceedings of the National Academy of Sciences of the United States of America 1997;94(25):13661-13665.
44. Brunetti V, Maiorano G, Rizzello L, Sorce B, Sabella S, Cingolani R, et al. Proceedings of the National Academy of Sciences of the United States of America 2010;107(14):6264-6269.
45. Radmacher JDaM. Langmuir 1998;14:3320-3325.
46. Kinney JH, Marshall GM, Marshall SJ. Archives of oral Biology 1999;44:813-822.
47. Kol N, Shi Y, Tsvitov M, Barlam D, Shneck RZ, Kay MS, et al. Biophysical Journal 2007;92(5):1777-1783.

48. G. W. Marshall MB, R. R. Gallagher, S. A. Gansky, S. J. Marshall. J Biomed Mat Res 2001;54:87-95.
49. Fan YW, Cui FZ, Chen LN, Zhai Y, Xu QY, Lee IS. Applied Surface Science 2002;187(3â€“4):313-318.
50. Fan YW, Cui FZ, Hou SP, Xu QY, Chen LN, Lee IS. Journal of Neuroscience Methods 2002;120(1):17-23.
51. Bates CA, Stelzner DJ. Experimental Neurology 1993;123(1):106-117.
52. Hasan S, Keirstead H, Muir G, Steeves J. Journal of Neuroscience 1993;13(2):492-507.
53. Yue-Teng Wei YH, Chand-Lei Xu, Ying Wang, Bing-Fang Liu, Xiu-Mei Wang, Xiao-Dan Sun, Fu-Zhai Cui, Qun-Yuan Xu. Journal of Biomedical Materials Research 2010;95B(1):110-117.
54. Abu-Rub MT, Billiar KL, Van Es MH, Knight A, Rodriguez BJ, Zeugolis DI, et al. Soft Matter;7(6):2770-2781.
55. Bregman BS, Kunkel-Bagden E, Schnell L, Dai HN, Gao D, Schwab ME. Nature 1995;378(6556):498-501.
56. Schnell L, Schwab ME. Nature 1990;343(6255):269-272.
57. Dill J, Wang H, Zhou F, Li S. Journal of Neuroscience 2008;28(36):8914-8928.
58. Kim WY, Zhou FQ, Zhou J, Yokota Y, Wang YM, Yoshimura T, et al. Neuron 2006;52(6):981-996.
59. Dergham P, Ellezam B, Essagian C, Avedissian H, Lubell WD, McKerracher L. Journal of Neuroscience 2002;22(15):6570-6577.
60. Lehmann MAF, Selles-Navarro I, Dergham P, Sebok, A Leclerc N, Tigyi G, McKerracher L. The Journal of Neuroscience 1999;19(17):7537-7547.
61. Alabed Y, Pool M, Tone S, Fournier A. J. Neuroscience 2007;27(7):1702-1711.

Claims

1. A biomaterial for use in medicine, wherein the biomaterial comprises poly(trimethylene carbonate-co-ε-caprolactone) (P(TMC-CL)).

2. A biomaterial for use in promoting neuronal regeneration in the central nervous system, wherein the biomaterial comprises poly(trimethylene carbonate-co-ε-caprolactone) (P(TMC-CL)).

3. The biomaterial for use according to claim 2, wherein the biomaterial is for use in treating damage to the central nervous system.

4. The biomaterial for use according to claim 3, wherein the damage is a traumatic injury.

5. The biomaterial for use according to claim 4, wherein the damage is a spinal cord injury (SCI).

6. The biomaterial for use according to claim 3, wherein the damage is as a result of a disease which causes damage to the CNS such as the spinal cord.

7. The biomaterial for use according to claim 3 or claim 6, wherein the damage is caused by: an infection such as poliomyelitis; neurodegeneration such as amyotrophic lateral sclerosis; a tumour; an autoimmune and/or inflammatory disease such as multiple sclerosis; or spinal stroke.

8. The biomaterial for use according to any preceding claim, wherein the molar ratio of trimethylene carbonate to ε-caprolactone in the P(TMC-CL) is between about 1:20 and about 1:3.

9. The biomaterial for use according to any preceding claim, wherein the molar ratio of trimethylene carbonate to ε-caprolactone in the P(TMC-CL) is between about 1:10 and about 1:6.

10. The biomaterial for use according to any preceding claim, wherein the molar ratio of trimethylene carbonate to ε-caprolactone in the P(TMC-CL) is about 11:89.

11. The biomaterial for use according to any preceding claim, wherein the P(TMC-CL) is coated with a molecule that promotes cell adhesion.

12. The biomaterial for use according to claim 10, wherein the molecule that promotes cell adhesion is poly(L-lysine) (PLL).

13. The biomaterial for use according to any preceding claim, wherein the P(TMC-CL) has a number average molecular weight of at least about 0.2×10^5.

14. The biomaterial for use according to any preceding claim, wherein the P(TMC-CL) has a number average molecular weight of less than about 2×10^5.

15. The biomaterial for use according to any preceding claim, wherein the P(TMC-CL) has a stiffness of between about 200 N/m and about 400 N/m.

16. The biomaterial for use according to any preceding claim, wherein the P(TMC-CL) has a hardness of between about 1×10^6 N/m2 and about 6×10^6 N/m2.

17. The biomaterial for use according to any preceding claim, wherein the P(TMC-CL) has a roughness of between about 10 nm and about 50 nm.

18. The biomaterial for use according to any preceding claim, wherein the biomaterial is in the form of a scaffold, a nerve guide, a fibre, a film, a bead, a microsphere, or a patch.

19. The biomaterial for use according to any preceding claim, wherein the biomaterial is in the form of a scaffold or a nerve guide.

20. The biomaterial for use according to any one of claims 1 to 17, wherein the biomaterial is in the form of a patch.

21. The biomaterial for use according to any preceding claim, wherein the biomaterial comprises one or more active pharmaceutical ingredients.

22. A method of promoting neuronal regeneration in the central nervous system of a subject, the method comprising administering a biomaterial comprising poly(trimethylene carbonate-co-ε-caprolactone) to a site of damage in the central nervous system of the subject.

Figure 1

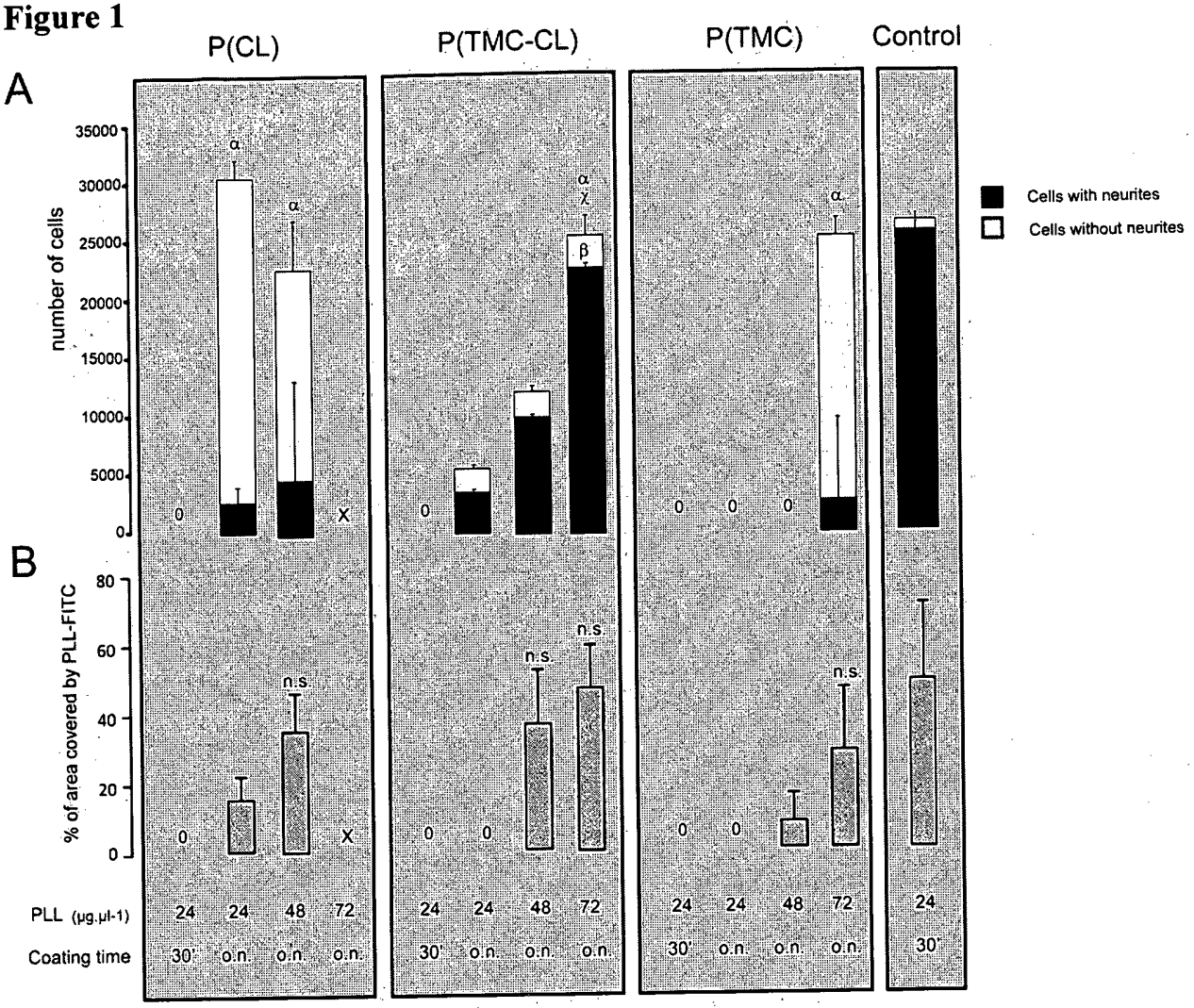
P(CL)
P(TMC-CL)
P(TMC)
Control
A
B
number of cells
% of area covered by PLL-FITC
Cells with neurites
Cells without neurites
PLL (µg.µl-1)
Coating time
n.s
o.n.

Figure 2

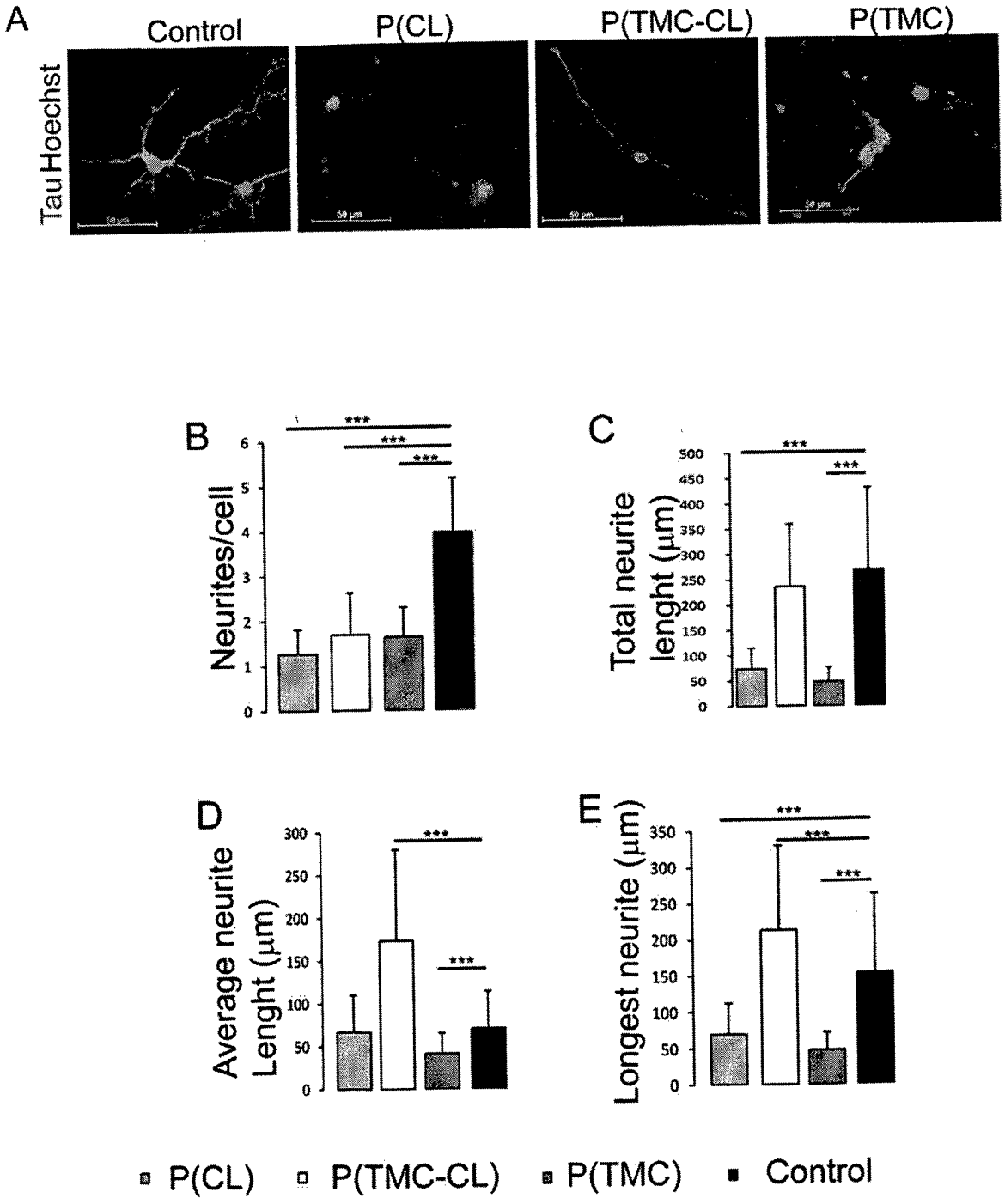
A
Control
P(CL)
P(TMC-CL)
P(TMC)
Tau Hoechst
B
Neurites/cell
C
Total neurite lenght (µm)
D
Average neurite Lenght (µm)
E
Longest neurite (µm)
***
P(CL)
P(TMC-CL)
P(TMC)
Control

Figure 3

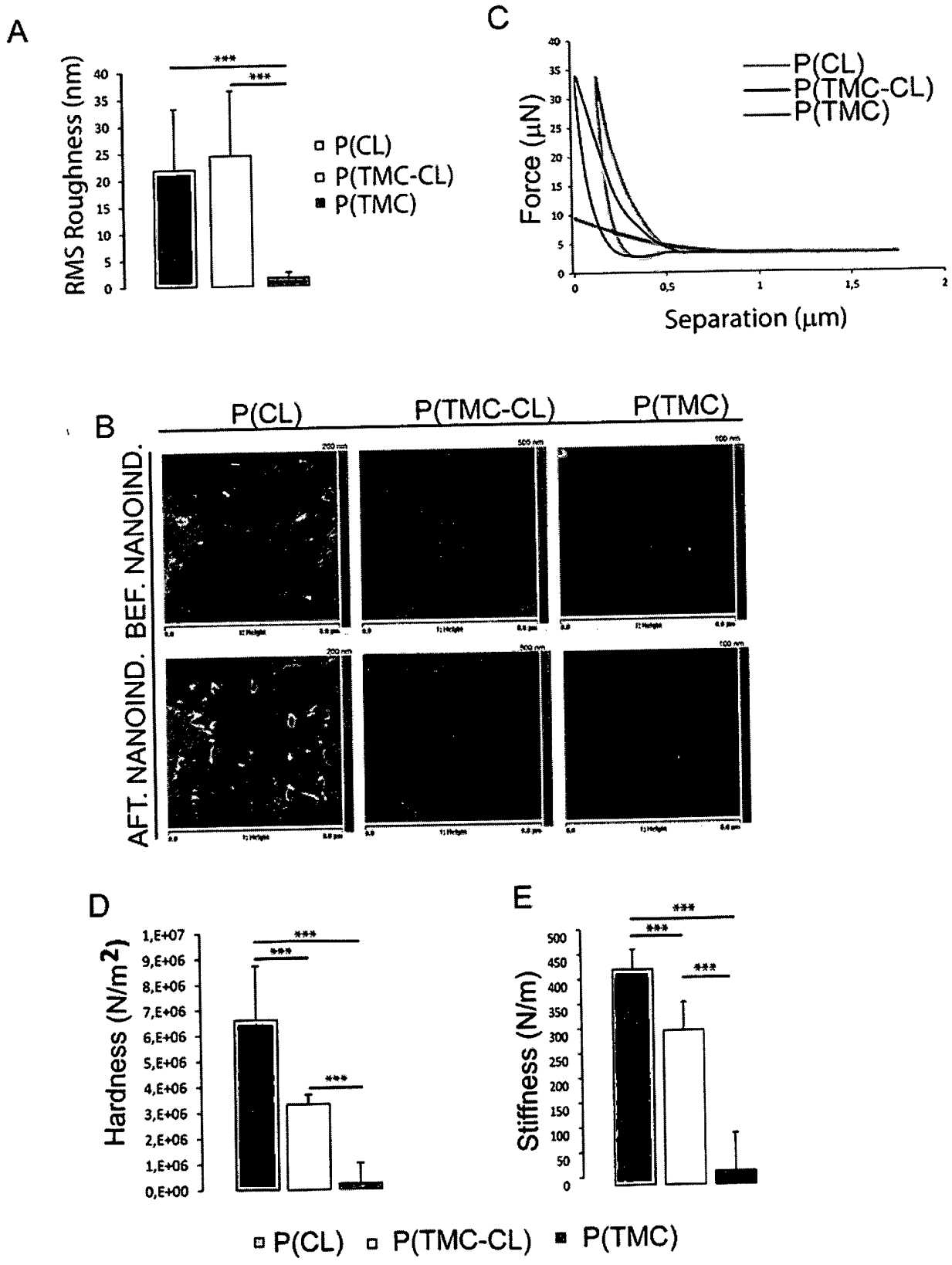
A
RMS Roughness (nm)
***
***
P(CL)
P(TMC-CL)
P(TMC)
C
Force (µN)
Separation (µm)
P(CL)
P(TMC-CL)
P(TMC)
B
P(CL)
P(TMC-CL)
P(TMC)
BEF. NANOIND.
AFT. NANOIND.
D
Hardness (N/m2)
E
Stiffness (N/m)
P(CL) P(TMC-CL) P(TMC)

Figure 4

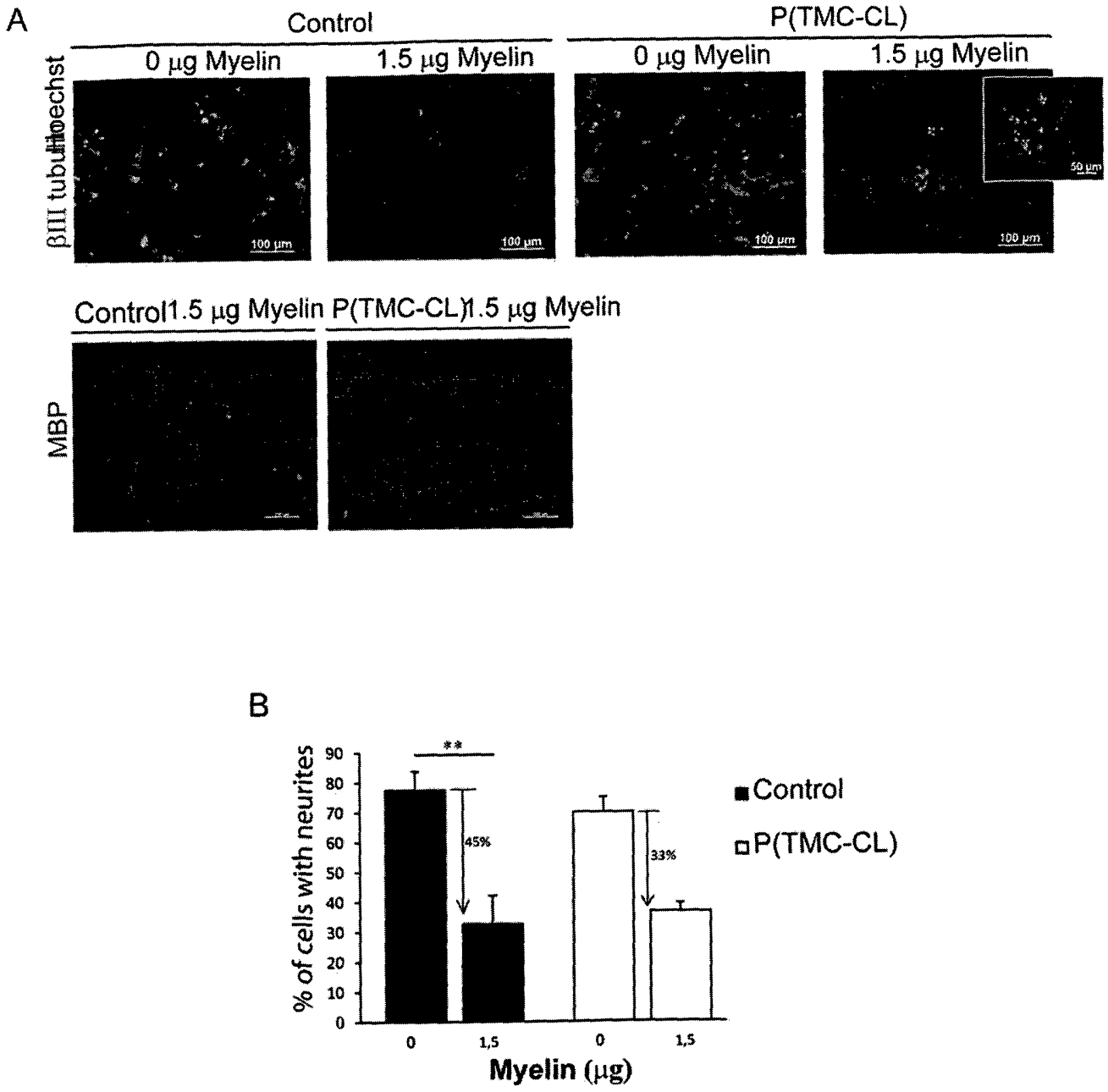
A
Control
P(TMC-CL)
0 µg Myelin
1.5 µg Myelin
0 µg Myelin
1.5 µg Myelin
βIII tubulin/Hoechst
100 µm
50 µm
Control1.5 µg Myelin
P(TMC-CL)1.5 µg Myelin
MBP
B
**
45%
33%
% of cells with neurites
90
80
70
60
50
40
30
20
10
0
0
1,5
0
1,5
Myelin (µg)
Control
P(TMC-CL)

Figure 5

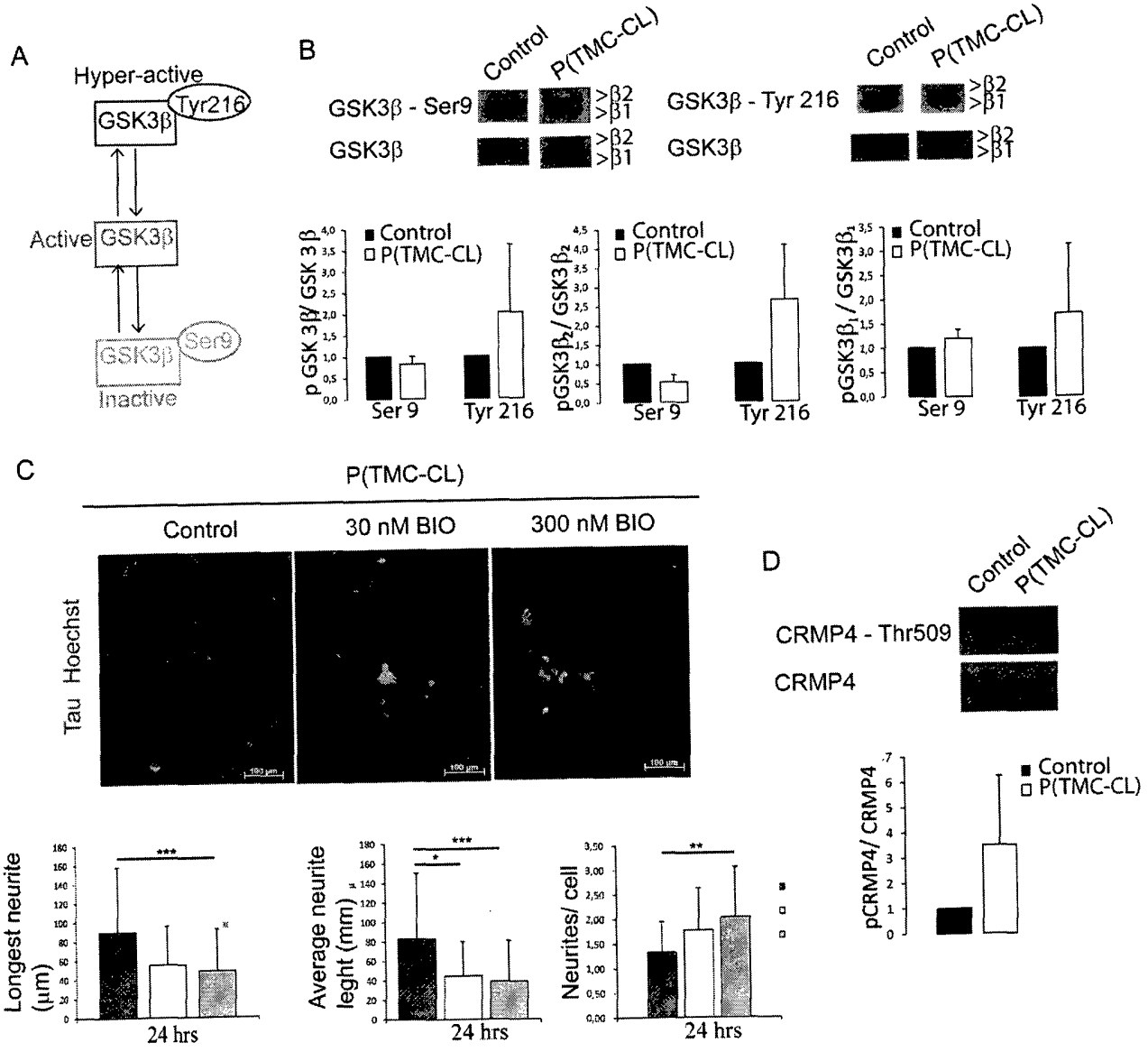
A
Hyper-active
GSK3β
Tyr216
Active GSK3β
GSK3β
Ser9
Inactive
B
Control
P(TMC-CL)
GSK3β - Ser9
GSK3β
>β2
>β1
GSK3β - Tyr 216
GSK3β
p GSK 3β/ GSK 3 β
pGSK3β2/ GSK3 β2
pGSK3β1 / GSK3β1
Control
P(TMC-CL)
Ser 9
Tyr 216
C
P(TMC-CL)
Control
30 nM BIO
300 nM BIO
Tau Hoechst
Longest neurite (µm)
Average neurite leght (mm)
Neurites/ cell
24 hrs
D
CRMP4 - Thr509
CRMP4
pCRMP4/ CRMP4

INTERNATIONAL SEARCH REPORT

International application No
PCT/PT2014/000006

A. CLASSIFICATION OF SUBJECT MATTER
INV. A61K31/765 A61L27/58 A61P25/00 A61K31/198
ADD.

According to International Patent Classification (IPC) or to both national classification and IPC

B. FIELDS SEARCHED

Minimum documentation searched (classification system followed by classification symbols)
A61K A61L

Documentation searched other than minimum documentation to the extent that such documents are included in the fields searched

Electronic data base consulted during the international search (name of data base and, where practicable, search terms used)
EPO-Internal, WPI Data, BIOSIS, EMBASE, CHEM ABS Data

C. DOCUMENTS CONSIDERED TO BE RELEVANT

Category*	Citation of document, with indication, where appropriate, of the relevant passages	Relevant to claim No.
X	VLEGGEERT-LANKAMP CARMEN L A M ET AL: "Effect of nerve graft porosity on the refractory period of regenerating nerve fibers - Laboratory investigation", JOURNAL OF NEUROSURGERY, vol. 109, no. 2, August 2008 (2008-08), pages 294-305, XP009177426, ISSN: 0022-3085 page 295, column 1, paragraph 2-4 page 299, column 1 ----- -/--	1-4, 8-11, 13-19,22

[X] Further documents are listed in the continuation of Box C.

[X] See patent family annex.

* Special categories of cited documents :

"A" document defining the general state of the art which is not considered to be of particular relevance

"E" earlier application or patent but published on or after the international filing date

"L" document which may throw doubts on priority claim(s) or which is cited to establish the publication date of another citation or other special reason (as specified)

"O" document referring to an oral disclosure, use, exhibition or other means

"P" document published prior to the international filing date but later than the priority date claimed

"T" later document published after the international filing date or priority date and not in conflict with the application but cited to understand the principle or theory underlying the invention

"X" document of particular relevance; the claimed invention cannot be considered novel or cannot be considered to involve an inventive step when the document is taken alone

"Y" document of particular relevance; the claimed invention cannot be considered to involve an inventive step when the document is combined with one or more other such documents, such combination being obvious to a person skilled in the art

"&" document member of the same patent family

Date of the actual completion of the international search	Date of mailing of the international search report
10 April 2014	22/04/2014

Name and mailing address of the ISA/	Authorized officer
European Patent Office, P.B. 5818 Patentlaan 2 NL - 2280 HV Rijswijk Tel. (+31-70) 340-2040, Fax: (+31-70) 340-3016	Allnutt, Sarah

2

Form PCT/ISA/210 (second sheet) (April 2005)

C(Continuation). DOCUMENTS CONSIDERED TO BE RELEVANT

Category*	Citation of document, with indication, where appropriate, of the relevant passages	Relevant to claim No.
X	LIETZ M ET AL: "PHYSICAL AND BIOLOGICAL PERFORMANCE OF A NOVEL BLOCK COPOLYMER NERVE GUIDE", BIOTECHNOLOGY AND BIOENGINEERING, WILEY & SONS, HOBOKEN, NJ, US, vol. 93, no. 1, 5 January 2006 (2006-01-05), pages 99-109, XP003005189, ISSN: 0006-3592, DOI: 10.1002/BIT.20688 page 106, column 1, paragraph 2 - page 107, column 1, paragraphs 1,3 see also abstract	1-5,11, 18,19, 21,22
X	WO 2004/041318 A1 (UNIV TWENTE [NL]) 3 August 2005 (2005-08-03) page 8, line 20 - line 33; claims 7,17,18; example 2; table 1	1,8-10, 13-19
X	PEGO A P ET AL: "In vivo behavior of poly(1,3-trimethylene carbonate) and copolymers of 1,3-trimethylene carbonate with D,L-lactide or epsilon-caprolactone: Degradation and tissue response", JOURNAL OF BIOMEDICAL MATERIALS RESEARCH, WILEY, NEW YORK, NY, US, vol. 67A, no. 3, 1 December 2003 (2003-12-01), pages 1044-1054, XP009177425, ISSN: 0021-9304	1,8-10, 13-19
Y	page 1045, column 1, paragraphs 2,3; table 1	1-22
Y	FABRE T ET AL: "Study of a (trimethylenecarbonate-co-@?-caprolactone) polymer-Part 2: in vitro cytocompatibility analysis and in vivo ED1 cell response of a new nerve guide", BIOMATERIALS, ELSEVIER SCIENCE PUBLISHERS BV., BARKING, GB, vol. 22, no. 22, 15 November 2001 (2001-11-15), pages 2951-2958, XP004301373, ISSN: 0142-9612, DOI: 10.1016/S0142-9612(01)00012-6 page 2954, column 2, lines 11-13 page 2956, column 1, paragraph 2 page 2956, column 2, lines 2-6,13-16,51-56 page 2957, column 2, paragraph 1	1-22

-/--

2

INTERNATIONAL SEARCH REPORT

International application No
PCT/PT2014/000006

C(Continuation). DOCUMENTS CONSIDERED TO BE RELEVANT

Category*	Citation of document, with indication, where appropriate, of the relevant passages	Relevant to claim No.
X,P	DANIELA NOGUEIRA ROCHA ET AL: "Poly(Trimethylene Carbonate-co-[epsilon]-Caprolactone) Promotes Axonal Growth", PLOS ONE, vol. 9, no. 2, 27 February 2014 (2014-02-27), page e88593, XP055112310, DOI: 10.1371/journal.pone.0088593 the whole document -----	1-22

2

Form PCT/ISA/210 (continuation of second sheet) (April 2005)

INTERNATIONAL SEARCH REPORT

Information on patent family members

International application No
PCT/PT2014/000006

Patent document cited in search report	Publication date	Patent family member(s)	Publication date
WO 2004041318 A1	03-08-2005	AT 454909 T	15-01-2010
		AU 2003288008 A1	07-06-2004
		EP 1558301 A1	03-08-2005
		ES 2339241 T3	18-05-2010
		NL 1021843 C2	07-05-2004
		US 2006241201 A1	26-10-2006
		WO 2004041318 A1	21-05-2004